

GIS-ENABLED MODELING OF MICHIGAN'S GROUNDWATER SYSTEMS

By

Mehmet Oztan

A DISSERTATION

Submitted to
Michigan State University
in partial fulfillment of the requirements
for the degree of

DOCTOR OF PHILOSOPHY

Civil Engineering

2011

ABSTRACT

GIS-ENABLED MODELING OF MICHIGAN'S GROUNDWATER SYSTEMS

By

Mehmet Oztan

In this paper we systematically evaluate a GIS-enabled and data-intensive modeling system to assess the system's capability to simulate the regional-scale ground water flow in 26 of 38 USGS 8-digit Hydrologic Unit Codes (HUCs) across Michigan's Lower Peninsula. All models simultaneously simulate the glacial and uppermost bedrock aquifer layer in the peninsula. Specifically, the modeling system is used to simulate the long-term average static water levels and base flow in the glacial aquifer, and long-term average piezometric heads in the bedrock aquifer. The results are compared with the measured ground water levels from Michigan's statewide ground water database (MSGWD) and USGS-estimated base flow values. The coupling between the models and data allows real-time and interactive analysis of the assumptions and boundary conditions used in the conceptual models. Overall, this paper presents the most extensive regional-scale modeling and evaluation effort in Michigan to date that provides critical insight into the state's ground water systems. We postulate that the results of this research will have significant implications on the sustainable management of Michigan's ground water resources and ground water dependent ecosystems.

Keywords: Michigan's ground water systems, Michigan's statewide ground water database, GIS-enabled ground water modeling, regional-scale ground water flow, coupling between data and model, Interactive Ground Water

MİŞİĞIN’IN YERALTISUYU SİSTEMLERİNİN CBS TABANLI MODELLEMESİ

Bu araştırma, CBS tabanlı ve çok sayıda arazi verisine dayalı bir nümerik modelleme sisteminin Mişigin Eyaleti’nin güney yarımadasında yer alan 26 büyük ölçekli yüzeysuyu havzasındaki yeraltısuyu akımını temsil etmekteki yeterliliğini değerlendirmektedir. Araştırma için geliştirilen bütün modeller eşzamanlı olarak havza dahilindeki buzul ve kaya akiferlerini kavramsallaştırmaktadır. Modelleme sistemi, buzul akiferdeki uzun zamanlı yeraltısuyu seviyeleri ve baz akım ile kaya akiferindeki piezometrik yükleri hesaplamakta kullanılmıştır. Sonuçlar Mişigin’ın yeraltısuyu veritabanında yer alan yeraltısuyu seviye ölçümleri ve USGS tarafından havza ölçeğinde gerçekleştirilmiş baz akım tahminleriyle karşılaştırılmıştır. Sayısal modelleri oluşturmak için kullanılan kesintisiz veri akışı, kavramsal modelde kullanılan varsayımların ve sınır koşullarının gerçek zamanlı ve etkileşimli analizini olası kılmaktadır. Genel olarak, bu araştırma Mişigin Eyaleti’nde günümüze kadar gerçekleştirilmiş en kapsamlı bölgesel ölçekli modelleme çalışması olup eyaletin yeraltısuyu sistemlerinin işleyişi hakkında önemli bilgiler sunmaktadır. Araştırma sonuçlarının, gelecekte eyaletin yeraltısuyu kaynakları ile devamlılığı bu kaynaklara bağlı olan ekosistemlerin sürdürülebilir yönetiminde önemli katkı sağlayacağı öngörülmektedir.

Anahtar Kelimeler: Mişigin’ın yeraltısuyu sistemleri, Mişigin’ın yeraltısuyu veritabanı, CBS tabanlı yeraltısuyu modellemesi, bölgesel ölçekli yeraltısuyu akımı, modelleme için kesintisiz veri akışı, Interactive Ground Water

Copyright by

MEHMET OZTAN

2011

*I dedicate this doctoral dissertation to my mother Ruveyde Leyla Oztan,
my father Prof. Sadi Yilmaz Oztan (1930-2003),
my uncle Prof. Yuksel Oztan (1933-2010), and to the graduate students who don't give up
despite all difficulties they experience through their education*

Mehmet Oztan, May 2011

Tampa, Florida

*Hayatımın en önemli eseri olan bu doktora tezini
canım annem R veyde Leyla  ztan'a,
değerli bilim adamları babam Prof. Dr. Şadi Yılmaz  ztan (1930-2003) ile
amcam Prof. Dr. Y ksel  ztan (1933-2010)'ın  l ms z hatıralarına ve
b y k zorluklarla m cadele ederek eēitimlerini s rd ren y ksek lisans  ērencilerine
ithaf ediyorum*

*Mehmet  ztan, Mayıs 2011
Tampa, Florida*

ACKNOWLEDGEMENTS

This dissertation would have not been possible without the help and support of professors, funding agencies, colleagues, my family, and friends. First of all, I would like to give my sincere thanks to Prof. Shu-Guang Li, my dissertation advisor, for his support and advice throughout my graduate studies at MSU.

I am grateful to my Ph. D. committee members Prof. Amirpouyan Nejadhashemi of Michigan State University and Dr. Howard W. Reeves of USGS for their detailed comments that have significantly improved the research and manuscript. Other committee members, Prof. Roger B. Wallace and Prof. Phanikumar Mantha also gave valuable feedback throughout the research.

I would like to give my sincere thanks to Prof. Ronald Harichandran, the chairperson of Department of Civil and Environmental Engineering and Prof. Thomas Voice at MSU, for their continuous support towards my degree completion.

I would like to thank Prof. Huasheng Liao, who is a visiting professor at MSU, and a professor at Sichuan University (China), for his invaluable comments and help throughout my research. I consider myself very lucky to know such a special person and admiring scientist.

This research was funded and made possible by the Michigan Department of Environmental Quality (MDEQ) and the National Science Foundation. Other funders include the Office for International Students and Scholars at MSU, and the American Water Works Association. I would like to thank Mr. Richard Mandle from the MDEQ for his help and guidance regarding the research tasks I completed.

The groundwater modeling research group at MSU is a big family. I am very happy to be a part of this family and especially thankful to fellow researchers Hassan Abbas, Dr. Dipa Dey, and Adrian Zhou with who I closely worked in the last four years.

Lori Lerner, administrative assistant in the Department of Civil and Environmental Engineering at MSU, was the person who helped me with every single administrative issue that alone I wouldn't be able to resolve.

I am grateful to Prof. M. Yavuz Corapcioglu who encouraged and supported me to come to MSU for my Ph. D. research.

I am very grateful to Mrs. K. Setenay Arikan, Dr. M. Firat Arikan, and Mr. Ilhan Kubilay Geckil for their valuable friendship and moral support throughout my graduate studies at MSU.

Finally, I would like to thank my family, specifically my mother Ms. Ruveyde Leyla Oztan and my cousin Ms. Aysegul Kucukgocmen for their existence and endless support, my wife Prof. Amy S. Thompson, Dr. Lowery Thompson, Mrs. Barbara Thompson, Ms. Laura Thompson, and all family friends who have been my encouragement not only in this endeavor, but all in others.

There is someone else who keeps living deep in my heart, my father Prof. Sadi Yilmaz Oztan, who I am very thankful for being my role model for hard work and for teaching me that honesty and human values are above any scientific research.

Mehmet Oztan

May 2011

TABLE OF CONTENTS

LIST OF TABLES	x
LIST OF FIGURES	xii
LIST OF ABBREVIATIONS.....	xviii
GIS-BASED REGIONAL-SCALE MODELING OF GROUND WATER FLOW IN MICHIGAN’S LOWER PENINSULA	1
INTRODUCTION	1
MODEL DEVELOPMENT.....	4
Conceptual Model.....	4
Governing Equations and Boundary Conditions.....	8
Numerical Model.....	10
MODEL EVALUATION	14
Statistical analysis.....	22
Conceptual messages.....	26
Base flow comparison.....	32
CONCLUSIONS	34
APPENDICES	37
Appendix A: Michigan’s Statewide Groundwater Database.....	38
Appendix B: Conceptual Difference between HCOND1 and HCOND2	68
Appendix C: Data Analysis and Management.....	71
Appendix D: Analysis of the Hydraulic Connection between the Great Lakes and Regional-Scale Heads	101
Appendix E: Analysis of the Simulated Heads.....	107
Appendix F: Analysis of Pumping in the Southern Lower Peninsula	151
Appendix G: Definition of the Additional Model Statistics	155
Appendix H: Detailed List of the Model Statistics.....	158
Appendix I: MATLAB Script for the Calculation of the Model Statistics.....	162
LITERATURE CITED	168

LIST OF TABLES

Table 1: Model settings and basic information for model analysis.	13
Table 2: Explanation of the abbreviations given in Figure 3.	16
Table 3: Summary of the significant messages illustrated in Figure 4.	18
Table 4: Summary of the significant messages illustrated in Figure 5.	20
Table 5: Summary of the significant messages illustrated in Figure 6.	22
Table 6: Summary of the model statistics for the glacial aquifer simulations.	25
Table 7: Adjusted $L'w$ values.	33
Table 8: Hydraulic conductivity classification based on the land systems of Michigan (GWIM, 2006).	57
Table 9: Essential modeling parameters recorded in the NHD.	60
Table 10: Basic specifications of IGW.	72
Table 11: Basic features of the main computer used in the research.	73
Table 12: Basic features of the advanced computer used for some of the simulations.	73
Table 13: Criteria used for eliminating the bad data.	75
Table 14: Ranges for the color transmissivity map.	96
Table 15: Prescribed head values assigned for the shorelines of the Great Lakes.	100
Table 16: Temporal analysis of the SWL based on the Great Lakes' water level periods.	103
Table 17: Temporal analysis of the SWL based on the annual quarters.	103

Table 18: Statistics that are used to quantify the head comparisons.....	155
Table 19: Statistics for the model residuals, glacial aquifers.....	158
Table 20: Statistics for the model performances, glacial aquifers.	159
Table 21: Statistics for the model residuals, bedrock aquifers.	160
Table 22: Statistics for the model performances, bedrock aquifers.....	161

LIST OF FIGURES

Figure 1: Illustration of the boundary conditions used in the conceptual model. For interpretation of the references to color in this and all other figures, the reader is referred to the electronic version of this dissertation.	7
Figure 2: Conceptual use of the statewide data, and the general cross-section of the conceptual model.....	8
Figure 3: Locations of the modeled watersheds.	15
Figure 4: Simulated (y axis) and measured (x axis) water levels in the watersheds across the regional-scale recharge zones. GL: Glacial aquifer, BR: Bedrock aquifer. Scale of the color map is non-linear.	17
Figure 5: Simulated (y axis) and measured (x axis) water levels in the watersheds across the transition zones between regional-scale recharge and discharge zones. GL: Glacial aquifer, BR: Bedrock aquifer. Scale of the color map is non-linear.....	19
Figure 6: Simulated (y axis) and measured (x axis) water levels in the watersheds with shale formations, karst formations, and confining layers. GL: Glacial aquifer, BR: Bedrock aquifer..	21
Figure 7: a) Distribution of the simulated piezometric heads, Shiawassee Watershed, and b) Simulated and measured piezometric heads.	27
Figure 8: a) Simulated piezometric heads in the shale formations, St. Joseph Watershed, and b) Simulated and measured piezometric heads.	28
Figure 9: a) Model boundaries before and after the boundary expansion, and b) Comparison between the simulated and measured water levels before and after the boundary expansion.	29
Figure 10: Simulated and measured water levels in the Manistee Watershed, glacial aquifer.....	30
Figure 11: Simulated and measured water levels in the bedrock aquifer along the northern tip of the Lower Peninsula: a) Black Watershed, and b) Cheboygan Watershed.....	31
Figure 12: Correlation between the simulated and USGS-estimated base flow values.....	33

Figure 13: Comparison between the seepage discharge values when streams are modeled as one-way and two-way head dependent flux model features.	34
Figure 14: Glacial thickness map for Michigan's Lower Peninsula. Values are subject to change due to the resolution of the raster-based data.....	40
Figure 15: Major bedrock aquifers in Michigan.	43
Figure 16: Time-based spatial distribution of the water wells in the glacial aquifers in Michigan.	45
Figure 17: Time-based spatial distribution of the water wells in the bedrock aquifers in Michigan.	46
Figure 18: Time-based change in the representation of the hydraulic conductivity (K) field in the Kalamazoo County.....	47
Figure 19: Distribution of the oil and gas wells in Michigan.	49
Figure 20: Raster-based bedrock surface map of Michigan.	50
Figure 21: Watersheds of Michigan.....	52
Figure 22: Sub-watersheds of the Muskegon Watershed.	53
Figure 23: Conceptualization of the calculation interval for the HCOND1 parameter.	54
Figure 24: Conceptualization of the calculation interval for the HCOND2 parameter.	55
Figure 25: Stream segments with missing stream stage data in the NHD of Michigan.	61
Figure 26: Raster-based recharge map of Michigan.	64
Figure 27: Locations of the stream gauging stations in Michigan.....	67
Figure 28: Hydraulic conductivity field of the Tittabawassee Watershed. Above HCOND1, and Below: HCOND2.....	69
Figure 29: Comparison between the model results with HCOND1 and HCOND2. Black Dots: Results for HCOND1, and Blue Circles: Results for HCOND2.	70

Figure 30: Error map for the DEM information in Wellogie.....	77
Figure 31: Location of an area in the western Lower Peninsula where DEM error is extremely high.	79
Figure 32: Simulated and measured heads for the model area shown in Figure 31. Above: comparison using vector-based DEM, and Below: comparison using raster-based DEM with 10 m (sampled from 30 m) resolution.....	80
Figure 33: Identifying bad SWL data using model-based analysis, Thornapple Watershed, bedrock aquifer.	81
Figure 34: Identifying the outliers for the Clinton Watershed, bedrock aquifer.	83
Figure 35: Analysis of the outliers based on the model results in the Clinton Watershed, bedrock aquifer.	84
Figure 36: Error locations for the bedrock surface map of the Upper Peninsula.	86
Figure 37: Magnifying the error in the bedrock surface map and available data points in the Upper Peninsula.	87
Figure 38: Conceptual picture of the possible reason for the error in the bedrock surface map. .	88
Figure 39: USGS 90 m raster-based DEM.	91
Figure 40: Raster-based hydraulic conductivity maps interpolated from the data.	93
Figure 41: Color map for the transmissivity ranges generated based on the aquifer test data.	95
Figure 42: High order streams with artificial lines along the shores of the Great Lakes.	97
Figure 43: Conceptualization of the stream cells in the models.	99
Figure 44: Location of the test area for temporal SWL analysis.	102
Figure 45: Temporal SWL analysis for annual quarters in the Kalamazoo and Van Buren County.	104
Figure 46: Temporal analysis for the Great Lakes water level periods in the Kalamazoo and Van Buren County.	105

Figure 47: Analysis of the simulated heads in the Au Gres-Rifle Watershed, glacial aquifer. ..	107
Figure 48: Analysis of the simulated heads in the Au Gres – Rifle Watershed, bedrock aquifer.	108
Figure 49: Analysis of the simulated heads in the Au Sable Watershed, glacial aquifer.	109
Figure 50: Analysis of the simulated heads in the Birch/St. Clair watersheds, glacial aquifer. .	110
Figure 51: Analysis of the simulated heads in the Birch/St. Clair watersheds, bedrock aquifer.	111
Figure 52: Analysis of the simulated heads in the Black Watershed, glacial aquifer.....	112
Figure 53: Analysis of the simulated heads in the Black Watershed, bedrock aquifer.	113
Figure 54: Analysis of the simulated heads in the Cass Watershed, glacial aquifer.	114
Figure 55: Analysis of the simulated heads in the Cass Watershed, bedrock aquifer.	115
Figure 56: Analysis of the simulated heads in the Cheboygan Watershed, glacial aquifer.....	116
Figure 57: Analysis of the simulated heads in the Cheboygan Watershed, bedrock aquifer.....	117
Figure 58: Analysis of the simulated heads in the Clinton Watershed, glacial aquifer.	118
Figure 59: Analysis of the simulated heads in the Clinton Watershed, bedrock aquifer.....	119
Figure 60: Analysis of the simulated heads in the Flint Watershed, glacial aquifer.	120
Figure 61: Analysis of the simulated heads in the Flint Watershed, bedrock aquifer.	121
Figure 62: Analysis of the simulated heads in the Huron Watershed, glacial aquifer.....	122
Figure 63: Analysis of the simulated heads in the Huron Watershed, bedrock aquifer.....	123
Figure 64: Analysis of the simulated heads in the Kalamazoo Watershed, glacial aquifer.....	124
Figure 65: Analysis of the simulated heads in the Kalamazoo Watershed, bedrock aquifer.....	125
Figure 66: Analysis of the simulated heads in the Kawkawlin Watershed, glacial aquifer.....	126

Figure 67: Analysis of the simulated heads in the Kawkawlin Watershed, bedrock aquifer.	127
Figure 68: Analysis of the simulated heads in the Lower Grand River Watershed, glacial aquifer.	128
Figure 69: Analysis of the simulated heads in the Lower Grand River Watershed, bedrock aquifer.	129
Figure 70: Analysis of the simulated heads in the Manistee Watershed, glacial aquifer.	130
Figure 71: Analysis of the simulated heads in the Maple Watershed, glacial aquifer.....	131
Figure 72: Analysis of the simulated heads in the Maple Watershed, bedrock aquifer.....	132
Figure 73: Analysis of the simulated heads in the Muskegon Watershed, glacial aquifer.	133
Figure 74: Analysis of the simulated heads in the Pere-Marquette Watershed, glacial aquifer.	134
Figure 75: Analysis of the simulated heads in the Pigeon Watershed, bedrock aquifer.....	135
Figure 76: Analysis of the simulated heads in the Pine Watershed, glacial aquifer.	136
Figure 77: Analysis of the simulated heads in the Raisin Watershed, glacial aquifer.....	137
Figure 78: Analysis of the simulated heads in the Raisin Watershed, bedrock aquifer.....	138
Figure 79: Analysis of the simulated heads in the Shiawassee Watershed, glacial aquifer.....	139
Figure 80: Analysis of the simulated heads in the Shiawassee Watershed, bedrock aquifer.	140
Figure 81: Analysis of the simulated heads in the St. Joseph Watershed, glacial aquifer.....	141
Figure 82: Analysis of the simulated heads in the St. Joseph Watershed, bedrock aquifer.....	142
Figure 83: Analysis of the simulated heads in the Thornapple Watershed, glacial aquifer.....	143
Figure 84: Analysis of the simulated heads in the Thornapple Watershed, bedrock aquifer.	144
Figure 85: Analysis of the simulated heads in the Thunder Bay Watershed, glacial aquifer.	145
Figure 86: Analysis of the simulated heads in the Thunder Bay Watershed, bedrock aquifer...	146

Figure 87: Analysis of the simulated heads in the Tittabawassee Watershed, glacial aquifer. ..	147
Figure 88: Analysis of the simulated heads in the Tittabawassee Watershed, bedrock aquifer.	148
Figure 89: Analysis of the simulated heads in the Upper Grand River Watershed, glacial aquifer.	149
Figure 90: Analysis of the simulated heads in the Upper Grand River Watershed, bedrock aquifer.	150
Figure 91: Interpolated SWL in the city of Lansing.	152
Figure 92: Revisiting the model results for the Upper Grand River. Circled area indicate the pumping effect.	153
Figure 93: Identifying biases similar to that of the Upper Grand River case. Circled areas might potentially indicate the pumping effect. Above: Flint Watershed, Below: Shiawassee Watershed.	154

LIST OF ABBREVIATIONS

1/d: One per day

ac: acre

DEM: Digital Elevation Model

ft: feet

ft/d: feet per day

ft²/d: square feet per day

ft³/s: cubic feet per second

GIS: Geographic Information System

GWIM: Groundwater Inventory and Mapping Project

HUC: Hydrological Unit Code

in/yr: inch per year

K: Hydraulic conductivity

LERCMM: Laboratory of Excellence for Real-time Computing and Multi-scale Modeling

m: meter

m/d: meter per day

m/s: meter per second

m³/s: cubic meter per second

mi²: square mile

MDEQ: Michigan Department of Environmental Quality

MDNRE: Michigan Department of Natural Resources and Environment

MSGWD: Michigan's Statewide Groundwater Database

MSU: Michigan State University

NED: National Elevation Dataset

NHD: National Hydrography Dataset

NOAA: National Oceanic and Atmospheric Administration

RASA: Regional Aquifer Systems Analysis

SRTM: Shuttle Radar Topography Mission

SWL: Static water level

T: Transmissivity

USGS: United States Geological Survey

GIS-BASED REGIONAL-SCALE MODELING OF GROUND WATER FLOW IN MICHIGAN'S LOWER PENINSULA

INTRODUCTION

In the last two decades, advances in information and computational technologies and increasing demands in ground water use have shifted the focus of ground water investigations from stand-alone models towards GIS-based modeling (Barazzuoli et al., 1999; Batelaan et al., 1993; El-Kadi et al., 1994; Gogu et al., 2001; Henriksen et al., 2003; Hoaglund et al., 2002; Hojberg et al., 2007; Li et al., 2009; Liao et al., 2010; Lubczynski and Gurwin, 2005; Mende et al., 2007; Michael et al., 2005; Refsgaard et al., 2009; Tim et al., 1996). Recently, Li *et al.* at Michigan State University (MSU) developed a data-integrated, interactive and graphically oriented modeling system, Interactive Ground water (IGW), to investigate Michigan's ground water systems in collaboration with Michigan Department of Natural Resources and Environment (MDNRE) (Li and Liu, 2006). IGW enables real-time two-dimensional and three-dimensional modeling, visualization, and analysis for many ground water problems (Li and Liu, 2006; Zheng, 2010). Most importantly, IGW provides a coupling between process-based models and Michigan's existing statewide ground water database (MSGWD) in a way that allows the definition of the model parameters almost everywhere in the state and at the time of numerical model creation, a unique feature that makes the regional-scale statewide ground water modeling possible. In this paper, we take full benefit of this feature to evaluate the modeling system's capability to simulate regional-scale ground water flow in Michigan's Lower Peninsula. This evaluation helps us to improve the understanding of the regional-scale ground water flow in the glacial aquifer and its interaction with the bedrock aquifer across the peninsula.

MSGWD is a pre-processed GIS-based database and has been assembled by the Michigan Department of Environmental Quality (now MDNRE) to contain most of the data needed for regional-scale ground water flow simulations across the state (GWIM, 2006). The database has been created based on the requirement made by the Public Act 148, Section 32802 (2003) that aims to improve the statewide environmental and water resources management. All data are available in geo-referenced digital files throughout our application domain, and spatial variations of the aquifer parameters in the models are defined with these data. Specifically, MSGWD includes the data for defining numerical model domains (e.g. watershed boundaries), aquifer elevations (e.g. digital elevation models (DEMs), aquifer lithologies), aquifer stresses (e.g. estimated ground water recharge, streams), aquifer properties (e.g. hydraulic conductivities, transmissivities), and calibration data (e.g. static water levels (SWL), base flow).

We focus on the ground water flow in two aquifer layers in the Lower Peninsula: the glacial and uppermost bedrock aquifer. The most critical conceptual questions we ask are the following: Can we simulate the dominant variations in regional-scale ground water flow in these two aquifers and explain the variations in measured ground water levels by assigning only one computational layer for each aquifer in the numerical model? What is the controlling factor of the bedrock flow along the regional-scale discharge zones and in the watersheds with shale units, relatively small glacial thickness and local confining layers? Can we conceptualize the bedrock aquifer as a collection of geologic sub-crops that are in contact with the glacial aquifer and that represent the effective transmissivity field? What is the impact of modeling glacial aquifer with one computational layer in the regional-scale recharge zones? Can we use surface-watershed boundaries to represent the regional-scale no-flow ground water boundaries everywhere in the peninsula? For which watersheds is the modeling system insufficient to simulate the ground

water flow, and why? We seek the answers to these conceptual questions by simulating ground water flow for 26 of 38 USGS 8-digit Hydrologic Unit Codes (hereafter referred as watersheds) across the peninsula. We tested the modeling system on a large number of watersheds in order to ensure that the capability of this system is generalizable. Extending the analysis over such a large area enables the coverage of the aquifers that are apart and that -at a regional-scale- have different hydrogeologic and physical properties (e.g. different recharge/discharge patterns, different aquifer thicknesses, different lithologies, different watershed sizes, and variations in the magnitude of vertical flow). Furthermore, maximizing the number of the modeled watersheds provides the opportunity to systematically test the capability of the simple two-layer conceptual models to represent the regional-scale ground water flow in the glacial and bedrock aquifers in the peninsula. Additionally, we assume that the watershed boundaries coincide with the regional-scale ground water basin boundaries to evaluate the accuracy of the boundary conditions used in the models.

We use IGW v. 5.20 to develop all of the models. Along with IGW, Arc/Info and MATLAB software applications are used for the model evaluation. Goodness of fit of the simulated long-term static water levels in the glacial aquifers and long-term piezometric heads in the bedrock aquifers to measured water level data from MSGWD is evaluated with model statistics. Similarly, simulated base flow values are systematically compared to USGS-estimated base flow values to evaluate the goodness of model calculations. Additionally, the comparisons between the simulated and measured water levels in each watershed are used to point out the most critical hydrogeologic aspects of the regional-scale ground water flow in the peninsula, and to evaluate the assumptions used in the conceptual models.

MODEL DEVELOPMENT

Conceptual Model. The conceptual model focuses on two regional aquifer layers: the glacial aquifer and uppermost bedrock aquifer. The watershed boundaries (USGS, 2011) are the model boundaries, and are initially assumed to coincide with the regional-scale ground water basin boundaries (Figure 1). Main purpose of this assumption is to test whether the watershed boundaries can be used for regional-scale ground water modeling across the Lower Peninsula of Michigan. Another assumption is that there is no lateral ground water flux coming to or from the glacial and bedrock aquifer through the watershed boundaries. Lateral flow only occurs into the Great Lakes through the watershed boundaries along the lake shorelines. The base of the bedrock aquifer is assumed to be impermeable.

The upper elevation of the glacial aquifer (i.e. land surface elevation) is defined by the USGS 90 m National Elevation Dataset (NED) (USGS, 2006). Where applicable, land surface is conceptualized as the seepage surface. That is, discharge to the land surface is zero when water levels in the model cells adjacent to the land surface are equal to or less than the assigned land surface elevation (Anderson and Woessner, 2002). All polygon-based surface water bodies (e.g. inland lakes, ponds, wetlands) are also assumed to be the components of the seepage surface. Steady-state water levels in these water bodies are assigned from the USGS 90 m NED. The bottom elevation of the glacial aquifer (bedrock surface) across the state is defined based on almost 150,000 well logs of water, and oil and gas wells. The locations and information in the water wells are provided with the state's electronic water well database, *Wellogic* (GWIM, 2006). The database for the oil and gas wells is compiled by the Michigan Department of Natural Resources and Environment (GWIM, 2006). The statewide effective horizontal hydraulic

conductivity field of the glacial aquifer is defined on the basis of lithologic descriptions recorded in more than 200,000 water well records from the statewide Wellog database (GWIM, 2006). The vertical hydraulic conductivity of the glacial aquifer is defined based on the vertical anisotropy given with $\frac{K_x}{10} = \frac{K_y}{10} = K_z$ where K_x is the effective hydraulic conductivity in x direction, K_y is the effective hydraulic conductivity in y direction, and K_z is the effective hydraulic conductivity in z direction. The statewide effective transmissivity (T_x for the effective transmissivity in x direction and T_y for the effective transmissivity in y direction) field of the bedrock aquifer is pre-defined based on the spatial interpolation of more than 1,400 aquifer test data provided by the USGS. The bedrock aquifer thickness is assumed to be constant and approximately 76 m. Since the T_x and T_y terms are pre-defined, changing the thickness only has an impact on the vertical flux [Equation (4)] between the glacial and bedrock aquifer. However, based on the available well depths that are provided with the USGS aquifer test database, a bedrock aquifer thickness of 76 m was found to be reasonable, even though the depths of the wells in the database are not necessarily the same.

It is assumed that the source of ground water to the glacial aquifer is from precipitation recharge. The statewide long-term average ground water recharge to the glacial aquifer is estimated by the USGS with hydrograph separation for more than 400 stream flow hydrographs, and landscape attributes (Neff *et al.*, 2005). The only source of water to the bedrock aquifer is maintained through the vertical leakage from the overlying glacial aquifer. The locations of the streams are defined with the USGS National Hydrography Dataset (NHD) for all 1st to 6th order streams (USGS, 2011). Steady-state water levels in the stream segments are assigned to all

streams from the USGS 30 m NED (USGS, 2006). The *leakance* (L') parameter is used to define the hydraulic connection between the seepage surface/streams and ground water [Equation (1)].

$$L' = \frac{K'}{b'} \quad (1)$$

where K' is the hydraulic conductivity of the stream/seepage surface bed and b' is the thickness of stream/seepage surface bed. All streams are assumed to be effluent streams since the stream gauging stations and miscellaneous measurements in Michigan show that most streams are gaining streams in the state (Holtschlag and Nicholas, 1998). Where applicable, the water elevations along the shorelines of the Great Lakes are assumed to be equal to the long-term average of the observed lake levels reported by the National Oceanic and Atmospheric Administration (NOAA) (NOAA, 2011). These levels are represented in the watershed models for both the glacial and bedrock aquifers as prescribed-head boundaries (Figure 1).

Conceptual use of the data and a general cross-section of the conceptual model are illustrated in Figure 2.

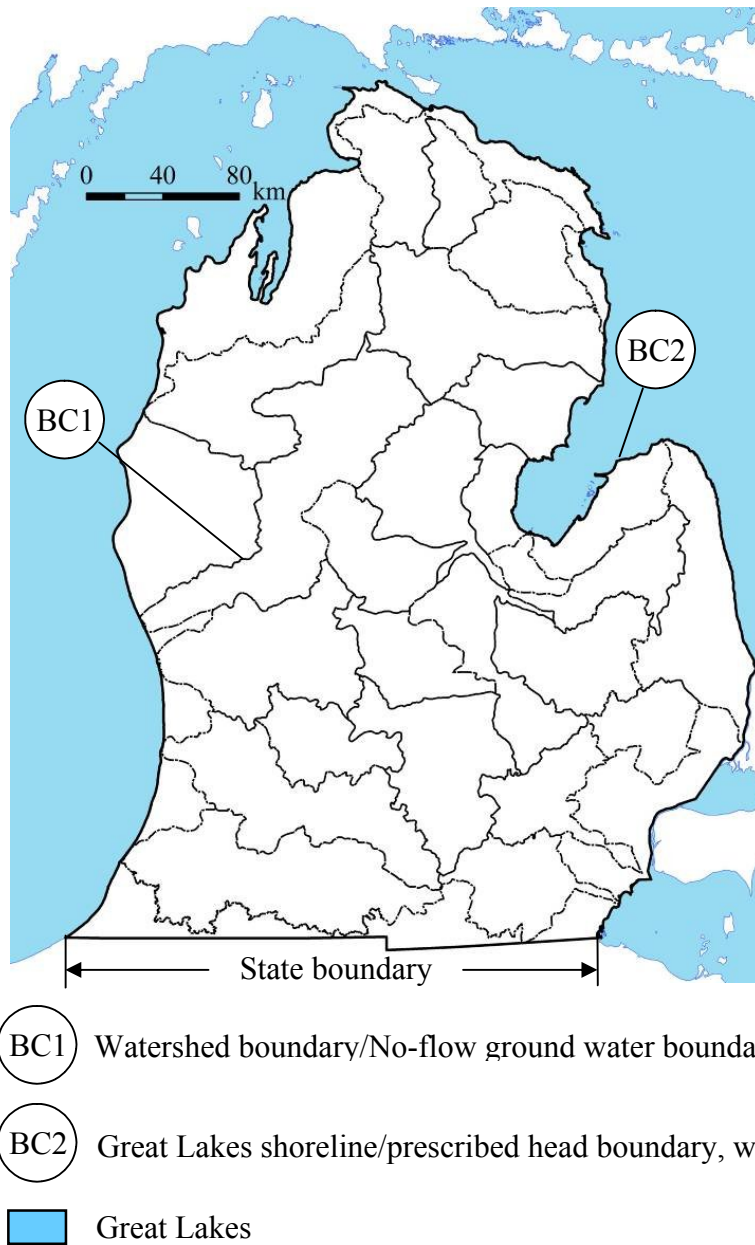


Figure 1: Illustration of the boundary conditions used in the conceptual model. For interpretation of the references to color in this and all other figures, the reader is referred to the electronic version of this dissertation.

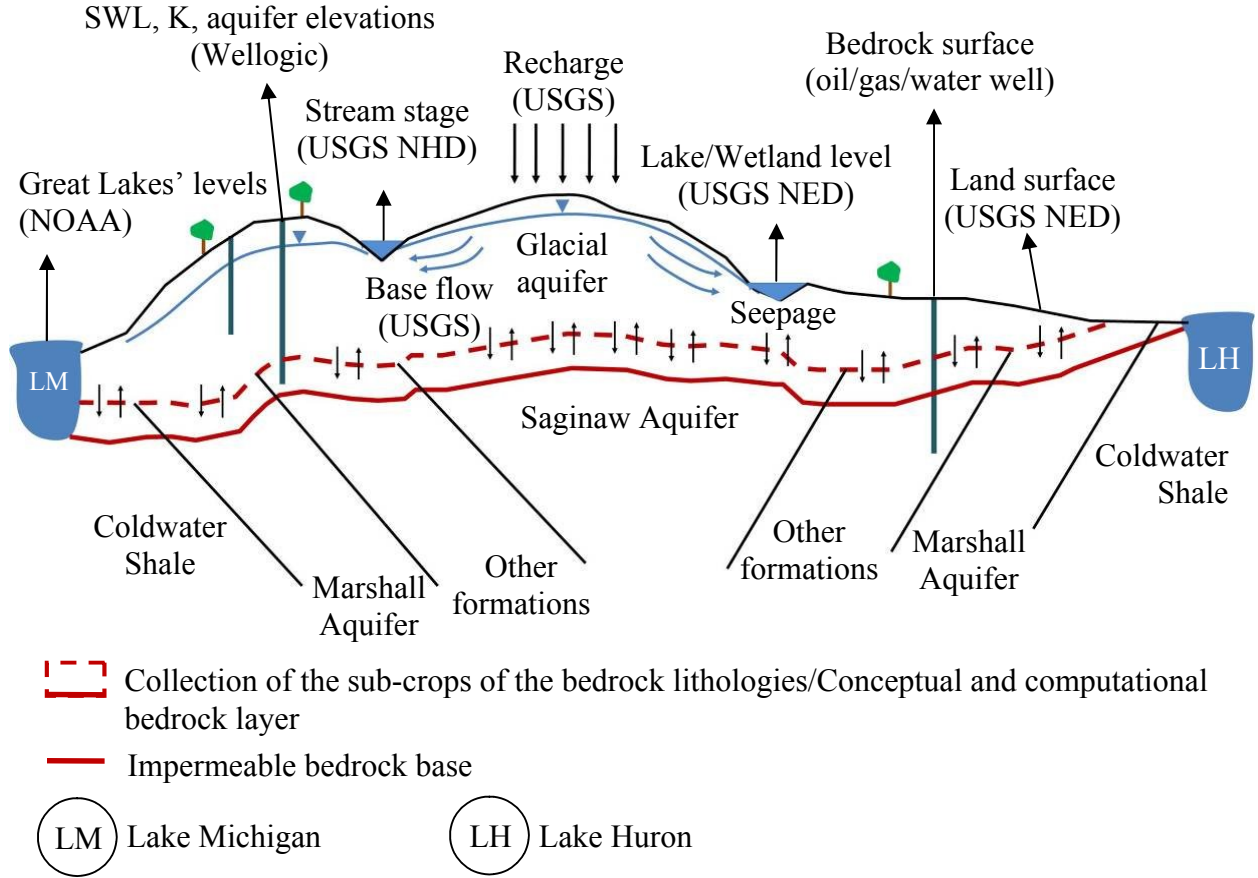


Figure 2: Conceptual use of the statewide data, and the general cross-section of the conceptual model.

Governing Equations and Boundary Conditions. Ground water flow in the glacial and bedrock aquifer is represented with [Equation (2)] and [Equation (3)], respectively:

$$\frac{\partial}{\partial x} \left(K_x (h_g - e) \frac{\partial h_g}{\partial x} \right) + \frac{\partial}{\partial y} \left(K_y (h_g - e) \frac{\partial h_g}{\partial y} \right) + q_g - q_v = 0 \quad (2)$$

where h_g is the ground water level in the glacial aquifer, e is the bottom elevation of the glacial aquifer, q_g is the source (i.e. recharge) and sinks (i.e. seepage, pumping where applicable), and

q_v is the vertical flux between the glacial and bedrock aquifer and expressed with [Equation (4)].

$$\frac{\partial}{\partial x} \left(T_x \frac{\partial h_b}{\partial x} \right) + \frac{\partial}{\partial y} \left(T_y \frac{\partial h_b}{\partial y} \right) + q_b + q_v = 0 \quad (3)$$

where h_b is the ground water level in the bedrock aquifer, q_b is the sinks (i.e. pumping where applicable).

$$q_v = \frac{K'_z}{d} (h_g - h_b) \quad (4)$$

where K'_z is the conductance between the glacial and bedrock aquifer, d is the arithmetic average of the aquifer thicknesses, and

$$K'_z = \frac{K_{zg} K_{zb} (b_g + b_b)}{b_g K_{zb} + b_b K_{zg}} \quad (5)$$

$$d = \frac{b_g + b_b}{2} \quad (6)$$

where K_{zg} is the vertical hydraulic conductivity of the glacial aquifer, K_{zb} is the vertical hydraulic conductivity of the bedrock aquifer, b_g is the glacial aquifer thickness, and b_b is the bedrock aquifer thickness.

Based on the conceptual model, two different boundary conditions given in [Equation (7)] and [Equation (8)] are used to solve [Equation (2)] and [Equation (3)]:

$$\left. \frac{\partial h_g}{\partial n} \right|_{\Gamma_1} = \left. \frac{\partial h_b}{\partial n} \right|_{\Gamma_1} = 0 \quad (7)$$

$$h_g|_{\Gamma_2} = h_b|_{\Gamma_2} = H(x, y) \quad (8)$$

where Γ_1 is watershed boundary, Γ_2 is the Great Lakes' shoreline, and $H(x, y)$ is the Great Lakes' long-term average water level.

Numerical Model. Quasi three-dimensional finite-difference numerical models are used to simulate the ground water flow in 26 of the 38 watersheds across Michigan's Lower Peninsula. The models are represented by rectangular grids discretized into rows and columns which construct the model cells. The values for the model input parameters in the model cells are assigned from the raster and vector-based GIS files (MSGWD) that are coupled with the numerical models to allow the representation of the aquifer heterogeneities. In the models, each aquifer layer (i.e. glacial and bedrock aquifer layer) is represented by one computational layer that simulates one average water level for the entire thickness of the aquifer.

At a regional scale, configuration of the water table is commonly a subdued replica of the land-surface topography (USGS, 1999). One computational layer is used to simulate the glacial aquifer based on the general practical rule that dictates that the Dupuit-Forchheimer approximation is acceptable when the distance between hydrologic boundaries, L , (here tens of

kilometers in most watersheds) is large compared to the saturated aquifer thickness, H , (Haitjema,2005) [Equation (9)]:

$$L \gg \sqrt{\frac{K_h}{K_v}} H \quad (9)$$

where K_h is the horizontal hydraulic conductivity, and K_v is the vertical hydraulic conductivity.

All models represent the steady-state flow conditions for which the simulated ground water levels are the long-term average values and water levels don't change with time. However, measured water levels in the wells span many years, in some cases over fifty years, and models do not incorporate the temporal variations in measured water levels due to the impacts of seasonal fluctuations and ground water withdrawals.

Cell sizes used in the models are not fine enough to capture the head variations induced by small-scale spatial heterogeneities (e.g. perched aquifers, local confining layers). Even though these small-scale details are not the focus of this paper, it should be noted that they contribute to the error in the simulations. Additionally, streams become strong boundary conditions as the stream order and the hydraulic connection (i.e. leakance) between the stream and ground water increases, and the ground water levels simulated in the models converge to the stream stages in these stream cells. Cell sizes are not fine enough to capture the small-scale variations in stream levels along the stream courses.

Most of the wells recorded in Wellogic do not have a pumping rate. More than 90% of the wells are household wells, and if it is assumed that each well in the watersheds is active and

pump ground water with an average discharge rate of $4 \times 10^{-6} \text{ m}^3/\text{d}$, then in none of the watersheds, magnitude of the ratio between total discharge through the wells and total ground water recharge is more than 10^{-2} . Furthermore, at a regional-scale, it is not possible to capture the actual drawdown created with small-scale pumping. Because of these reasons, pumping wells are not simulated in the models.

The information regarding the number of the cells, and the grid sizes used in the models, the model area and the number of the water-well records (i.e. number of measured water level data) used for the analysis of the simulations are given in Table 1.

Table 1: Model settings and basic information for model analysis.

Watershed Name	NX	NY	ΔX (m)	ΔY (m)	Model Area (km²)	No. of Glacial Wells	No. of Bedrock Wells
Au Gres – Rifle	130	87	654	653	2,593	1,834	562
Au Sable	150	103	837	835	5,323	3,184	7
Birch – St. Clair	150	363	437	437	4,552	2,770	1,234
Black	50	91	768	768	1,560	369	158
Cass	150	108	636	635	2,335	109	2,159
Cheboygan	71	103	768	768	2,429	1,446	77
Clinton	150	138	404	405	1,903	12,057	181
Flint	150	116	569	566	3,499	3,611	9,750
Huron	150	139	574	573	2,432	19,938	2,358
Kalamazoo	150	97	982	978	5,220	12,730	2,884
Kawkawlin	150	245	238	238	1,294	623	1,735
L. Grand River	150	124	732	732	5,185	14,162	1,298
Manistee	150	137	845	847	4,925	5,222	2
Maple	150	106	571	572	2,413	1,173	1,106
Muskegon	150	153	1,022	1,025	7,066	15,054	17
Pere – Marquette	150	212	521	522	5,192	10,227	6
Pigeon	150	147	503	502	2,239	22	1,308
Pine	150	121	581	580	2,677	4,305	15
Raisin	150	96	636	633	2,641	4,403	1,733
Shiawassee	150	185	630	629	3,198	10,307	2,829
St. Joseph	250	101	676	673	6,174	15,448	972
Thornapple	150	109	525	525	2,203	5,034	1,508
Thunder Bay	100	91	768	768	3,257	1,035	230
Tittabawassee	150	186	544	543	3,685	5,744	223
U. Grand River	150	173	612	610	4,500	2,032	17,579

MODEL EVALUATION

At a regional-scale, resolution of the water-well data (i.e. Wellogic) is several magnitudes greater than that of the traditionally collected data, which is a unique feature that makes the GIS-enabled regional-scale ground water modeling possible almost everywhere in the State of Michigan. The GIS interface of IGW maximally benefits from the data-rich structure of Wellogic. The measured water levels are readily available in Wellogic, and can be brought into IGW through the GIS interface in real-time and interactively. The coupling between the data and models is used to evaluate the simulations by systematically comparing the simulated water levels to the measured water levels (Figure 4, Figure 5, and Figure 6). IGW calculates the simulated water levels at the nodes of each cell, and then using the information at the nodes, applies bi-linear interpolation to predict the water levels at the location of the water wells. Measured water levels that are used for model comparison are the water levels recorded in the water wells after the wells are developed, prior to pumping (GWIM, 2006). Please refer to Figure 3 and Table 2 for the locations and identifications of the simulated watersheds. Summary of the significant messages illustrated in Figure 4, Figure 5, and Figure 6 is provided in Table 3, Table 4, and Table 5.

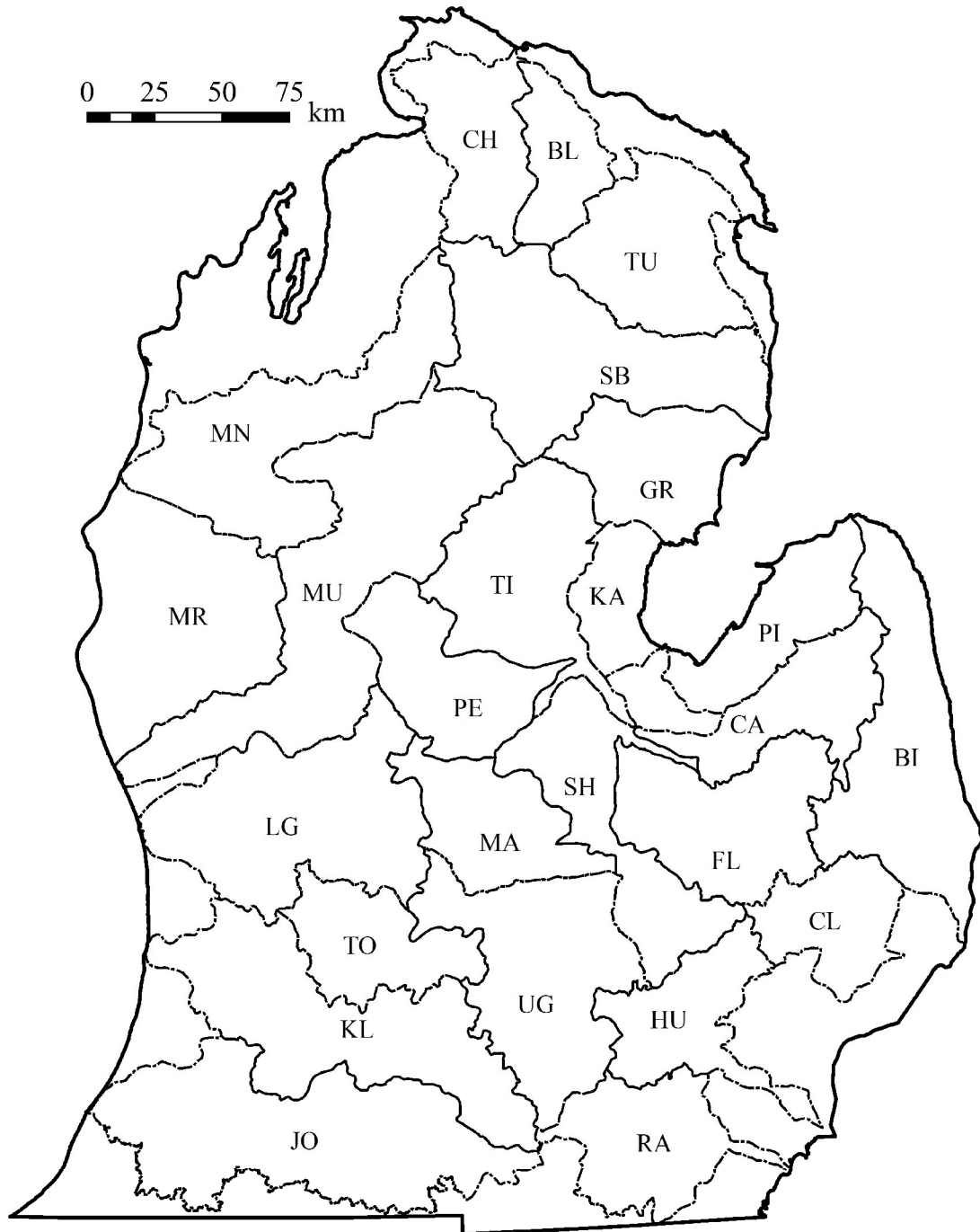


Figure 3: Locations of the modeled watersheds.

Table 2: Explanation of the abbreviations given in Figure 3.

Watershed Name	Abbreviation
Au Gres – Rifle	GR
Au Sable	SB
Birch – St. Clair	BI
Black	BL
Cass	CA
Cheboygan	CH
Clinton	CL
Flint	FL
Huron	HU
Kalamazoo	KL
Kawkawlin	KA
Lower Grand River	LG
Manistee	MN
Maple	MA
Muskegon	MU
Pere-Marquette	MR
Pigeon	PI
Pine	PE
Raisin	RA
Shiawassee	SH
St. Joseph	JO
Thornapple	TO
Thunder Bay	TU
Tittabawassee	TI
Upper Grand River	UG

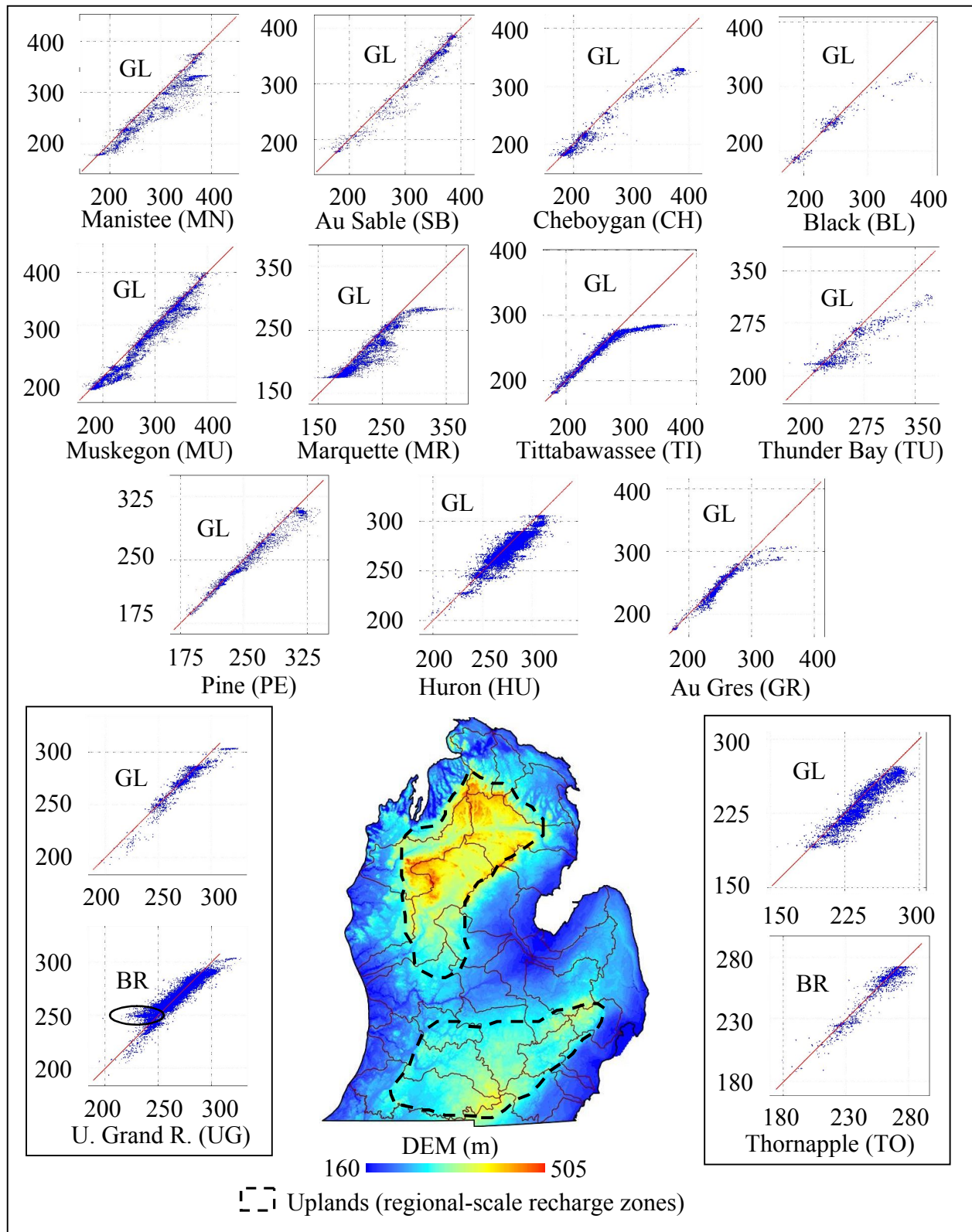


Figure 4: Simulated (y axis) and measured (x axis) water levels in the watersheds across the regional-scale recharge zones. GL: Glacial aquifer, BR: Bedrock aquifer. Scale of the color map is non-linear.

Table 3: Summary of the significant messages illustrated in Figure 4.

<p><i>Northern upland (NU)</i>: Largest glacial thickness, significant vertical flow, deep bedrock aquifers (i.e. very few wells for model validation)</p> <ul style="list-style-type: none"> - On NU: Simulated glacial heads are averaged over large aquifer depths and systematically under predict measured heads (e.g. MN, MR, MU, SB) - Around NU: Simple no-flow boundaries cannot be used on watershed boundaries to model glacial flow (e.g. BL, CH, GR, MR, TI, TU)
<p><i>Southern upland (SU)</i>: Glacial thickness is moderate with respect to NU, significant vertical flow</p> <ul style="list-style-type: none"> - On SU: Systematic model under prediction still exists but not as strong as in NU (e.g. HU (GL), UG (GL), PE (GL), TO (GL)) - Around SU: Simple no-flow boundaries cannot be used on watershed boundaries for ground water modeling, bias at high heads are less due to smaller gradient/lateral flow at the boundaries (e.g. HU (GL), TO (BR), UG (GL)) - In major pumping centers, simulated heads locally over predict the measured heads since pumping wells are not modeled (e.g. circled area in UG (BR))

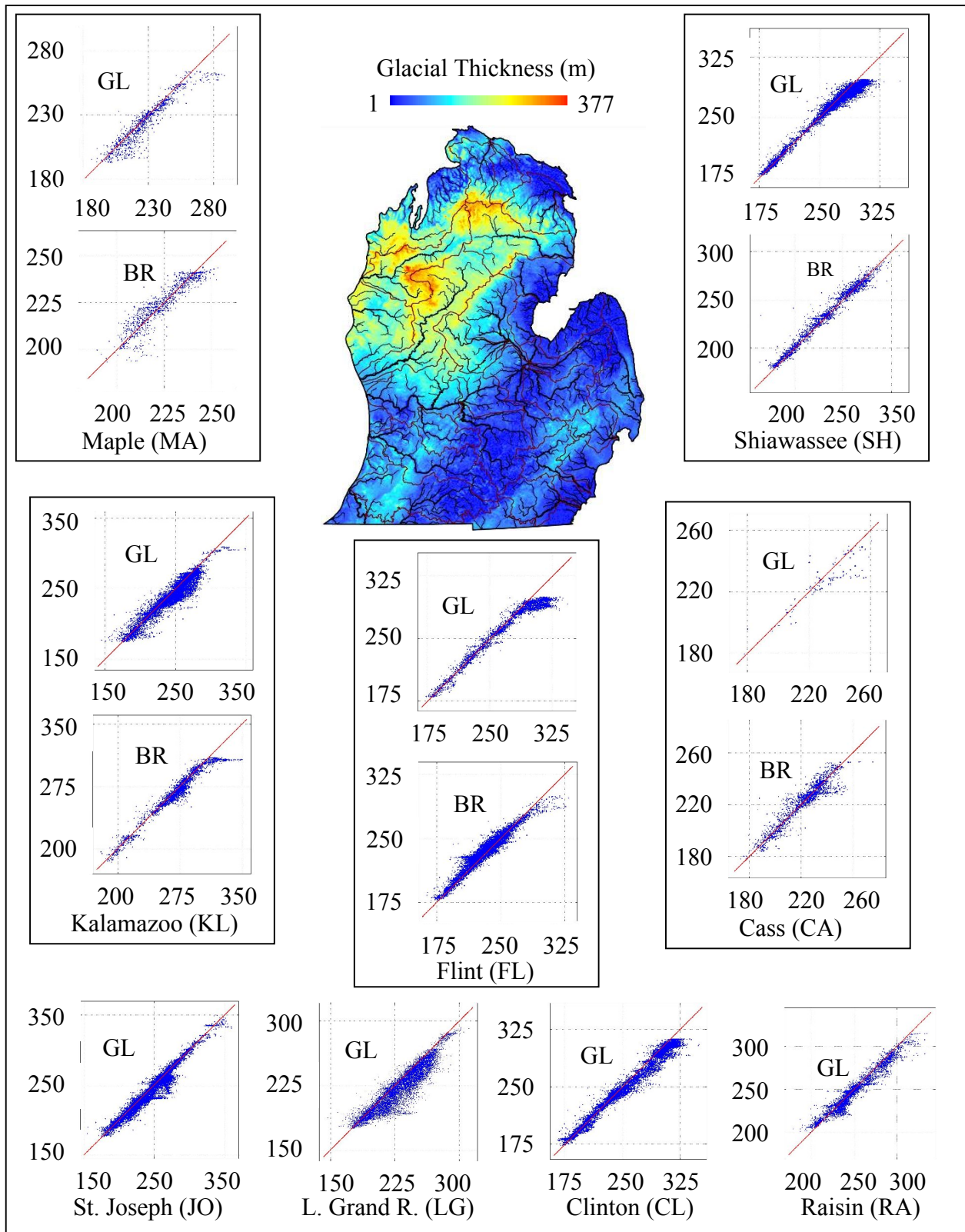


Figure 5: Simulated (y axis) and measured (x axis) water levels in the watersheds across the transition zones between regional-scale recharge and discharge zones. GL: Glacial aquifer, BR: Bedrock aquifer. Scale of the color map is non-linear.

Table 4: Summary of the significant messages illustrated in Figure 5.

Transition zones:

- Glacial thickness gradually decreases from uplands towards discharge zones along lowlands (regional-scale drainage along the central peninsula), and the Great Lakes shores
- At low elevations, major streams function as strong boundary conditions and control glacial flow (e.g. CL, FL, KL, LG, SH)
- Through vertical hydraulic connection, major streams also control bedrock flow at lower elevations and in regions where bedrock is very close to land surface (e.g. CA, FL, KL, SH)
- Even in watersheds where glacial aquifer is intercalated with confining layers at low elevations, major streams control bedrock flow (e.g. FL, CA, SH)
- Underneath recharge mounds close to regional-scale discharge zones, simulated glacial heads are averaged over moderate glacial thickness (e.g. CL, KL, LG, MA, RA)
- At high elevations, simulated heads under predict due to boundary conditions (e.g. CA (GL and BR), FL (GL and BR), JO (GL), KL (GL and BR), LG (GL), MA (GL and BR), SH (GL))

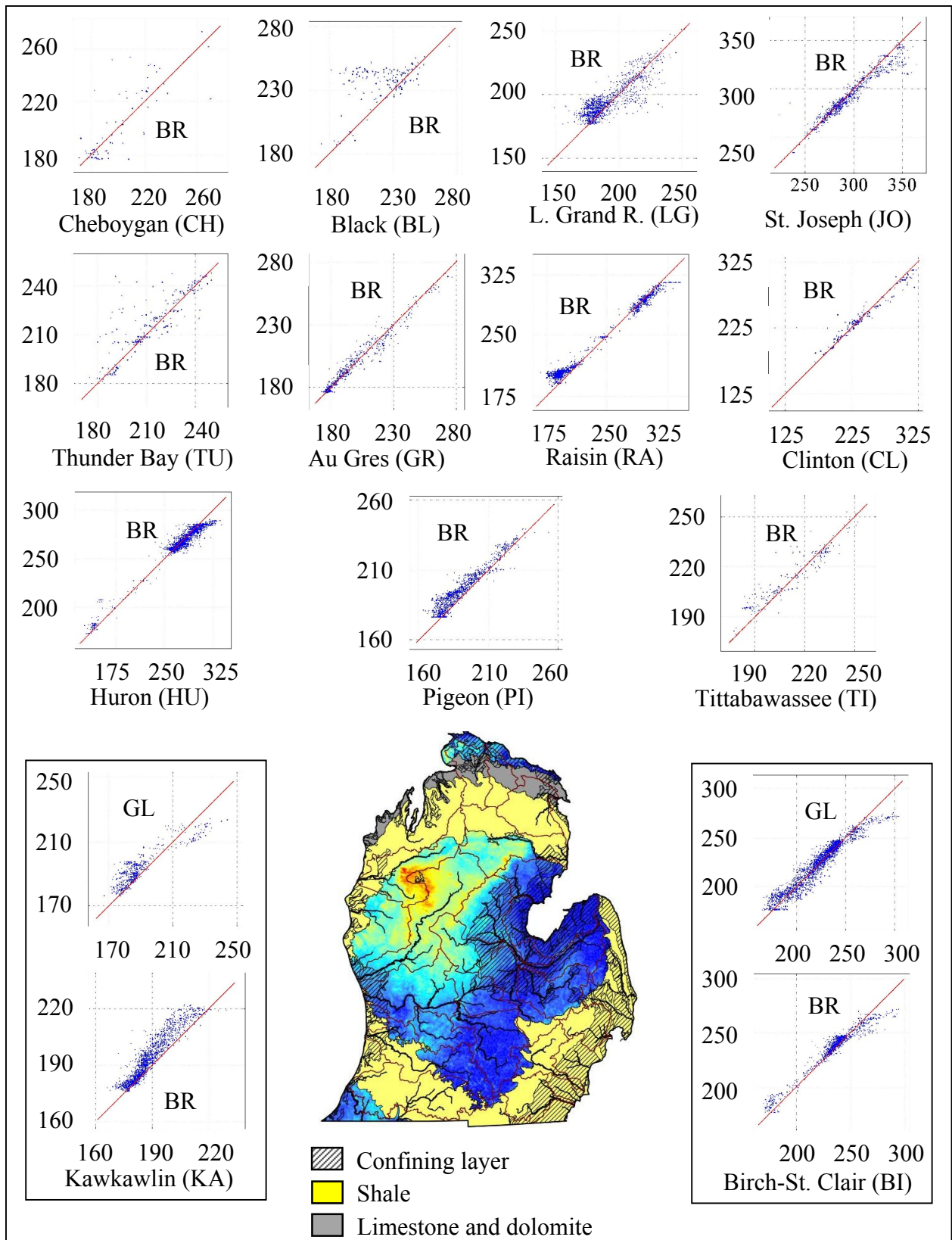


Figure 6: Simulated (y axis) and measured (x axis) water levels in the watersheds with shale formations, karst formations, and confining layers. GL: Glacial aquifer, BR: Bedrock aquifer.

Table 5: Summary of the significant messages illustrated in Figure 6.

<p><i>Shale formations:</i></p> <ul style="list-style-type: none"> - Glacial thickness above shale units gradually decreases from southern uplands towards the Great Lakes shorelines - Hydraulic connection between glacial and bedrock aquifer is maintained through vertical flow - Major streams in glacial aquifers connect with bedrock aquifers through cracks in shale formations and control bedrock flow (e.g. CL, HU, JO, RA)
<p><i>Confining layers along the shores:</i></p> <ul style="list-style-type: none"> - Glacial thickness significantly decreases in the watersheds close to the Great Lakes - At high elevations, ground water in bedrock aquifers regionally discharges into the Great Lakes through deep bedrock flow system underneath the confining layers along the shores - Artesian wells exist in the watersheds next to the Great Lakes (e.g. GR, KA) - Systematic over prediction in glacial aquifers above the confining layers is partially related to pumping near the shores since wells are not simulated (e.g. KA, LG) - Systematic over prediction in bedrock aquifers underneath the confining layers may potentially be related to the under estimation of transmissivity values due to low data resolution (e.g. BI, GR, KA, PI, RA, TI)
<p><i>Karstic formations:</i> Significant bias in the simulated heads, Darcy's Law doesn't apply to the karstic bedrock aquifers along the northern tip of the peninsula (e.g. CH, BL, TU)</p>

Statistical analysis. The goodness-of-fit of the simulated water levels (Figure 4, Figure 5, and Figure 6) to the measured data is evaluated with the model statistics. These statistics are used to demonstrate the overall performance of each model through evaluating the average error in the models (Anderson and Woessner, 2002). Following statistics are used for the evaluation:

1) The arithmetic mean error (AME). Even though the positive and negative residuals (i.e. difference between the simulated and measured ground water levels) may cancel each other out, the AME allows quantifying the average model bias through a simple calculation (Anderson and Woessner, 1991; El-Kadi (Ed.), 1995).

$$AME = \frac{\sum_{i=1}^n (h_{mi} - h_{si})}{n} \quad (10)$$

where n is the total number of measurements in a watershed, h_{mi} is the measured ground water level, and h_{si} is the simulated ground water level.

2) The normalized standard deviation of the residuals (NSDR). Generally, if the range of the measured water-level data is large, there is a larger standard deviation in residual errors. In ground water investigations, a good fit to the data would be reflected if this ratio is approximately 0.1 or less indicating that the residuals are generally less than 10 percent of the range in altitude of the observations (Kuniansky *et al.* 2004; Hunt *et al.* 2003).

$$NSDR = \frac{\sqrt{\frac{\sum_{i=1}^n (r_i - \mu)^2}{n+1}}}{DR} \quad (11)$$

where r_i is the particular absolute residual, μ is the residual mean, and DR is the data range (Walton, 1992).

3) The coefficient of determination (R^2). R^2 indicates the strength of the fit between the simulated and measured ground water levels through the dispersion in the comparison. R^2 can be expressed as:

$$R^2 = \frac{\sum_{i=1}^n (h_{mi} - \overline{h_m})(h_{si} - \overline{h_s})}{\sqrt{\sum_{i=1}^n (h_{mi} - \overline{h_m})^2} \sqrt{\sum_{i=1}^n (h_{si} - \overline{h_s})^2}} \quad (12)$$

where $\overline{h_m}$ is the average of the measured ground water levels, and $\overline{h_s}$ is the average of the simulated ground water levels. The range of R^2 changes between 0 and 1 where a value of 0 indicates no correlation and, ideally, a value of 1 means that the dispersion of the prediction is equal to that of the observation (Krause *et al.* 2005).

A summary of the model statistics is provided in Table 2. The AME, and NSDR are generally within 10% of the total head difference (DR) within the watersheds, and R^2 values indicate that for most watersheds more than 85% of the total variation in the graphical comparisons (Figure 4, Figure 5, and Figure 6) can be explained with the linear relation between the simulated and measured water levels.

Table 6: Summary of the model statistics for the glacial aquifer simulations.

Watershed Name	Glacial Aquifer				Bedrock Aquifer			
	DR (m)	AME (m)	NSDR (%)	R ²	DR (m)	AME (m)	NSDR (%)	R ²
Au Gres – Rifle	232	5.7	4.8	0.89	105	-0.1	4.4	0.96
Au Sable	268	6.1	4.4	0.96	-	-	-	-
Birch – St. Clair	139	-0.7	5.0	0.92	125	-1.5	4.8	0.94
Black	228	6.9	7.4	0.91	100	-13.2	17.4	0.26
Cass	83	3.9	9.5	0.78	102	-0.1	5.7	0.87
Cheboygan	253	16.6	8.5	0.96	105	-1.9	14.8	0.67
Clinton	185	3.9	3.8	0.98	212	-0.9	6.2	0.88
Flint	170	7.1	6.0	0.95	166	-2.4	3.7	0.93
Huron	139	3.8	4.4	0.83	140	1.2	3.6	0.95
Kalamazoo	205	3.4	3.9	0.90	171	3.3	4.1	0.95
Kawkawlin	77	-3.8	8.5	0.80	63	-4.7	6.8	0.80
L. Grand River	164	8.2	6.0	0.86	102	-3.2	8.6	0.73
Manistee	294	20.4	6.5	0.91	-	-	-	-
Maple	102	3.3	6.0	0.89	64	-0.2	7.9	0.84
Muskegon	284	11.5	4.4	0.96	-	-	-	-
Pere – Marquette	230	12.0	5.4	0.89	-	-	-	-
Pigeon	-	-	-	-	90	-5.2	5.2	0.91
Pine	168	5.3	4.3	0.97	-	-	-	-
Raisin	156	2.4	4.1	0.94	172	-5.7	5.0	0.99
Shiawassee	174	3.2	3.7	0.97	144	-1.5	3.4	0.97
St. Joseph	205	2.7	3.1	0.95	141	2.7	5.1	0.93
Thornapple	140	8.0	5.8	0.86	107	2.1	5.2	0.90
Thunder Bay	206	12.7	8.3	0.82	75	-3.1	13.4	0.71
Tittabawassee	217	17.6	10.1	0.89	74	-1.9	8.7	0.89
U. Grand River	139	2.8	4.0	0.91	133	-0.1	4.4	0.89

Conceptual messages. When combined with the model statistics listed in Table 6, evaluation of the comparisons shown in Figure 4, Figure 5, and Figure 6 provides the following conceptual messages regarding the ground water systems in the Lower Peninsula of Michigan:

- The conceptual model assumes that the watershed boundaries are no-flow ground water boundaries. In other words, the hydraulic connection between the glacial and bedrock aquifer is only maintained through the vertical flow between two aquifer layers. Based on this assumption and the evaluation of the simulated heads, it is concluded that contrary to common belief, in the southern Lower Peninsula, bedrock aquifers are well-connected with the surface water network, especially where the glacial thickness is relatively small and even in areas where the aquifer lithology is intercalated with confining geologic formations. Specifically, highly permeable beds of the major (i.e. 4th to 6th order) streams embedded in the glacial aquifer maintain a strong hydraulic connection with bedrock aquifer, and control the ground water flow in the aquifer (Figure 5). This hydraulic connection can be observed from Figure 7b where the simulated water levels have a very good fit to data, and bend around and follow the streamlines (Figure 7a).

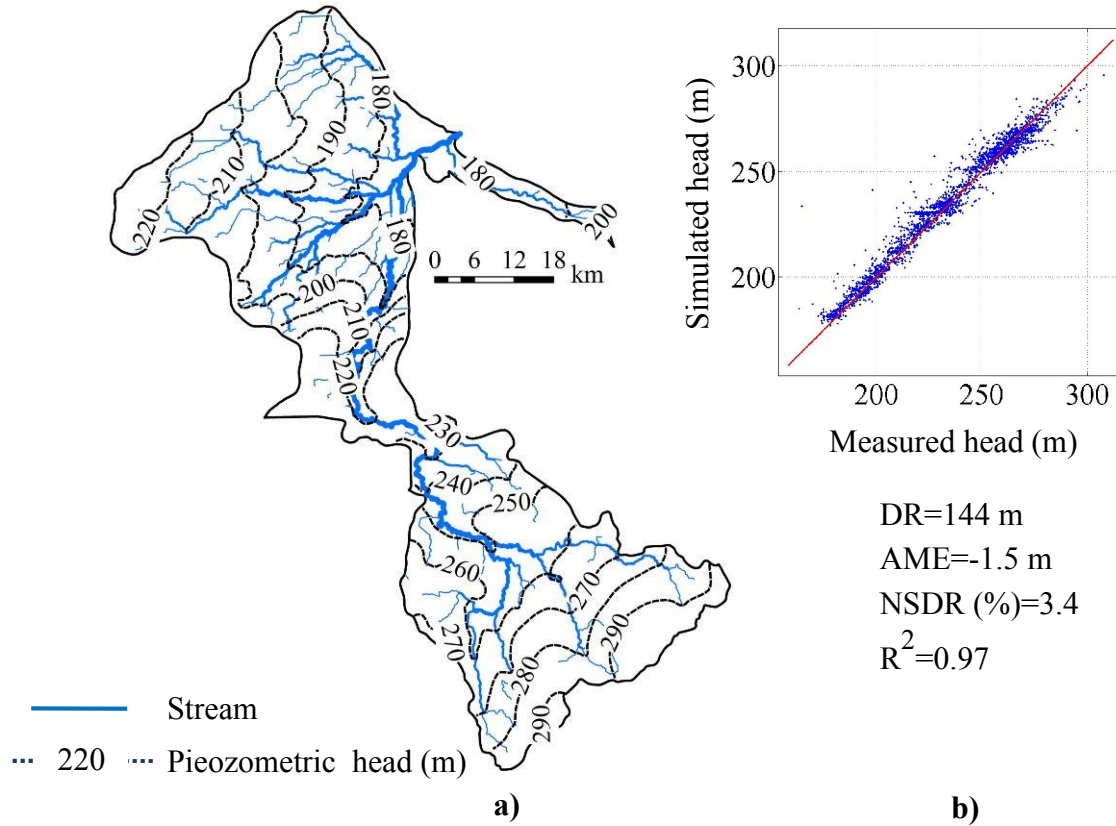


Figure 7: a) Distribution of the simulated piezometric heads, Shiawassee Watershed, and b) Simulated and measured piezometric heads.

In some watersheds across the southern Lower Peninsula, ground water is located in the low-yielding shale formations. Water wells are drilled in the cracks of these formations where the glacial thickness is relatively smaller and the bedrock aquifer is closer to the land surface. Based on the evaluation of the simulations, it is concluded that the strong hydraulic connection between the surface water network and shale formations also exists through the vertical flow between two aquifer layers (Figure 8).

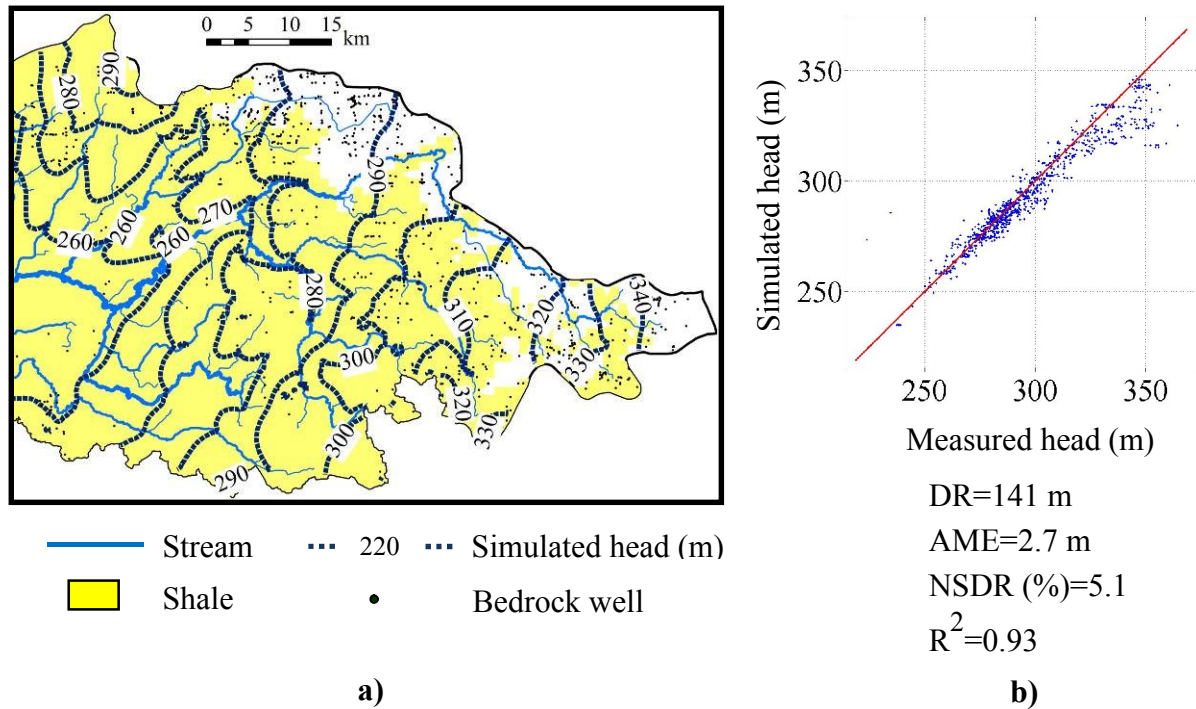


Figure 8: a) Simulated piezometric heads in the shale formations, St. Joseph Watershed, and b) Simulated and measured piezometric heads.

- No-flow (i.e. Neumann) ground water boundary conditions can be used on the watershed boundaries to model the ground water flow in both aquifer layers, except for several watersheds that are located on the edge of Michigan's two major uplands in northern and southern Lower Peninsula (Figure 4). These two uplands represent the regional-scale recharge areas and there is a significant amount of flow across watershed boundaries from topographic highs to the discharge zones located at lower elevations. To reduce the model deviations that occur due to the watershed boundaries, a careful examination is needed. Specifically, numerical model boundaries need to be expanded to the extent for which the real no-flow ground water basin boundaries are maintained (Figure 9).

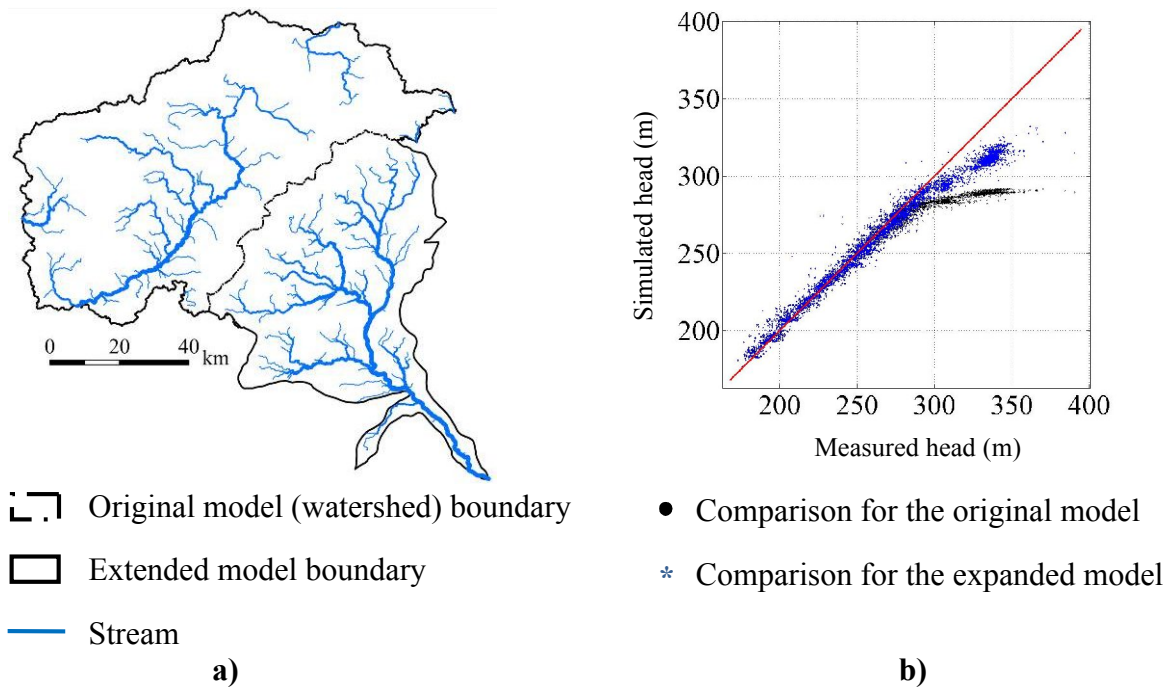


Figure 9: a) Model boundaries before and after the boundary expansion, and b) Comparison between the simulated and measured water levels before and after the boundary expansion.

- In general, simulating glacial aquifer flow with one computational layer causes variable magnitudes of model under predictions. Specifically, ground water flow in the watersheds located on the uplands must be modeled with caution because of the presence of the significant vertical flow. In these watersheds, simulated water levels represent the average values over a large aquifer depth and are not comparable to the measured water levels in the water wells (Figure 10). To capture more details vertically, the computational layer needs to be divided into multiple hydrostratigraphic layers. Similarly, since the depth of the wells in this region range between 30-45 m, hydraulic conductivity data used in the models only represent a small portion of the glacial deposits. As a result, any non-aquifer materials that may exist at deeper locations are not

included in the conductivity estimation which may potentially cause model under predictions in the region.

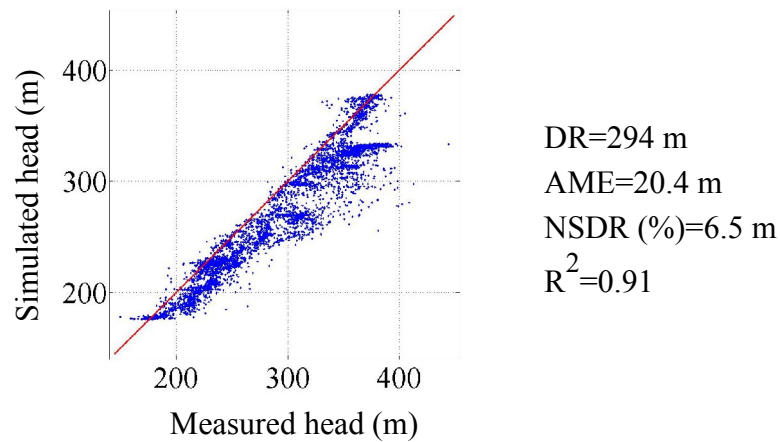


Figure 10: Simulated and measured water levels in the Manistee Watershed, glacial aquifer.

- The models can be used to identify the watersheds for which the modeling system is insufficient to simulate the ground water flow. For example, along the northern tip of the Lower Peninsula, the bedrock aquifers in the lowlands of the watersheds are composed of karstic limestone and dolomite geologic formations (Rheaume, 1991). Through a real-time analysis, it was found out that the two-layer conceptual models that adopt Darcy's Law for flow simulation do not apply to these watersheds. Because of this, there is a significant bias between the simulated and measured water levels (Figure 11).

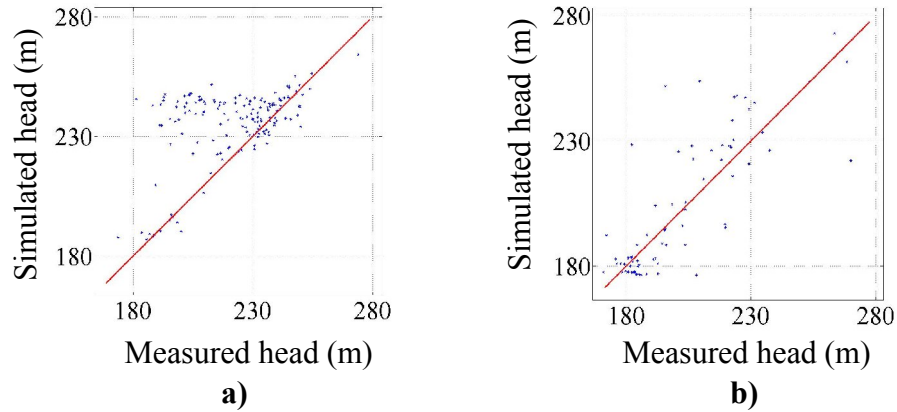


Figure 11: Simulated and measured water levels in the bedrock aquifer along the northern tip of the Lower Peninsula: a) Black Watershed, and b) Cheboygan Watershed.

- In some watersheds (i.e. Au Sable, Manistee, Muskegon, Pere-Marquette, Pine) located in the northern Lower Peninsula, because of the high glacial thickness, bedrock aquifer is rarely used for ground water supply (Rheaume, 1991). Since the number of data is very few in these watersheds, the performance of the modeling system in the deep bedrock aquifer is not validated.
- Relatively speaking, in the Lower Peninsula, glacial aquifers have more spatial heterogeneity than the bedrock aquifers. Because of this, data definitions of the parameters that have an impact on flow variations are smoother in the bedrock aquifers than that of the glacial aquifers in a way that helps the models predict the ground water levels better in the bedrock aquifers. Head comparisons and model statistics also indicate that defining effective transmissivity fields for bedrock aquifers through a collection of different geologic sub-crops is sufficient for modeling regional-scale bedrock flow in most watersheds.
- Data in MSGWD can be relatively crude and involve different sources of uncertainties such as driller variability, inaccuracies in well locations, and processing and recording

errors. Therefore before evaluating the simulations, certain queries (e.g. excluding the water-wells for which the measured water levels are lower than the well's bottom elevation, excluding negative static water levels) are applied to eliminate particular data errors. On the other hand, it is not possible to detect all “bad data” in the database, and these data adversely affect the goodness-of-fit of the models.

Base flow comparison. The purpose of the base flow comparison is to show that the models presented in this paper can reproduce the USGS-estimated base flow values within each watershed, after testing model parameters for a selected set of watersheds.

In the models, the source of water that enters the glacial aquifer layer is ground water recharge from precipitation. This recharge is eventually discharged from the glacial aquifer as base flow into streams. To define the connection between ground water and the streams, and to match the USGS-estimated base flow values, different sets of leakance values were tested in selected watersheds. In nature, stream width and streambed conductivity vary frequently along the course of a stream so that it becomes practically very difficult to measure these parameters. Because of this, the leakance values were introduced through a lumped parameter, $L'w$, where L' represents the streambed leakance, and w represents the stream width. Different sets of values were tested for the $L'w$ parameter based on the goodness of the comparison between the model-simulated and USGS-estimated base flow values. Once an optimum set of values was determined, those values were applied to all watershed models. In other words, the leakance parameter was not thoroughly calibrated for each watershed but adjusted to provide an acceptable prediction of the USGS base flow estimates in the watersheds. The resulting set of $L'w$ varies depending on the stream orders (Table 7).

Table 7: Adjusted $L'w$ values.

Stream order	$L'w$ (m/d)
1	3
2	5
3	10
4	20
5	50
6	100

To check the accuracy of the base flow calculations for all watersheds, the model-simulated base flow values are compared to the USGS-estimated values (Figure 12). The coefficient of determination (R^2) for this comparison is found to be 0.98. This value indicates that the same set of $L'w$ values can be applied to all watershed models.

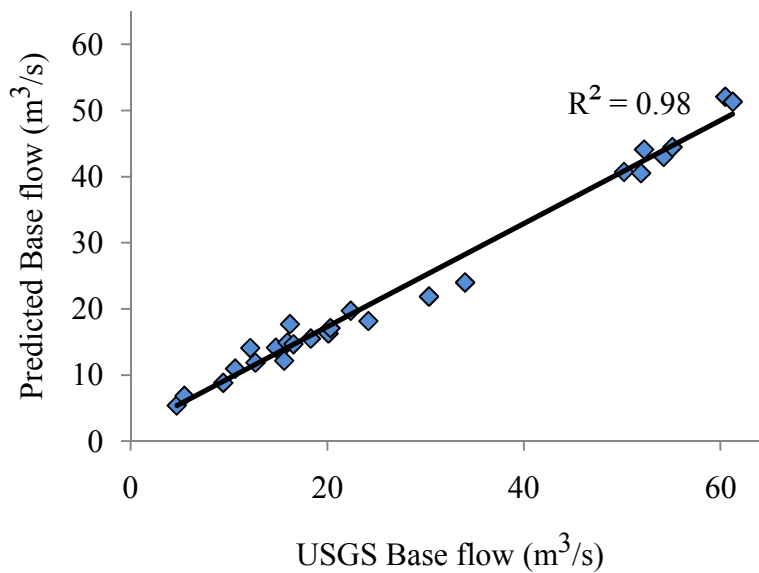


Figure 12: Correlation between the simulated and USGS-estimated base flow values.

Additionally, it was found out that modeling the small (i.e. 1st and 2nd order) streams as two-way head-dependent flux features lead to gross water budget errors (Figure 13). Instead, conceptualizing all streams in the watersheds as effluent streams is a justifiable assumption since it provides accurate base flow and seepage discharge calculations.

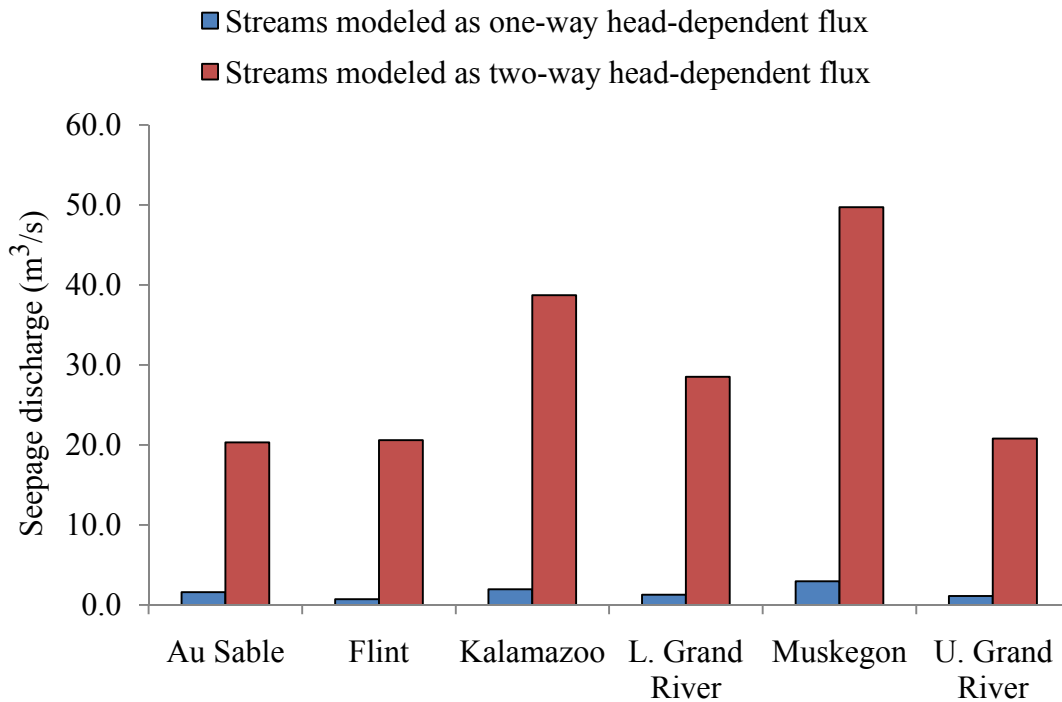


Figure 13: Comparison between the seepage discharge values when streams are modeled as one-way and two-way head dependent flux model features.

CONCLUSIONS

Li *et al.* at MSU recently designed a modeling system that maximally benefits from the data-rich structure of MSGWD and that maintains the coupling between the data and ground water models. In this paper, we systematically test the capability of this system to simulate the regional-scale ground water flow in most watersheds across Michigan's Lower Peninsula.

Overall, our investigation shows that the modeling system represents the regional-scale aquifer dynamics and significantly enhances our ability to understand the critical hydrogeologic aspects of the ground water systems in the peninsula. Model statistics show that the AME and NSDR are generally less than 10 percent. The values of R^2 are usually above 85 percent. For the watersheds where the model performances are relatively low, the comparisons between the simulated and measured ground water levels gave us the opportunity to visually and interactively examine the accuracy of the assumptions used in the conceptual model.

Specifically, the comprehensive modeling and evaluation effort presented in this research provides the following messages:

- The relatively simple two-layer models are able to capture the dominant variations in regional-scale ground water flow, including the interaction between the upper glacial and lower bedrock aquifers.
- Contrary to common belief, the bedrock aquifers are well connected with the surface water network, even in the watersheds where confining layers exist, and generally the high (i.e. 4th to 6th) order streams that are linked to the glacial aquifer control the bedrock flow.
- No-flow boundary conditions can be imposed on the watershed boundaries to simulate ground water flow in the glacial and bedrock aquifers, except for the watersheds around the northern and southern uplands (or the regional-scale recharge zones) of the Lower Peninsula, due to the substantial amount of ground water flow from high to low elevations.

- Simulated heads in the glacial aquifers on the uplands represent the average heads over large aquifer depths, and are not comparable to the measured static water levels in the region, because of the significant amount of vertical flow.
- Performance of the modeling system in the deep bedrock aquifer underneath the uplands is not validated because of lack of measured data.
- Modeling the small streams as two-way head-dependent flux features lead to gross water budget errors, and these streams should be represented as effluent streams.
- Darcy's Law cannot be applied to simulate the ground water flow in the bedrock aquifers along the northern tip of the peninsula, because of the karstic nature of the bedrock in this region.

The GIS-enabled ground water models presented in this research significantly reduced the time and financial costs needed to collect field data, and shifted the focus to conceptual modeling and critical thinking. This provides a very useful tool that can be utilized for cost-effective ground water management in Michigan. In the future, results of this research can be used to calibrate the simulations to the static water levels from the well records and the stream flow data from the USGS gauging stations for site-specific ground water problems.

APPENDICES

Appendix A: Michigan's Statewide Groundwater Database

Michigan's statewide groundwater database (MSGWD) consists of four main data categories:

- Geological/hydrological framework which provides the spatial distributions of the aquifer parameters
- Physical framework which helps to define the geometry of the aquifers
- Groundwater systems' stress factors which are imposed to the models through the source and sink terms
- Calibration parameters which are used for the model validation

MSGWD uses the Michigan Georeference projected coordinate system and the GCS North American geographic coordinate system. Unit systems used in the database are the US Customary System and the International System of Units.

Data categories are available in two different geographical model formats:

- Raster data models which appear in finite difference models and represent two-dimensional spatial variations by assigning a single value to each cell in a fixed rectangular array. For example, a layer might represent the spatial variation of depth to groundwater in a layer constructed by conducting interpolation between data located at different measurement locations (Goodchild, 1996).
- Vector data models which represent spatial variation through irregularly distributed points, lines, and polygons. The meaning of layer for vector systems is more complex

than that of raster data models. While mainly a vector layer provides a parameter (e.g. hydraulic conductivity, SWL, stream elevation) to a groundwater model; it can also facilitate display (e.g. county boundary, road) by grouping one or more classes of points, polylines, or polygons (Goodchild, 1996).

Current trend in water resources management in the United States is to develop a hydrological data network (Consortium of Universities for the Advancement of Hydrologic Science, CUAHSI) that could be accessed by anyone through web services using a stand-alone computer. MSGWD is readily available to be connected to this system since the state's groundwater data can be downloaded and mapped through the state's online geographic information system (<http://www.michigan.gov/cgi>) and the GWIM's webpage (<http://gwmap.rsgis.msu.edu/>) which is the result of a collaborative effort between the MDEQ, the USGS, and Michigan State University. Most important advantages of these online services are that all data provided through the services have consistent data structures and that these data can be directly visualized and processed through GIS tools. Data that were produced for the GWIM are briefly discussed in the following sections.

Hydrogeological Setting of Michigan

The regional aquifer system of Michigan's Lower Peninsula consists of the unconsolidated glacial aquifer, and the two major bedrock aquifers (Saginaw and Marshall Aquifer) separated by confining layers. The Coldwater Shale forms the base of the regional aquifer system (Barton *et al.*, 1996; Westjohn and Weaver, 1998).

The glacial deposits cover nearly all of the Lower Peninsula. The glacial thickness map of the Lower Peninsula is shown in Figure 14. This map is generated by subtracting the raster-based bedrock surface map (with a resolution of 500 m) provided with the GWIM from the raster-based USGS 90 m SRTM land surface map.

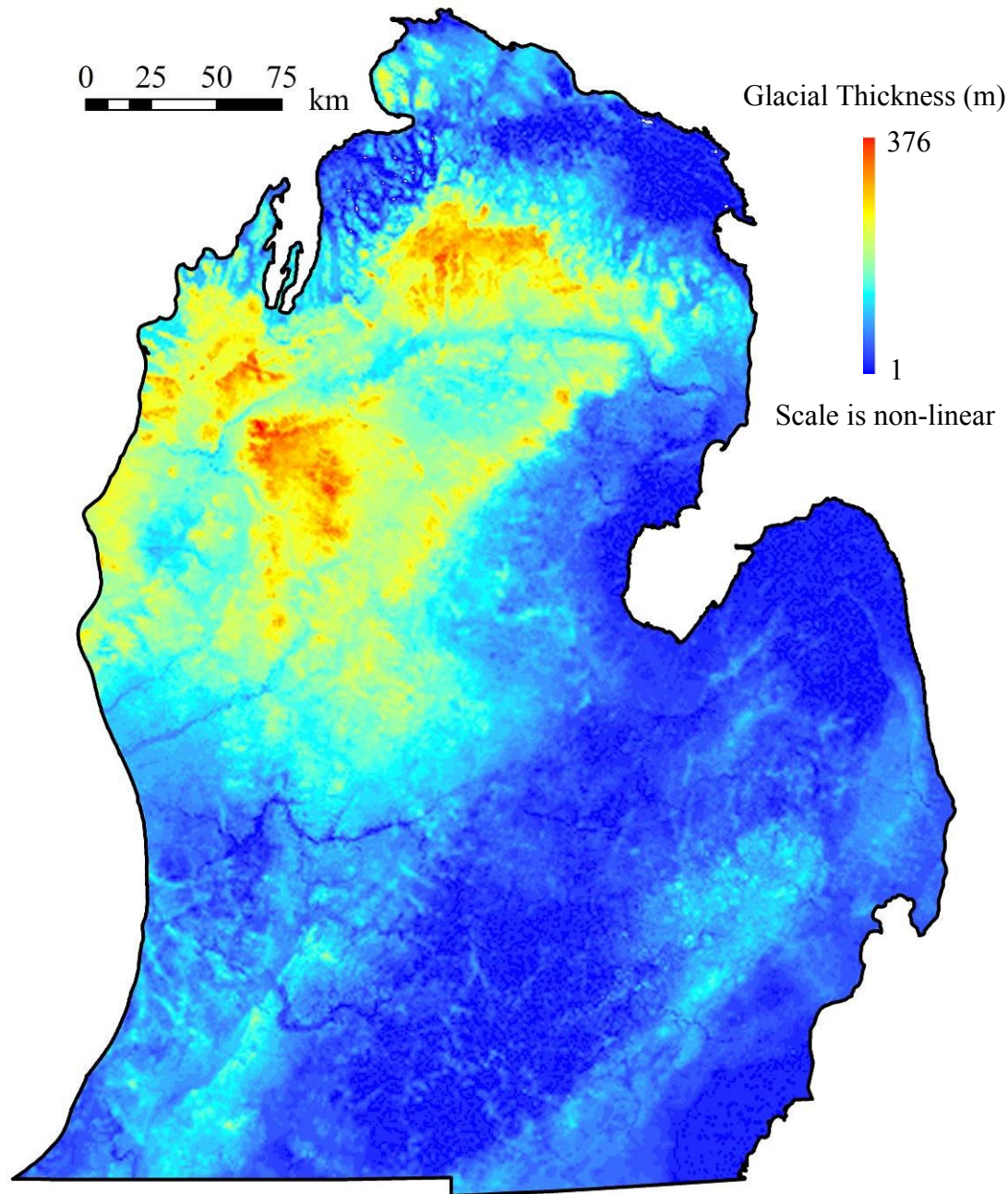


Figure 14: Glacial thickness map for Michigan's Lower Peninsula. Values are subject to change due to the resolution of the raster-based data.

The glacial deposits are the largest reservoir of fresh groundwater in the Lower Peninsula and primarily consist of thick sequences of sand and gravel, but in some areas also consist of sand and gravel layers within till or other fine-grained deposits (Barton *et al.*, 1996; Westjohn and Weaver, 1998).

The Saginaw Aquifer consists of sandstone lenses, and typically ranges in thickness from 100 to 350 ft in areas where this unit is used for water supply. In the western-central part of the aquifer system, the Saginaw Aquifer is separated from the glacial deposits by 100 to 150 ft of red beds. The red beds consist of mudstone and poorly consolidated red shale, gypsum, and minor amounts of sandstone. Together with fine-grained glacial and lacustrine deposits, the red beds form the sub-regional confining units that separate the glacial aquifer from the underlying Saginaw Aquifer (Barton *et al.*, 1996; Westjohn and Weaver, 1998).

The Marshall Aquifer, the basal aquifer in the basin, includes sandstones that overlie the Coldwater confining unit. The Marshall Aquifer consists of two or more permeable sandstones in the central part of the basin; but in and near areas where the aquifer is a sub-crop of the glacial deposits, it consists of one permeable sandstone unit. In areas where more than one sandstone unit exists, alternating carbonate, shale, siltstone, and evaporites separate permeable sandstones. The thickness of permeable sandstones is typically from 75 to 200 ft. The Marshall Aquifer is regionally confined except where it is a sub-crop of the glacial aquifer (Barton *et al.*, 1996).

The bedrock aquifers (Traverse Group) along the northern tip of the Lower Peninsula are covered with relatively thin glacial lacustrine deposits. Traverse Group consists of limestone and dolomite formations which are the primary source of most groundwater supplies in the area. The

transmissivities of these karstic aquifers depend on the interconnection of fractures and solution channels in the aquifers (Rheaume, 1991).

Bedrock layer is exposed in most parts of the Upper Peninsula. Here, major aquifers are the crystalline-rock aquifer and the Jacobsville Aquifer. The crystalline-rock aquifer is located in the western part of the peninsula. Groundwater generally moves through secondary openings, such as joints, fractures, or faults, in the crystalline rocks. The Jacobsville Aquifer is found running under large portions of the Upper Peninsula along the Lake Superior shore. It is composed of feldspathic and quartzitic sandstone and shale formations. Although the aquifer consists of sandstone, it is well cemented and has a low permeability. Groundwater moves through joints and fractures which decrease to insignificance at depths of 100 and 150 ft. The aquifer is considered a confined aquifer (Marsicek, 2002).

Approximate boundaries of the major bedrock aquifers beneath the surficial glacial aquifer are shown in Figure 15.

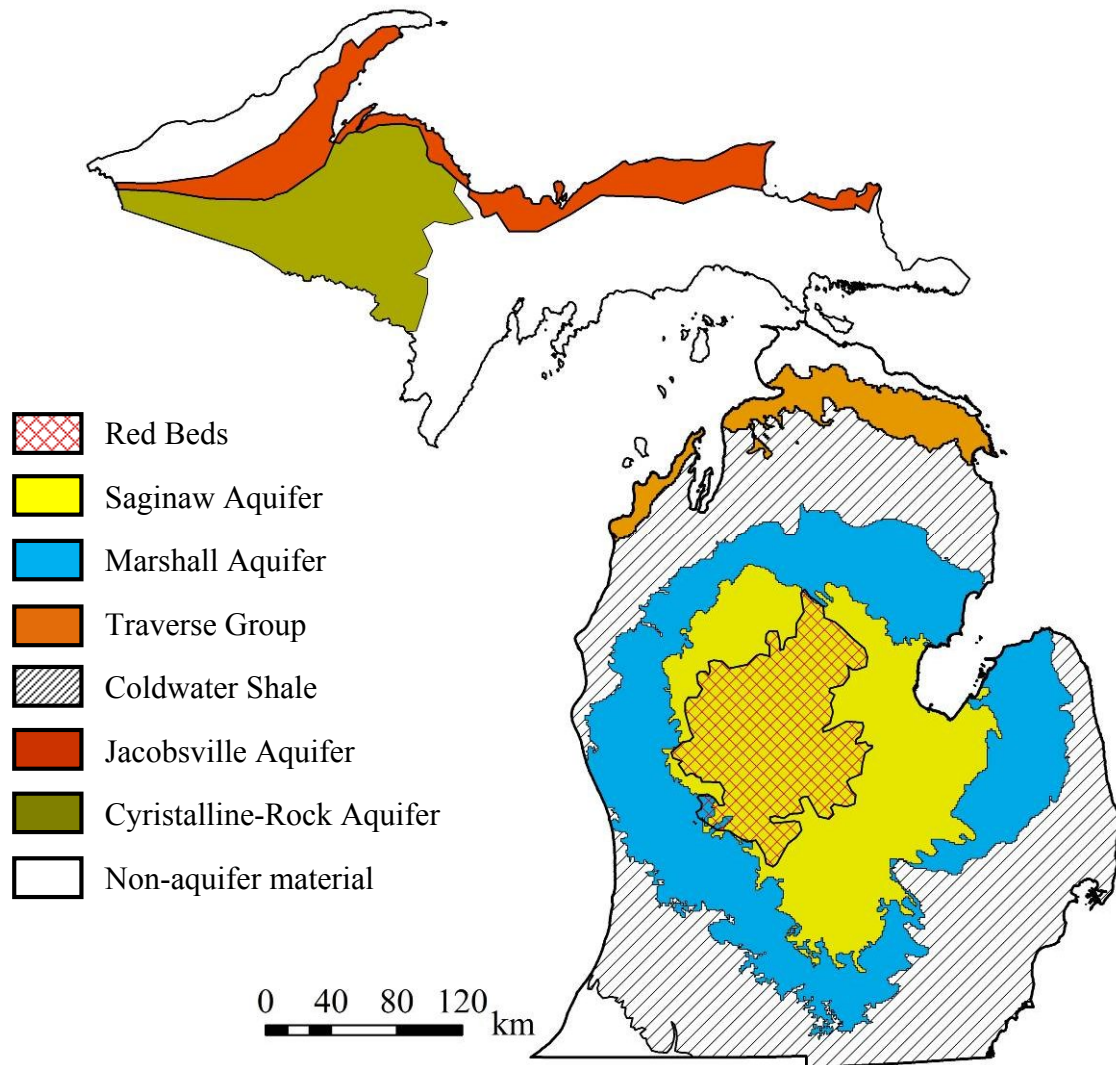


Figure 15: Major bedrock aquifers in Michigan.

Wellogic

The paper logs of the water wells that had been drilled in Michigan since 1960's were scanned and processed by the MDEQ to make almost 300,000 (totally in the glacial and the bedrock aquifers) data points (as of 2006) usable in Wellogic. MSU and the MDEQ systematically work together to update the database with the most recent well data. The data is stored in the shapefiles where the wells are recorded with a unique Well ID along with the

attributes that summarize the location of the wells and the spatial data to provide the information for the hydrogeological and the physical framework of Michigan's aquifers.

Number of the water wells in Wellogic increases by approximately an amount of 1,500 every month (GWIM, 2006). Even though data resolution is not uniform throughout the state, since the amount of the data in the database is steadily increasing, in the near future, in the areas where the data amount is poor, resolution will be much better than that of today. Change of the number of the statewide data with respect to time is illustrated in Figure 16 and Figure 17.

Wellogic comes with the following advantages:

- Data is available almost everywhere in the state, free, and open to public
- If made full use of it, massive data structure reduces both the monetary costs and the time required to conduct field investigations
- Data resolution is significantly higher than that of the traditionally collected data
- Even though it is not uniform and because of the uncertainties involved, it is not as good as of the traditionally collected data, data quality improves with time (Figure 18) shows the increase in the number of the data points from 1970 to 2006 and how this improvement translates into the map of the hydraulic conductivity field for the Kalamazoo County, MI.

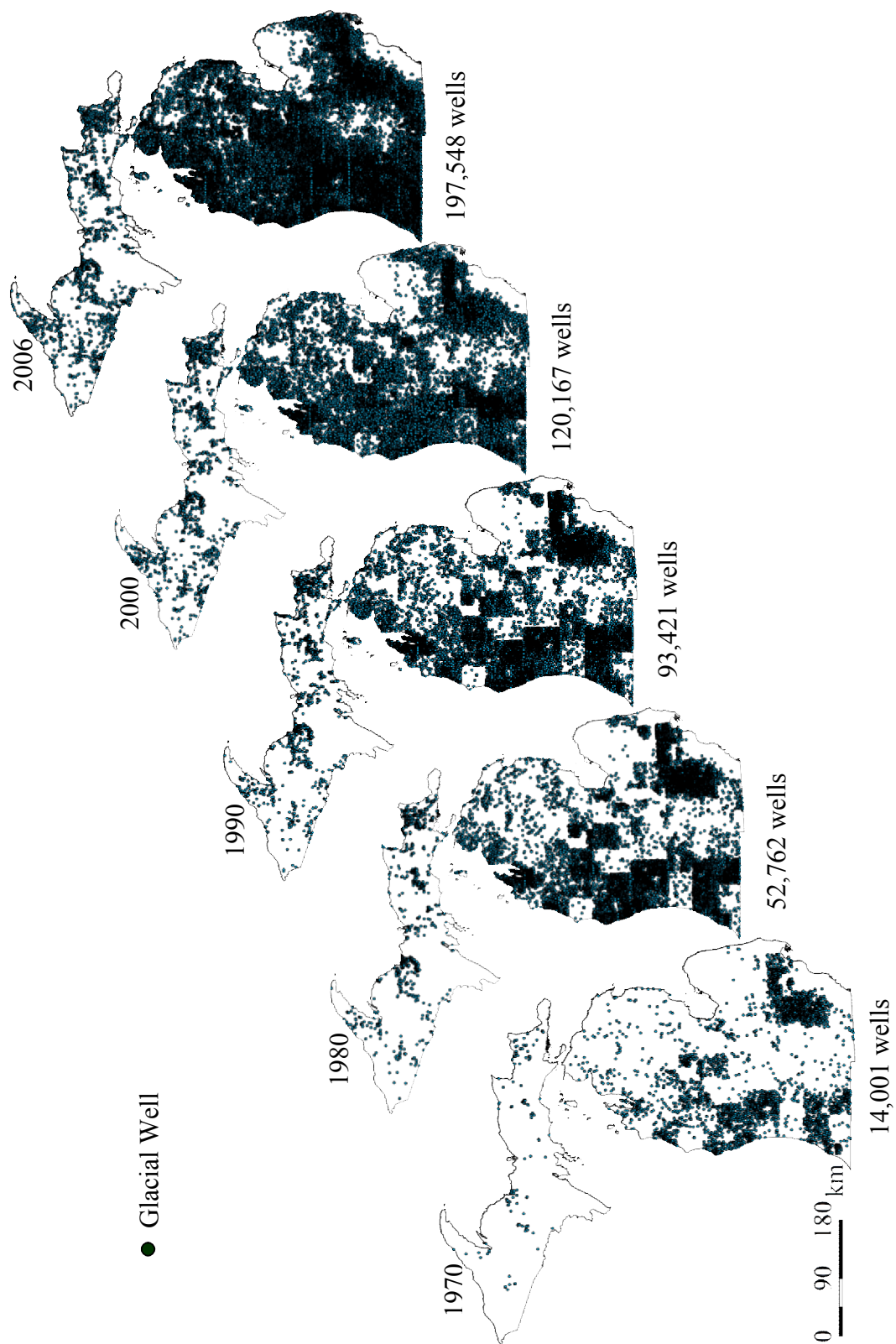


Figure 16: Time-based spatial distribution of the water wells in the glacial aquifers in Michigan.

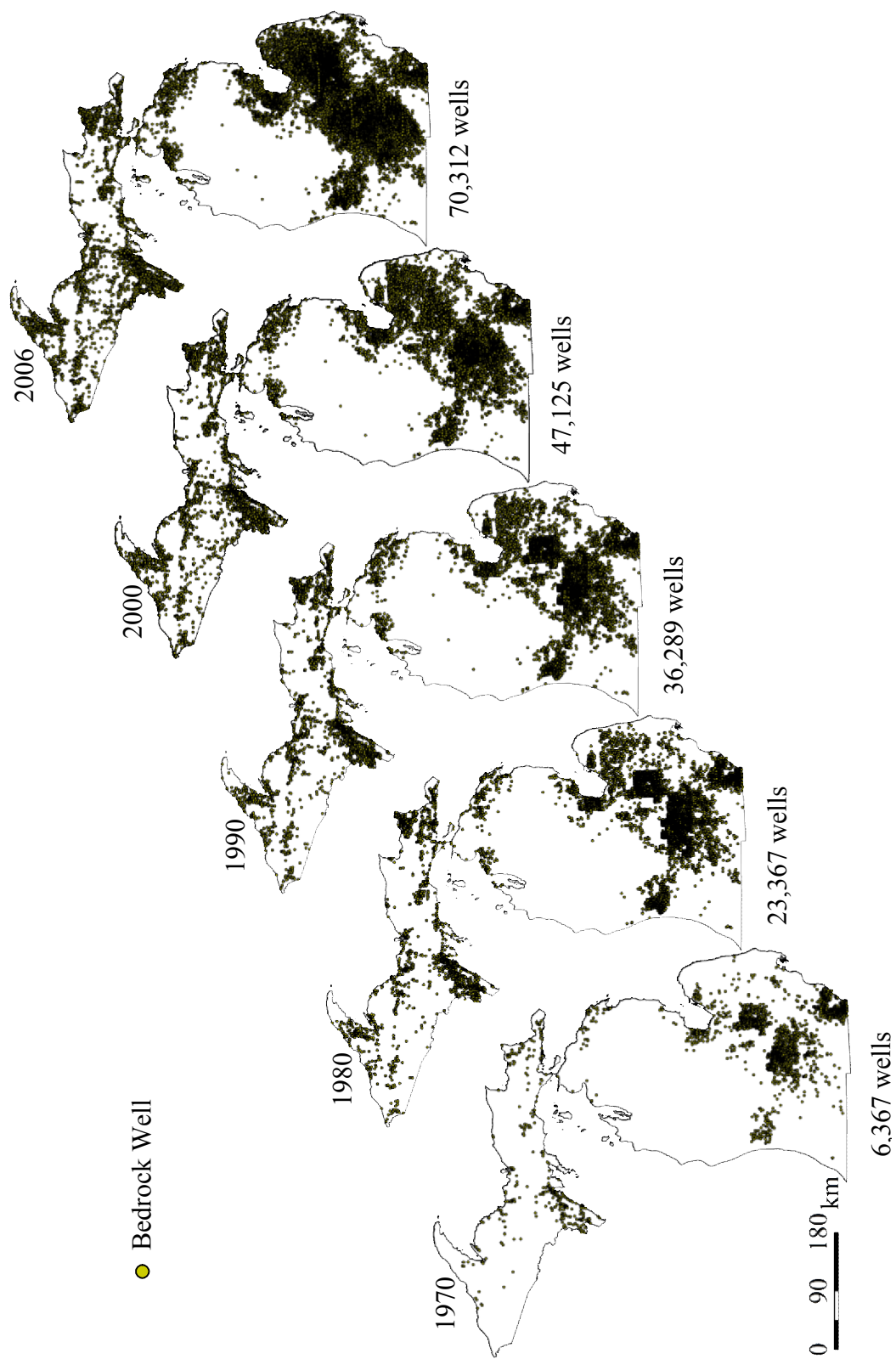


Figure 17: Time-based spatial distribution of the water wells in the bedrock aquifers in Michigan.

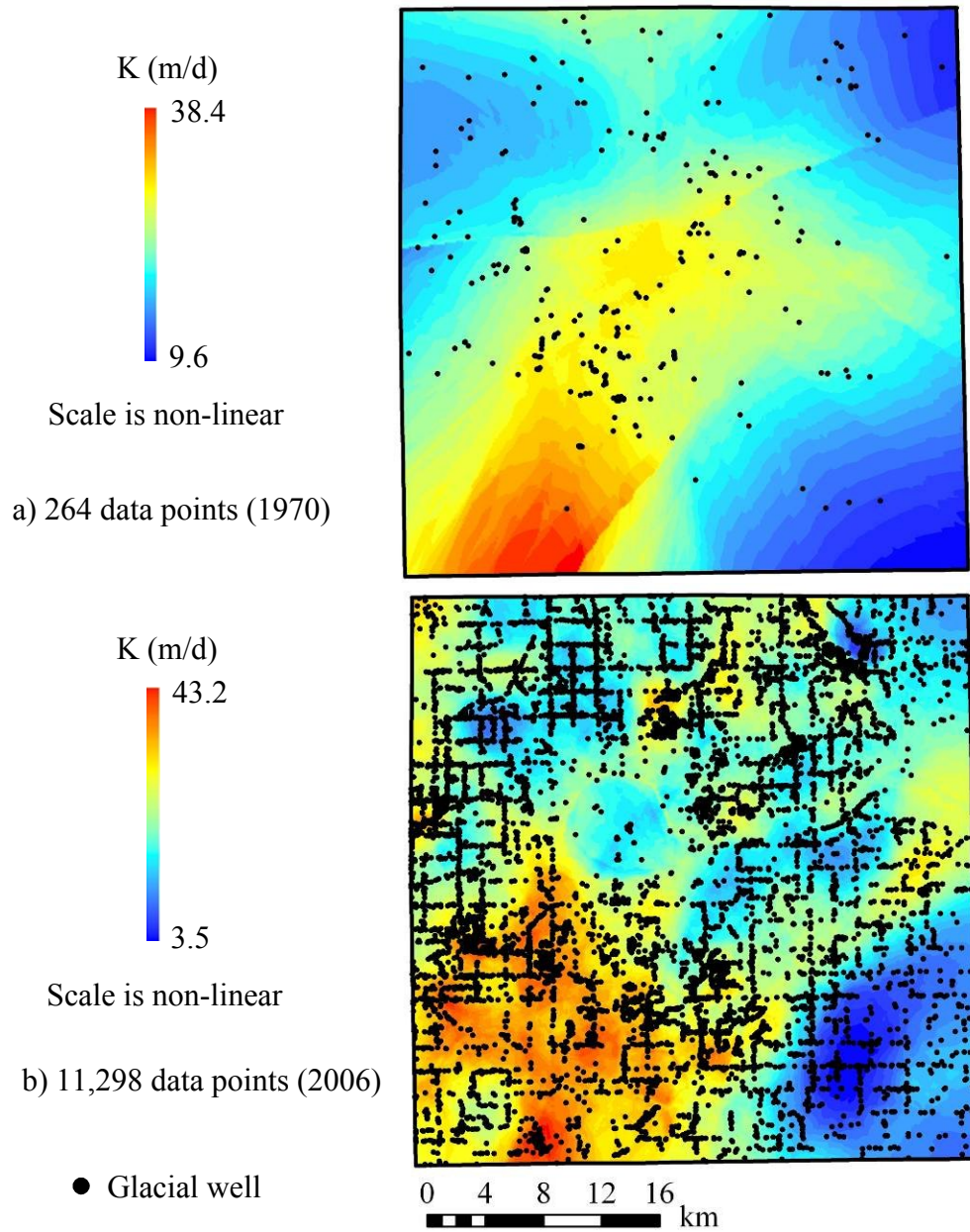


Figure 18: Time-based change in the representation of the hydraulic conductivity (K) field in the Kalamazoo County.

Physical Framework

Land surface elevation. All wells recorded in Wellogic have an attribute that provides the land surface elevation at the well's location. This attribute was generated from the raster-based 30 m (7.5 minute) *Digital Elevation Model (DEM)* provided in the *USGS National Elevation Dataset, NED*. For the GWIM, following steps were applied to extract the elevation data for each well by using ArcGIS 8.3 (GWIM, 2006).

- NED coverage of the state was downloaded in multiple geographical tiles from the USGS's related website
- The raster data in the tiles were converted into integer grids
- Tiles were merged into a statewide DEM map
- The statewide map was projected into Michigan's coordinate system and the map unit was converted into decimal meters
- The unit of the data was converted into ft and these new values were added to the database
- The statewide map was divided into the counties (totally 83) with an exterior buffer of 1 mile to the outside of the county boundaries
- The county-based NED data grid was used to sample the land surface elevation at the location of the water wells

More detailed information for the NED and a discussion of the method that is used to generate the raster-based DEM database for this research can be found in Appendix C (p. 89).

Surface elevation of the bedrock layers. Statewide oil and gas wells (i.e. deep wells) compiled by the MDEQ, and the water wells which intersect the bedrock layers where the glacial thickness is small (the Upper Peninsula or the southern Lower Peninsula), were used to map the surface of the bedrock aquifer (GWIM, 2006). Total number of the wells that were used for mapping was approximately 53,000 (Figure 19).

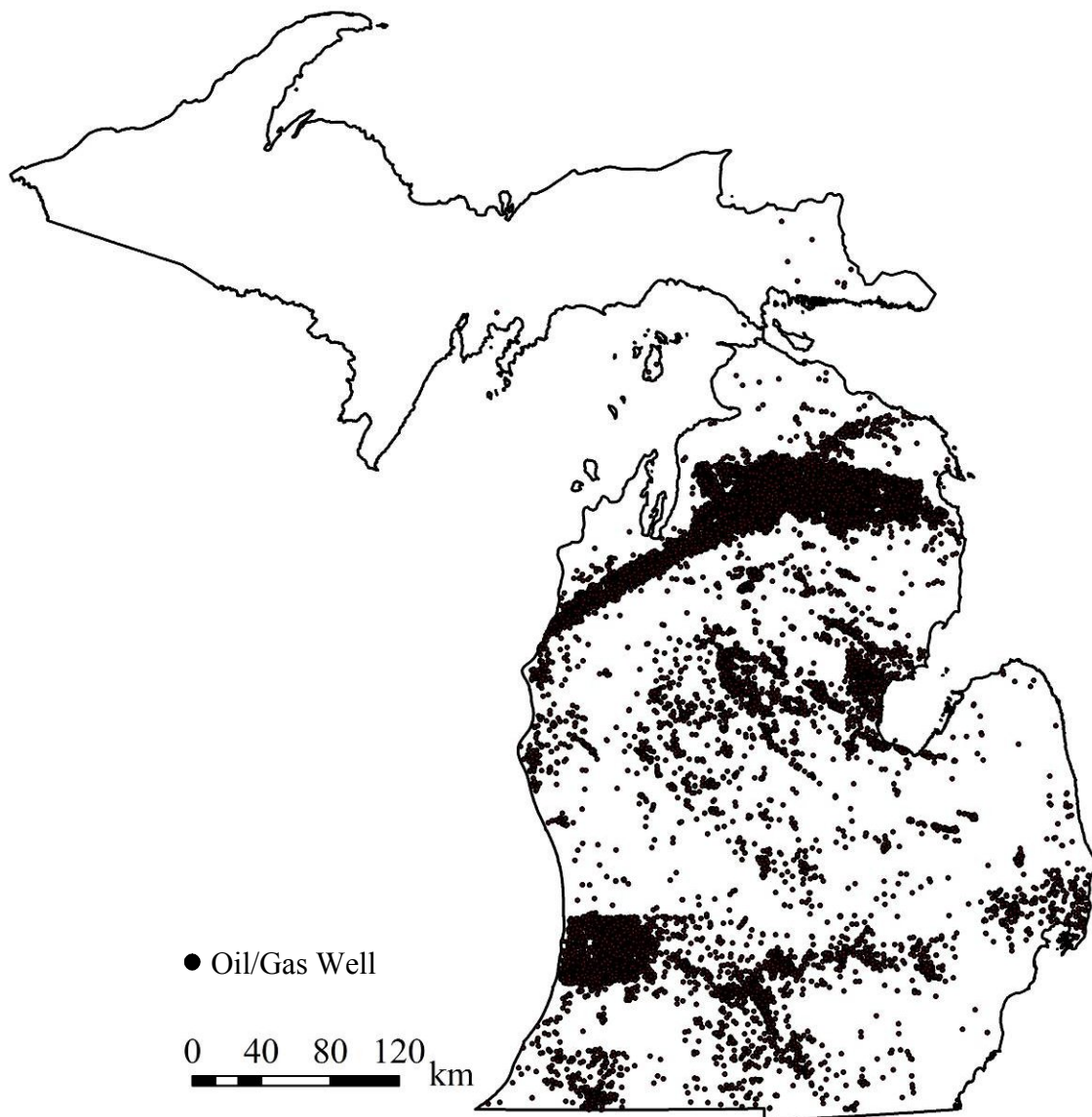


Figure 19: Distribution of the oil and gas wells in Michigan.

In the point-based well shapefile, the maximum recorded value of the surface elevation of the bedrock layer is 1,430 ft where the minimum is -982 ft. A raster map with a 500 m of resolution was generated by interpolating the information provided in the database (Figure 20).

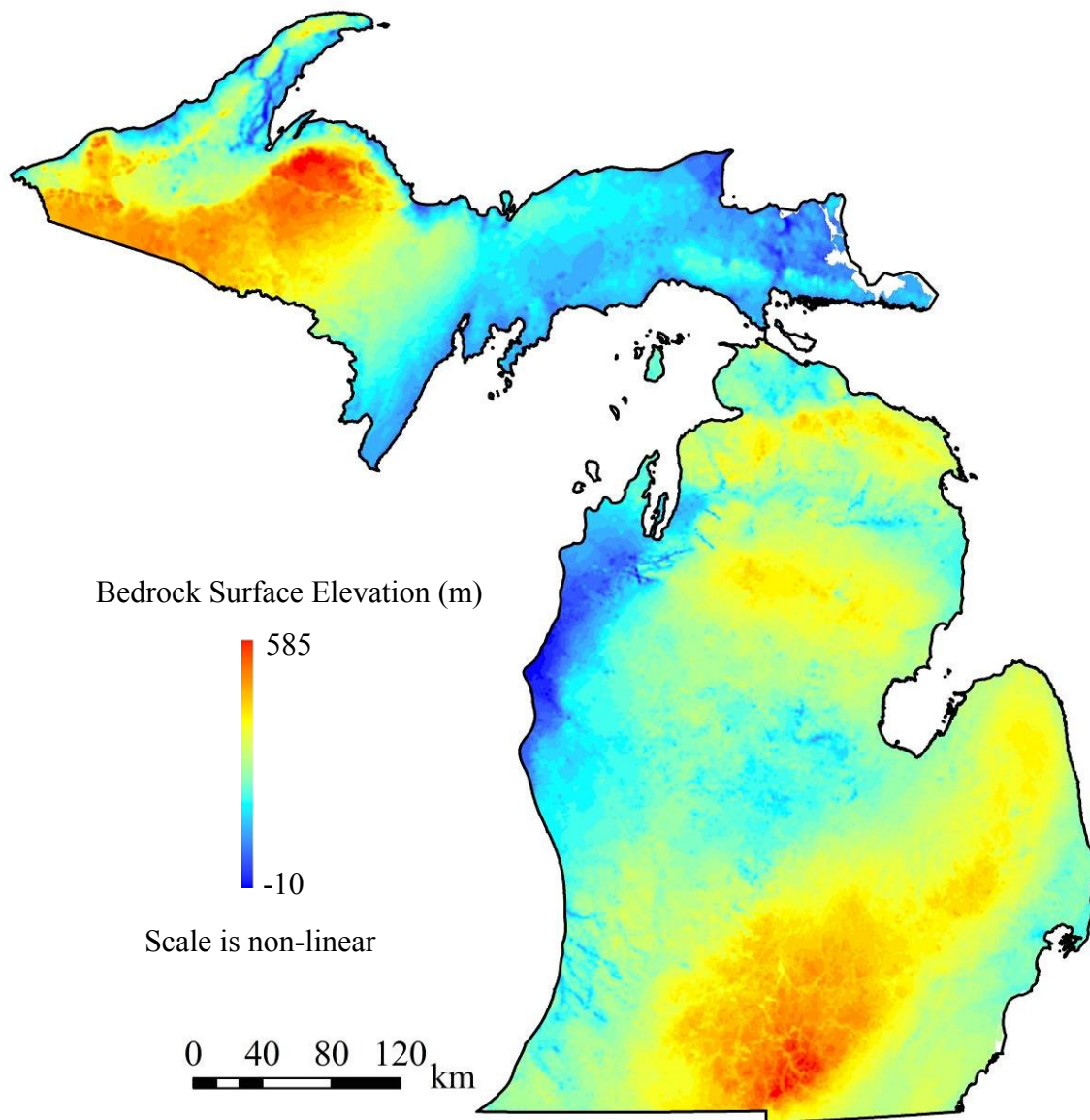


Figure 20: Raster-based bedrock surface map of Michigan.

A discussion on the existing bedrock surface map can be found in Appendix B (p. 85).

Watershed boundaries. The USGS delineated the watersheds in the United States using a nationwide hydrological system that divides and subdivides the country into hierarchical levels. These levels of sub-divisions, which are used for organization of the hydrological data, are called *hydrological units*. Hydrological units are used to collect and organize the data and these units can be defined as the land areas that catch precipitation and drain it to rivers, streams, wetlands, lakes, or groundwater (Seaber *et al.*, 1987).

The largest unit in the hydrological unit system is called *region* and represents either the drainage area of a major river or the combined drainage areas of a series of rivers. Watersheds are the smallest subdivisions of the regions. Each watershed includes the area drained by a river system or a section of a river (i.e. stream) and its tributaries in that reach (Seaber *et al.*, 1987).

The watersheds are identified with an 8-digit identification number which is called *hydrological unit code (HUC)*. A hydrological unit code consists of 2 digits for each hydrological level that describes the relation of the hydrological units to each other to represent the way the smaller watersheds get together to form the larger watersheds. The hydrological system has a scale of 1:2,000,000 (1 cm = 20 km) and divides the country into 2,264 watersheds, 60 of which are located in Michigan (Figure 21). The USGS provides not only the boundaries but also the surface areas (in acres) of the watersheds in the corresponding shapefiles (Seaber *et al.*, 1987).

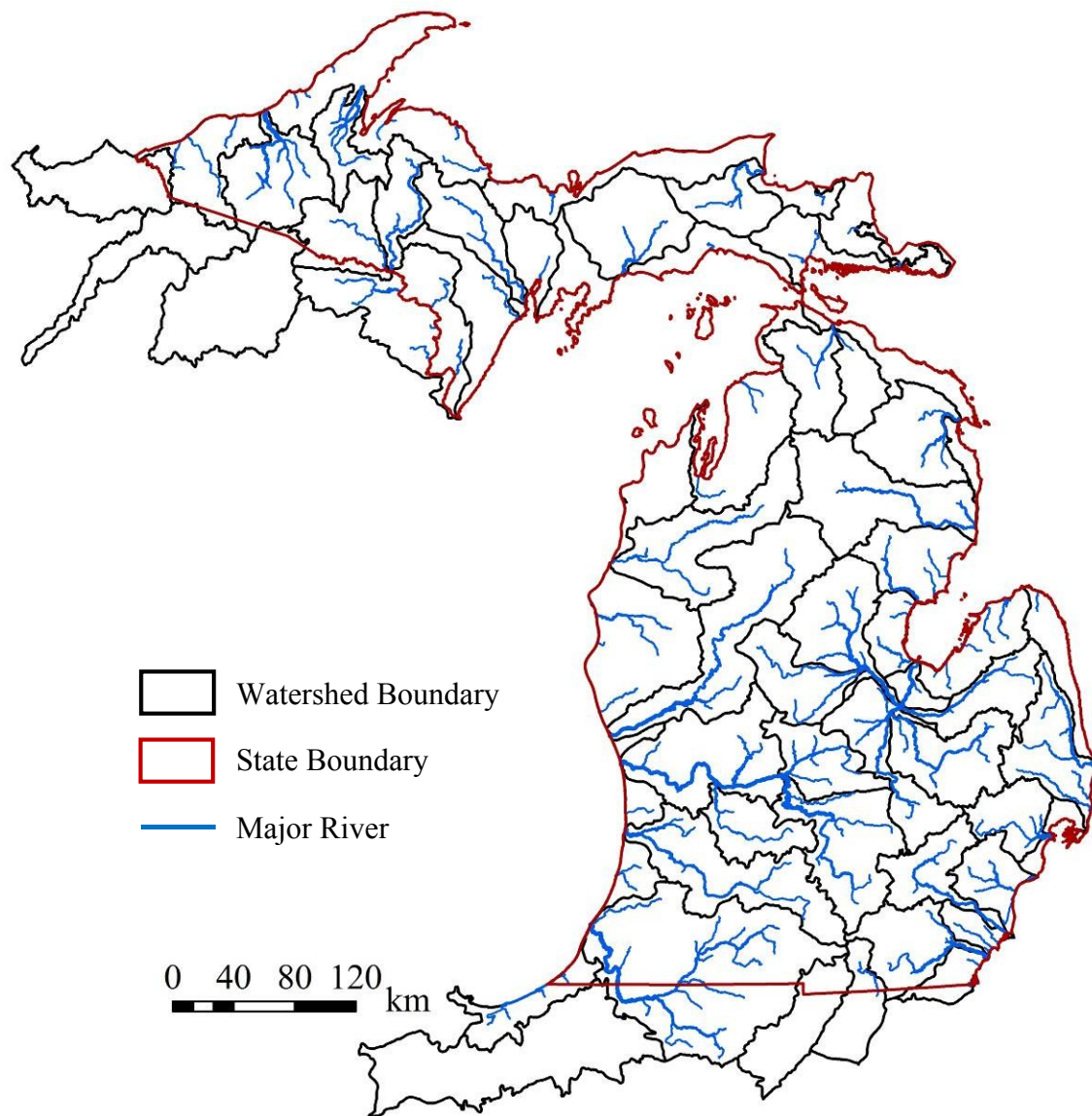


Figure 21: Watersheds of Michigan.

The USGS also provides a statewide GIS database for *sub-watersheds* that divides the existing watersheds into smaller drainage areas. This GIS database was generated from the 1:24,000 (1 cm = 240 m) scale topographic maps which are also known as 7.5-minute quadrangles. Totally there are 2,287 sub-watersheds in Michigan's sub-watershed system

(Seaber *et al.*, 1987). A set of sub-watersheds located in the Muskegon Watershed is shown in Figure 22.

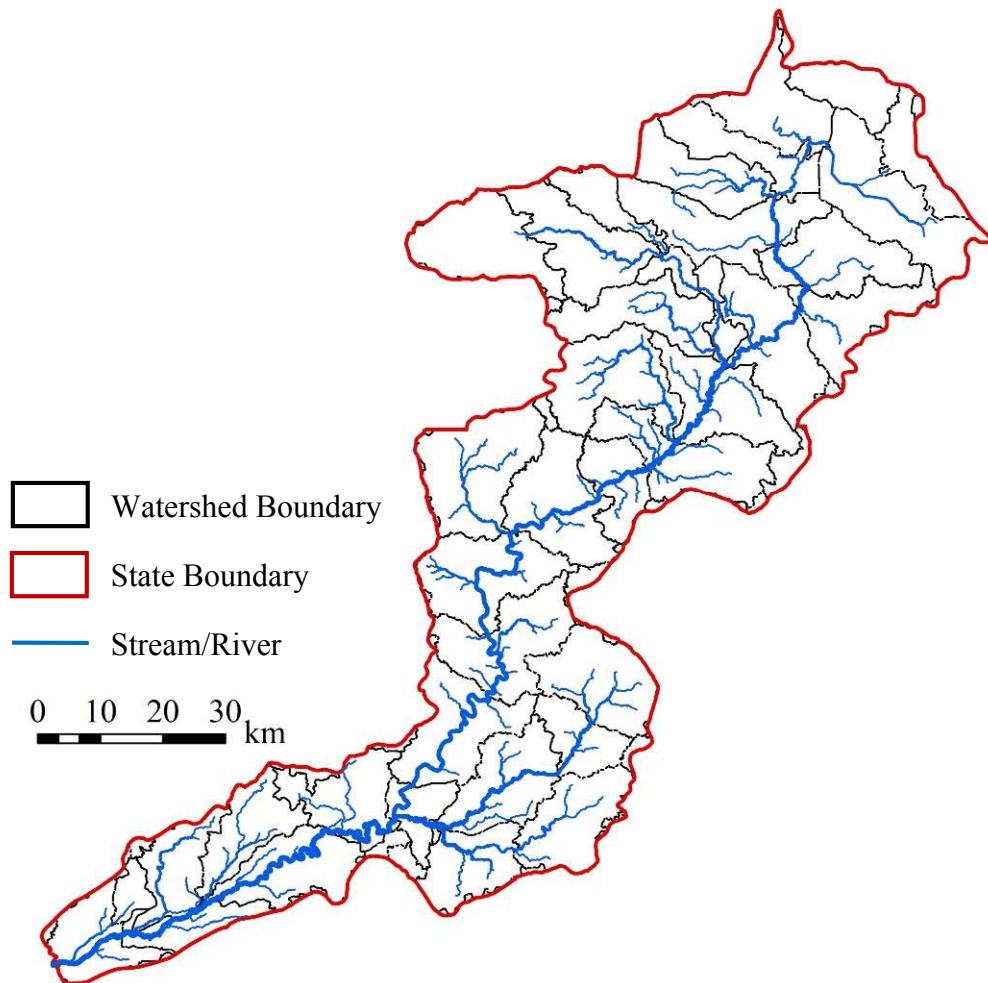


Figure 22: Sub-watersheds of the Muskegon Watershed.

Hydrogeological Framework

Hydraulic conductivity of the glacial aquifer. In GWIM, equivalent horizontal hydraulic conductivity for each water well drilled in the glacial aquifer was estimated (in ft/d) from the lithology information reported in Wellogic (GWIM, 2006). Two hydraulic conductivity

values were calculated for each well: Horizontal Hydraulic Conductivity 1 (HCOND1) and Horizontal Hydraulic Conductivity 2 (HCOND2).

HCOND1 is defined as the equivalent hydraulic conductivity of the lithologies from the bottom of the well to the first confining layer (Figure 23). However, HCOND1 recorded in the system is most of the times equal to the lithology in the well screen. Since the well screen is built within the most conductive geological material, magnitude of HCOND1 is most of the times has ranges between 10 and 10^2 .

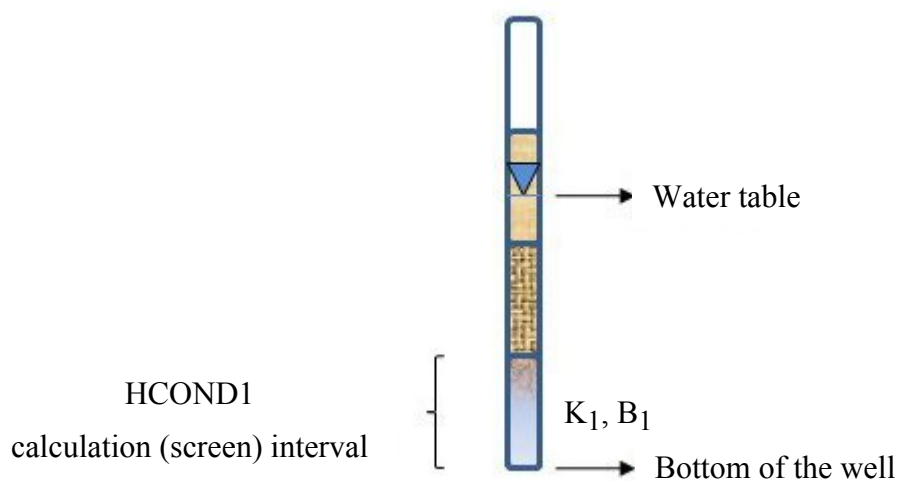


Figure 23: Conceptualization of the calculation interval for the HCOND1 parameter.

Calculation of HCOND2 is different than that of HCOND1. HCOND2 value was calculated based on the lithology from the water table to the bottom of the well or the top of bedrock for the wells completed in the bedrock aquifers underlying the glacial aquifers. In other words, HCOND2 represents the hydraulic conductivity of the saturated thickness (Figure 24).

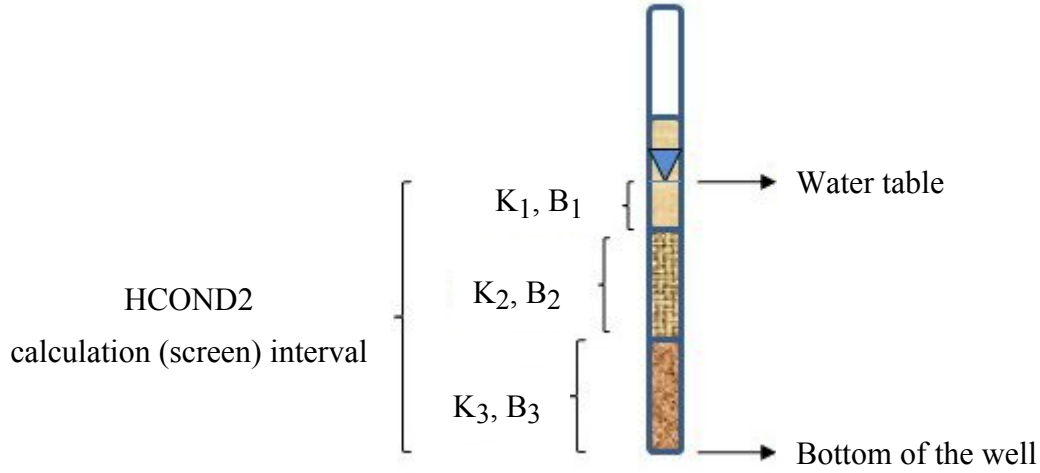


Figure 24: Conceptualization of the calculation interval for the HCOND2 parameter.

Assuming that all lithologies within the wells are layered horizontally, equivalent horizontal hydraulic conductivity in the wells was calculated with the thickness-weighted average formula [Equation (13)] (Freeze and Cherry, 1979):

$$K_h = \frac{\sum_{i=1}^n K_i B_i}{B} \quad (13)$$

where

K_h : equivalent horizontal hydraulic conductivity in the water well, $\left[\frac{L}{T}\right]$

n : number of lithologies within the calculation interval,

K_i : hydraulic conductivity of the lithological unit, $\left[\frac{L}{T}\right]$

B_i : thickness of the lithological unit, $[L]$

B : saturated thickness, $[L]$

In general, the equivalent horizontal hydraulic conductivity is controlled by the lithology with the highest hydraulic conductivity. The hydraulic conductivity values that were assigned to the lithologies had been adopted from the Source Water Assessment Program conducted by the MDEQ in 2004 by using a textbook range of values. For each lithology, three different (minimum, intermediate, maximum) hydraulic conductivity values were defined. Depending on the land system that the water wells were drilled in, one of the three values was assigned for the corresponding lithology. Full list of these values are available in the GWIM Technical Report (GWIM, 2006). Some of the selected values along with the land system classification are given in Table 8.

For some wells, equivalent vertical hydraulic conductivity value was also calculated depending on the availability of data, and using [Equation (14)] (Freeze and Cherry, 1979):

$$K_v = \frac{B}{\sum_{k=1}^m \frac{B_k}{K_k}} \quad (14)$$

where

K_v : equivalent vertical hydraulic conductivity in the water well, $\left[\frac{L}{T} \right]$

m : number of lithologies within the calculation interval,

K_k : hydraulic conductivity of the lithological unit, $\left[\frac{L}{T} \right]$

B_k : thickness of the lithological unit, $[L]$

B : thickness of the calculation interval, $[L]$

Table 8: Hydraulic conductivity classification based on the land systems of Michigan (GWIM, 2006).

Lithology	Land system		
	Bedrock Lacustrine fine Lakes	Ice-marginal till Lacustrine coarse Lodge till/fine supraglacial drift	Coastal dunes Ice-contact outwash Proglacial outwash
	Hydraulic conductivity (ft/d)		
	Minimum	Intermediate	Maximum
Clay	10^{-4}	10^{-4}	10^{-4}
Clay & Gravel	3×10^{-4}	10^{-3}	10^{-2}
Clay & Sand	3×10^{-4}	10^{-2}	10^{-2}
Clay & Silt	10^{-4}	10^{-4}	10^{-4}
Gravel	50	100	300
Gravel & Clay	10^{-2}	10^{-2}	10^{-2}
Gravel & Sand	1	50	100
Gravel & Silt	1	1	1
Sand	1	50	100
Sand & Clay	10^{-4}	0.1	1
Sand & Gravel	1	50	100
Sand & Silt	1	1	10
Silt	10^{-1}	1	1
Silt & Clay	10^{-4}	10^{-3}	10^{-2}
Silt & Gravel	10^{-1}	1	1
Silt & Sand	10^{-1}	1	1

The conceptual difference between the HCOND1 and the HCOND2 parameters is demonstrated in Appendix B. Final products that are generated to implement HCOND1 and HCOND2 into the groundwater models developed in this research are discussed in Appendix C.

Transmissivity of the bedrock aquifer. Transmissivity map of the bedrock layer was generated by interpolating a total number of 233 point-based transmissivity data (GWIM, 2006). The sources of the transmissivity data used in the interpolation are given below:

- The MDEQ collected the paper records of the aquifer tests conducted by the consulting companies in various municipal wells across the state
- The USGS compiled the aquifer test records throughout the state as a part of the Michigan Basin Regional Aquifer System Analysis (RASA) Program

Existing transmissivity map of the bedrock aquifers in the state is improved for this research. Further discussion on the improvement can be found in Appendix C (p. 85).

Stress Factors

Surface water network. MSGWD uses the medium resolution (1:100,000) USGS NHD for the identification of Michigan's surface water network. The NHD provides comprehensive digital spatial data that represent the surface water network of the United States through common features such as streams, rivers, lakes, and ponds. These data are designed to be used in general mapping and the analysis of surface water systems and surface water-groundwater interactions through GIS. For mapping and analysis purposes, the NHD is used with

other data themes such as the surface elevation and feature boundaries to produce general reference maps (USGS, 2000).

The features in the NHD were organized into polylines and polygons. The stream lines were broken up into shorter segments stretching from confluence to confluence and these segments were linked together to trace the flow of water. Artificial lines that go through inside lakes represent the flow of water through a lake. The polygons typically represent the water bodies such as lakes and ponds where the lines were used to digitize the streams (USGS, 2000).

Streams were labeled with a unique and permanent identifier (reach code) which gives the streams an identity for inventory and analysis. This makes it easier to perform calculations in GIS such as determining the distance to the stream flow gauging stations and calculating base flow. Linear referencing also makes it easy to link additional data to the NHD without having to customize it (USGS, 2000).

The NHD is available for different resolutions. In this research, a medium resolution NHD which was generated with 1:100,000 (1 cm = 1 km) scale topographic mapping is used for groundwater modeling (USGS, 2000).

The NHD GIS files were updated by appending quite a few different parameters for every stream segment and lake recorded in Michigan (GWIM, 2006). However, number of the essential parameters for modeling is limited to a few. Table 9 shows the attribute names and the definitions of these parameters.

Table 9: Essential modeling parameters recorded in the NHD.

Feature	Parameter	Definition	Unit
Stream	Order (Strahler number)	Stream size based on the hierarchy of the tributaries (available 1 through 6)	-
	F_Elev	Upstream elevation of the stream segment	m
	T_Elev	Downstream elevation of the stream segment	m
	Base flow	Groundwater discharge to streams	ft ³ /s
	Name	Stream name	-
	Length	Length of the stream segment	m
Lake	Lake_Elev	Lake elevation	m
	Area	Surface area of the lake	ac
	Name	Lake name	-

In the NHD GIS files, for some stream segments a generic value of -9,999 for the attributes that define the upstream and the downstream elevations of those segments is detected (Figure 25). This value indicates the stream segment locations where there is no data available for the stream stages. Stream stages in the vector-based stream segments were generated by extracting the land surface elevations from the USGS 30 m NED (GWIM, 2006). For this research, statewide raster-based stream stage maps are used to directly extract the stage values. Final product for the stream network used in the groundwater models is discussed in Appendix C (p. 96).

Lately, the USGS, in cooperation with the U.S. Environmental Protection Agency (USEPA) evaluated different methods to delineate catchments of the medium resolution

(1:100,000-scale) NHD with a goal to estimate stream flow and velocity to support water quality modeling. The results of this study are the first national dataset that links the mapped stream network to the landscape. The data, called NHDPlus, are distributed for all states, except Alaska, through the website <http://www.epa.gov/waters> (Johnston *et al.*, 2009).

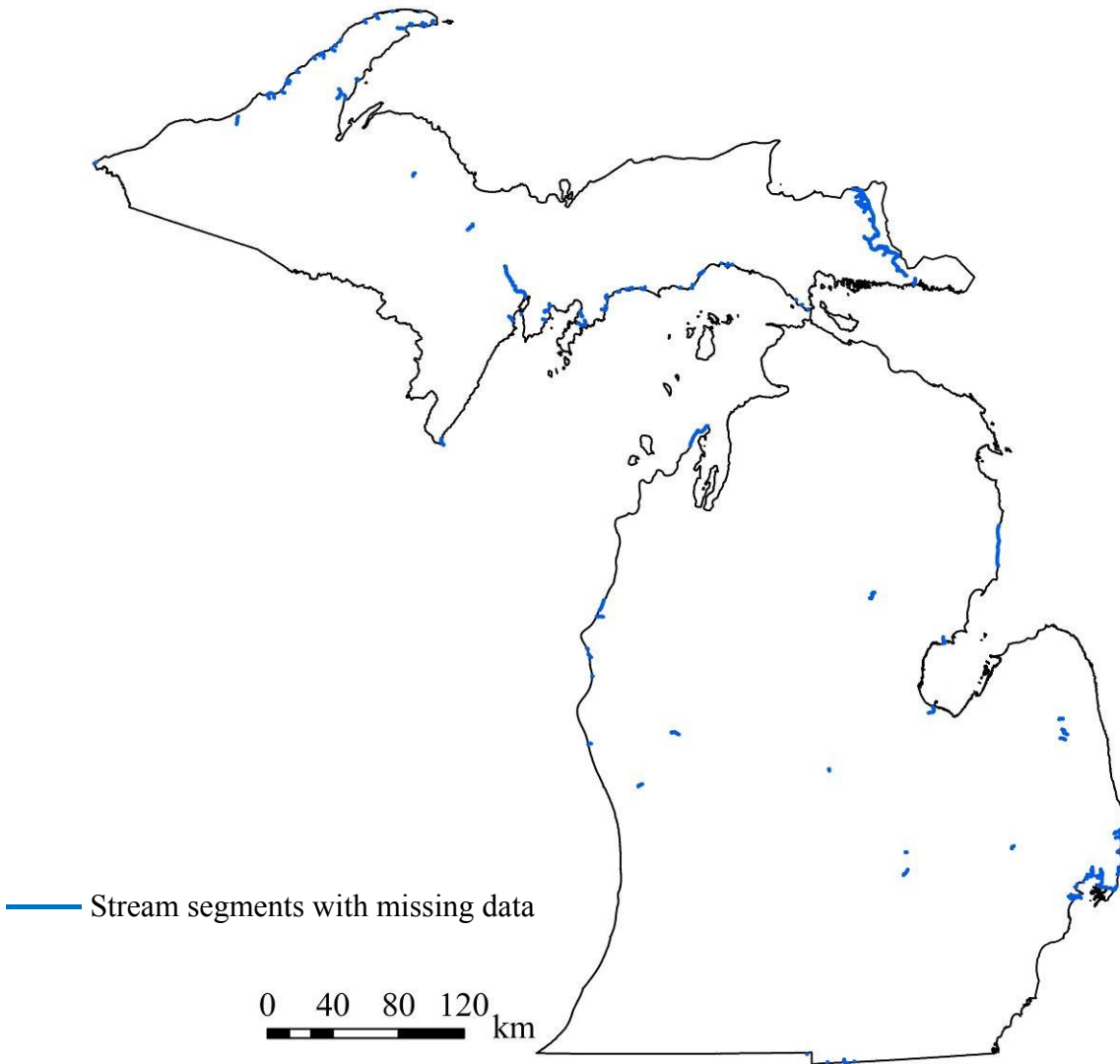


Figure 25: Stream segments with missing stream stage data in the NHD of Michigan.

Estimated shallow groundwater recharge. In this research, groundwater recharge is defined as the precipitation that infiltrates the land surface, moves downward through

the unsaturated zone, and enters the water table. The long-term average base flow values were assumed by the USGS to be equal to the long-term average groundwater recharge (i.e. total water entering the soil minus losses to evapotranspiration before it reaches the water table) in the surrounding watershed. Steps for calculating the estimates of recharge are given below (Neff *et al.*, 2006):

- Long term stream flow records from the 162 stream flow gauging stations in the Lower Peninsula and the 46 stream flow gauging stations in the Upper Peninsula out of totally 416 stations (Figure 27) were used to determine the stream flow component that results from groundwater discharge (base flow) into the streams
- Base flow was supplemented by direct runoff during and immediately after precipitation or snowmelt events, resulting in peaks on a hydrograph showing stream flow through time
- Peaks on the hydrographs were divided into base flow and stream flow components by using the hydrograph separation technique
- Watersheds were delineated for each of the 208 gauging stations, and the state was divided into three regions (i.e. the eastern Lower Peninsula, the western Lower Peninsula, and the Upper Peninsula) based on the distribution of base flow yield (base flow per unit area)
- For the ungauged areas, multivariate linear regression models were used to relate the base flow information in the gauged areas to landscape attributes (e.g. agricultural land use, urban land use, annual growing degree days, annual precipitation, percentage of the watershed underlain by the lacustrine deposits) in the surrounding watersheds for each of the three regions

- A base recharge (mean base flow yield) value was estimated within each of the three regions by dividing the base flow to the total area of each of the three regions
- As an initial estimate, mean base flow yield value was multiplied by the watershed area for each station
- A residual value was then calculated by subtracting the measured base flow at each station from the area-based prediction
- A second set of linear regression models was created to predict these residuals based on the same watershed attributes used in the previous regression model
- The resulting regression models were then applied to estimate the residual in each section of 1 mi² of area
- Finally, the residuals were added to the initial estimated yields to come up with an estimate of the total recharge for each section

The spatial resolution of the estimates of recharge in the Upper Peninsula is not as detailed as of the Lower Peninsula because the number of stream flow gauging stations in the Upper Peninsula is not good enough to provide a sufficient number of observations to support the incorporation of land cover or surface geology into the models.

The estimated recharge values for each recharge polygon with an area of 1 mi² were tabulated into a shapefile (GWIM, 2006). For this research, this shapefile is converted to a raster-based map to be used in the groundwater models (Figure 26). It is observed that, in the original vector-based GIS file, there are local zones for which recharge data is missing. Locations and extensions of these polygons are also shown in Figure 26.

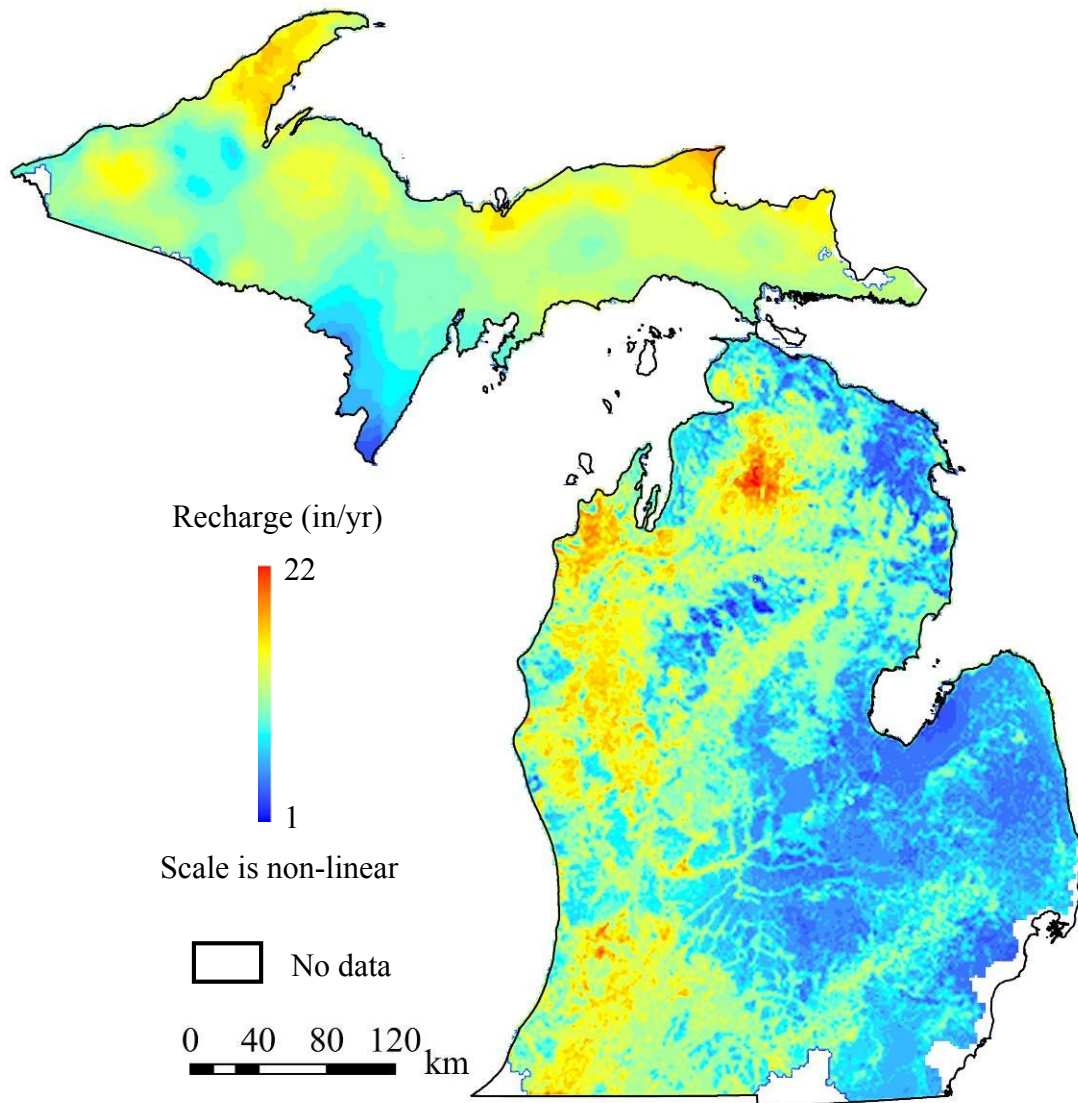


Figure 26: Raster-based recharge map of Michigan.

Calibration Parameters

Static water level. Wellogis contains more than 45 years of water level data which makes this data set ideal to demonstrate the long-term regional-scale behavior of the groundwater level distributions across the state. The static water level (SWL, in ft) recorded in the database is defined as the depth from the land surface to the water table in the corresponding

well. The SWL reported here is the water level in the well after the well is developed, prior to pumping.

In this research, SWL information is used to conduct the comparison between the groundwater levels simulated with the watershed-scale models and measured groundwater levels in the water wells.

Base flow. Base flow can be defined as groundwater discharge into streams. Precipitation that is not returned to atmosphere by evapotranspiration either flows across the land surface, discharging directly into wetlands, lakes, and rivers, or infiltrates into land surface, recharging groundwater system and ultimately resulting in groundwater discharge that contributes to base flow. The partitioning of precipitation between runoff and infiltration is controlled by the capacity of groundwater system to receive and transmit water. This partitioning is a result of landscape attributes (p. 61), and the characteristics of the shallow subsurface materials which are the principal constraints in the estimation. Coarse-textured unconsolidated sediments and permeable and fractured bedrock are typically associated with above average infiltration, whereas fine-textured unconsolidated sediments and low-permeability bedrock are typically associated with above average surface runoff (Neff *et al.*, 2005; Neff *et al.*, 2006).

The USGS used two fundamental models to calculate a base flow index (BFI, i.e. ratio of base flow to stream flow) for the estimation of base flow in each watershed in Michigan (Neff *et al.*, 2005): (1) G-Model which develops an empirical relation (from stepwise regression analysis), between each surface material class (bedrock, tills, organic sediments, coarse-textured sediment, fine-textured sediment) and the BFI in each gauged watershed. Here, it was assumed that groundwater discharge is most closely related to surface geology, and that the averaged

values of BFI approximate the portion of stream flow that is the result of groundwater discharge.

(2) G-SW model, which along with the geological interpretation used in G-model, takes the surface water features into account by incorporating the proportion of surface water network within a gauged watershed, and develops an empirical relation to calculate the BFI.

The USGS used the stream flow records from the stream flow gauging stations (Figure 27) to estimate the long term average stream flow in each HUC (here watershed) across the state. Base flow was then determined by multiplying model-simulated BFI with the estimated total stream flow for each HUC. Further details for the model equations and the parameter weights used in the models can be found in (Neff *et al.*, 2005).

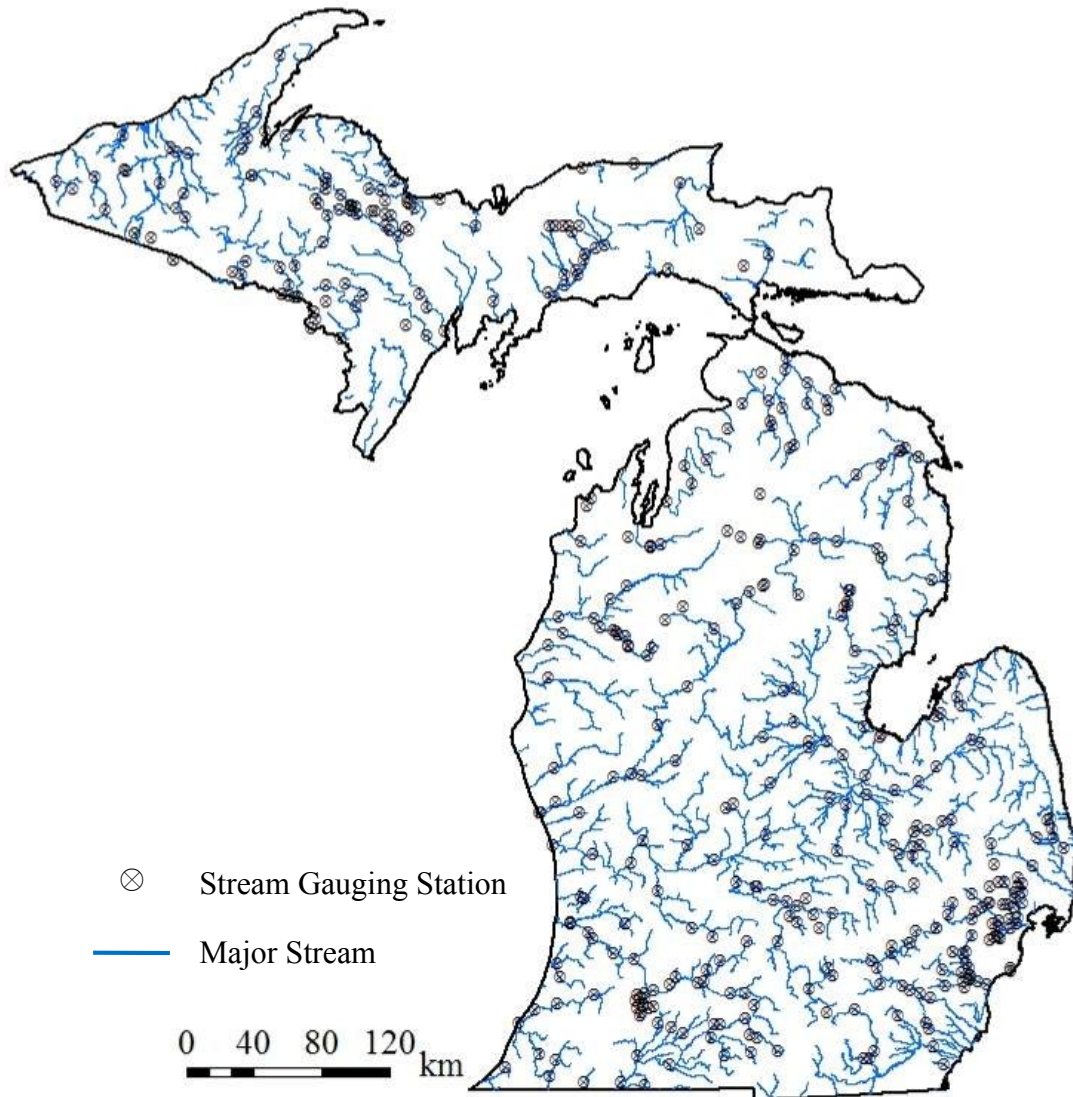


Figure 27: Locations of the stream gauging stations in Michigan.

In gauged areas (i.e. areas that are tributaries to a given gauge or gauges), base flow estimates were calculated based on the hydrograph separation using the stream flow data extracted from the USGS Automated Data Processing System (ADAPS). To develop regression models to describe base flow in ungauged areas (watersheds that are represented by 8-digit HUCs which may also contain gauged areas), only the USGS stream flow gauging stations with a length of record of at least 36 months were used (Neff *et al.*, 2005).

Appendix B: Conceptual Difference between HCOND1 and HCOND2

As it was discussed in Appendix A, the HCOND1 values in the water wells represent the lithology of the screen intervals where the HCOND2 values represent the saturated thickness in the water wells (or the saturated thickness of the glacial aquifer where the aquifer thickness is small). Difference between the values of the HCOND1 and the HCOND2 parameters is shown in Figure 28.

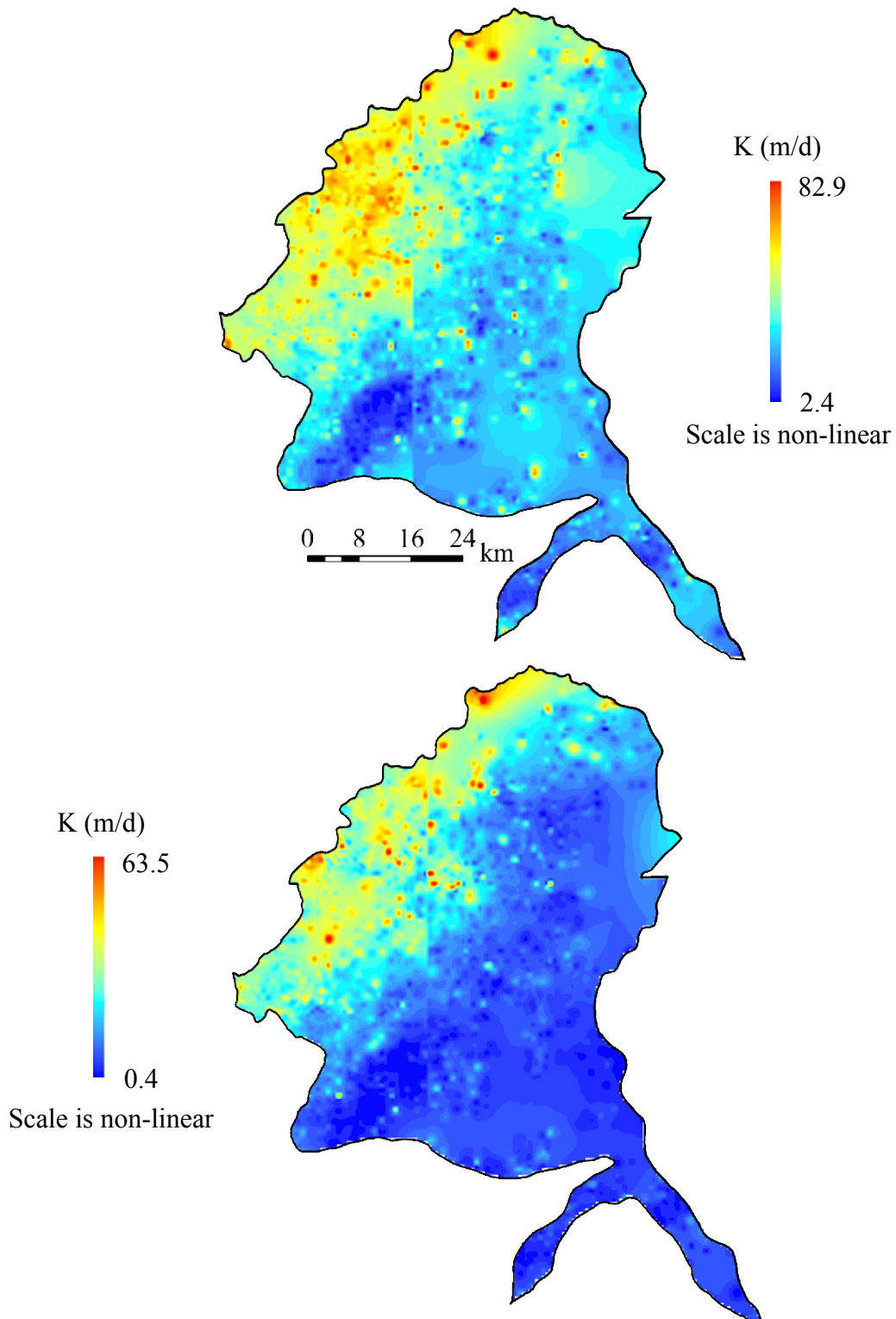


Figure 28: Hydraulic conductivity field of the Tittabawassee Watershed. Above HCOND1, and Below: HCOND2.

All models presented in this research utilize the HCOND2 parameter to generate the flow fields. For demonstration purposes, the model of the Tittabawassee Watershed is redone using the HCOND1 parameter, and the head comparisons from both conductivity fields are shown on the same plot (Figure 29). In this figure, it can be clearly seen that the model generated with the HCOND1 parameter predicts lower water levels (black dots) at the same locations than those of the HCOND2 parameter (blue circles). Even this comparison alone indicates that the HCOND1 parameter cannot be used for aquifer characterization and modeling purposes. The HCOND1 can be used for the applications where the screen interval of the water wells is of great importance in terms of determining the flow direction when the wells are pumped (e.g. well-head delineation).

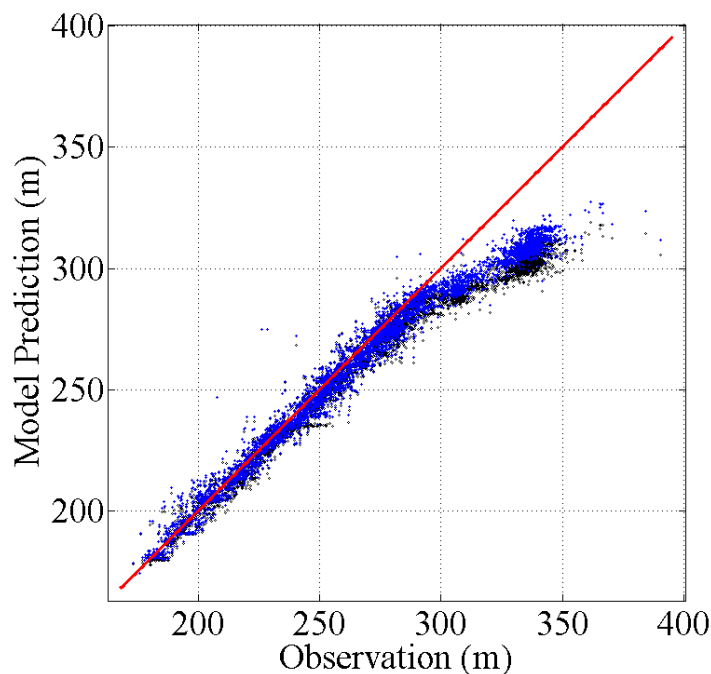


Figure 29: Comparison between the model results with HCOND1 and HCOND2. Black Dots: Results for HCOND1, and Blue Circles: Results for HCOND2.

Appendix C: Data Analysis and Management

Introduction

Model prediction is always uncertain to some degree, and it is of critical importance to have a reliable dataset for which data uncertainties are reduced so that the model's ability to represent the reality can be improved.

In MSGWD, while some parameters were presented as directly measured field data, some of them were calculated from those directly measured data, or estimated through interpolation of the existing data by using various geospatial modeling techniques (e.g. Kriging interpolation). While directly measured Wellogic data has uncertainties such as temporal variability, location inaccuracy, and driller variability, calculation and processing errors could also be introduced for the indirectly calculated parameters.

Interpolation can be justified if the data is abundant (Lubczynski and Gurwin, 2005). However, even in cases where data is abundant, generated maps come with problems that originate from the data errors and uncertainties, and the methods that are used for mapping. Because of all these potential problems, before developing the conceptual models of the state's watersheds, the data provided with the GWIM is revisited to check possible data problems, a step that is important to improve the quality of the models. Also, where it is projected that data smoothing won't significantly change the regional-scale data definitions while the computational efficiency will be improved, some vector data are converted into raster data by benefiting from the Kriging and the inverse distance weighting interpolation techniques.

In this research, for data analysis and groundwater modeling, mainly two programs are used: ArcGIS (version 9.2) and Interactive Groundwater (IGW, version 5.20P). IGW is a real-time, interactive, and hierarchical simulation environment with a GIS interface that allows data integration for deterministic, stochastic, and multi-scale finite difference groundwater flow and contaminant transport modeling. IGW has been developed and continuously improved in *the Laboratory of Excellence for Real-time Computing and Multi-scale Modeling (LERCMM)*, Department of Civil and Environmental Engineering, Michigan State University. Other basic specifications of the program are summarized in Table 10.

Table 10: Basic specifications of IGW.

Developers: Shu-Guang Li, Huasheng Liao, Qun Liu
Contact: A133 Engineering Research Complex, Michigan State University, East Lansing, MI 48824. E-mail: lishug@egr.msu.edu
Year first available: 1997
Hardware required: IBM compatible PC
Operating system: PC with Windows (NT/95/98/ME/2000/XP)
Programming language: Visual Basic 6, Visual FORTRAN 5
Space required for installation: 50 MB
Current version: IGW 5.2P
Availability: Downloadable version (version 4.7), with user's manual and supporting material, available at http://www.egr.msu.edu/igw/

Specifications of the computer that was used for most of the research are given in Table 11.

Table 11: Basic features of the main computer used in the research.

Processor: Pentium D CPU 3.20 GHz
Memory: 3.50 GB
Operating system: Microsoft Windows XP Professional (32-bit)

For more challenging analysis and modeling issues that needed better computational resources, the computer of which specifications are given in Table 12 was used:

Table 12: Basic features of the advanced computer used for some of the simulations.

Processor: Intel Xeon CPU X5482 3.20 GHZ
Memory: 8 GB
Operating system: Microsoft Windows XP Professional (64-bit)

Identifying and Eliminating the Data Uncertainties

Data uncertainties in Wellogic. Wellogic provides valuable information regarding the hydrogeological and the physical framework of Michigan's groundwater systems. On the other hand, efficiency of groundwater flow and contaminant transport models is significantly influenced by the "bad data" and uncertainties involved in the data (Simard, 2007; Tiedeman *et al.*, 2003). This fact comes along with the requirement of a systematic analysis for the identification of the data uncertainties which helps to improve the groundwater management.

Some of the uncertainties that are introduced with Wellogic are given below:

- Temporal variability: The wells were drilled in different times and measured time-dependent variables (e.g. SWL) only reflect the conditions at the drilling time. However, at a regional scale with the help of large amount of data, temporal variability is averaged and gives long-term trend that may be used in steady-state groundwater models.
- Vertical uncertainty: The data recorded (e.g. SWL, hydraulic conductivity) in the water wells reflect the conditions in the well screen. For the groundwater models developed in this research, the spatial data in the water wells are considered as they represent the vertical average values for the corresponding aquifer (i.e. glacial or bedrock) layer.
- Well location inaccuracy: The quality and location of Wellogic data is generally worse than that of the traditionally collected data especially because of the well locations that were recorded based on address matching, before the global positioning system technologies became popular.
- Driller variability: The water wells in the database are drilled by different drillers. Because of this, data quality from different drillers is different.

Vertical uncertainty discussed above can be explained by an example regarding the definition of the HCOND2 parameter provided in MSGWD. While HCOND2 is a good estimation for the saturated thickness in the water wells, where glacial deposits extend below the water wells and glacial thickness is extremely high (e.g. northern part of the Lower Peninsula), deeper lithologies are not incorporated into HCOND2.

In addition to the uncertainties discussed above, there are systematic inconsistencies, bad and missing values, and recording, processing, and typographic errors, along with wells with no data for specific parameters. Even though the number of these data points is not too many, it is

necessary to systematically eliminate them to improve the quality of the data-based analysis and the model results. Data elimination criteria and the number of the data eliminated using those criteria are shown in Table 13. The K data with zero and negative values don't exist in the current (2006) version of Wellogig, and the elimination criteria of $K \leq 0$ is added as a precaution.

Table 13: Criteria used for eliminating the bad data.

Data Elimination Criteria	No. of Wells	
	Glacial	Bedrock
$SWL \leq 0$	5196	2630
$SWL \geq 999$	-	1680
$DEM = 0$	120	95
$(DEM - SWL) \leq 0$	-	1640
$(SWL - \text{Well Depth}) \geq 0$	97	77
$K \leq 0$	-	-

Another observation regarding the data uncertainties is that for some water wells, well depth data with zero values exist, where the SWL data for those wells are recorded as positive values i.e. (SWL can't be bigger than well depth). This doesn't necessarily mean that the recorded SWL data for those wells are wrong, however, data inconsistencies must be recognized for this kind of cases with different comparable data combinations.

At this point, it is important to revisit the land surface elevation data provided with the water wells. The accuracy and reliability of the land surface data are very important since this parameter represents the upper boundary of the glacial aquifer, and it is needed to calculate the

measured heads above sea level. Furthermore, the stream stages in the 2006 version of Wellogis were derived from the land surface elevation data stored in the water wells.

To test the accuracy of the land surface elevation data in the water wells provided with the GWIM, following procedure is applied:

- First, the most recent raster-based USGS DEM (p. 89) with 10 m resolution (sampled from 30 m DEM) is used to extract the DEM data at each well location in Wellogis
- Then, a new shapefile, with the attributes of the DEM data from the GWIM and the DEM data extracted from the new datasets at the same well locations (almost 300,000 data points), is produced
- Finally, in the resulting shapefile, the data from the GWIM is subtracted from the new data to calculate the residuals
- For the areas where there are huge differences between the two datasets, the new DEM data is cross-validated by comparing the surface elevation data stored in the oil and gas wells

Residual map produced through the procedure discussed above is shown in Figure 30.

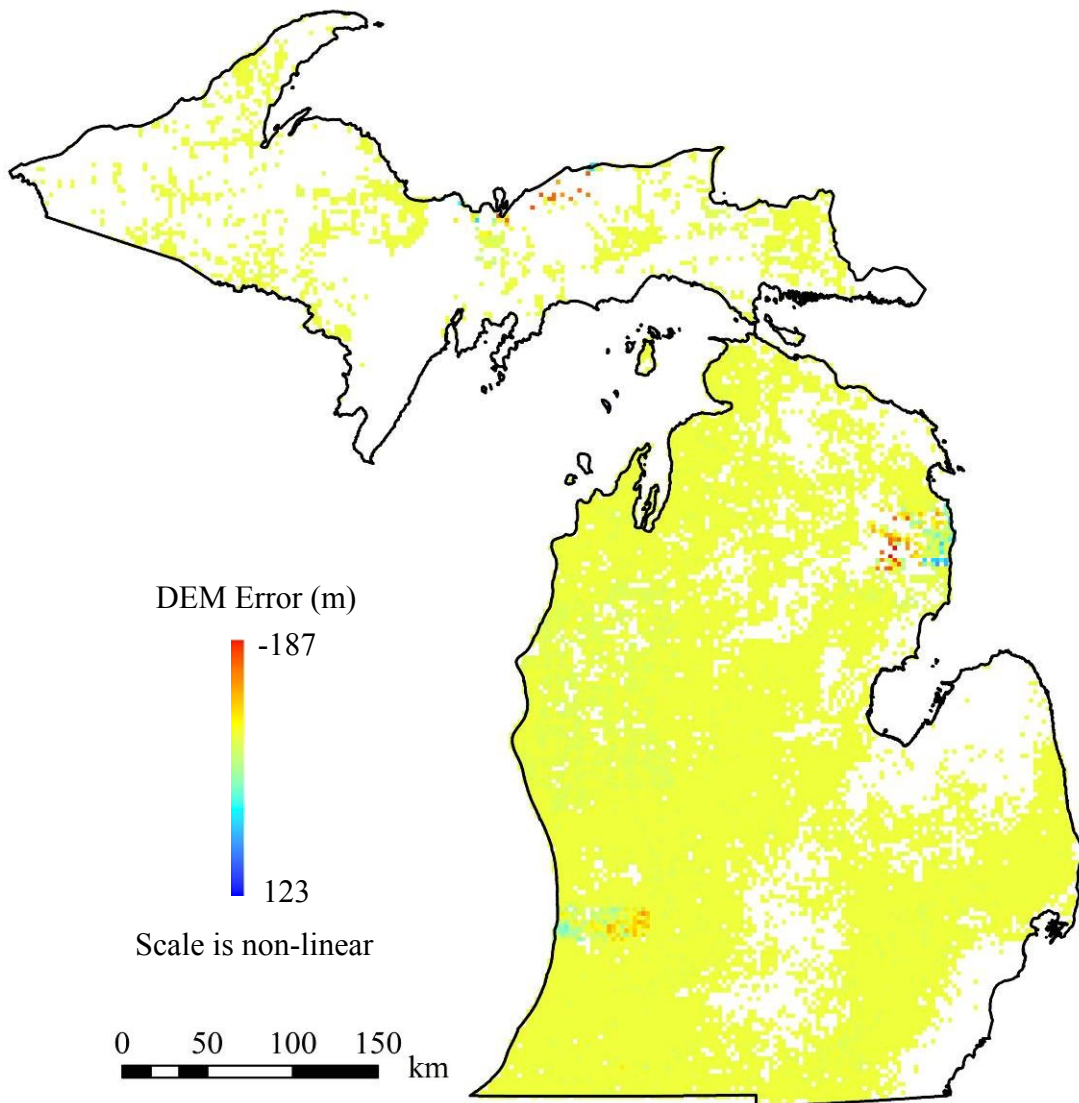


Figure 30: Error map for the DEM information in Wellogic.

Figure 30 shows that the residual between the two datasets can produce extremely big values at some locations. Final product provided with the GWIM doesn't directly use the raster data but instead converts it to point-based vector data that is defined at every water well location, after multiple procedures that go back and forth. Creating such a middle product, where the locations of the wells have also uncertainties, could introduce a new source of error. In order to demonstrate how the error in land surface elevation can adversely influence the simulated heads

(i.e. land surface elevation minus depth to water table), a test site is chosen where the DEM error becomes the highest (Figure 31).

Here, while the water table calculated from the point-based land surface data that was generated from the USGS raster-based 30 m DEM dataset produce extremely bad values, water level elevations calculated directly from the raster-based DEM data with the same resolution provides a much better final product (Figure 32).

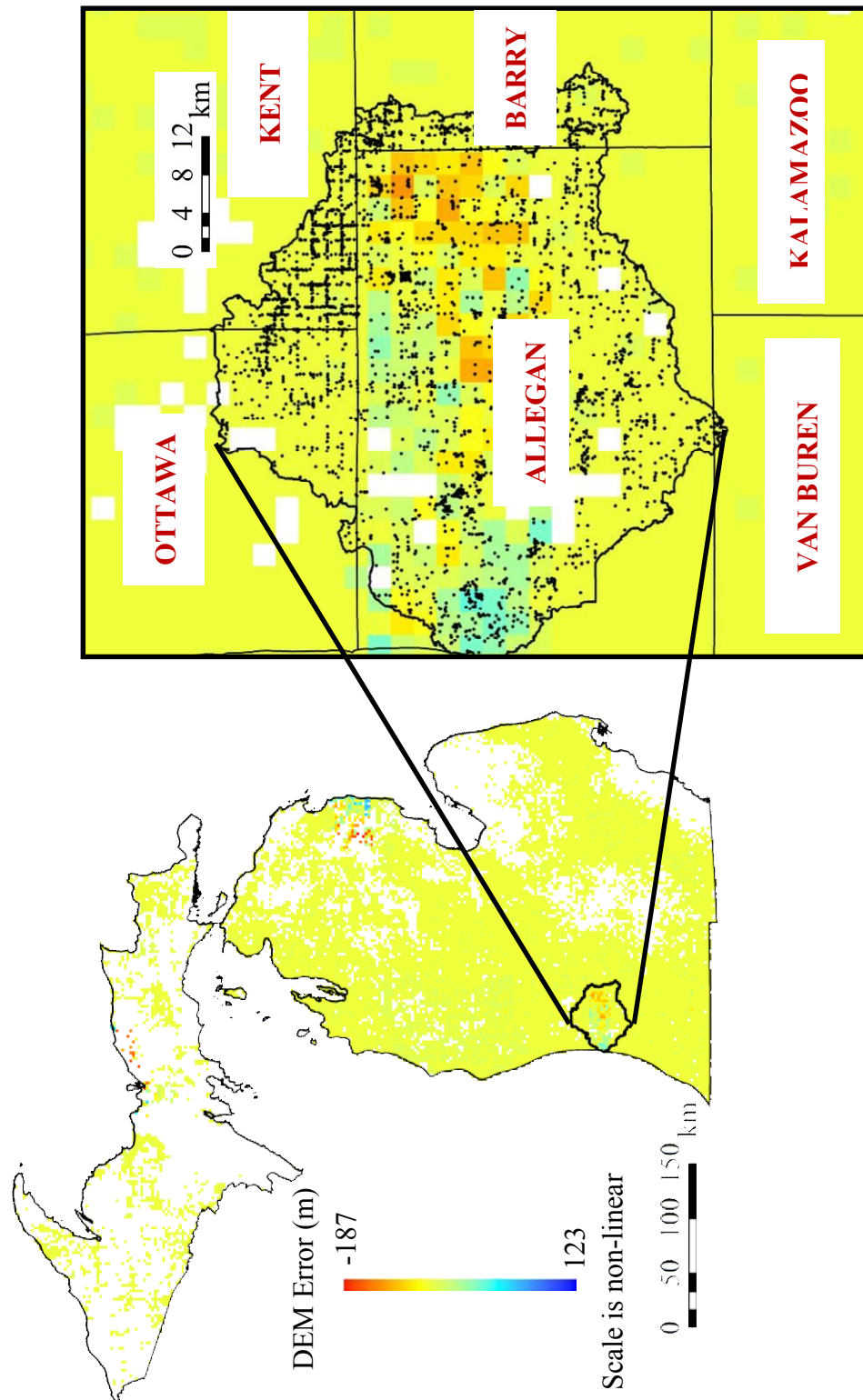


Figure 31: Location of an area in the western Lower Peninsula where DEM error is extremely high.

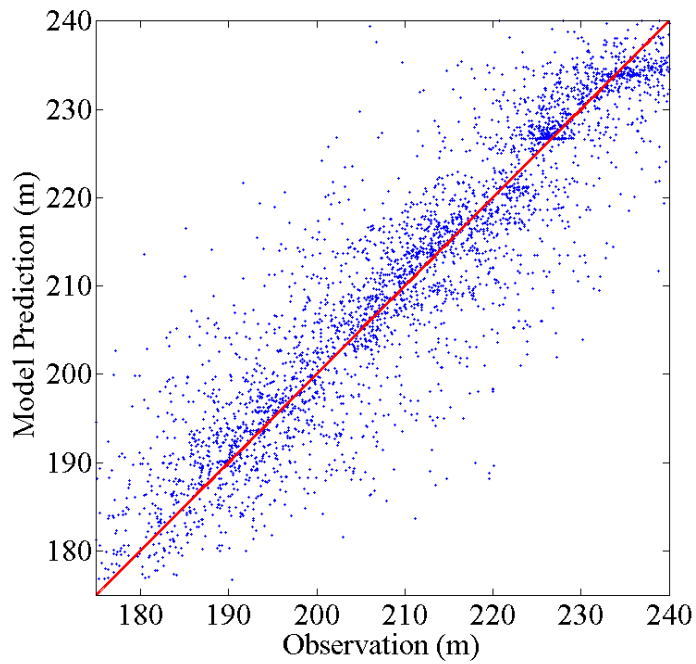
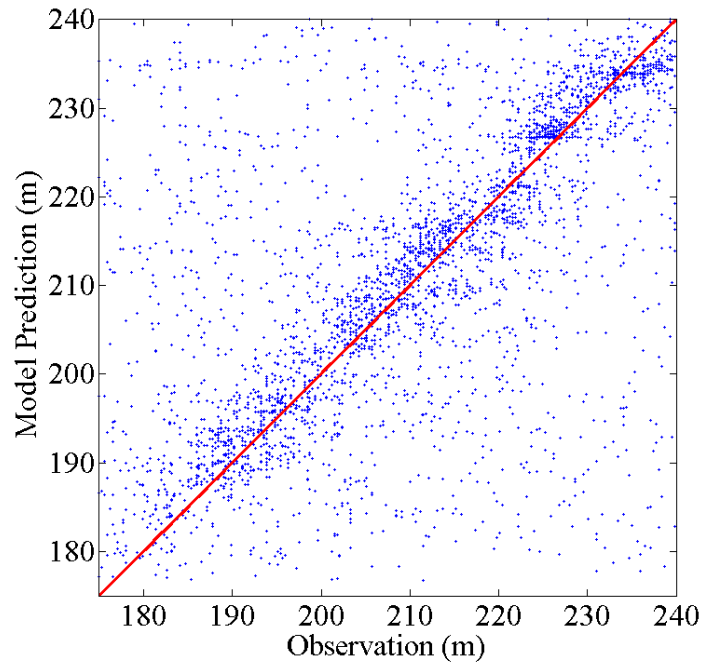


Figure 32: Simulated and measured heads for the model area shown in Figure 31. Above: comparison using vector-based DEM, and Below: comparison using raster-based DEM with 10 m (sampled from 30 m) resolution.

Another example that helped to identify the data uncertainties through a reverse (model-based) analysis is shown in Figure 33.

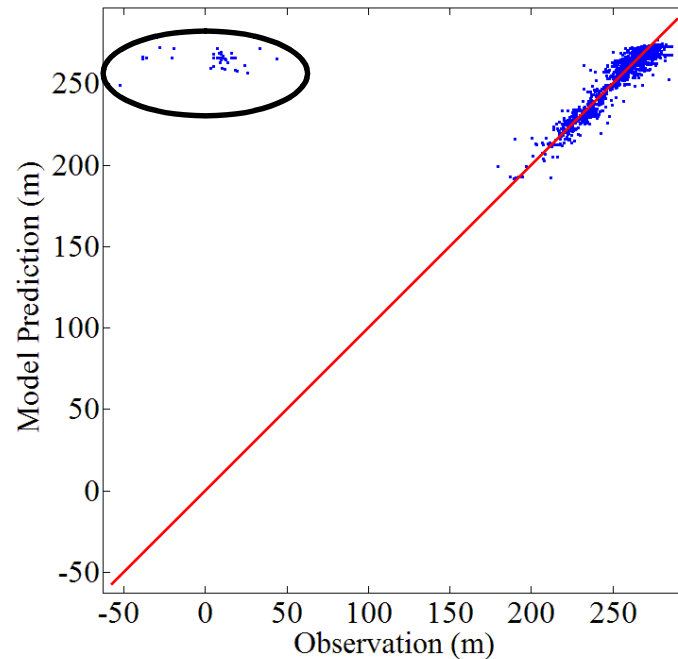


Figure 33: Identifying bad SWL data using model-based analysis, Thornapple Watershed, bedrock aquifer.

Figure 33 demonstrates the head comparison between the simulated and measured heads in the bedrock aquifer in the Thornapple Watershed (southern Lower Peninsula). The strong bias detected on the left side of the forty-five degree line indicates that there might be an uncertainty that needs to be examined by going back to the GIS files and look for a possible source of error. At the end, the bias in the comparison is found to be a result of the erroneous water well data for which the SWL information was recorded as water levels above sea level instead of depth to water table (i.e. possibly a processing and/or a recording error).

Outlier analysis. Elimination of the bad data in Wellogic was discussed before (p. 73). Errors in the calculation of the water level elevations are reduced by introducing the raster-based USGS DEM. However, it is a difficult task to detect the water wells with incorrect and anomalously high or low static water levels and these wells can sometimes be a major source of error. In this research, for the model evaluations, a systematic outlier analysis isn't conducted so that the effectiveness of the data can be judged in a better sense. On the other hand, the model-based analysis significantly helps to identify the data points with extreme values. Some of these points are can be identified with the NOSD parameter defined in Appendix G.

Hill-Rowley *et al.* (2003) states that using Wellogic data at local scales without processing might present “confused” groundwater flow patterns which are not consistent with the hydrogeological framework of the aquifer. Even though most of the issues related to these local data are lost at watershed scale, it is still possible to identify some of those points by comparing the data and models. In Figure 34, two extreme values in the bedrock wells can be easily detected using the comparative analysis.

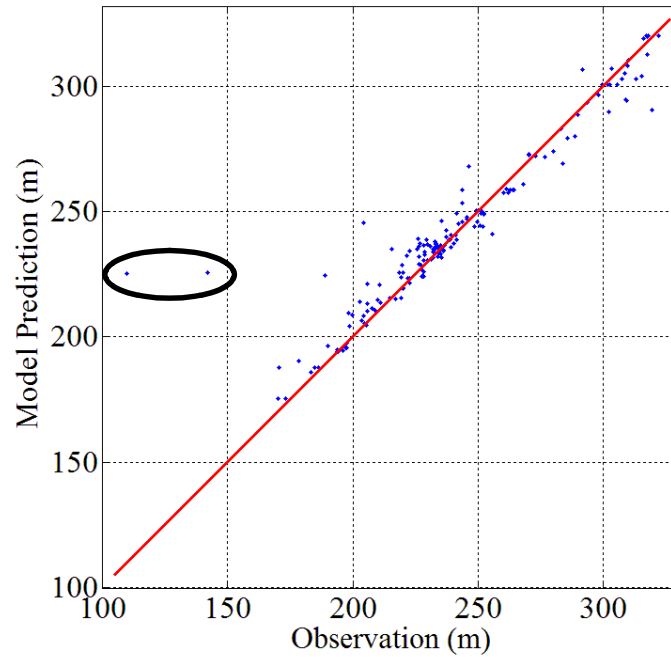


Figure 34: Identifying the outliers for the Clinton Watershed, bedrock aquifer.

The SWL values that were recorded in these wells (red box) are compared to those of the surrounding wells (Figure 35). Since within a very short distance, SWL is not expected to fluctuate anomalously, these two data points can be considered as the “bad data”.

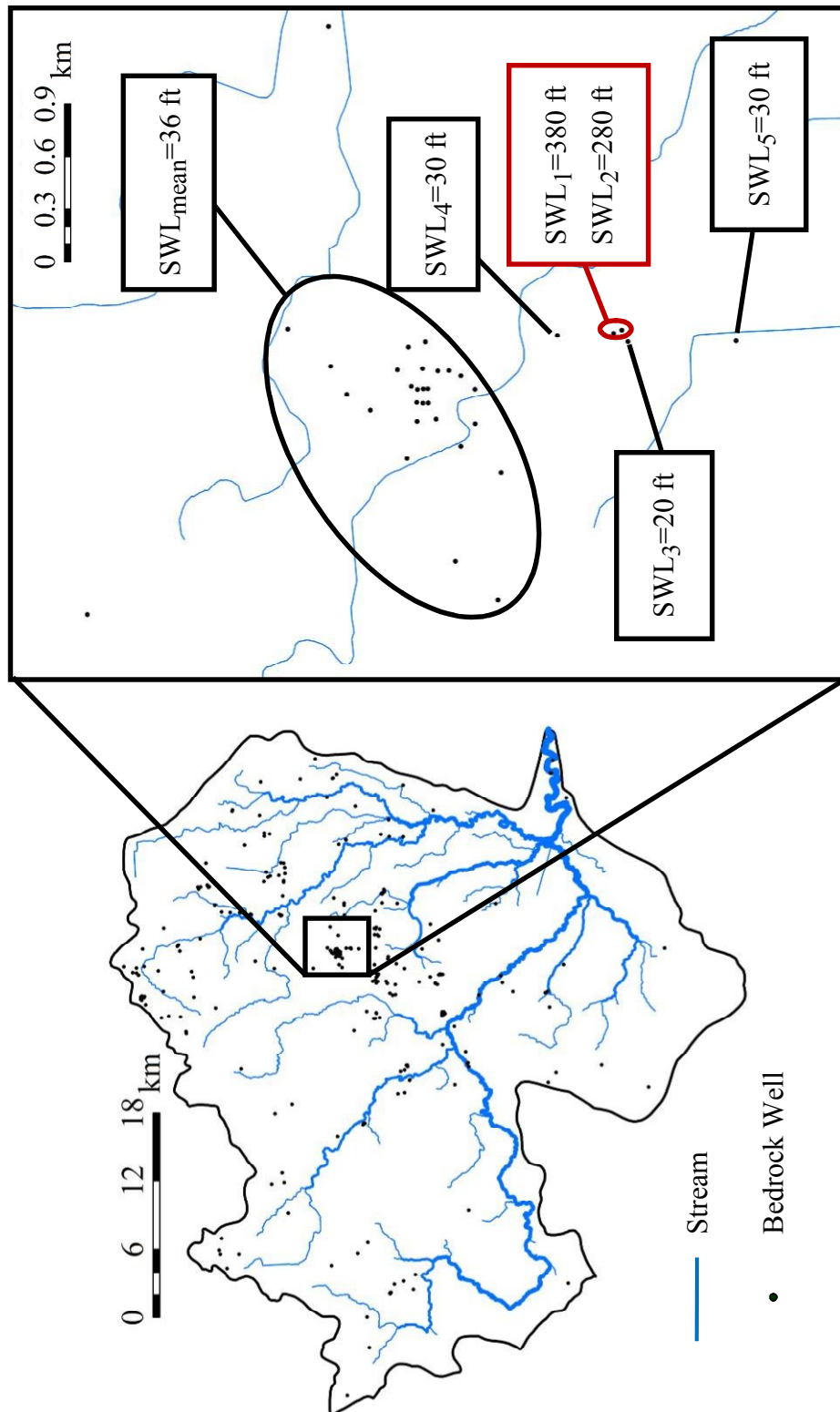


Figure 35: Analysis of the outliers based on the model results in the Clinton Watershed, bedrock aquifer.

Raster-based bedrock surface map. The accuracy of the bedrock surface map is important because this parameter defines the saturated thickness (water table minus bedrock surface) of the glacial aquifers. Raster-based bedrock elevation map was generated by interpolating the bedrock surface elevation data recorded in the oil, gas, and also deep water wells (GWIM, 2006). However, the data resolution for these wells (with bedrock surface elevation data) is not very good and especially for the Upper Peninsula, data is sparse.

In order to test the accuracy of the raster-based bedrock surface map (with 500 m of resolution), following steps are applied:

- Using IGW, 90 m SRTM land surface data for a portion of the Upper Peninsula, is remapped onto a grid with a cell size of 500 m resolution
- The resulting DEM grid is extracted into ArcGIS
- The raster-based bedrock surface data is subtracted from the raster-based DEM data
- The final product gives the glacial thickness

The reason that a statewide glacial thickness map with 500 m of resolution isn't generated is because it is computationally impossible to map the DEM data at state scale by using such small grids. Glacial thickness map created for the accuracy test, along with the wells that are used to produce the bedrock surface map, is shown in Figure 36.

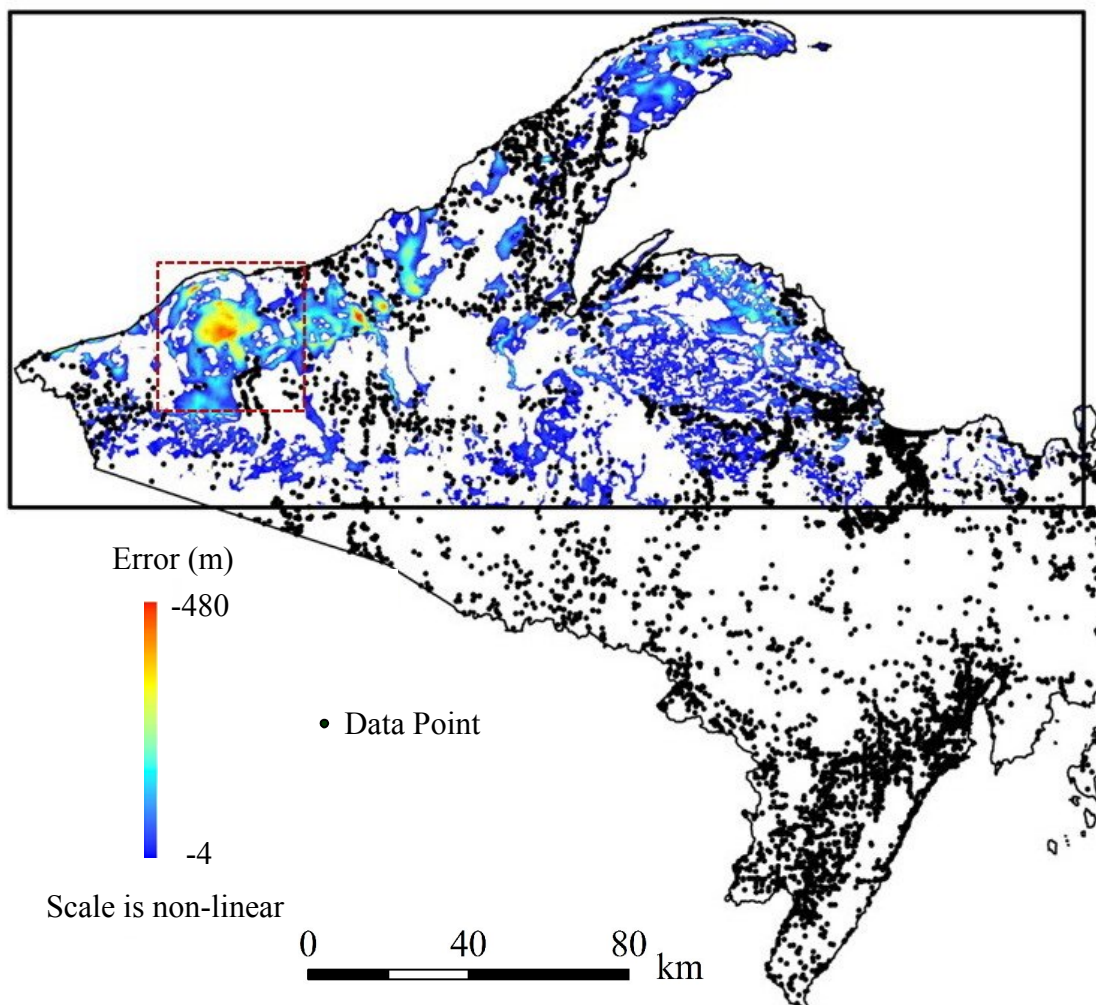


Figure 36: Error locations for the bedrock surface map of the Upper Peninsula.

Figure 37 zooms into the red box shown in Figure 36 to have a closer look at the data resolution used in the interpolation. It is observed that, at certain locations where there is no data available, error produced with the interpolation increases, as expected.

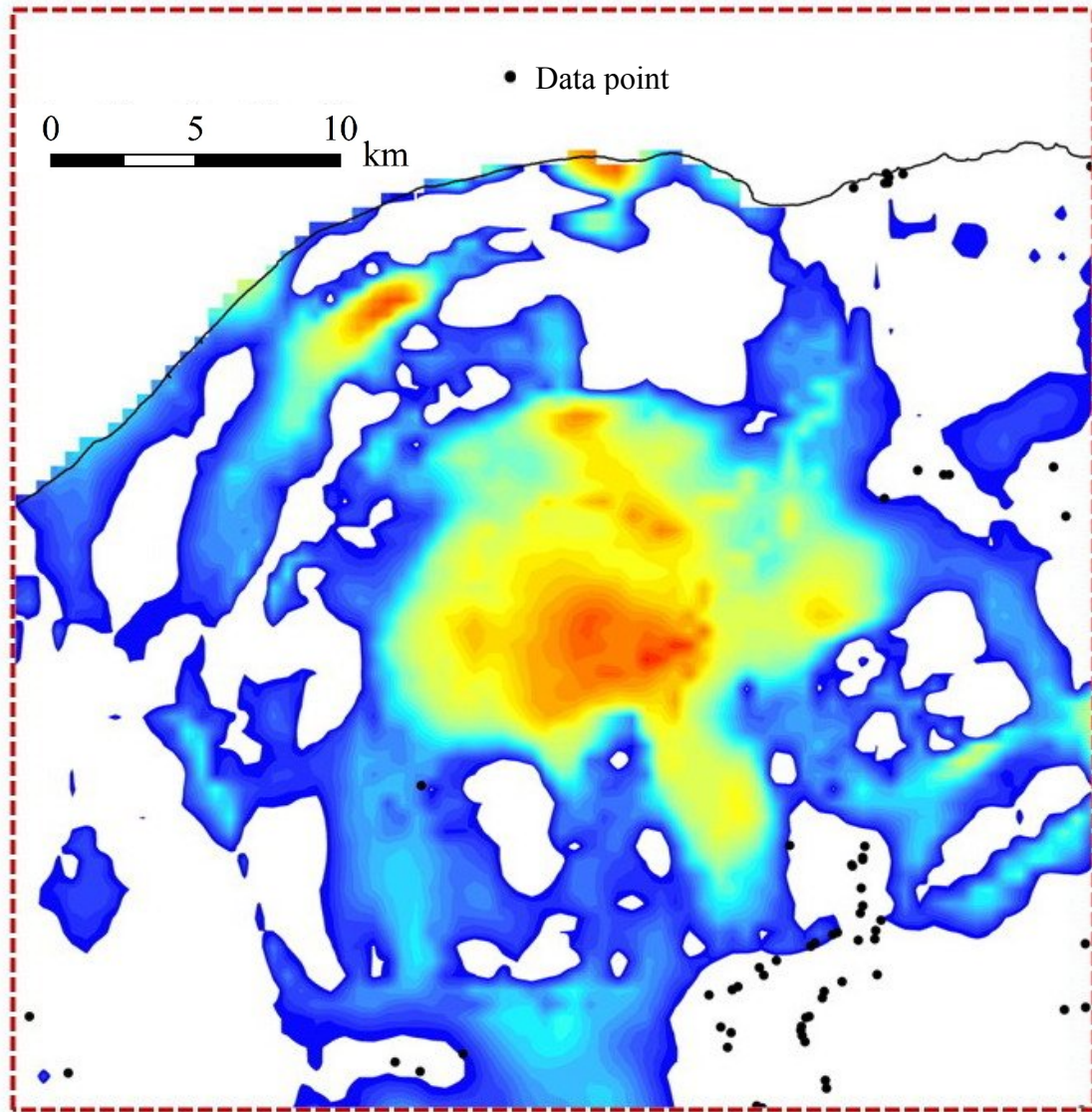


Figure 37: Magnifying the error in the bedrock surface map and available data points in the Upper Peninsula.

The cause of the interpolation artifacts shown in Figure 37 is also illustrated in Figure 38. While the interpolation uses the data at the well locations, if the data density in between those data points is not good enough, the interpolation might end up with very bad representations of the reality.

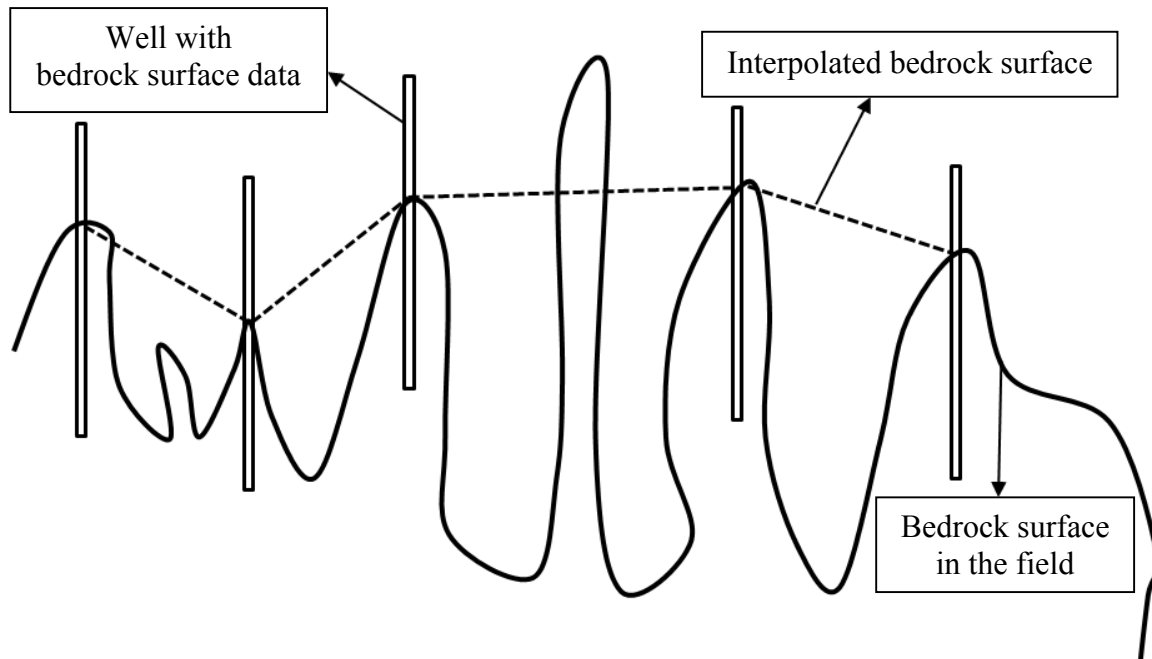


Figure 38: Conceptual picture of the possible reason for the error in the bedrock surface map.

Since in the Lower Peninsula, data resolution is much better than that of the Upper Peninsula, it is assumed that the raster bedrock surface map for the Lower Peninsula is a good representation of the reality.

Results from the analysis on the accuracy of the bedrock surface map indicate that there is a need for the revision of this map. However, for the groundwater models developed for this research, since there isn't a dataset available with a better resolution to generate a new bedrock surface map, existing map is used to define the bottom elevation of the glacial aquifer.

Reproduced GIS Files

To improve the computational efficiency, to develop seamless raster-based data definitions, and where possible, to improve the conceptual representation of the model

parameters, some of the statewide data files are reproduced. Final database is coupled with models to provide a flexible and interactive data environment that allows the simultaneous use of the vector-based and the raster-based geospatial data.

Raster-based land surface elevation. The USGS and Earth Resources Observation and Science (EROS) Data Center (EDC) provides access to *The National Map Seamless Server* (available online at <http://seamless.usgs.gov/>) which makes it possible to explore and retrieve countrywide land surface elevation data from the *National Elevation Dataset (NED)*. NED is the primary elevation product of the USGS and it is a seamless dataset with the best available raster elevation data of the United States. The NED data is distributed in geographic coordinates in units of decimal degrees, and in conformance with the North American Datum of 1983 (NAD 83). All elevation values are in meters and the NED of Michigan is available for 30 m (1 arc-second) of resolution everywhere in the state. NED provides data with a resolution of 10 meters (1/3 arc-second) or higher for only 85% of the United States, and most of Michigan is among the 15% where the 10 m DEM coverage was generated from oversampling of 30-meter DEM source data (USGS, 2006; 2009).

Other than the NED data, the USGS also provides *Shuttle Radar Topography Mission (SRTM)* data for the land surface elevation. SRTM is a joint project between the National Aeronautics and Space Administration (NASA) and National Geospatial-Intelligence Agency (NGA) to map the world in three dimensions. SRTM generates a digital topographic map of the Earth's land surface with data points spaced every 3 arc-second (about 90 meters) for global coverage of latitude and longitude (USGS, 2008).

Even though the DEM data provided by the USGS is pre-processed, it is still necessary to arrange the data in a way that makes it possible to use it for the groundwater models developed in this research. Following steps are applied to generate the GIS files for the model integration:

- The USGS raster-based NED and SRTM data for 10 m (sampled from 30 m DEM), 30 m, and 90 m resolutions are downloaded (from the National Map Seamless Server) in 485, 42, and 10 geographic tiles, respectively
- The numbers of the geographic tiles are optimized (e.g. each tile for 10 m dataset stores 50 MB of raster data) based on the limitations of the computational resources that are used to extract the data for the models
- A statewide polygon shapefile, that allows to locate the raster data for data transfer depending on the geographic extensions of the model area, is created

One of the final products, statewide 90 m DEM is shown in Figure 39.

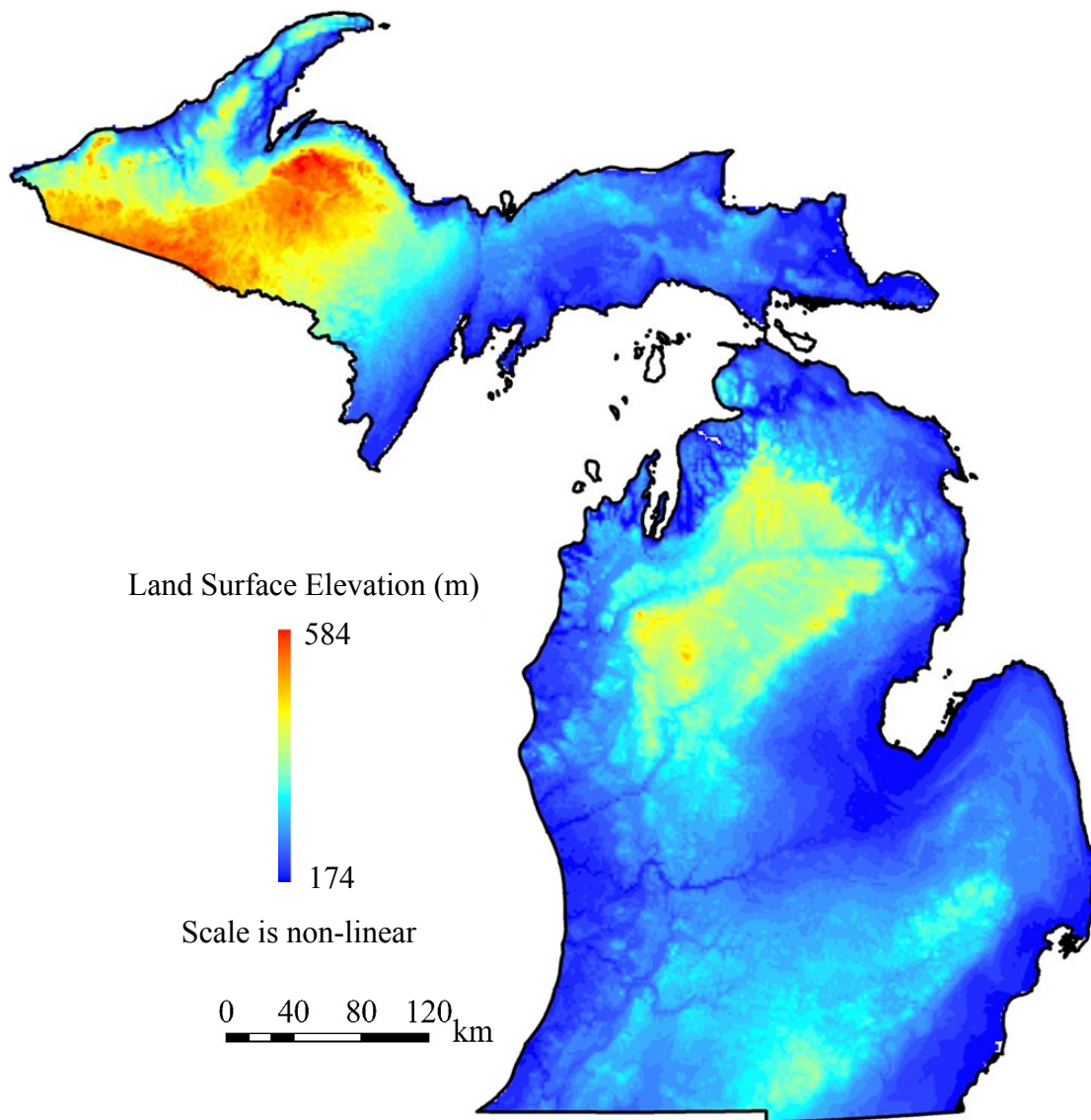


Figure 39: USGS 90 m raster-based DEM.

Raster-based hydraulic conductivity field. Along with the SWL data, hydraulic conductivity data is the most critical component needed for groundwater investigations. The distribution of water levels and hydraulic conductivity dictates the groundwater speed and direction. Both of these data are needed for most hydrogeological analyses such as contaminant transport predictions, remediation design, and well-head delineation (Simard, 2007).

Statewide raster-based hydraulic conductivity maps for HCOND1 and HCOND2 parameters are produced through the following steps:

- The state map of Michigan is divided into 8 seamless rectangular geographic tiles in ArcGIS
- The water wells (totally almost 200,000) for each tile are extracted in ArcGIS
- The HCOND1 and HCOND2 data in the water wells are interpolated (with a number of 300 nearest data points and a cell resolution of 540 m) within the tiles by using IGW's *Inverse Distance Weighting* interpolation interface
- After the conductivity fields for each tile are interpolated, they are extracted as the raster-based maps in IGW
- The resulting maps are merged in ArcGIS

Final products for the raster-based maps of the HCOND1 and HCOND2 parameters are shown in Figure 40.

Raster-based transmissivity. The statewide transmissivity map is improved through the following steps:

- The USGS point-based aquifer test analysis database is updated with the current available data which makes the use of 1,423 statewide data points where the previous map (GWIM) was generated based on 233 data points
- The polygons (USGS shapefiles), that were used to map the extent of the bedrock units based on the locations of the aquifer test wells and the interpretations of the county-based hydrogeological reports, are maintained from the MDEQ [*personal communication with Richard Mandle from the MDEQ*]

Even though the number of the data points used in the production of the transmissivity map is still not too many, it is a lot more than that of the ones provided with the GWIM, and the new map is considered as the best that can be created with the current available information.

The locations of the data points along with the bedrock geology polygons are shown in Figure 41. Here, the color map gives a general qualitative idea about the transmissivity distribution of the bedrock layers (Table 14).

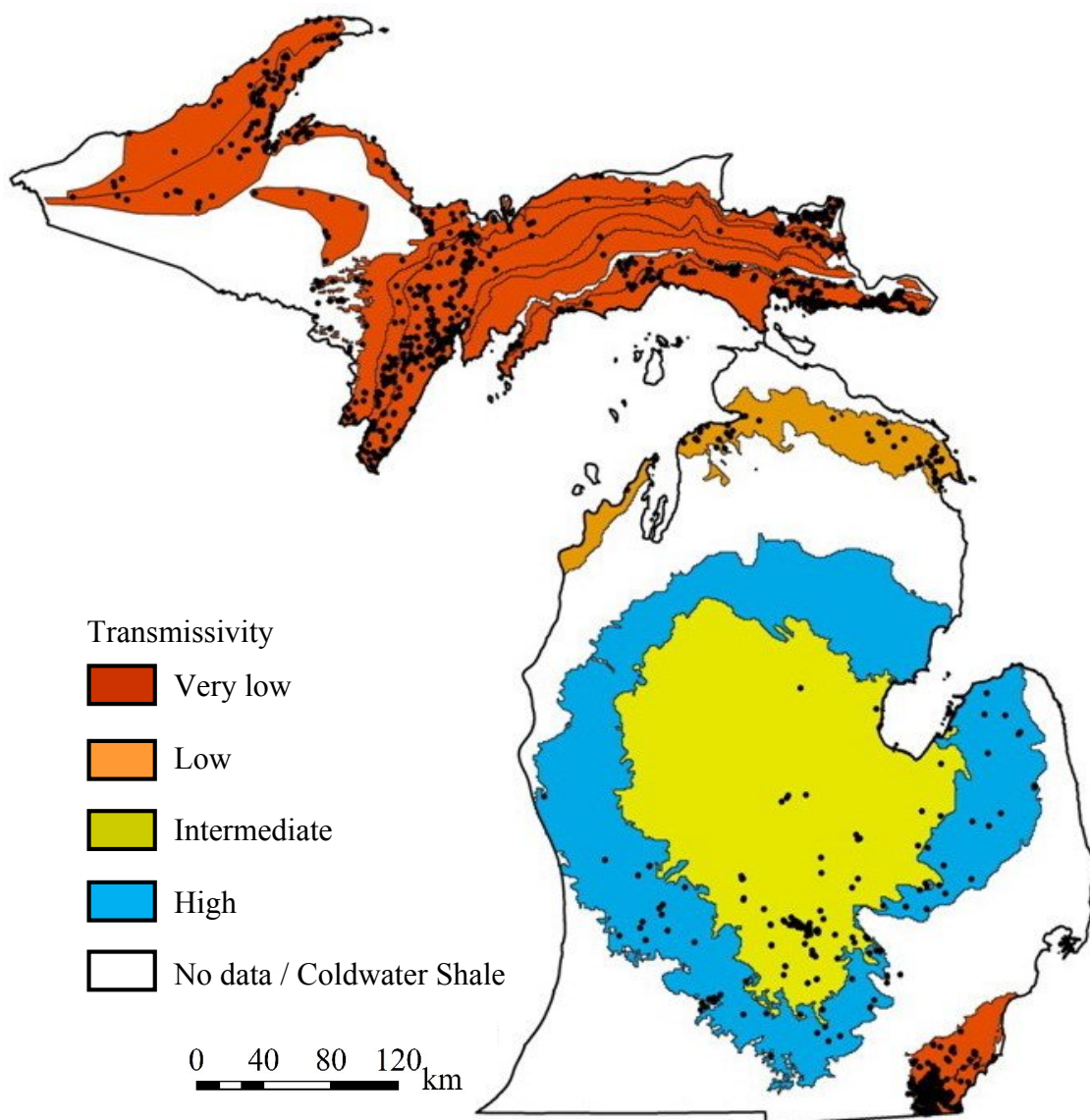


Figure 41: Color map for the transmissivity ranges generated based on the aquifer test data.

Table 14: Ranges for the color transmissivity map.

Class	Average T (ft ² /d)
Very low	< 500
Low	715
Intermediate	2,344
High	13,802

The minimum transmissivity value recorded in the database is 0.32 ft²/d and located in the western Upper Peninsula, where the maximum value is 142,062 ft²/d and located in the Lower Peninsula (Marshall Aquifer). For the Coldwater Shale unit, a constant value of 1 ft²/d was assigned to define the transmissivity used in the models.

After the data points are arranged based on the geological layers they represent, these data points are interpolated through the Kriging interpolation interface of IGW within the polygon coverage they are located in. The resulting transmissivity contour maps are then converted to the raster maps to produce the final statewide transmissivity database.

Raster-based stream data. In the NHD GIS files, for the streams of 3rd and greater orders, some polyline segments that follow the shorelines of the Great Lakes are detected. These segments are called the *coastline reaches* and they are artificial paths that were added to delineate the coasts (here the Great Lakes) of the country (USGS, 2000). Even though these artificial segments don't have a conceptual meaning in the groundwater models developed in this research, in the database, stream stages are also stored for these polyline features (Figure 42). In

the figure, only the 5th and 6th order streams with artificial lines on the boundaries of the Great Lakes are shown.

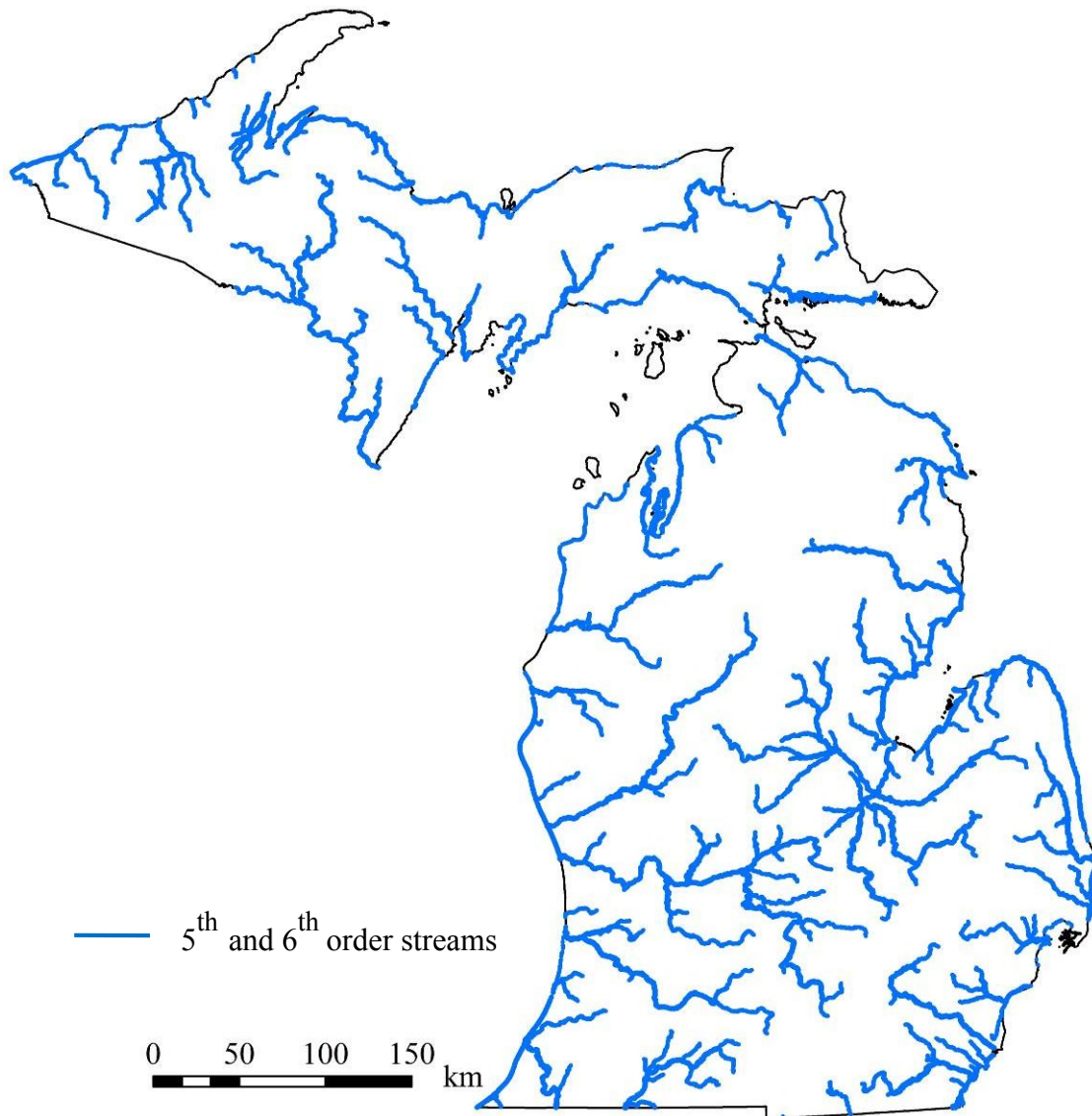


Figure 42: High order streams with artificial lines along the shores of the Great Lakes.

IGW still recognizes these artificial segments as streams in a way that might introduce artificial fluxes in the models. To resolve this issue, artificial paths along the shorelines of the

Great Lakes (Michigan's state boundaries) are removed, and a new stream data set for the stream network is generated.

In the raster-based DEM maps, land surface elevation in a stream segment of the NHD can be considered as the stream stage at that location. Since the raster-based USGS DEM data provided with this research improves the accuracy of the land surface elevation data, it can also quantitatively improve the stream stage information across the state. Within this context, Prof. Shu-Guang Li *et al.* at MSU developed a code to directly extract the stage information based on the NHD's polyline stream network coverage projected onto the raster-based DEM. According to this code, if the polyline passes through a raster cell, the code assigns that cell as a stream cell and records the DEM value stored in the raster cell's center as the stream stage for that cell (Figure 43).

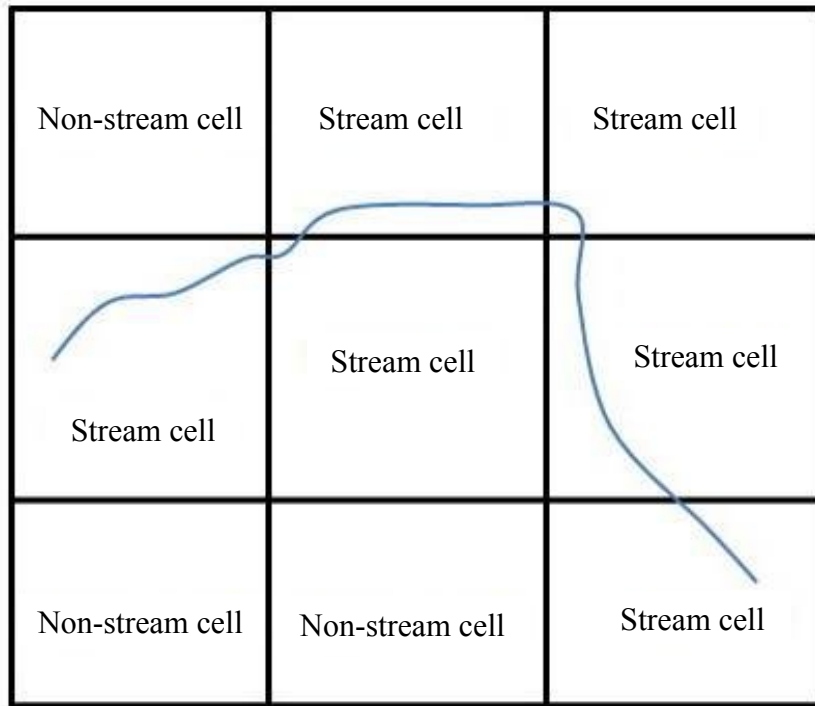


Figure 43: Conceptualization of the stream cells in the models.

DEM-based stream stage data is extracted, for all stream orders, from 30 m and 90 m USGS DEM. Currently, a stream stage data set based on the 10 m USGS DEM (sampled from 30 m DEM) is also available for only the streams with the orders of equal to and greater than 3.

Great Lakes boundary. A polyline coverage is created to delineate the shorelines of the Great Lakes. Long-term average lake levels that were provided by NOAA-Great Lakes Environmental Research Laboratory (website available at <http://www.glerl.noaa.gov/>) are assigned to the poylines along the shorelines (Table 15).

Table 15: Prescribed head values assigned for the shorelines of the Great Lakes.

Lake Name	Water Level (ft)
Erie	571
Huron-Michigan	578
St. Clair	574
Superior	600

Appendix D: Analysis of the Hydraulic Connection between the Great Lakes and Regional-Scale Heads

The primary driving forces that change the Great Lakes' levels are precipitation and evaporation. Water stored in the Great Lakes can change depending on the amount of the precipitation falling on the lakes and the runoff contributing from their surrounding watersheds. Based on the change in the water stored, the Great Lakes have had several major lake level (high or low) periods in the past. These temporary periods can be divided into six: 1960 – 1970, 1970 – 1976, 1976 – 1983, 1983 – 1989, 1989 – 1998, and 1998 – 2006 (GWIM, 2006; NOAA, 2010). To observe the temporal variations in the static water levels in connection with the lake level periods, glacial wells in the Van Buren County next to the Lake Michigan and the Kalamazoo County (Figure 44) next to the Van Buren County were separated into those periods, using IGW. Then the average SWL values for the corresponding periods were calculated for these wells and the results were plotted in Figure 45. Same water wells were also divided into annual quarters (January – March, April – June, July – September, October – December) for all times to observe the seasonal changes in the static water levels (Figure 46). The numbers of the wells for the periods used in the both analyses and the average static water levels from the analyses are shown in Table 16 and Table 17, respectively. Temporal comparisons show that while between the annual quarters, average SWL changes within a few feet of range (Figure 45), fluctuations within the Great Lakes level periods is a lot more (especially for the Van Buren County which is closer to the Lake Michigan) than that of the seasonal changes (Figure 46).

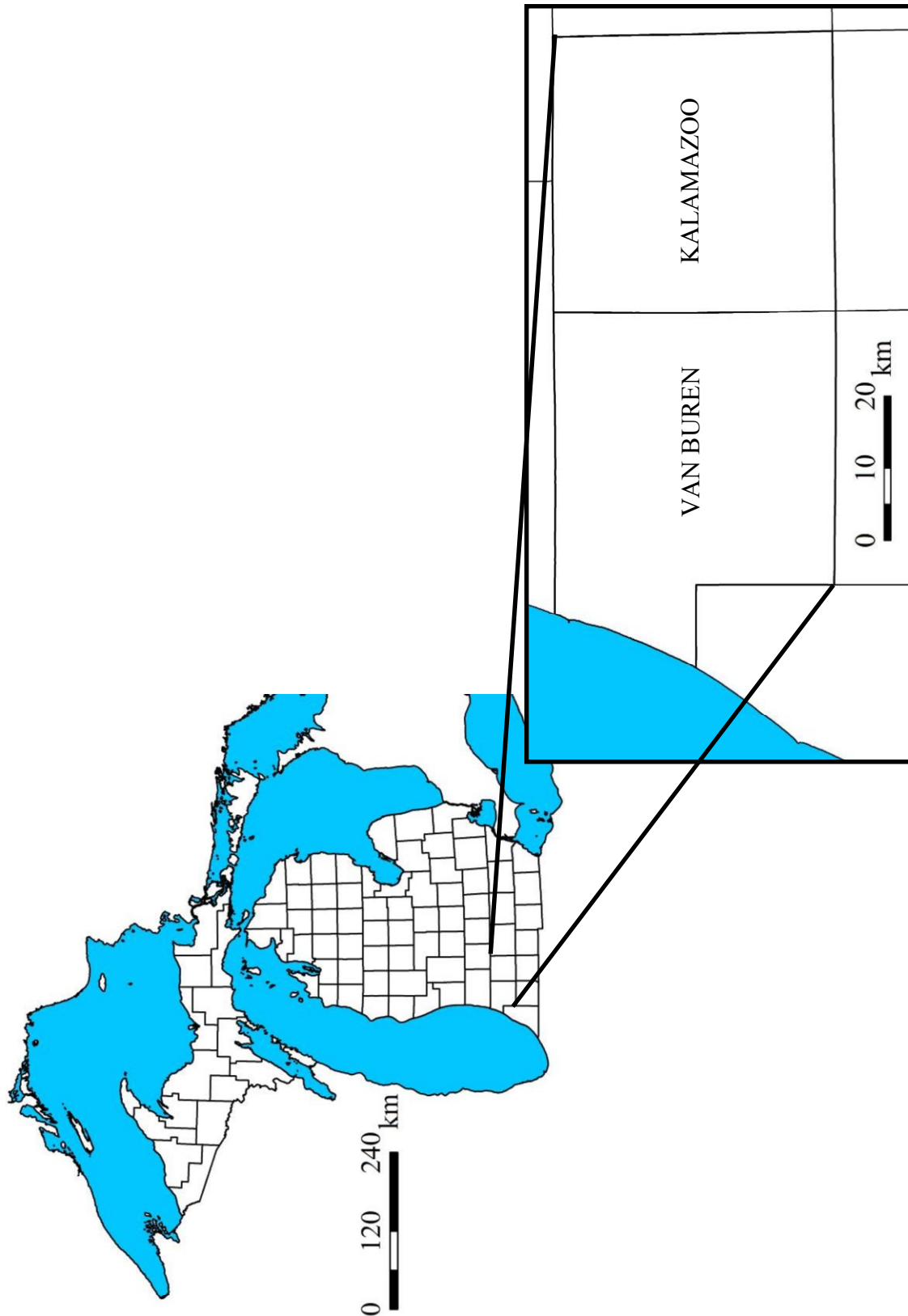


Figure 44: Location of the test area for temporal SWL analysis.

Table 16: Temporal analysis of the SWL based on the Great Lakes' water level periods.

Lake Level Period	Number of the Glacial Wells		Average SWL (ft)	
	Kalamazoo	Van Buren	Kalamazoo	Van Buren
1960 – 1970	266	283	843.50	723.48
1970 – 1976	531	914	844.77	719.04
1976 – 1983	1,320	808	846.97	710.74
1983 – 1989	2,094	901	849.29	729.57
1989 – 1998	4,088	83	847.41	753.72
1998 – 2006	3,036	2,206	842.26	725.49

Table 17: Temporal analysis of the SWL based on the annual quarters.

Annual Quarter	Number of the Glacial Wells		Average SWL (ft)	
	Kalamazoo	Van Buren	Kalamazoo	Van Buren
January – March	1,973	744	847.26	724.96
April – June	3,055	1,565	846.31	726.51
July – September	3,458	1,611	845.83	722.11
October – December	2,477	1,255	845.52	718.99

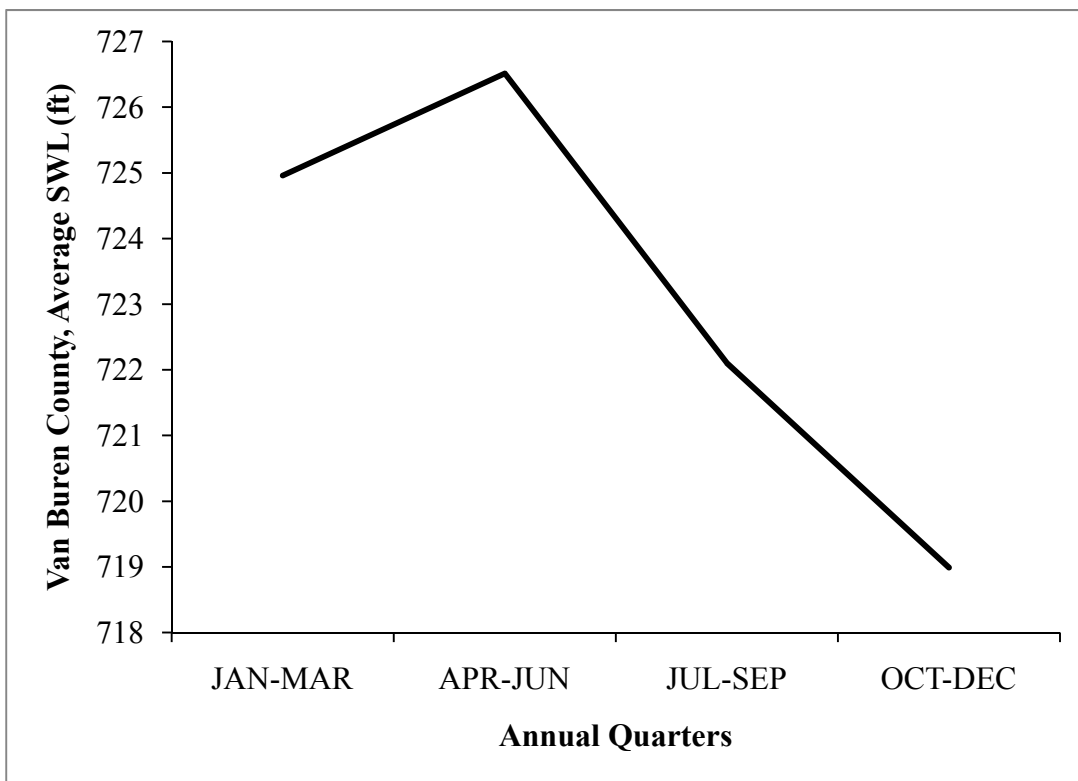
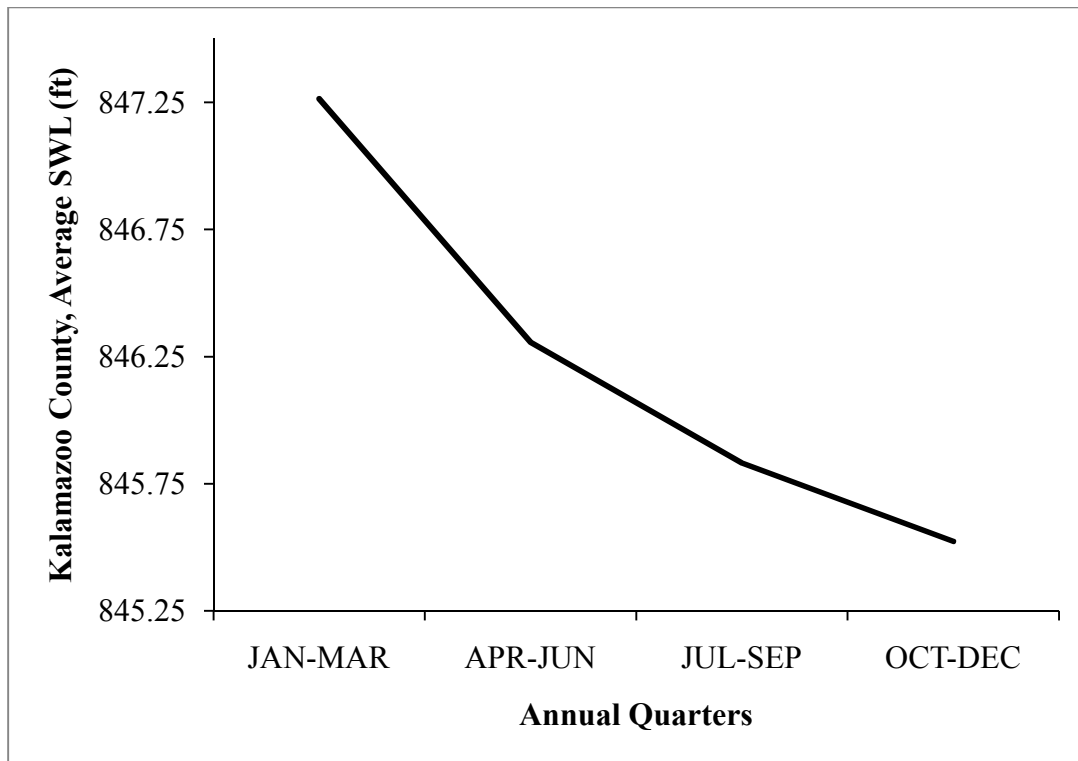


Figure 45: Temporal SWL analysis for annual quarters in the Kalamazoo and Van Buren County.

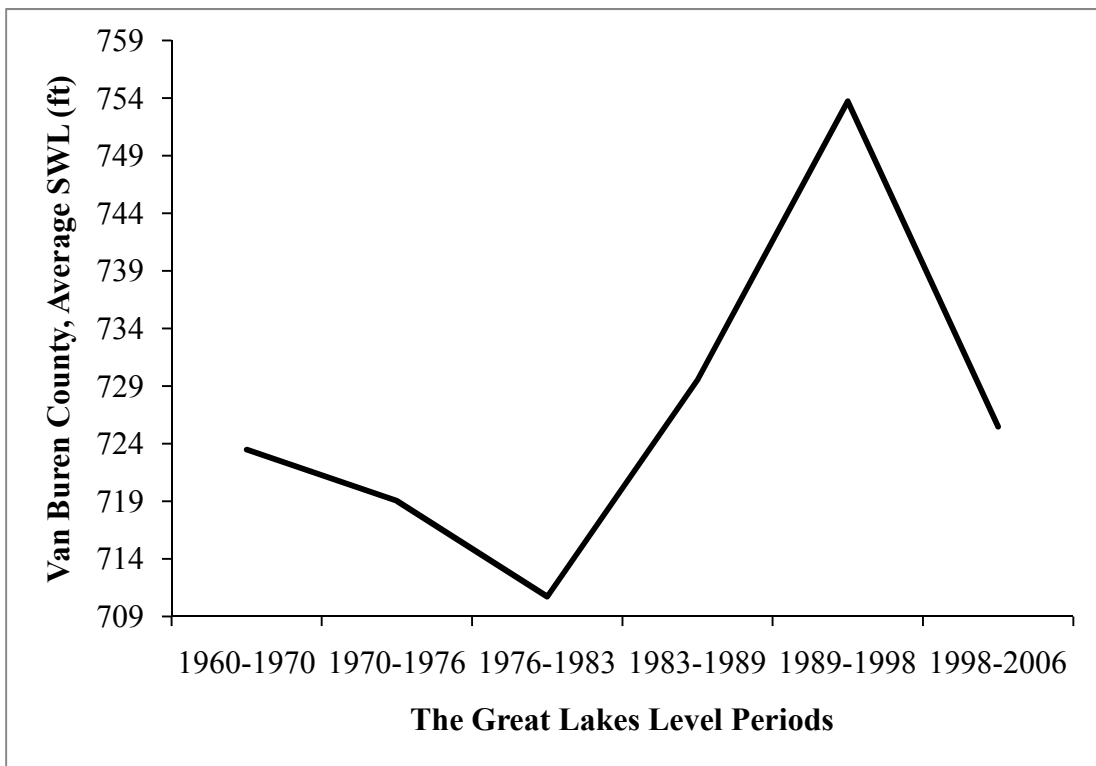
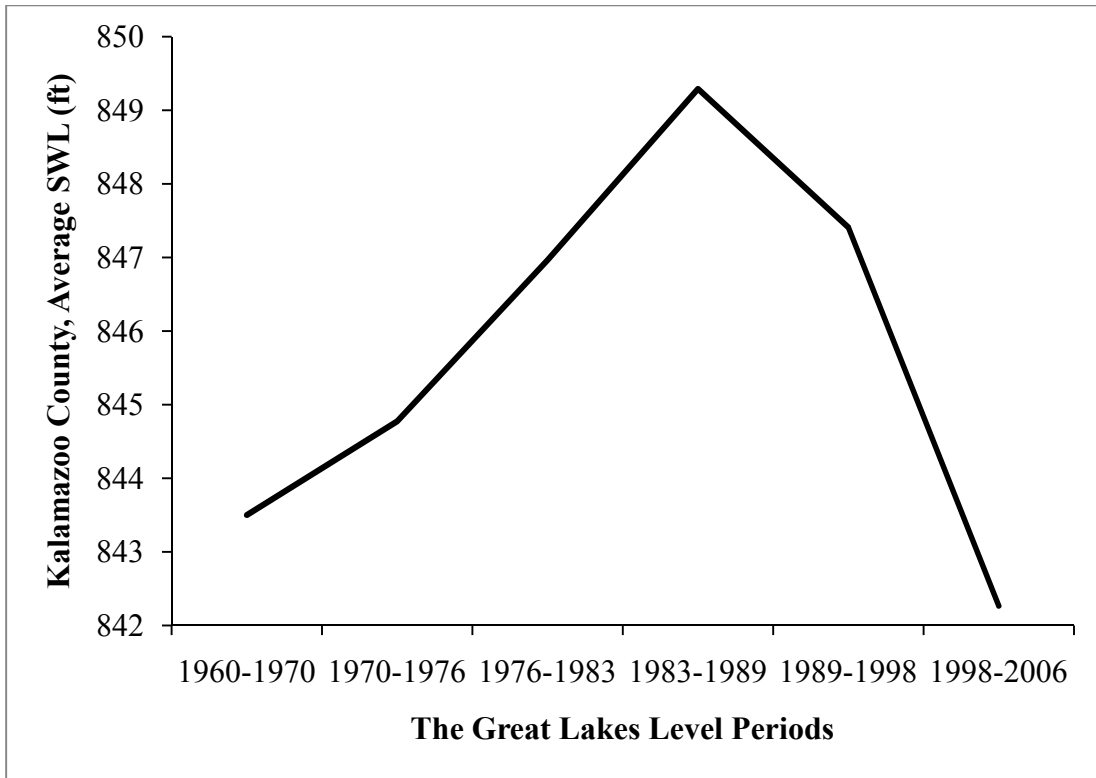


Figure 46: Temporal analysis for the Great Lakes water level periods in the Kalamazoo and Van Buren County.

The fluctuations in the groundwater levels are consistent with the high and low lake level trends in the corresponding periods. The results shown in Figure 46 are not surprising since groundwater and the Great Lakes are interconnected components of a regional hydrological system. Effects of the periodic climate changes in this system are observed in the Great Lakes and groundwater as water level changes. The connection between the Great Lakes' levels and the groundwater levels in both the glacial and bedrock aquifers along the shorelines of the Great Lakes can also be observed through the SWL values recorded in the water wells along the shores. The strong connection between the regional-scale groundwater flow dynamics and the Great Lakes maintains the main argument for the assumption of modeling the Great Lakes' shorelines as prescribed-head boundary condition.

Appendix E: Analysis of the Simulated Heads

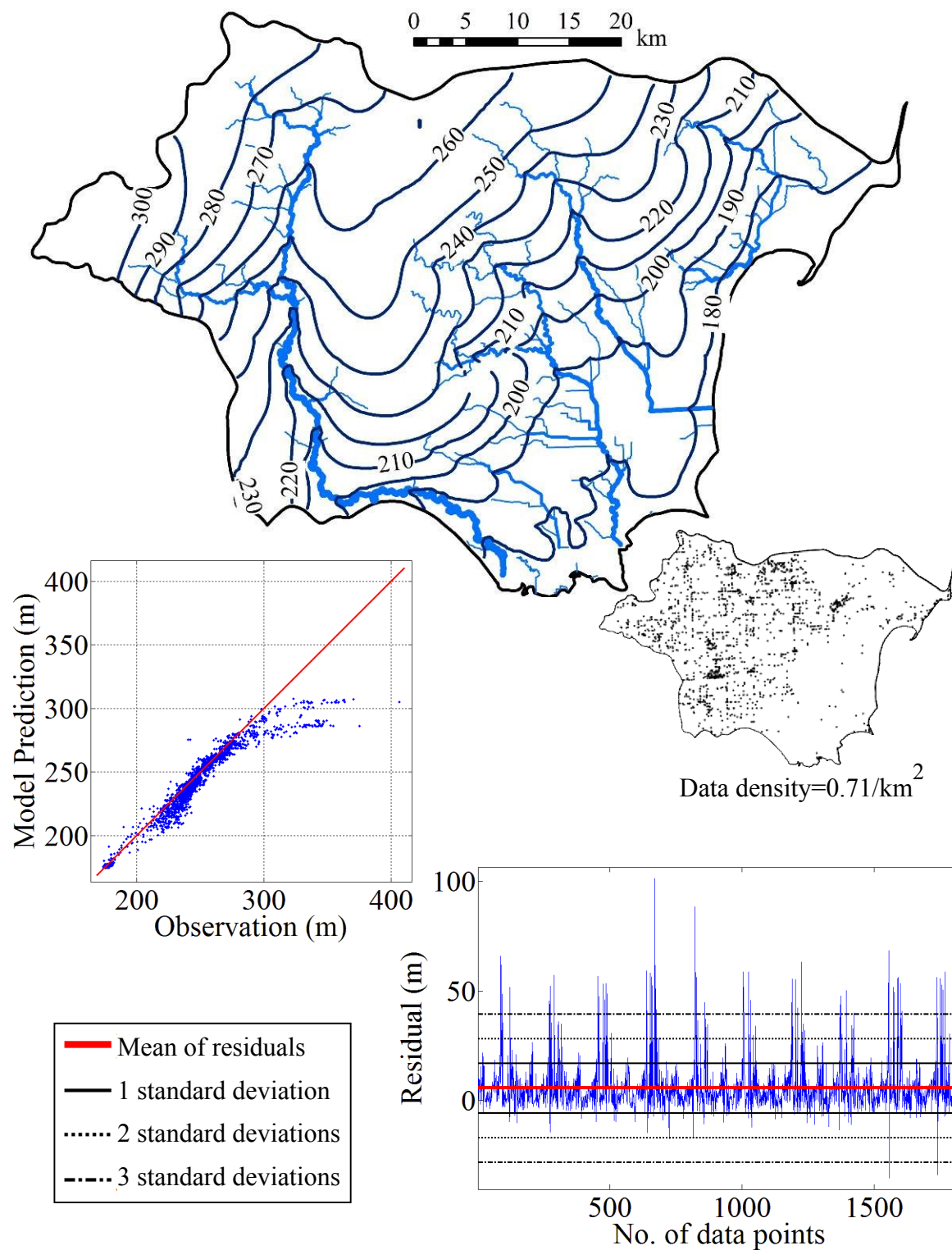


Figure 47: Analysis of the simulated heads in the Au Gres-Rifle Watershed, glacial aquifer.

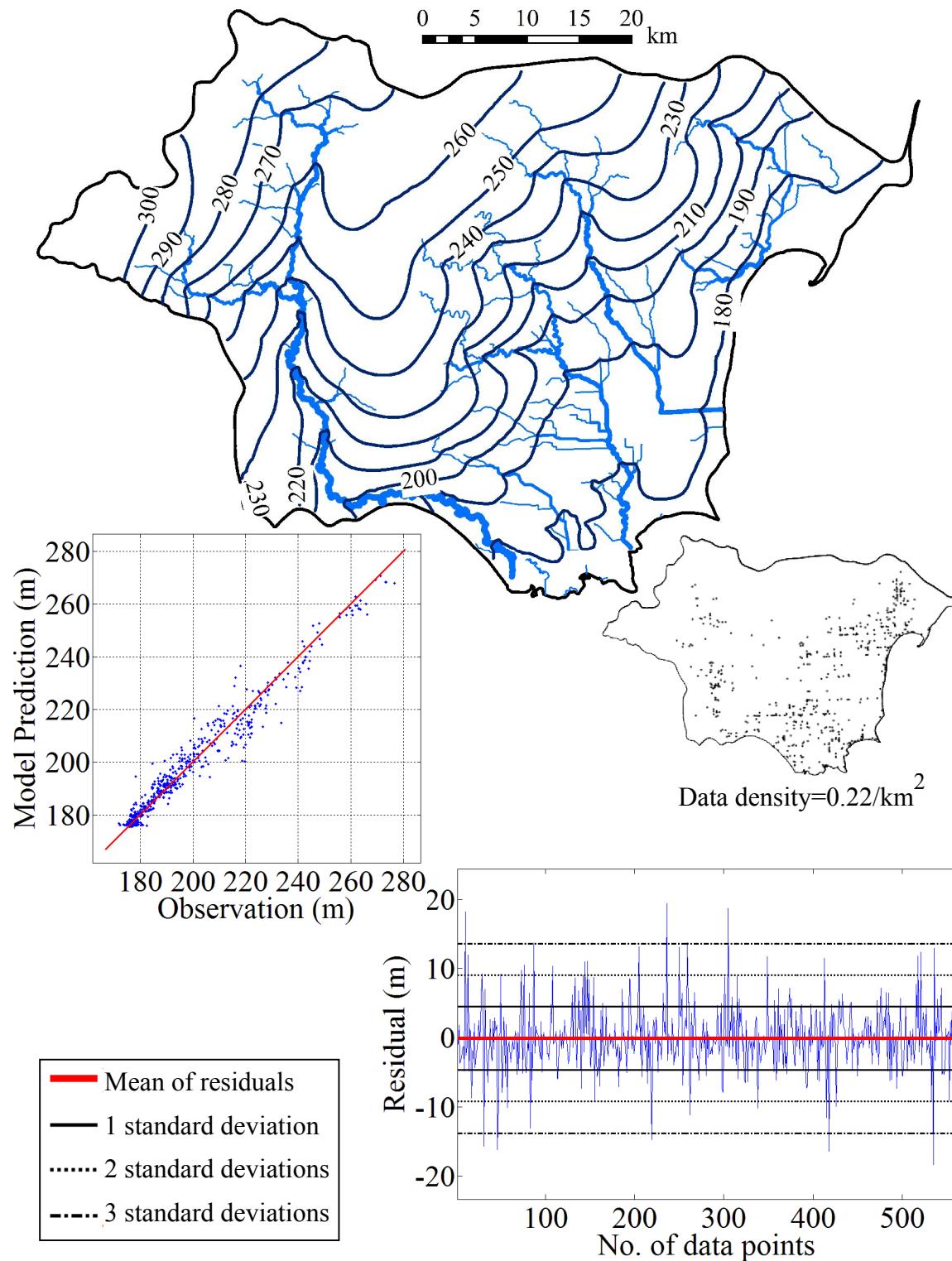


Figure 48: Analysis of the simulated heads in the Au Gres – Rifle Watershed, bedrock aquifer.

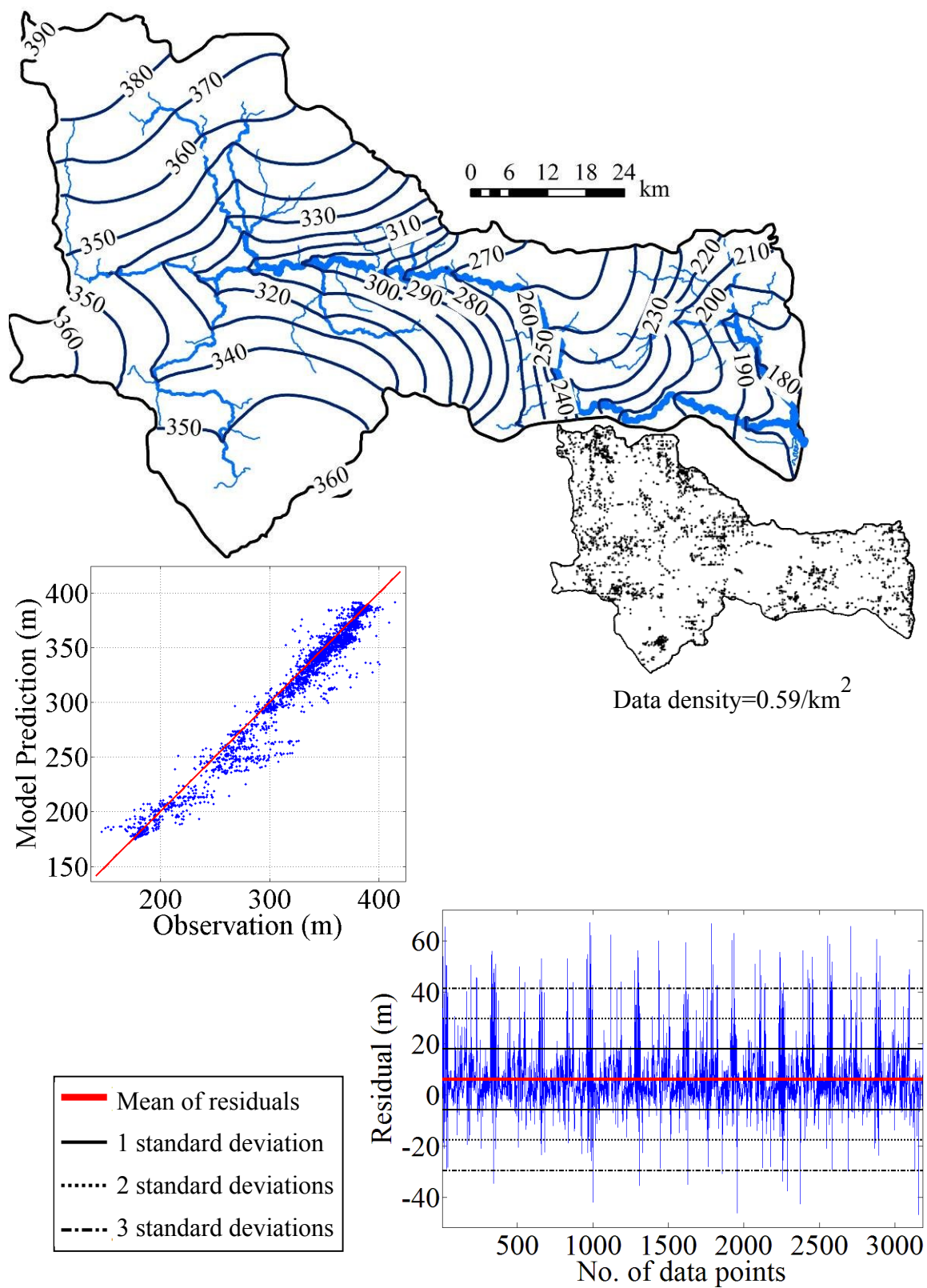
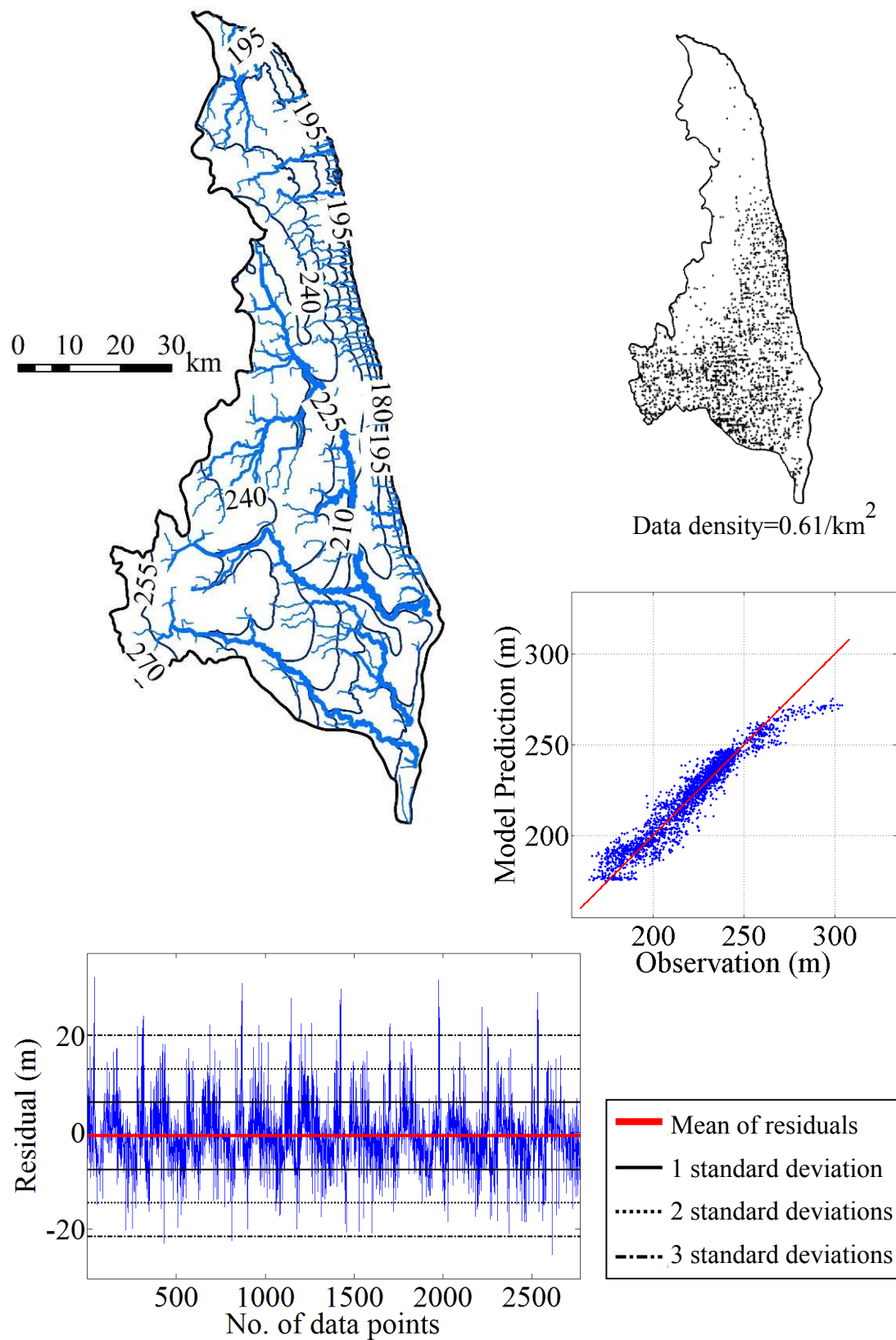


Figure 49: Analysis of the simulated heads in the Au Sable Watershed, glacial aquifer.



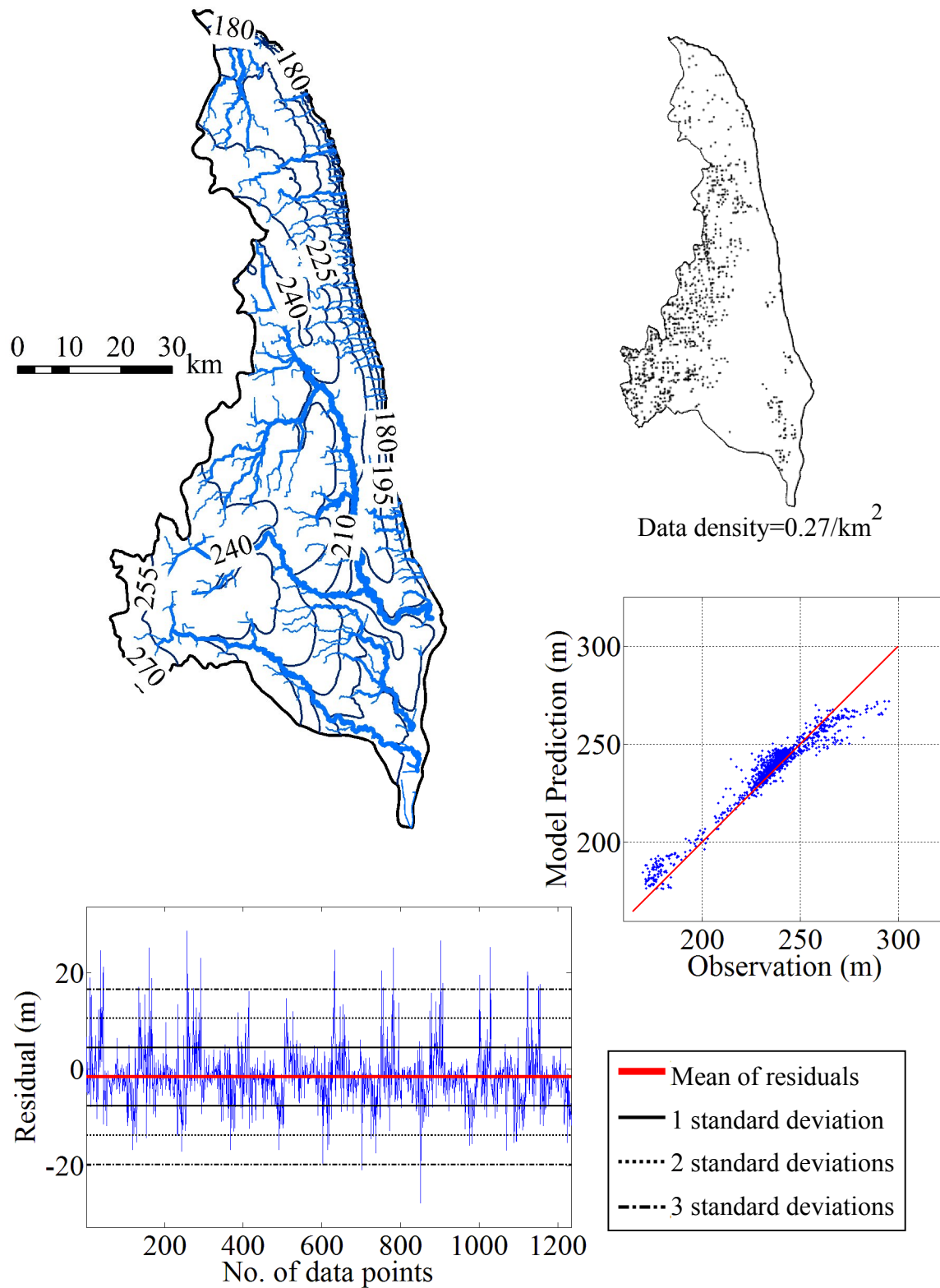


Figure 51: Analysis of the simulated heads in the Birch/St. Clair watersheds, bedrock aquifer.

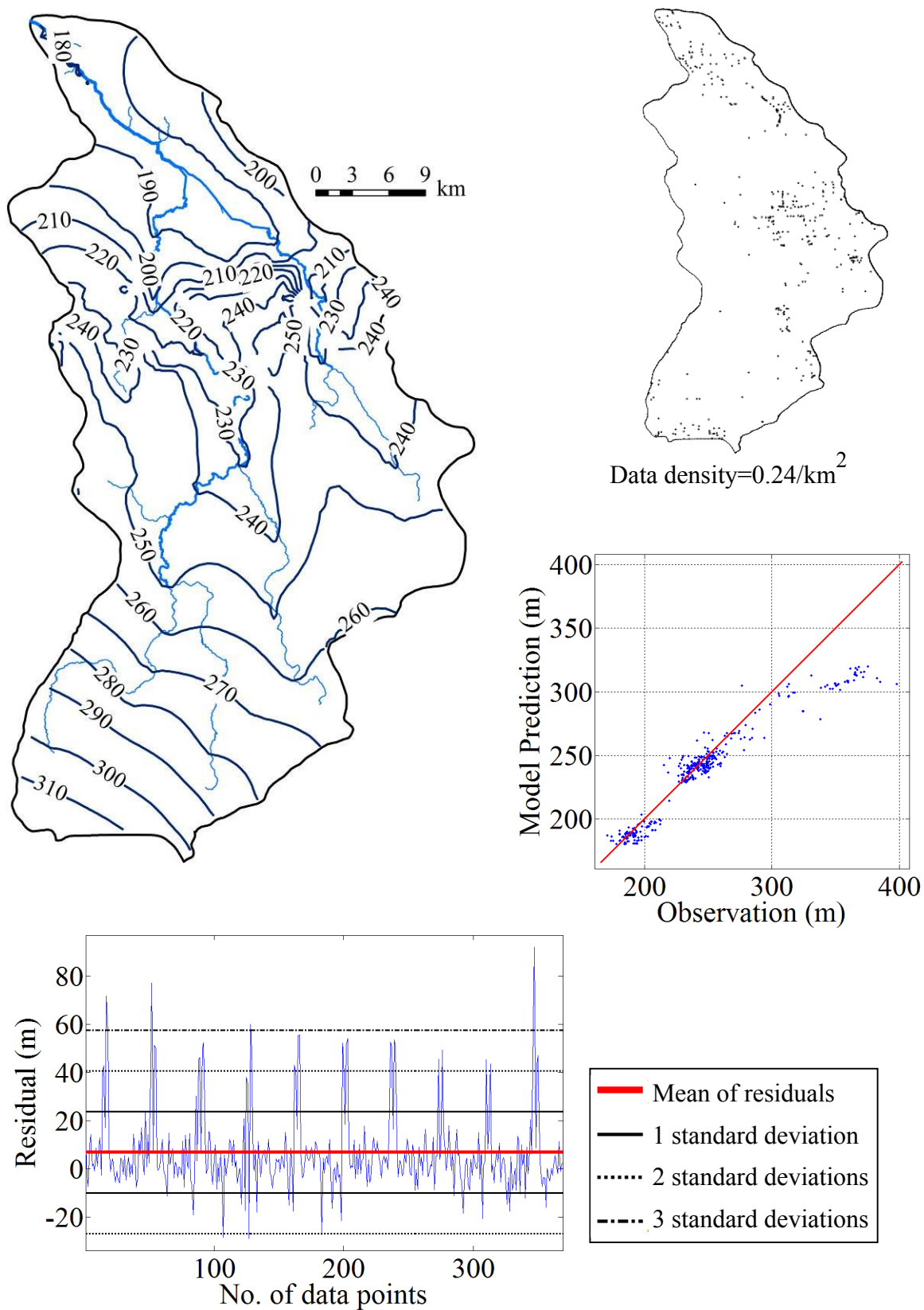


Figure 52: Analysis of the simulated heads in the Black Watershed, glacial aquifer.

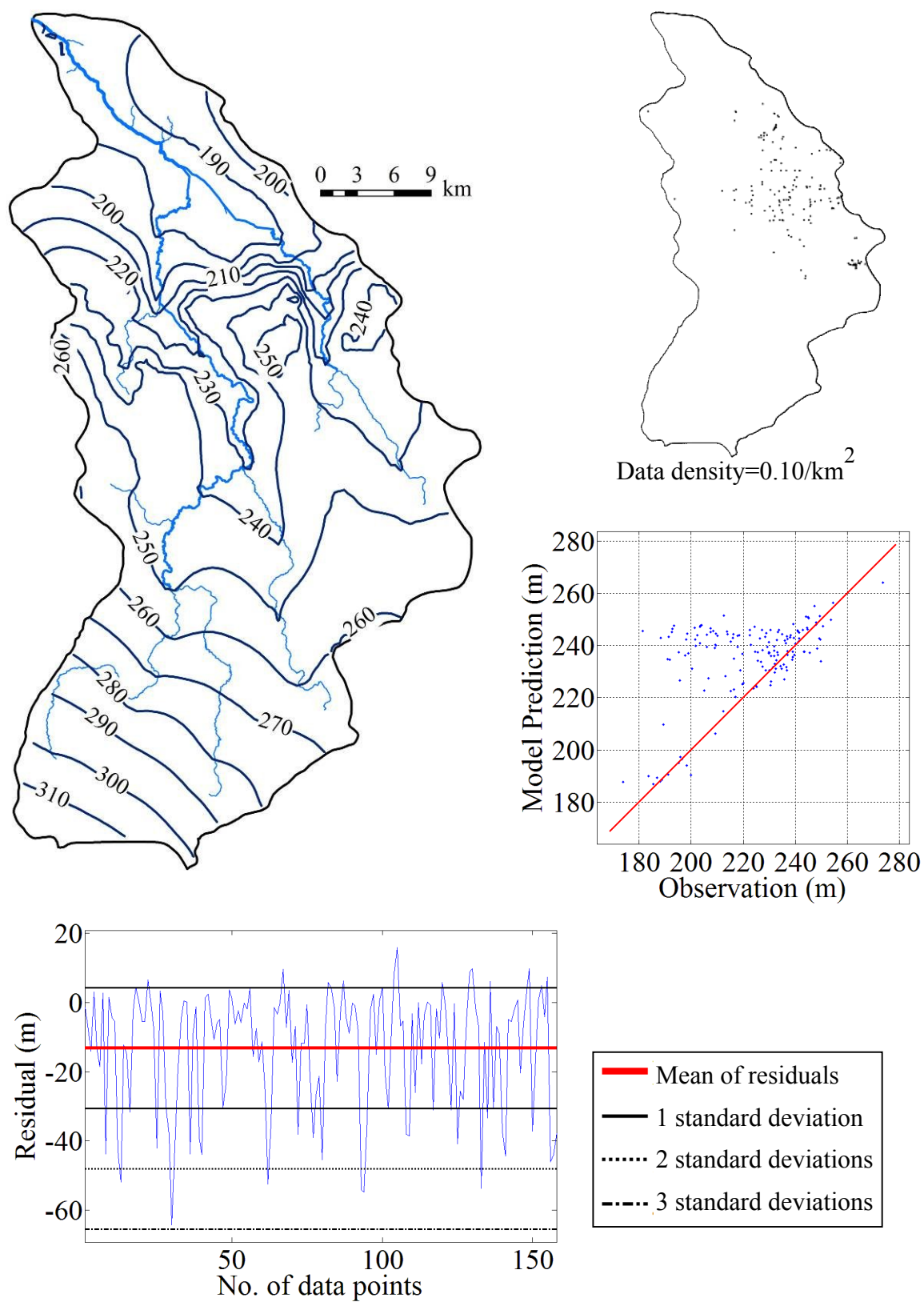


Figure 53: Analysis of the simulated heads in the Black Watershed, bedrock aquifer.

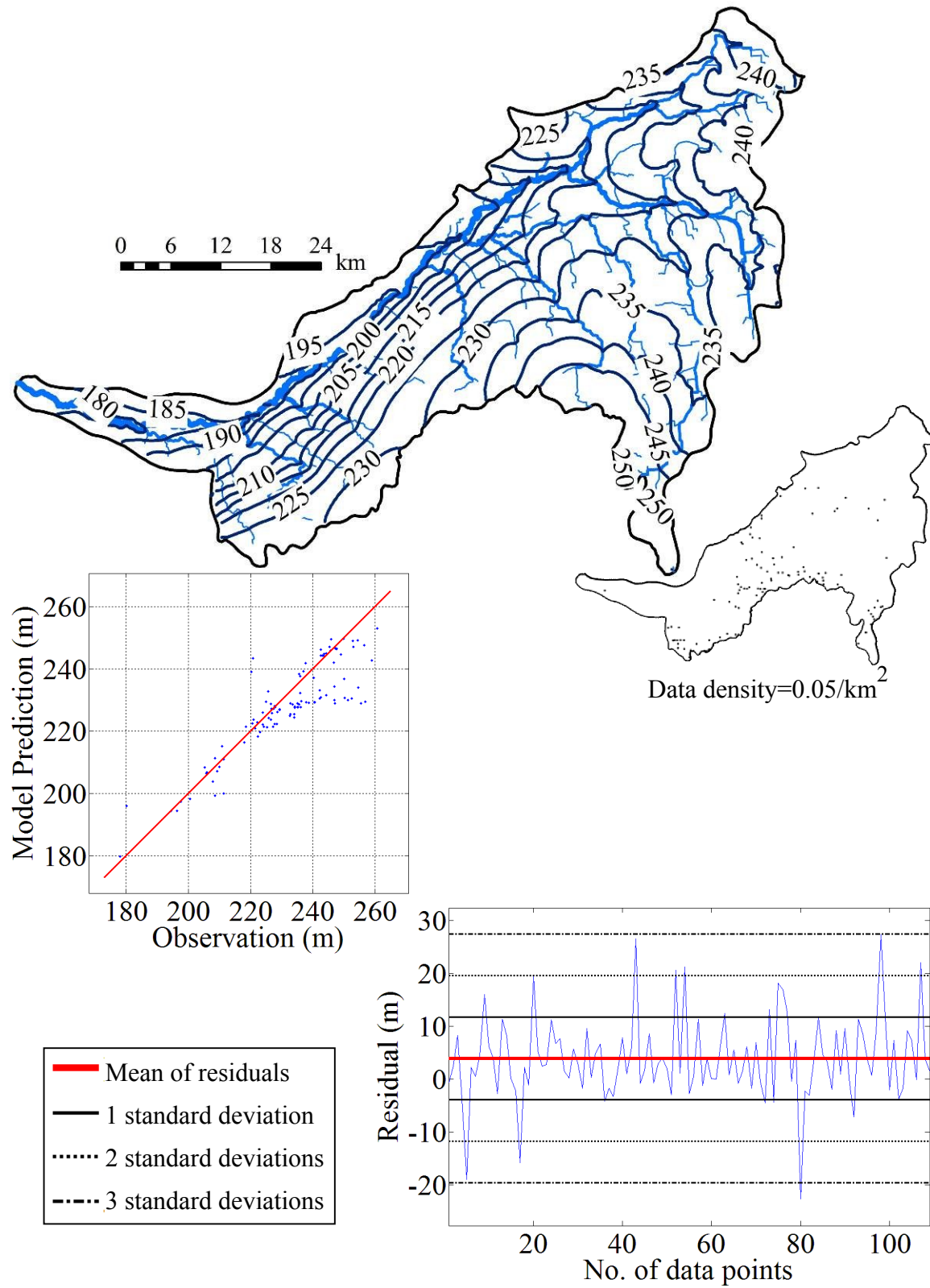


Figure 54: Analysis of the simulated heads in the Cass Watershed, glacial aquifer.

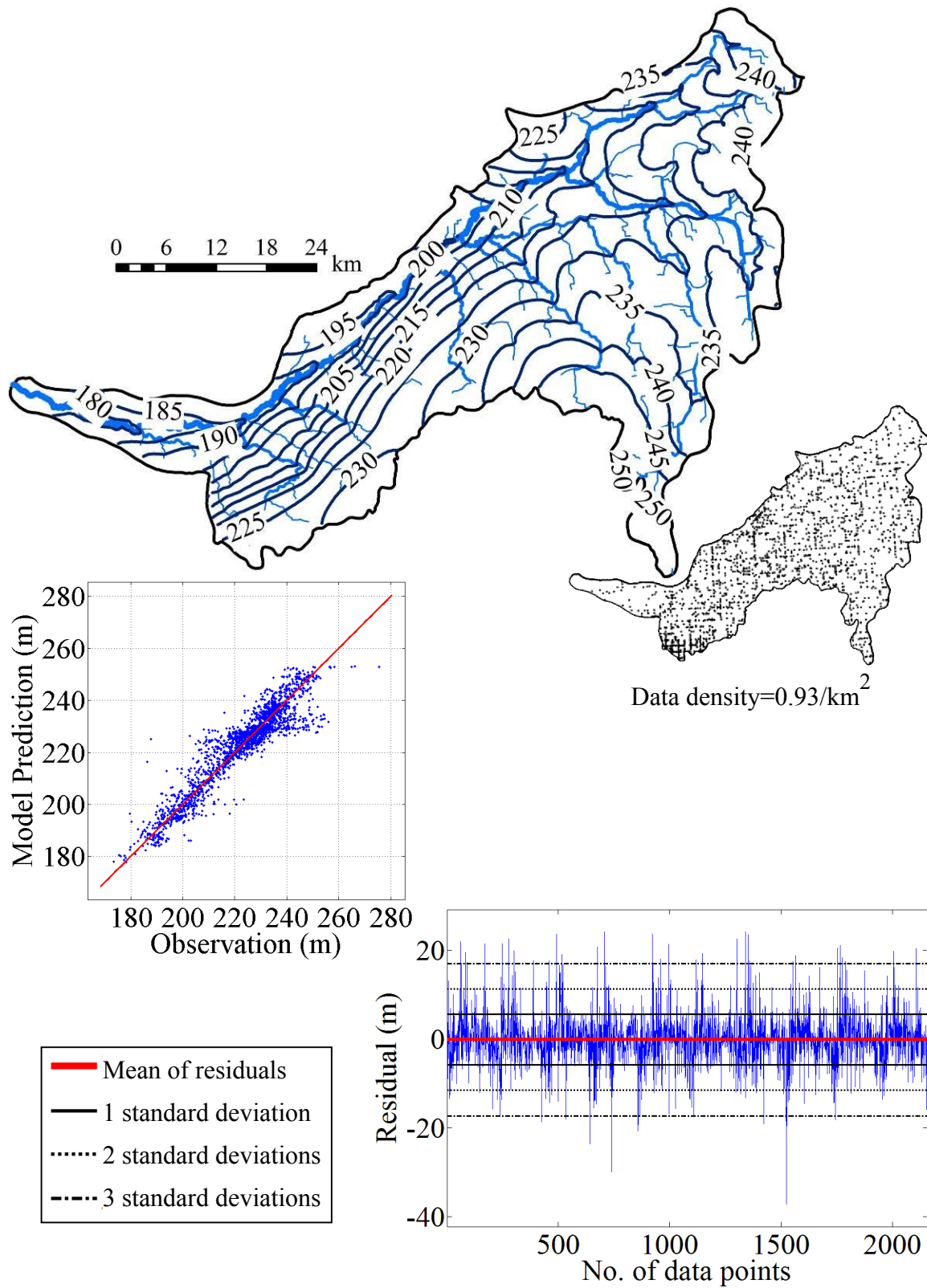


Figure 55: Analysis of the simulated heads in the Cass Watershed, bedrock aquifer.

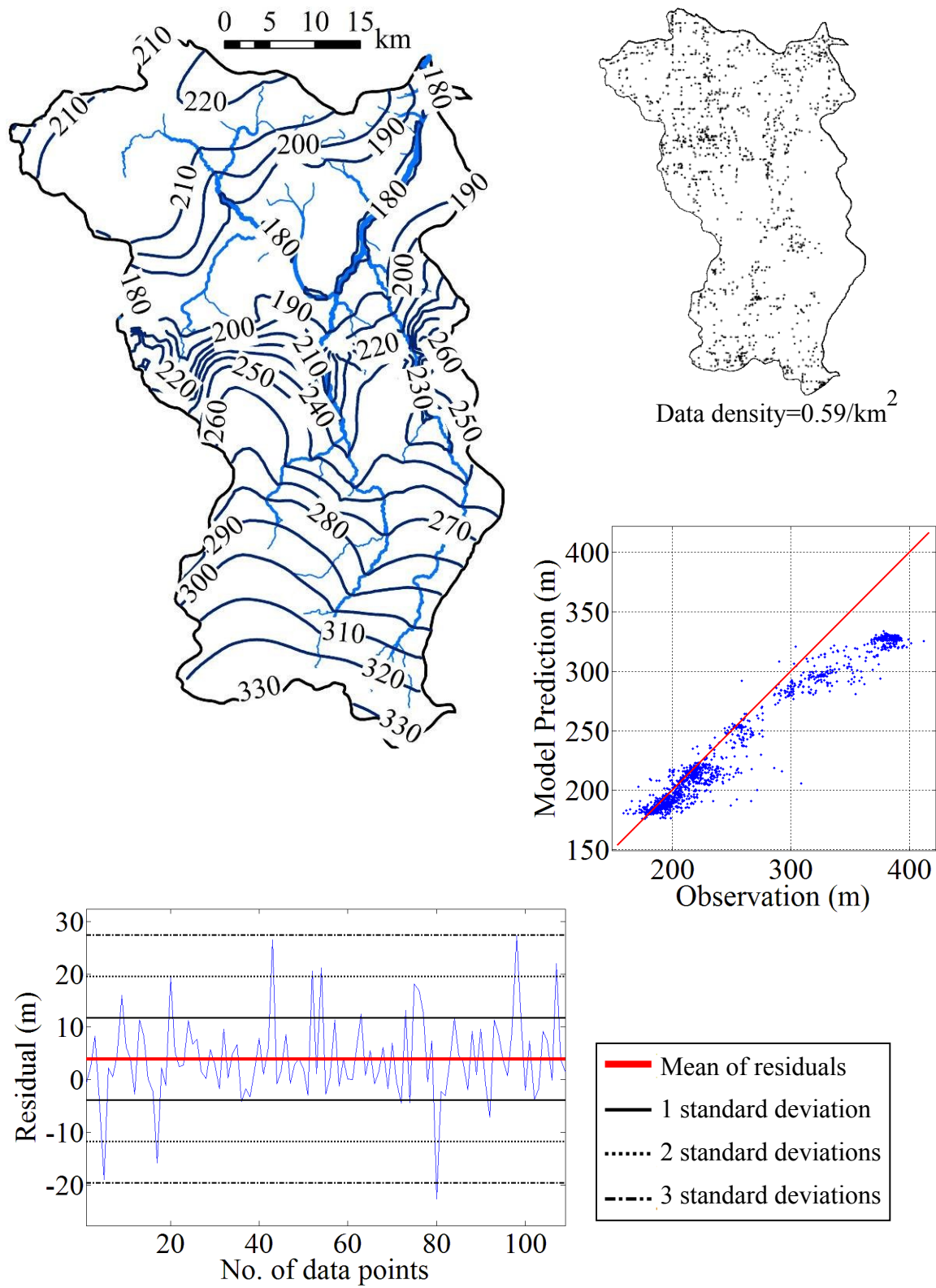


Figure 56: Analysis of the simulated heads in the Cheboygan Watershed, glacial aquifer.

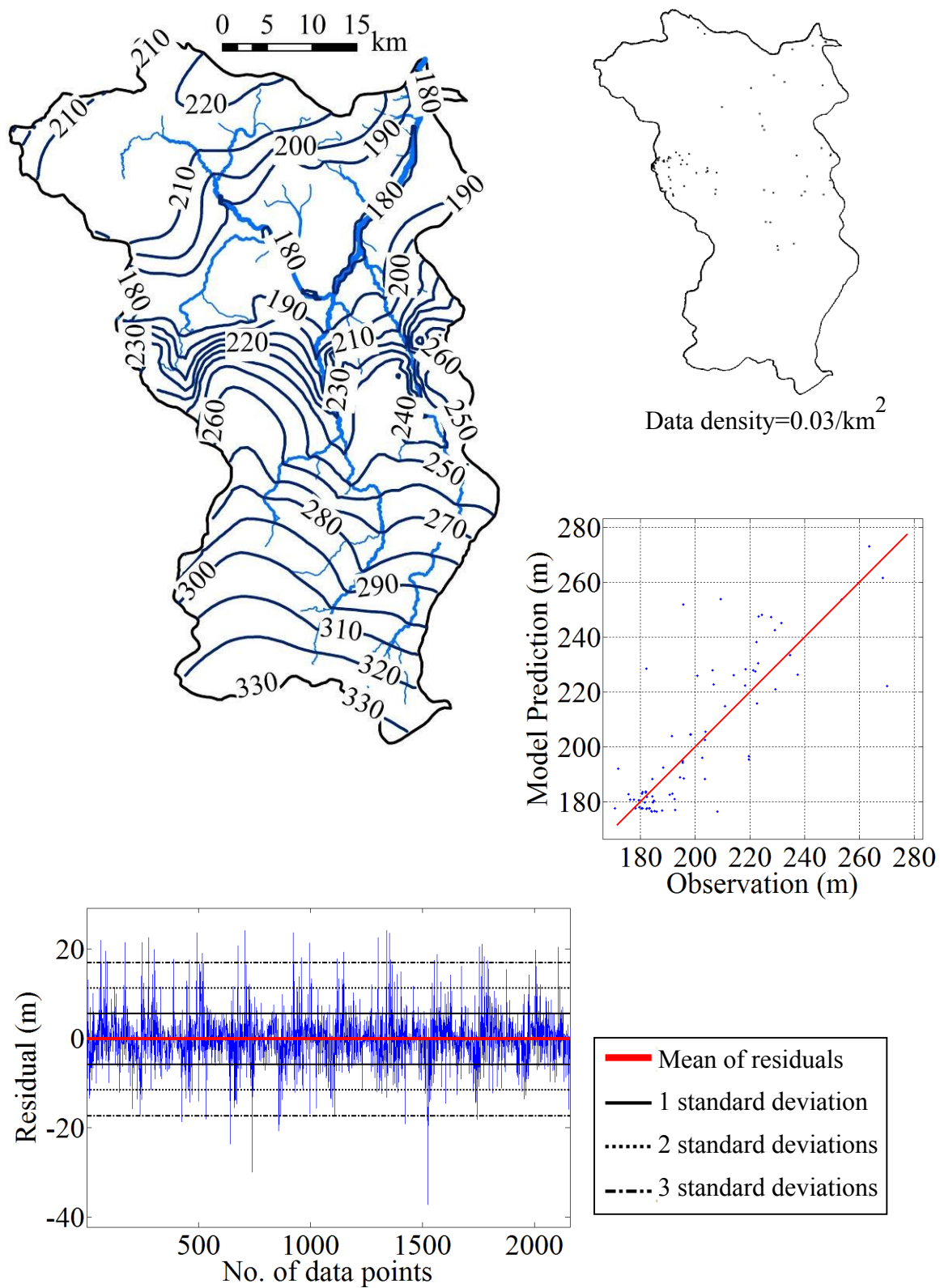


Figure 57: Analysis of the simulated heads in the Cheboygan Watershed, bedrock aquifer.

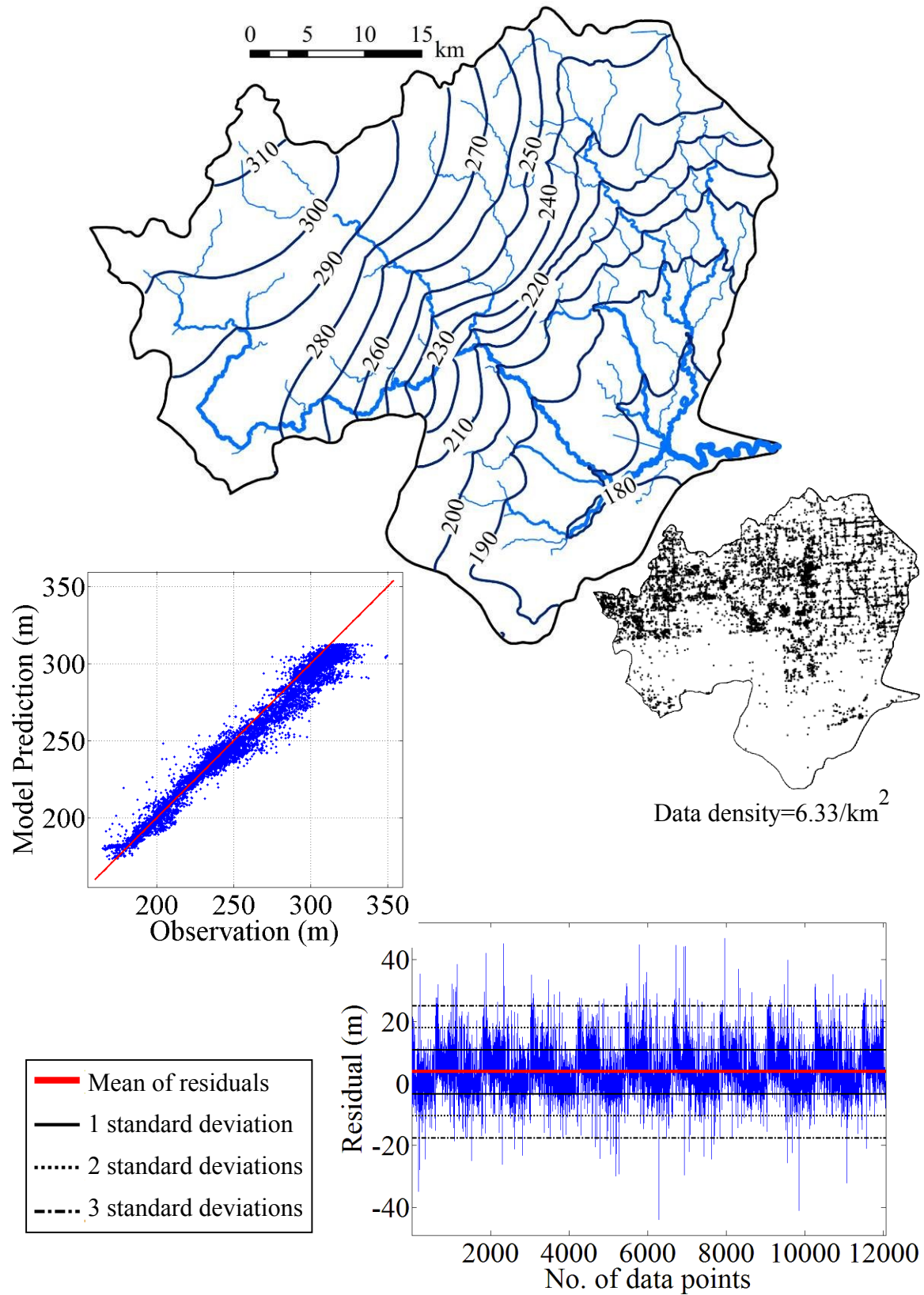


Figure 58: Analysis of the simulated heads in the Clinton Watershed, glacial aquifer.

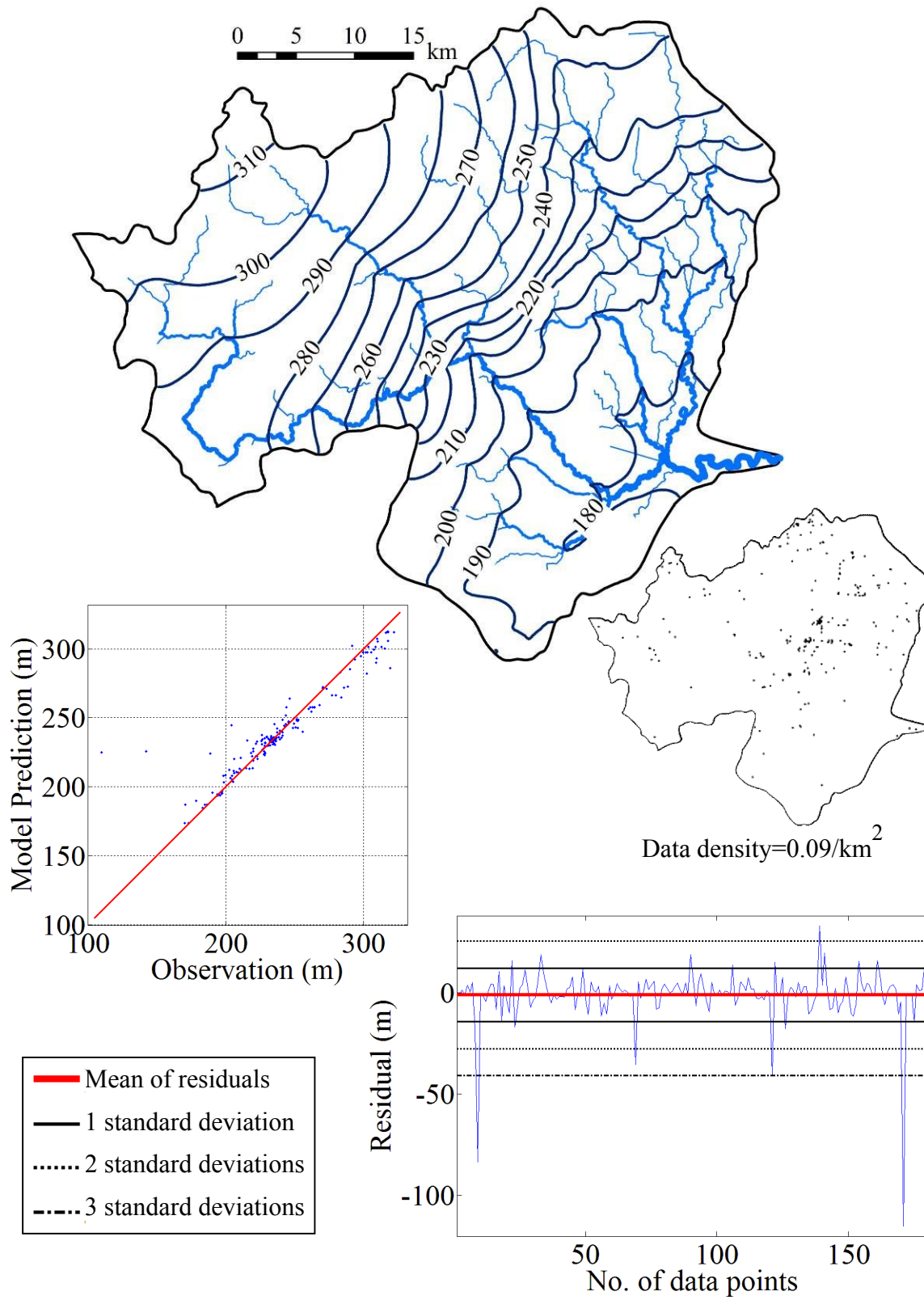


Figure 59: Analysis of the simulated heads in the Clinton Watershed, bedrock aquifer.

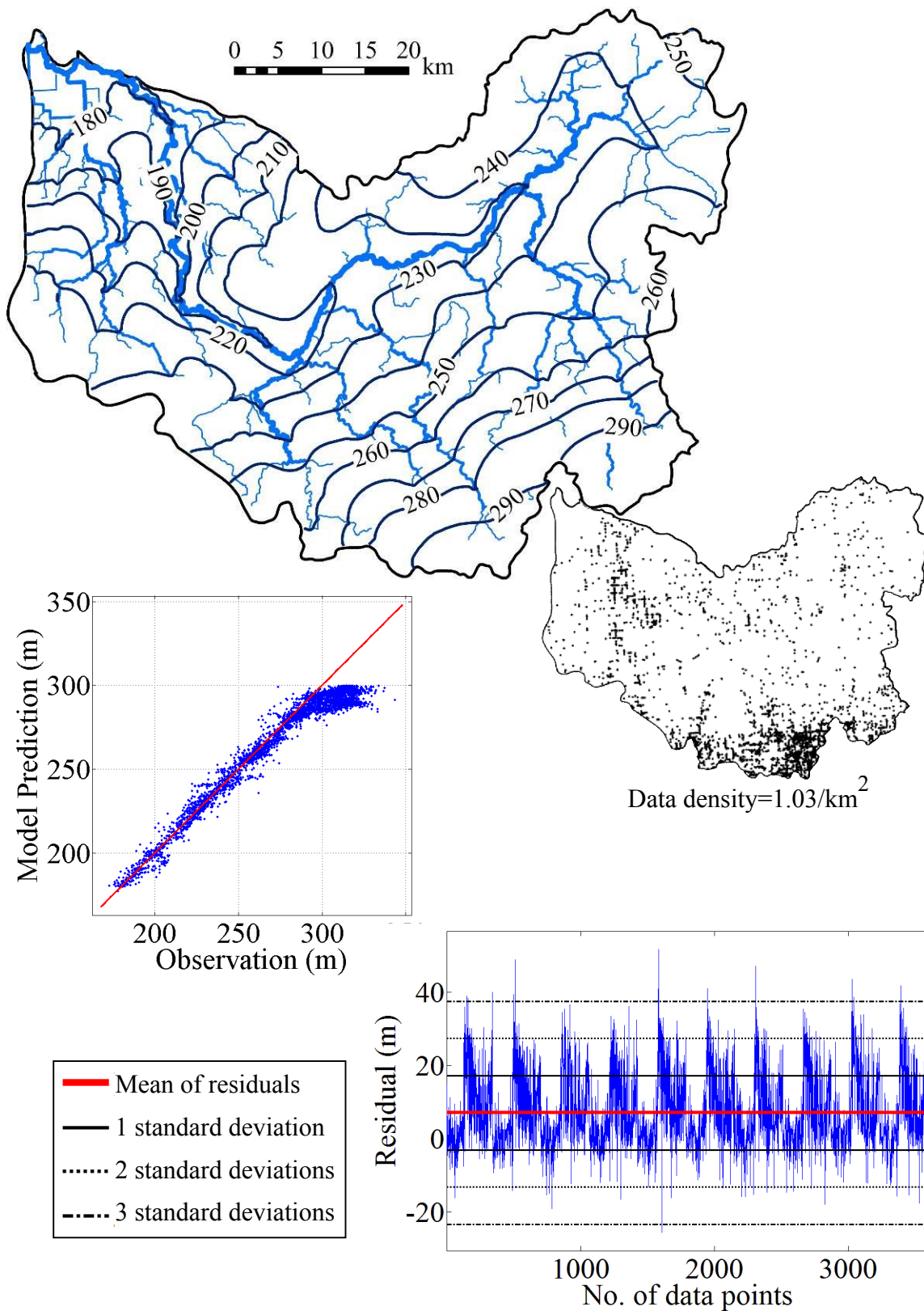


Figure 60: Analysis of the simulated heads in the Flint Watershed, glacial aquifer.

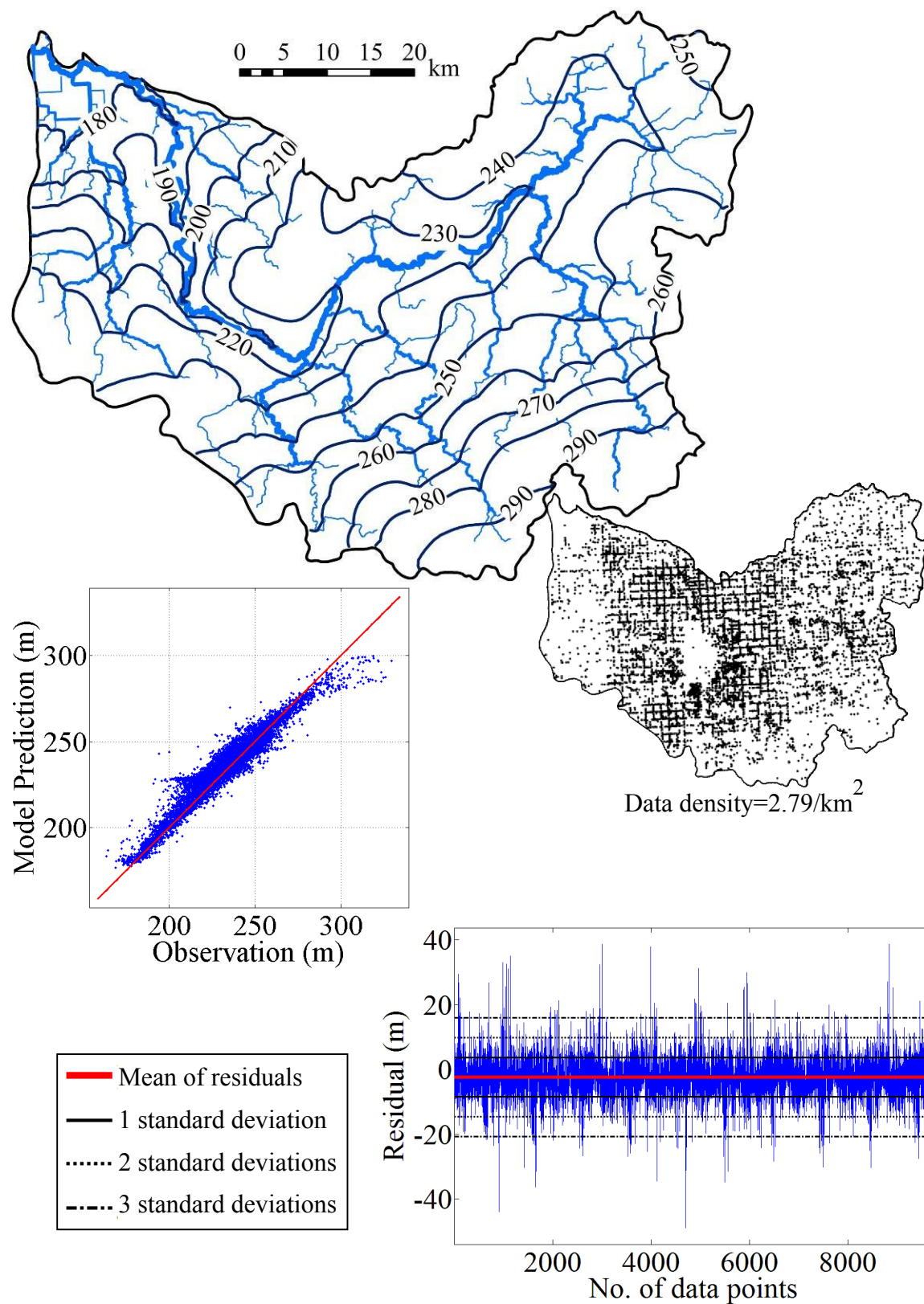


Figure 61: Analysis of the simulated heads in the Flint Watershed, bedrock aquifer.

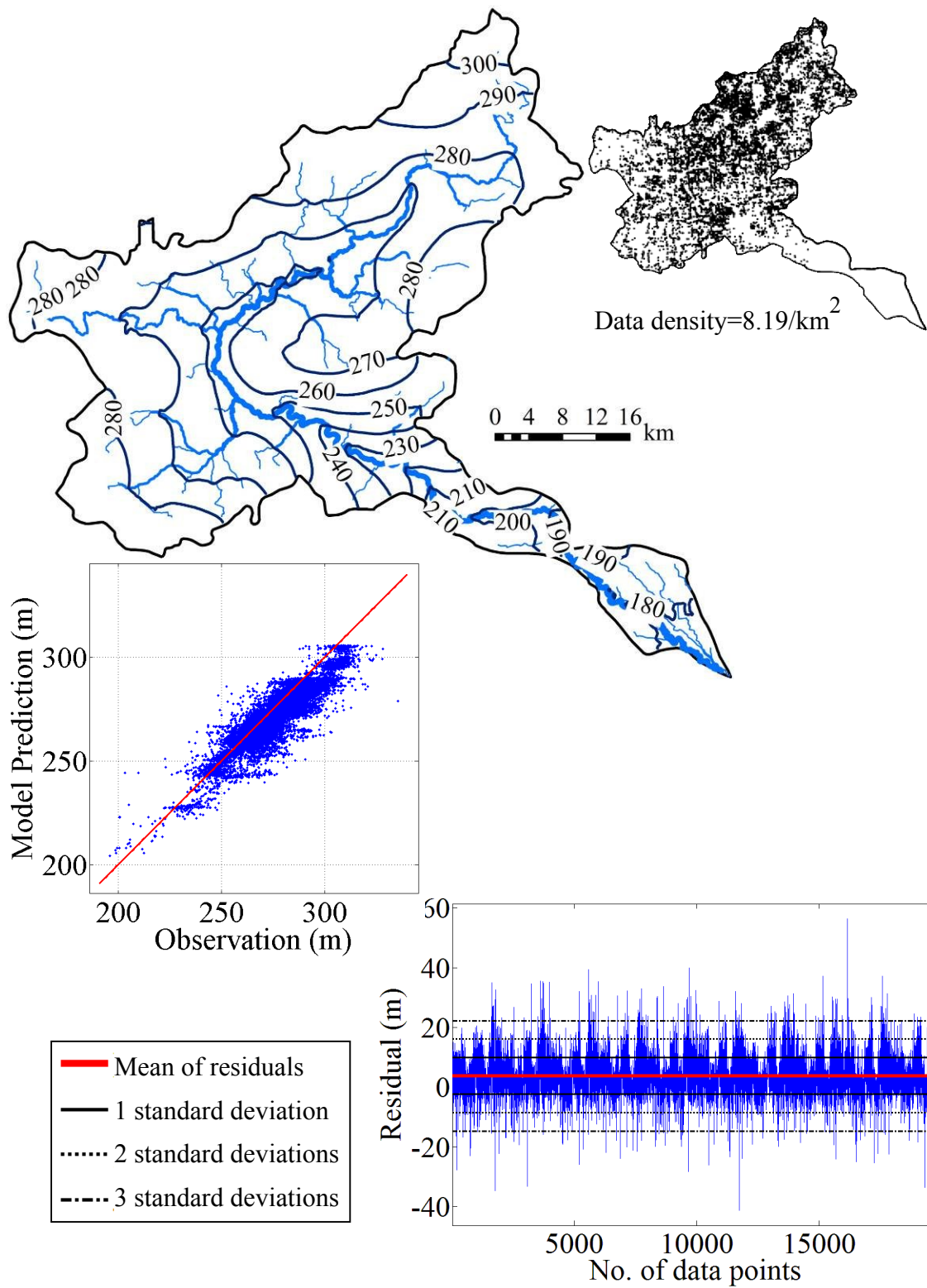


Figure 62: Analysis of the simulated heads in the Huron Watershed, glacial aquifer.

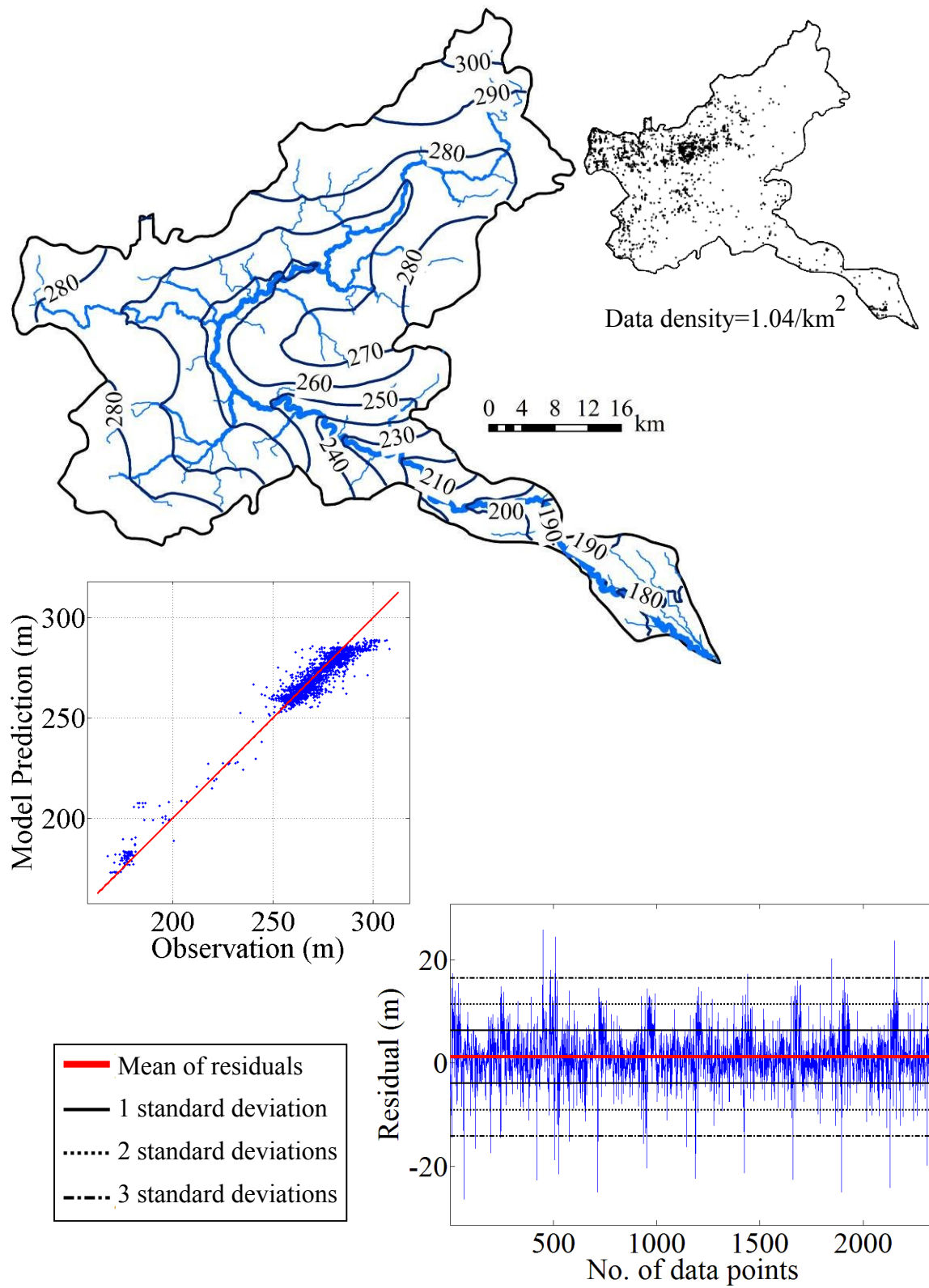


Figure 63: Analysis of the simulated heads in the Huron Watershed, bedrock aquifer.

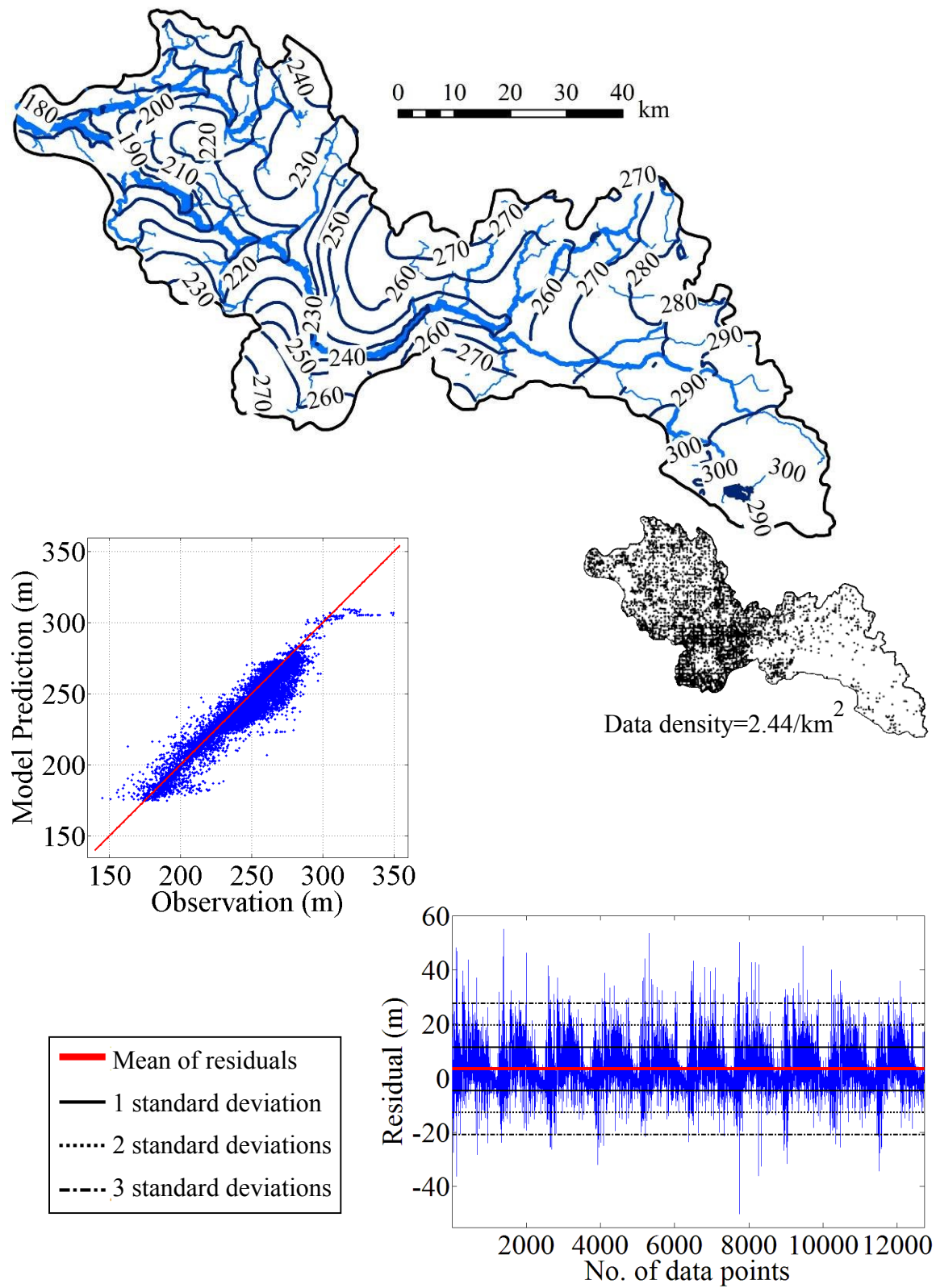


Figure 64: Analysis of the simulated heads in the Kalamazoo Watershed, glacial aquifer.

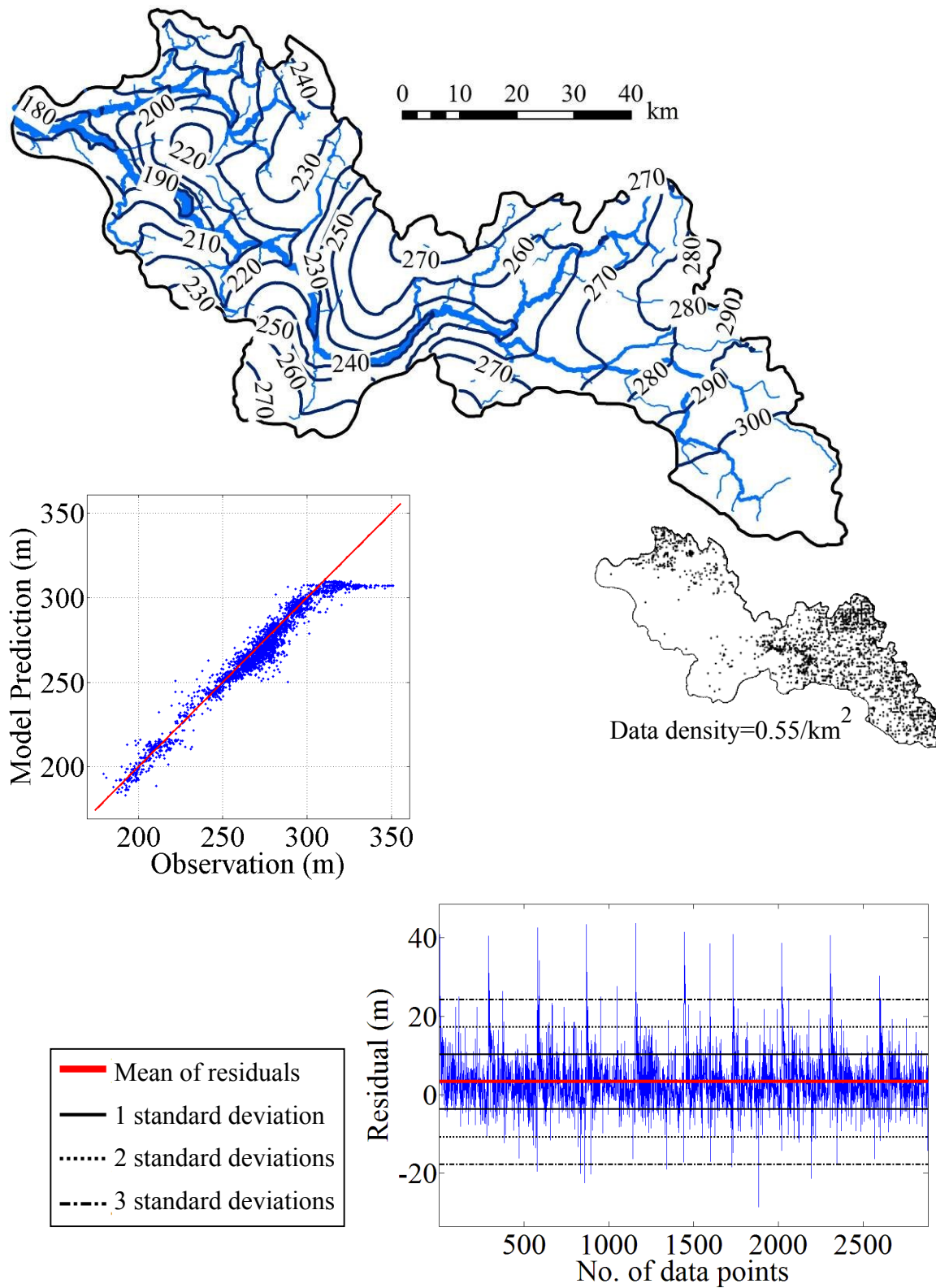


Figure 65: Analysis of the simulated heads in the Kalamazoo Watershed, bedrock aquifer.

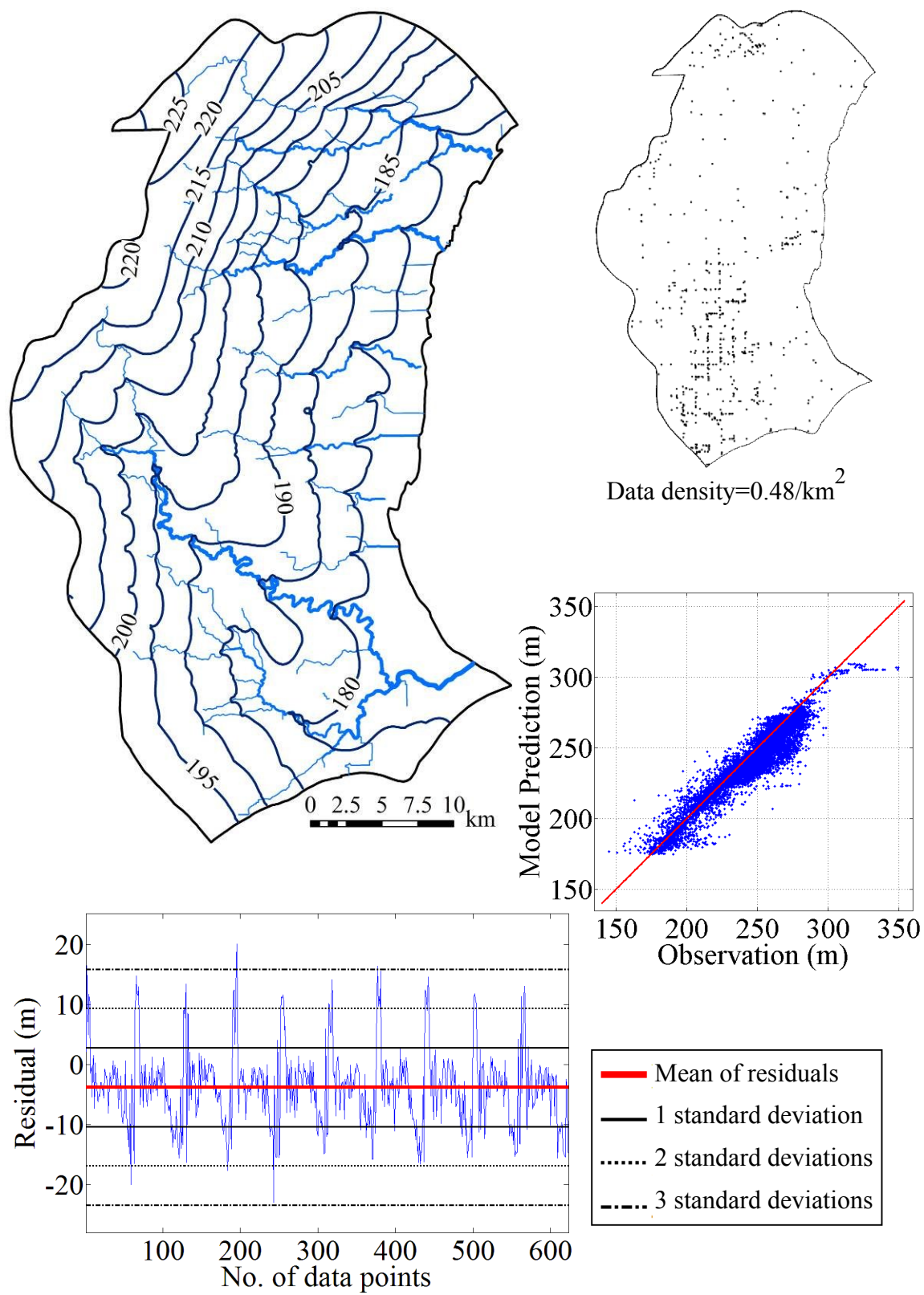


Figure 66: Analysis of the simulated heads in the Kawkawlin Watershed, glacial aquifer.

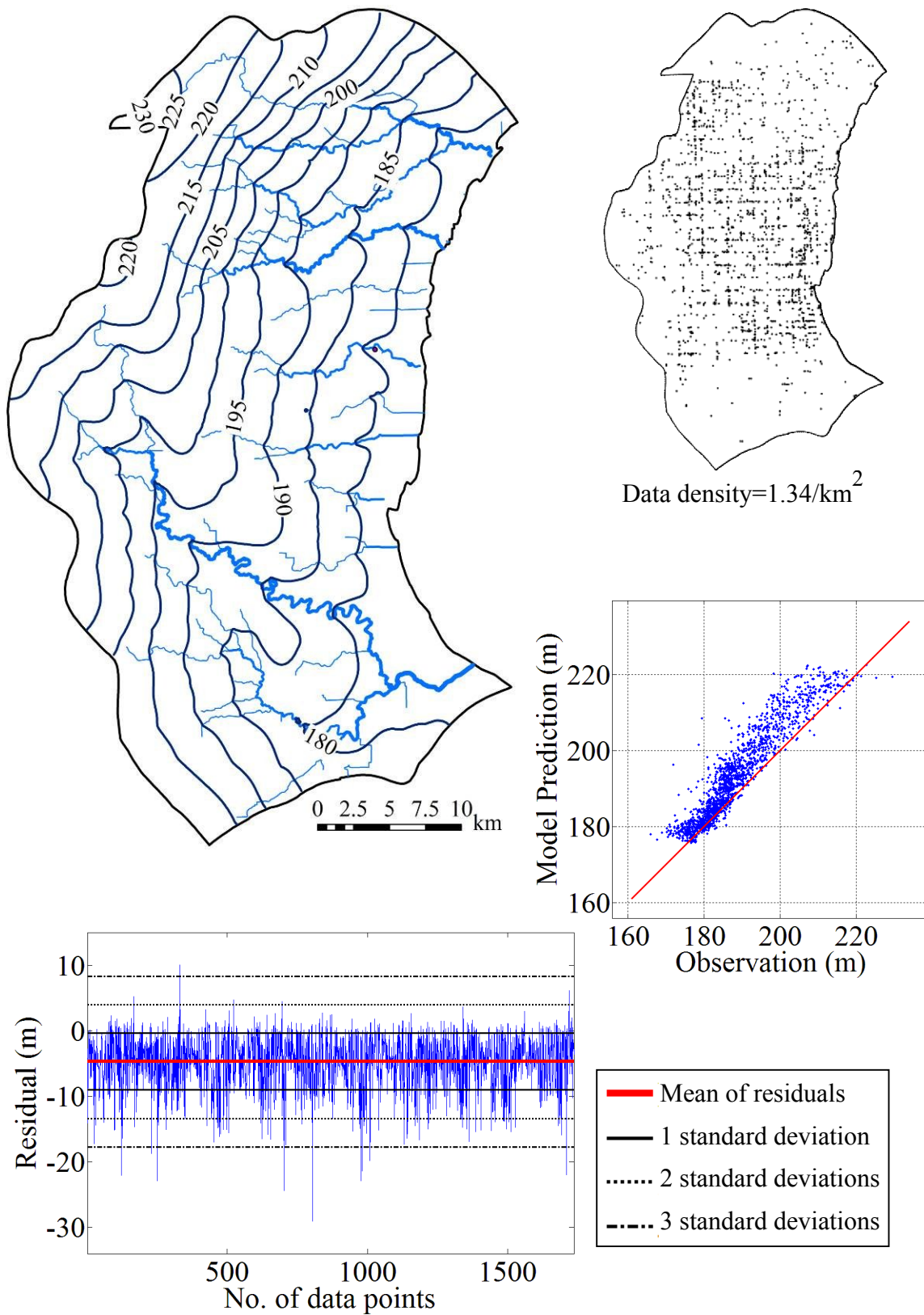


Figure 67: Analysis of the simulated heads in the Kawkawlin Watershed, bedrock aquifer.

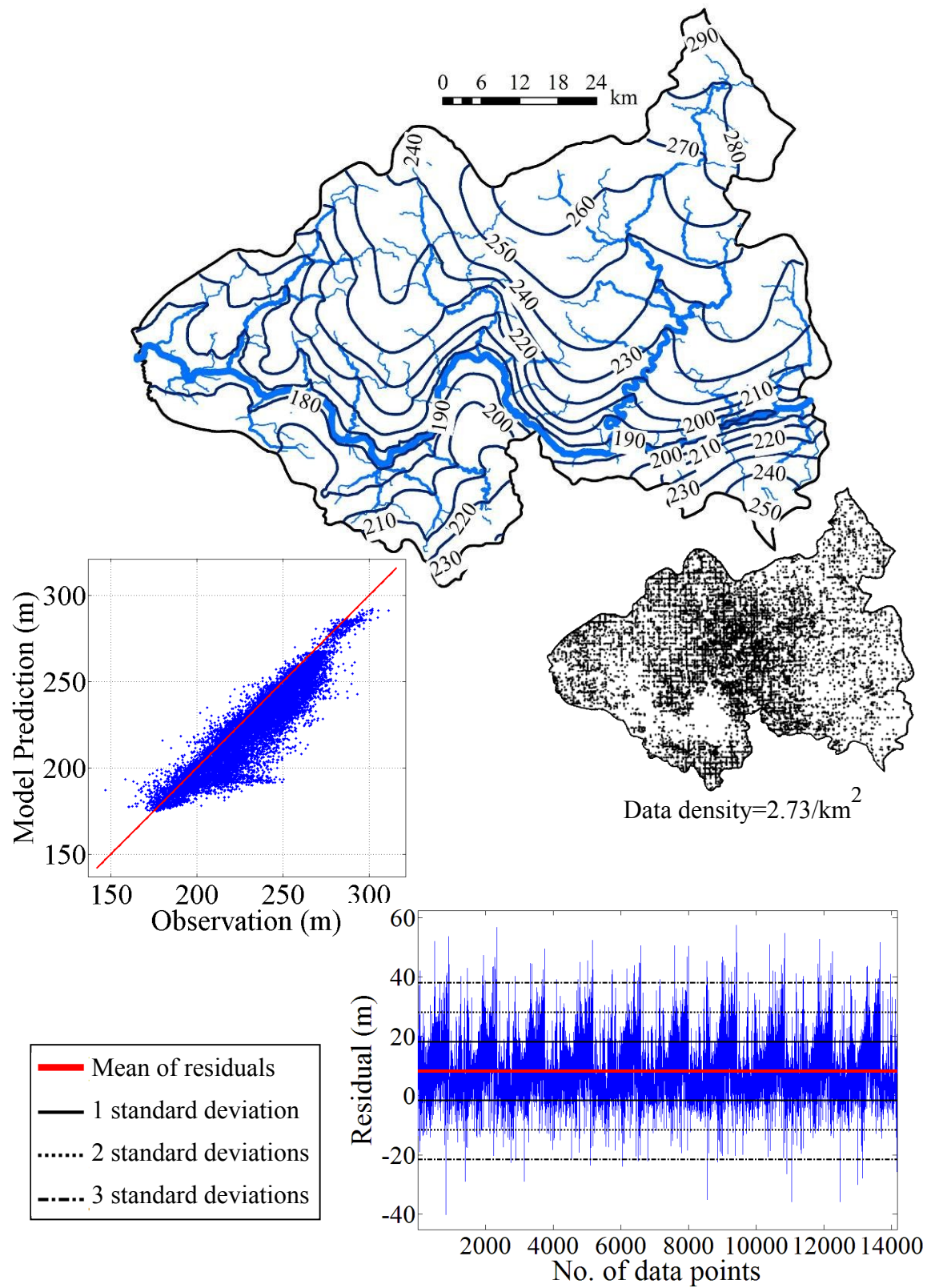


Figure 68: Analysis of the simulated heads in the Lower Grand River Watershed, glacial aquifer.

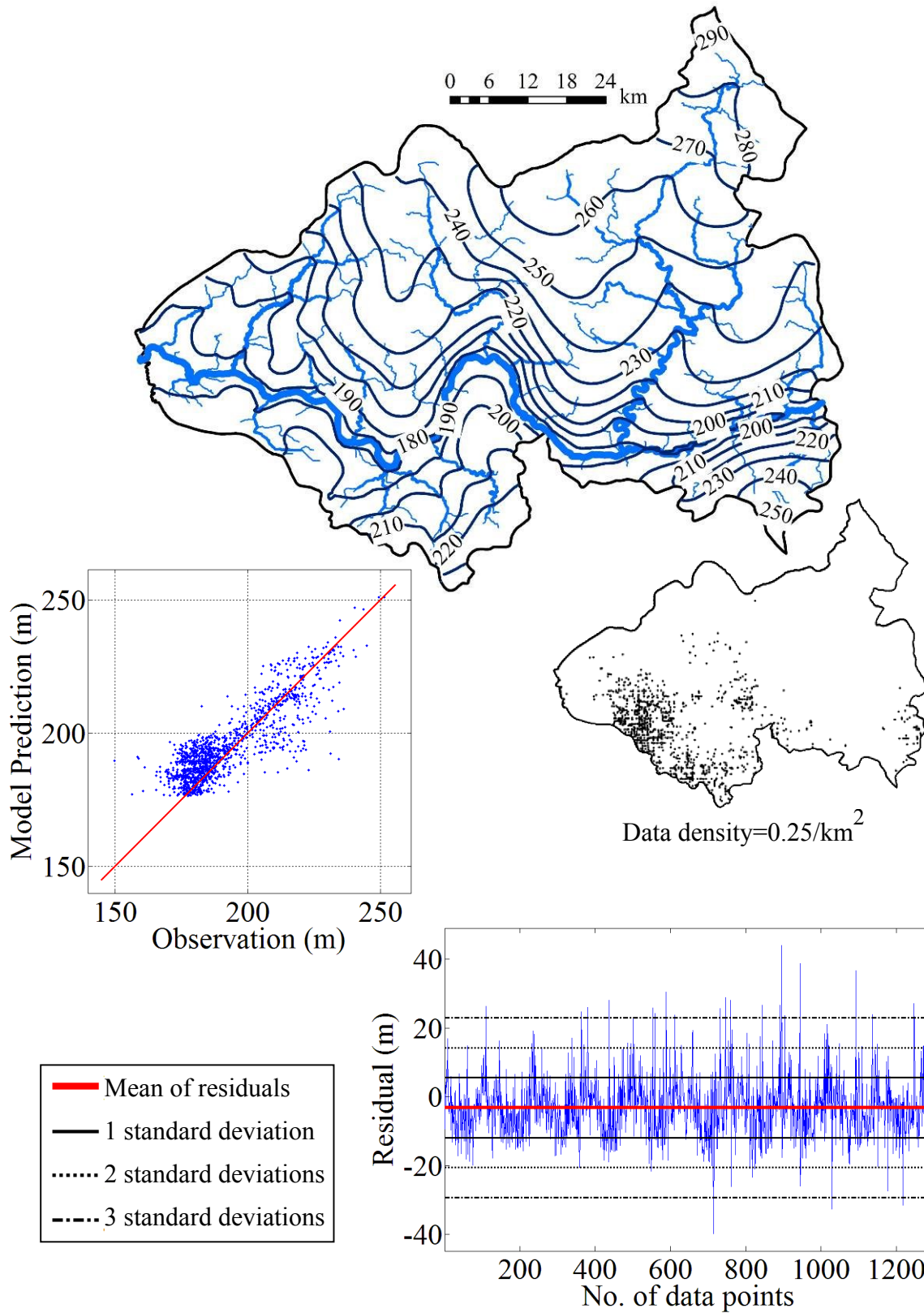


Figure 69: Analysis of the simulated heads in the Lower Grand River Watershed, bedrock aquifer.

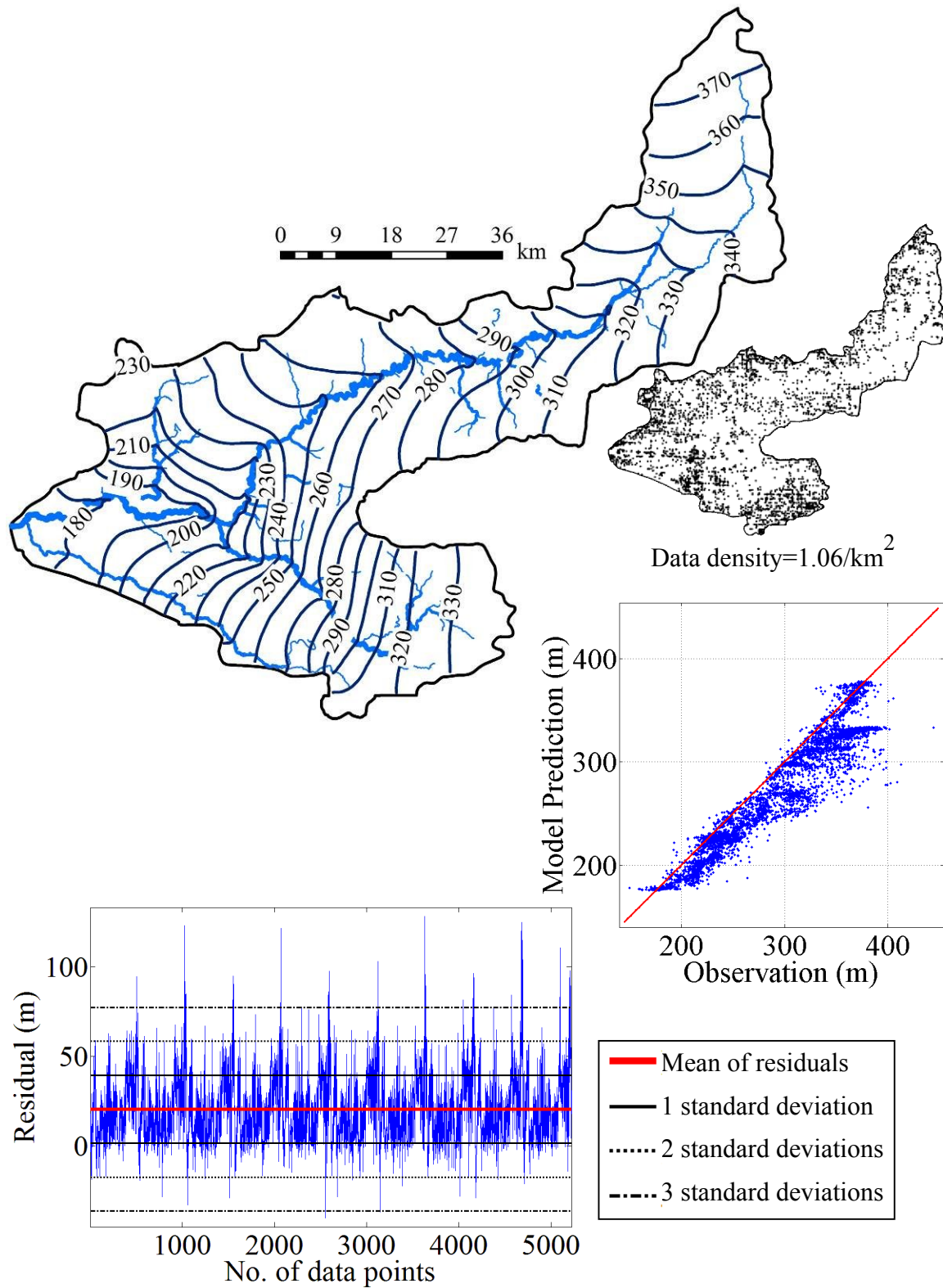


Figure 70: Analysis of the simulated heads in the Manistee Watershed, glacial aquifer.

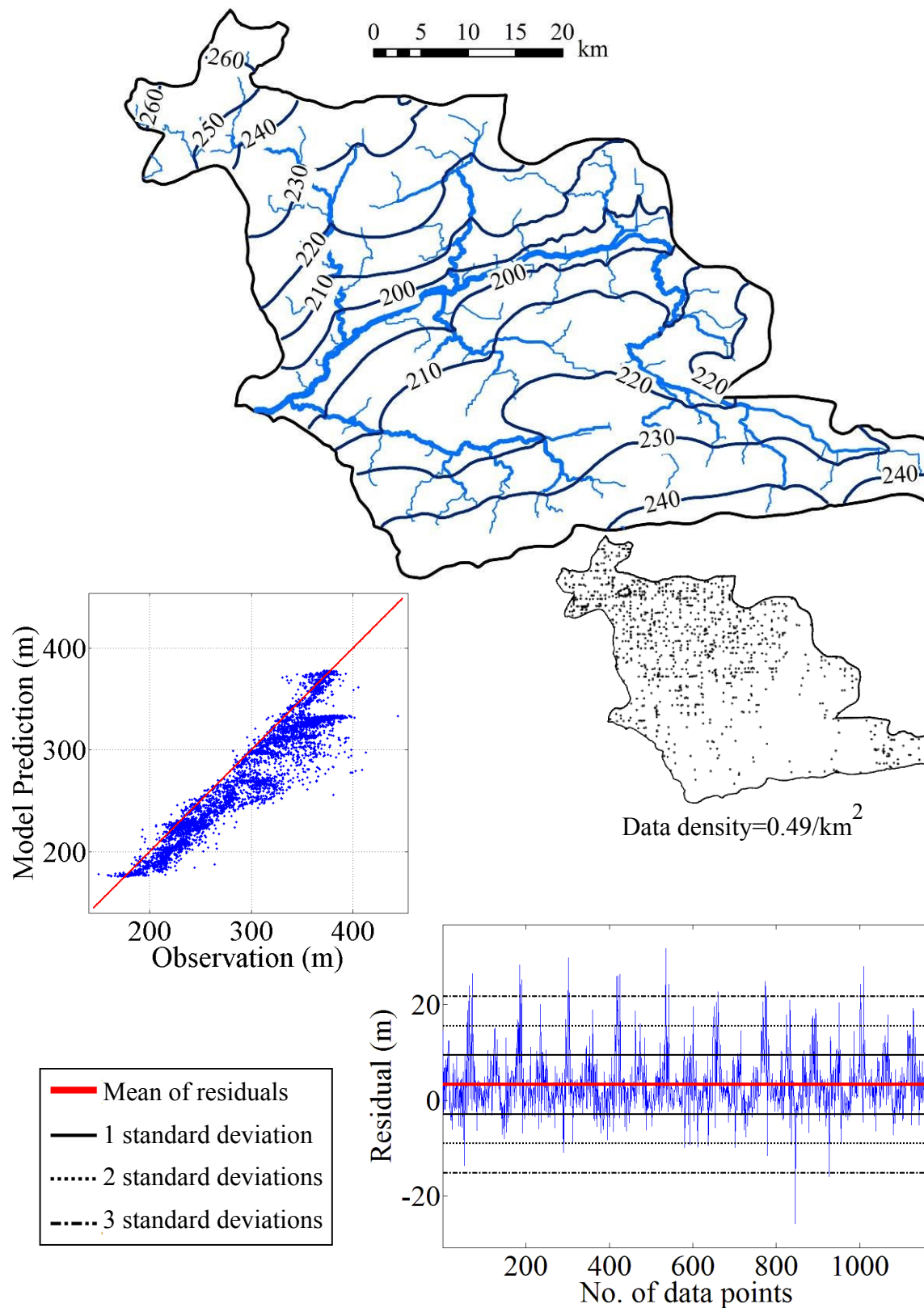


Figure 71: Analysis of the simulated heads in the Maple Watershed, glacial aquifer.

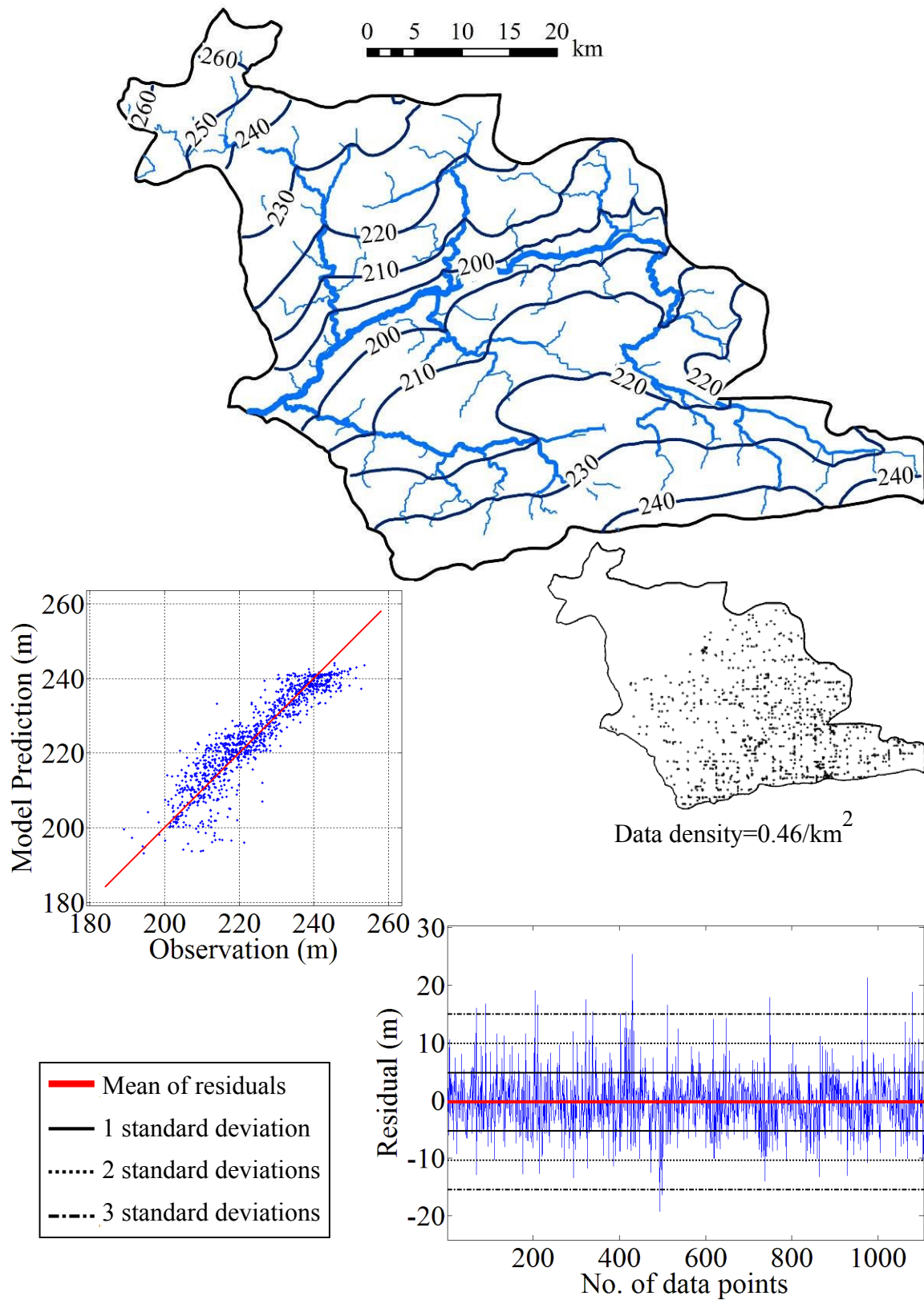


Figure 72: Analysis of the simulated heads in the Maple Watershed, bedrock aquifer.

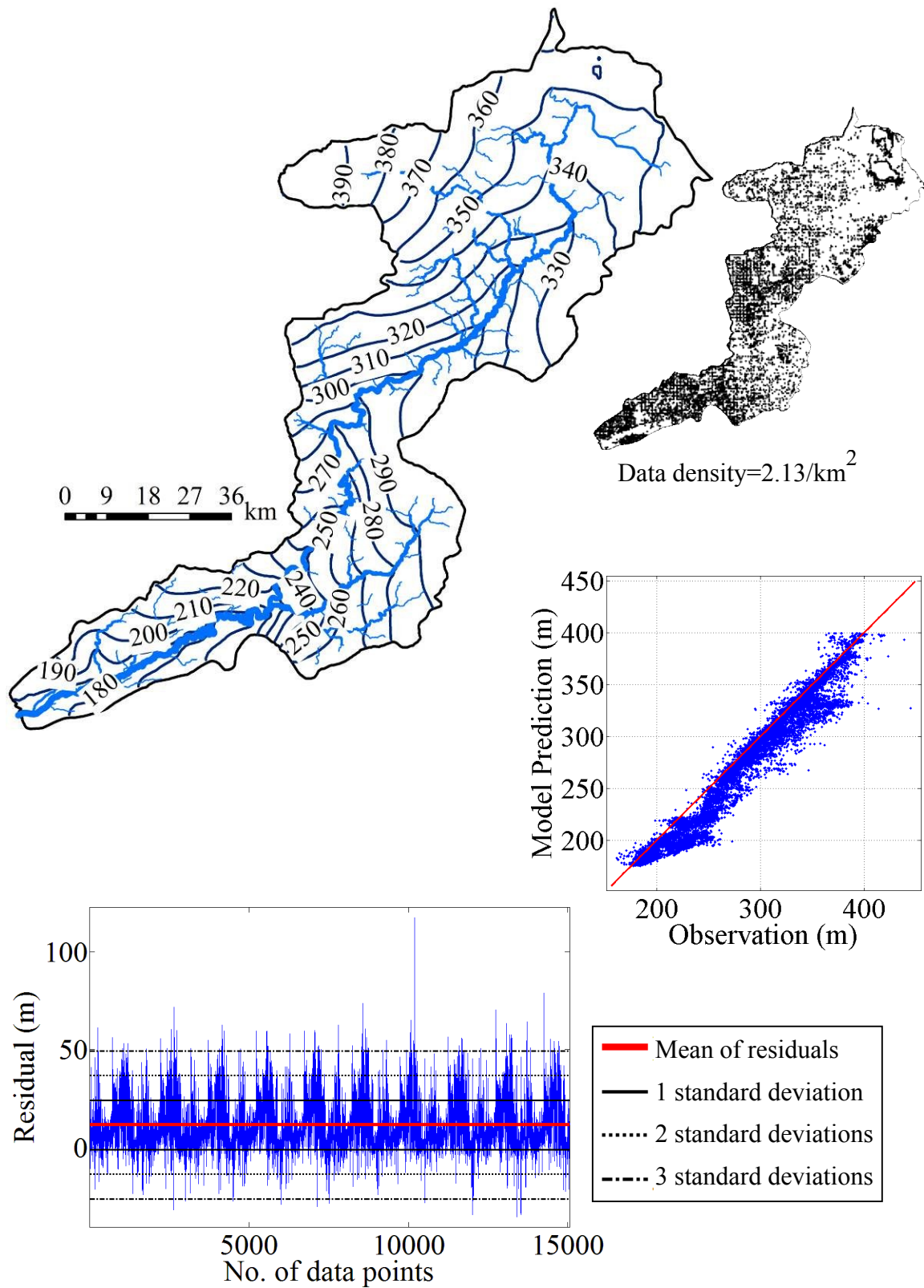


Figure 73: Analysis of the simulated heads in the Muskegon Watershed, glacial aquifer.

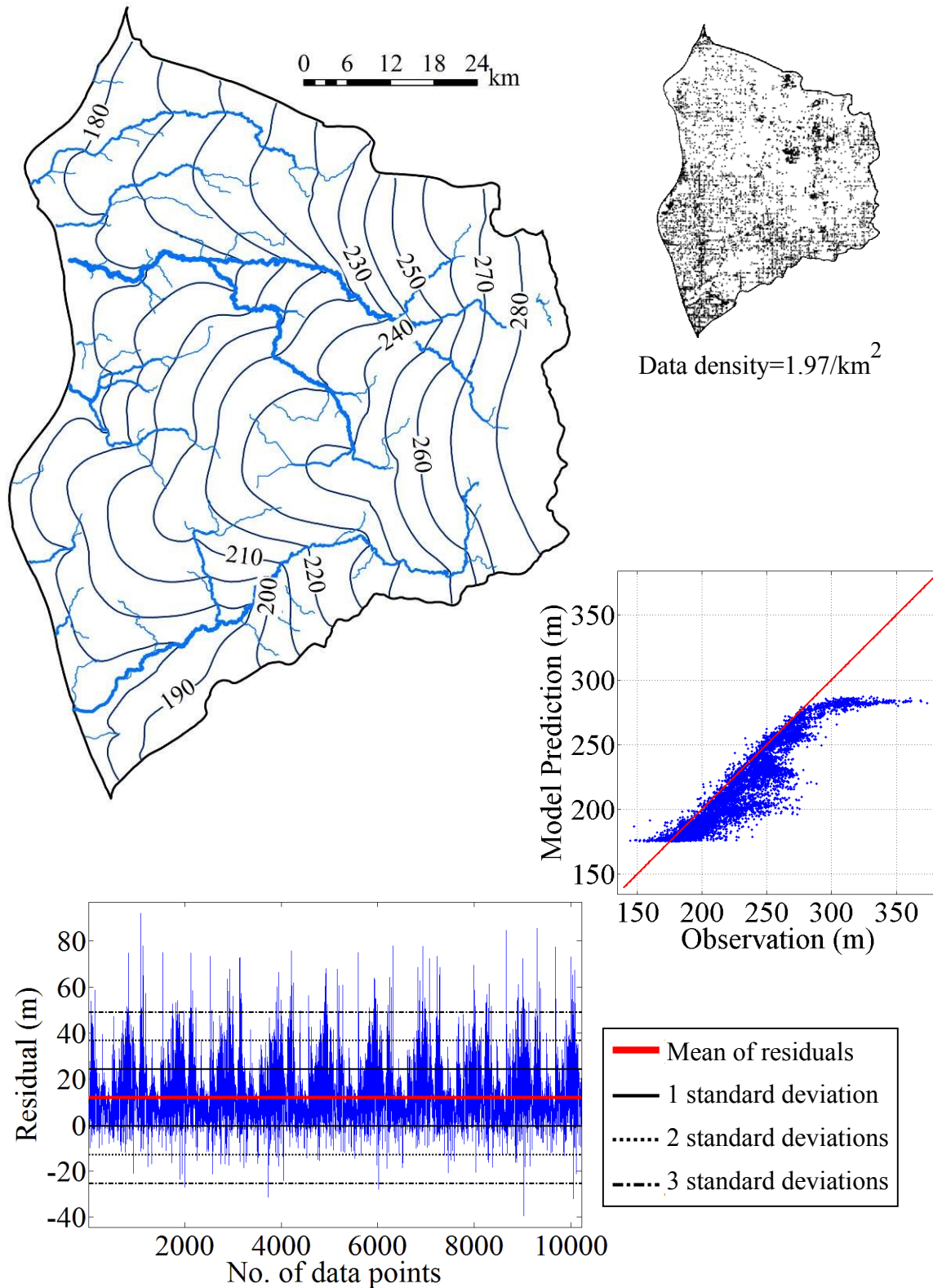


Figure 74: Analysis of the simulated heads in the Pere-Marquette Watershed, glacial aquifer.

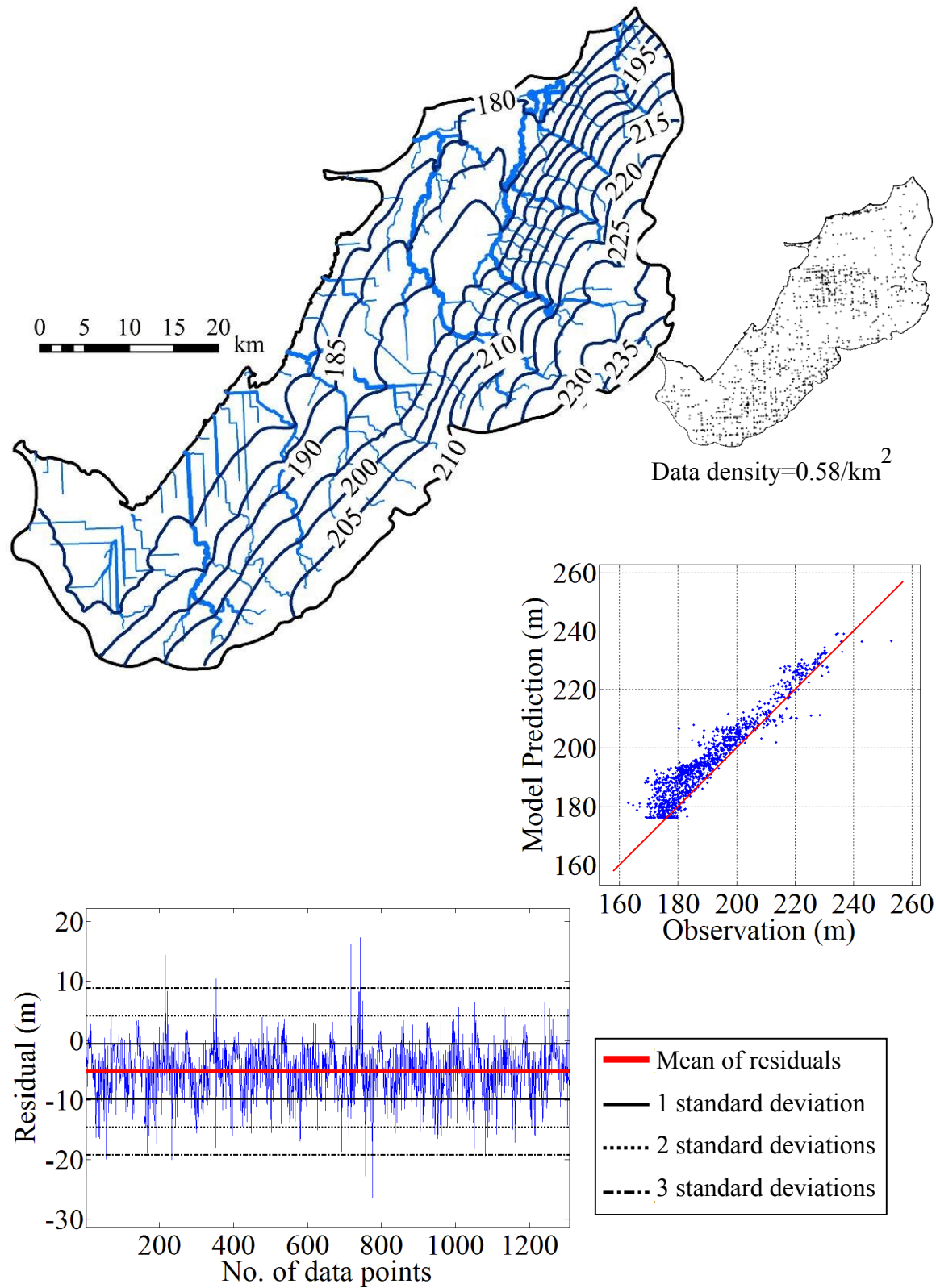


Figure 75: Analysis of the simulated heads in the Pigeon Watershed, bedrock aquifer.

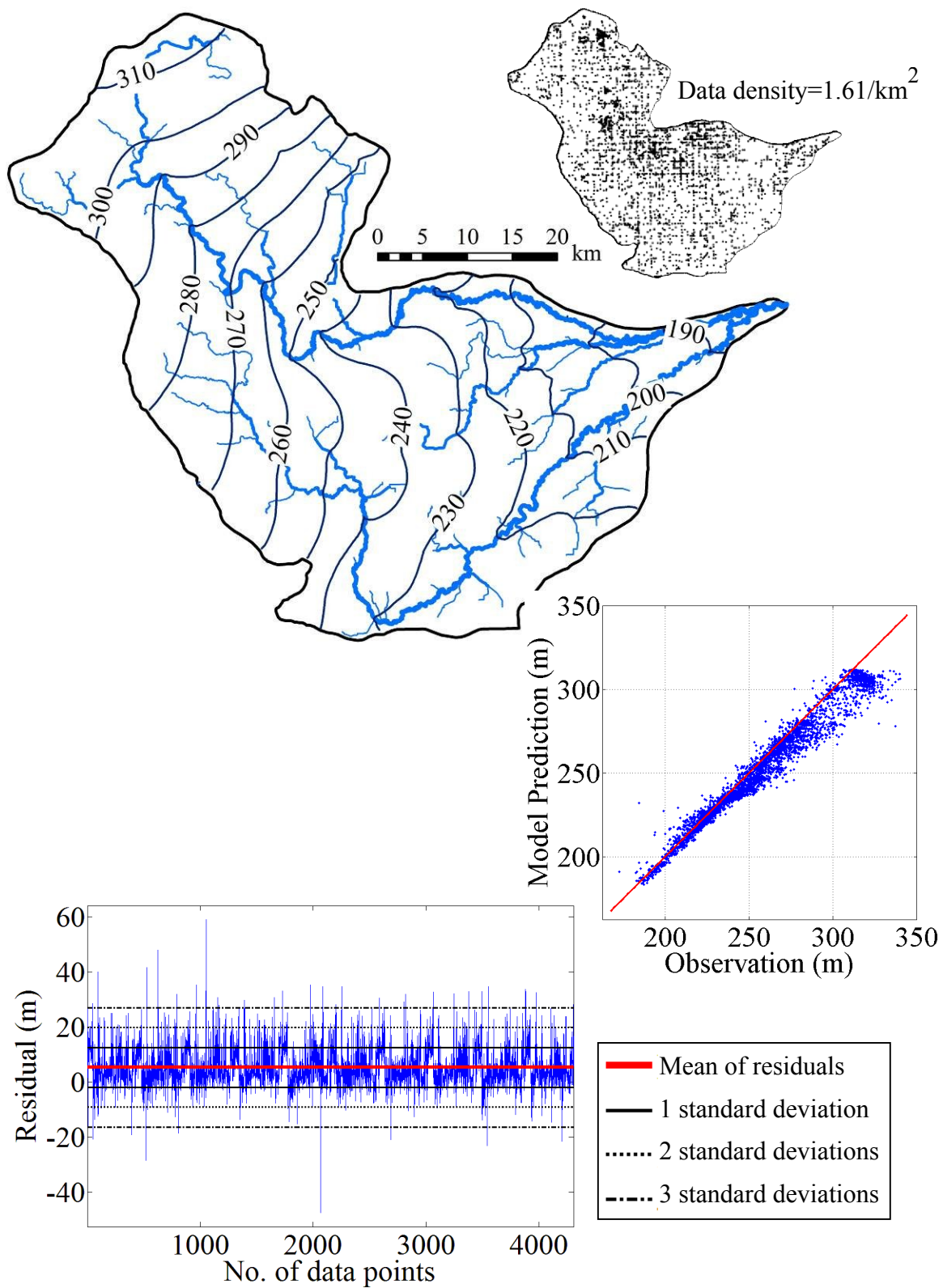


Figure 76: Analysis of the simulated heads in the Pine Watershed, glacial aquifer.

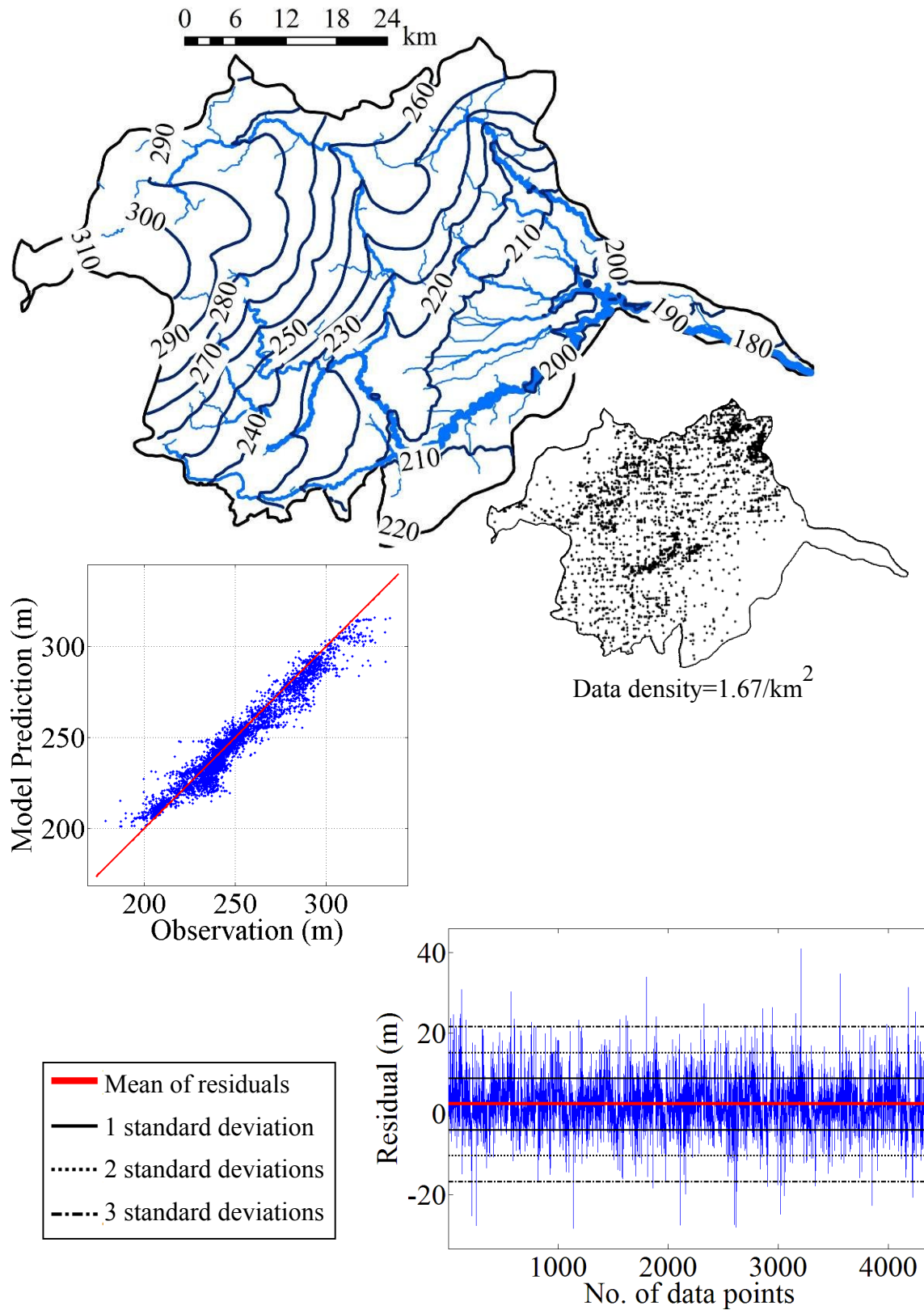


Figure 77: Analysis of the simulated heads in the Raisin Watershed, glacial aquifer.

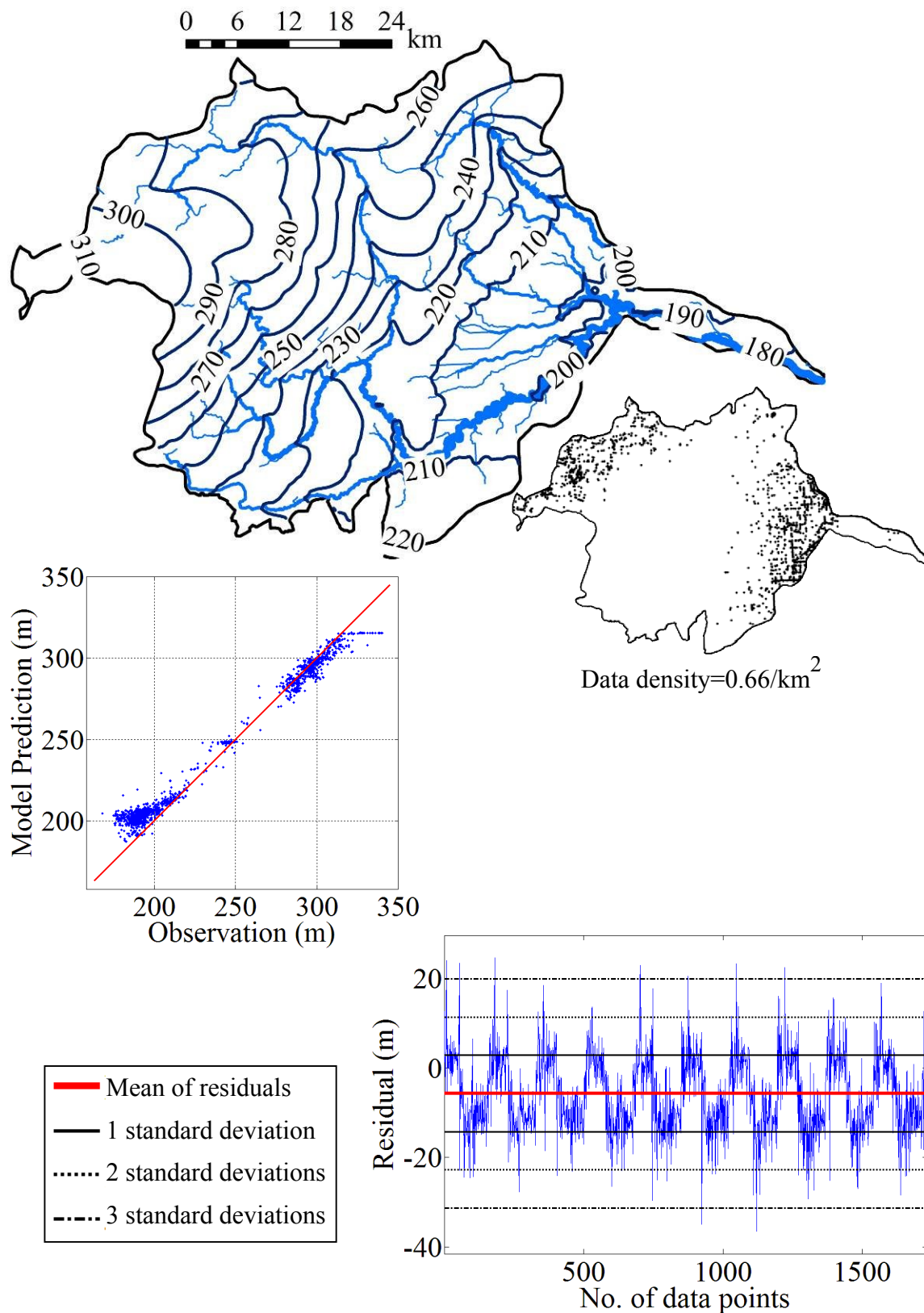


Figure 78: Analysis of the simulated heads in the Raisin Watershed, bedrock aquifer.

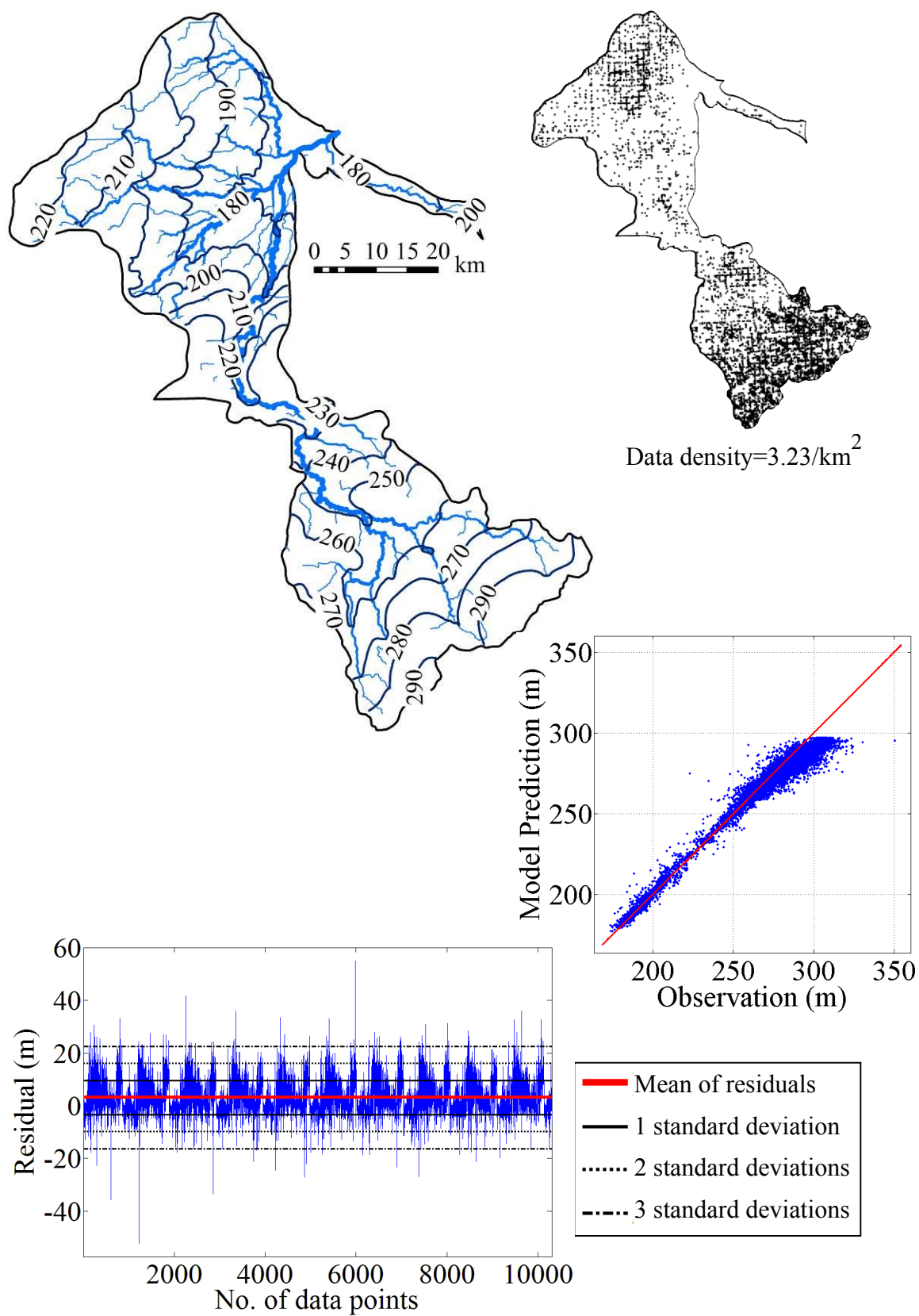


Figure 79: Analysis of the simulated heads in the Shiawassee Watershed, glacial aquifer.

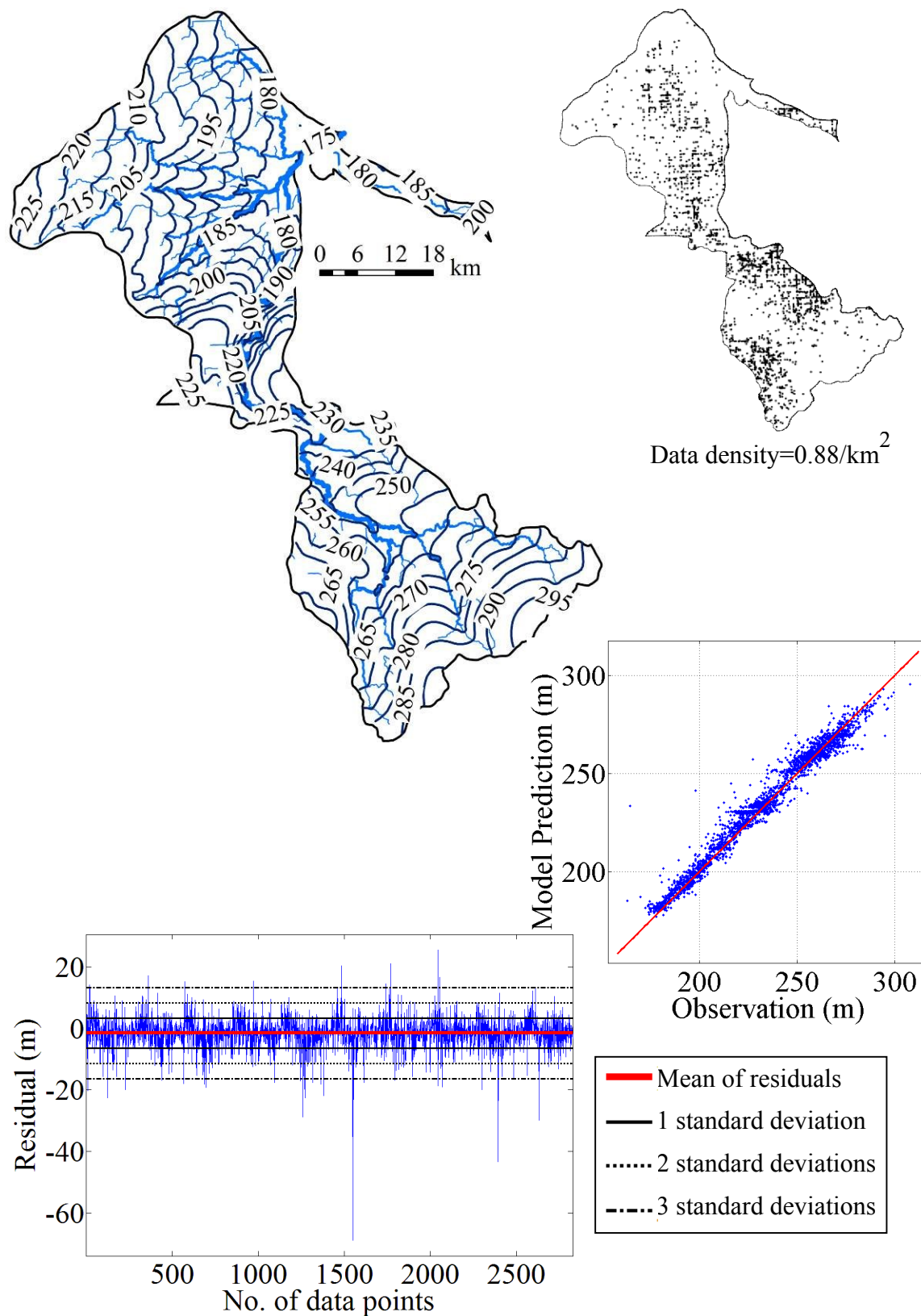


Figure 80: Analysis of the simulated heads in the Shiawasseee Watershed, bedrock aquifer.

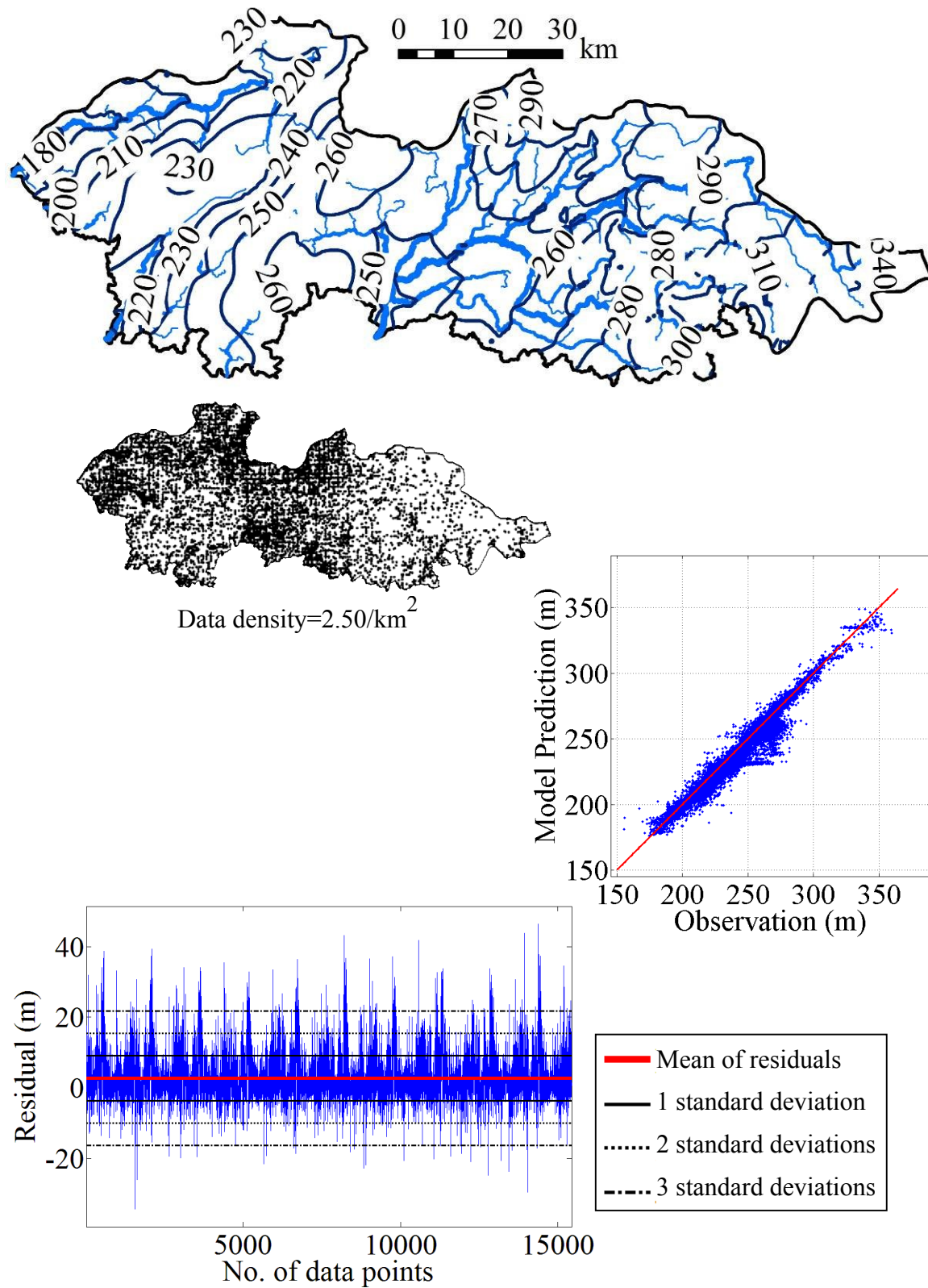


Figure 81: Analysis of the simulated heads in the St. Joseph Watershed, glacial aquifer.

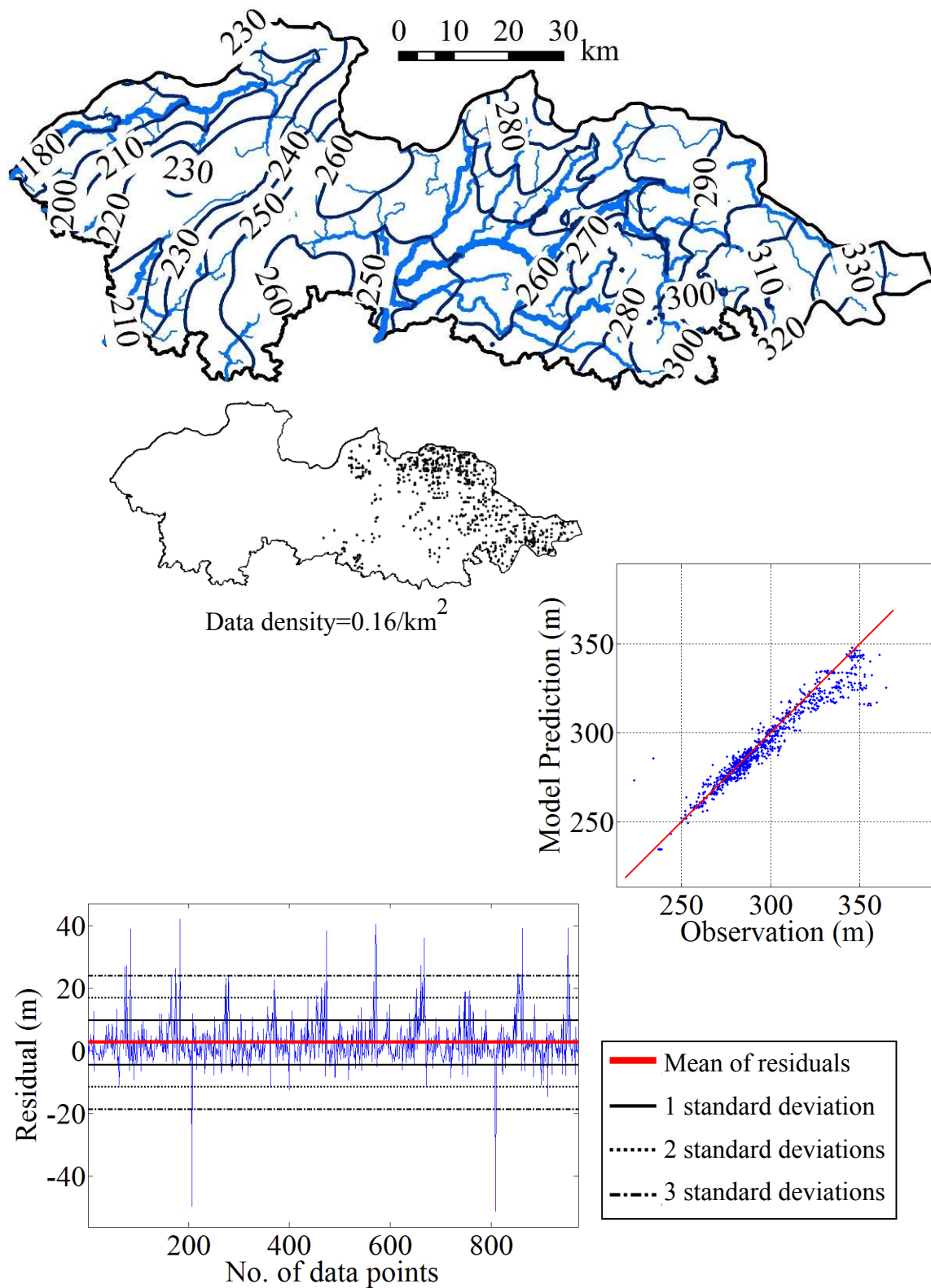


Figure 82: Analysis of the simulated heads in the St. Joseph Watershed, bedrock aquifer.

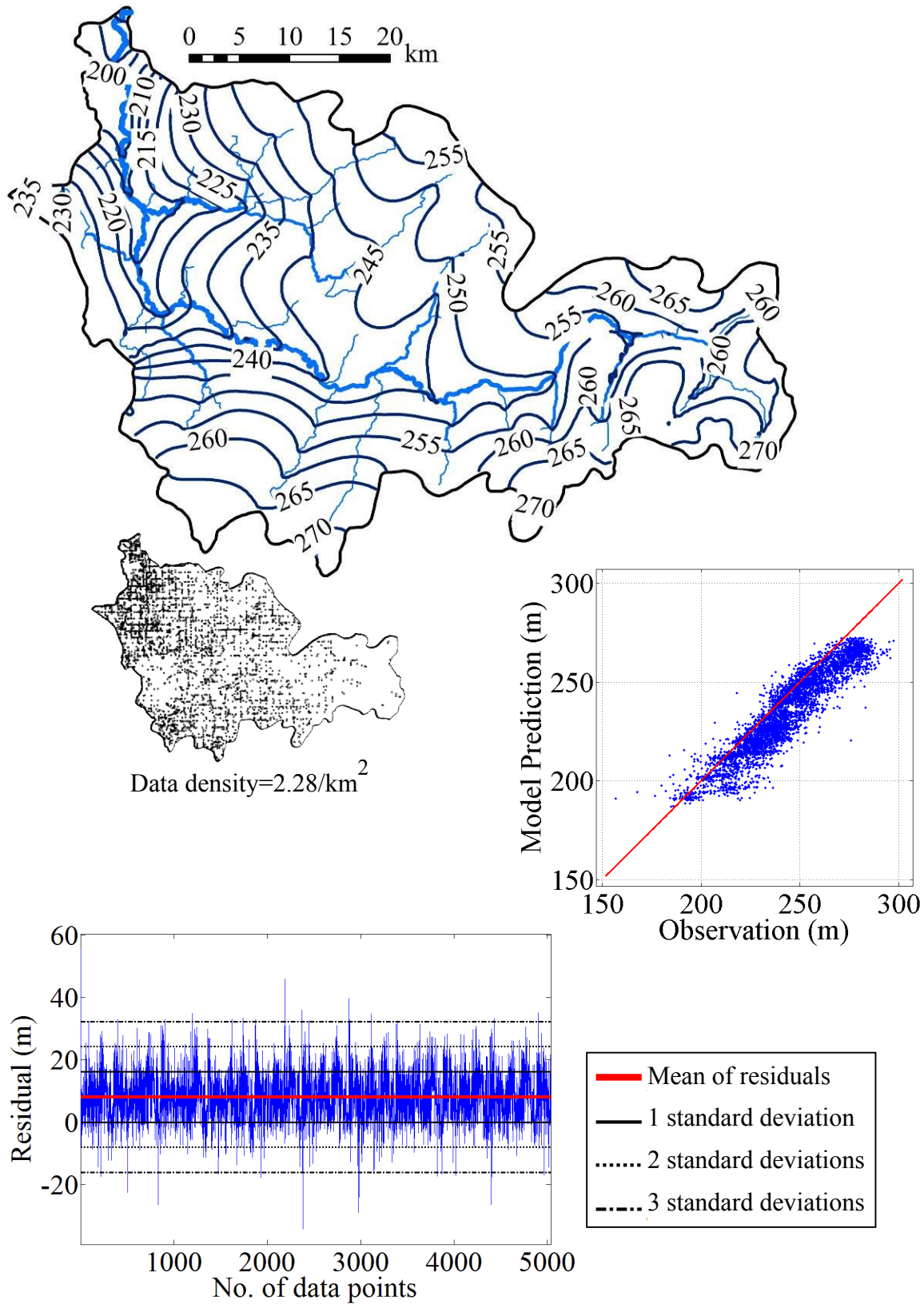


Figure 83: Analysis of the simulated heads in the Thornapple Watershed, glacial aquifer.

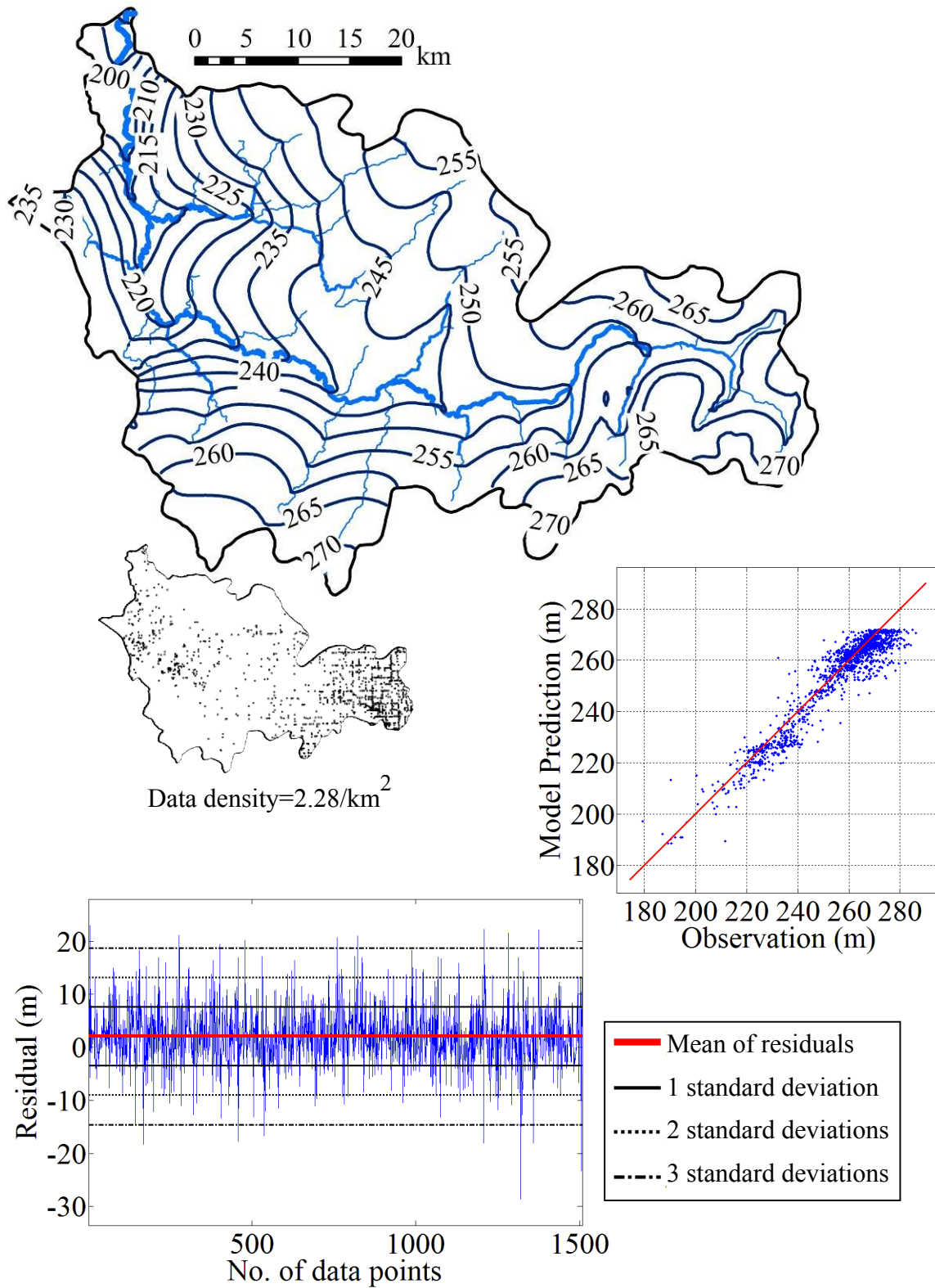


Figure 84: Analysis of the simulated heads in the Thornapple Watershed, bedrock aquifer.

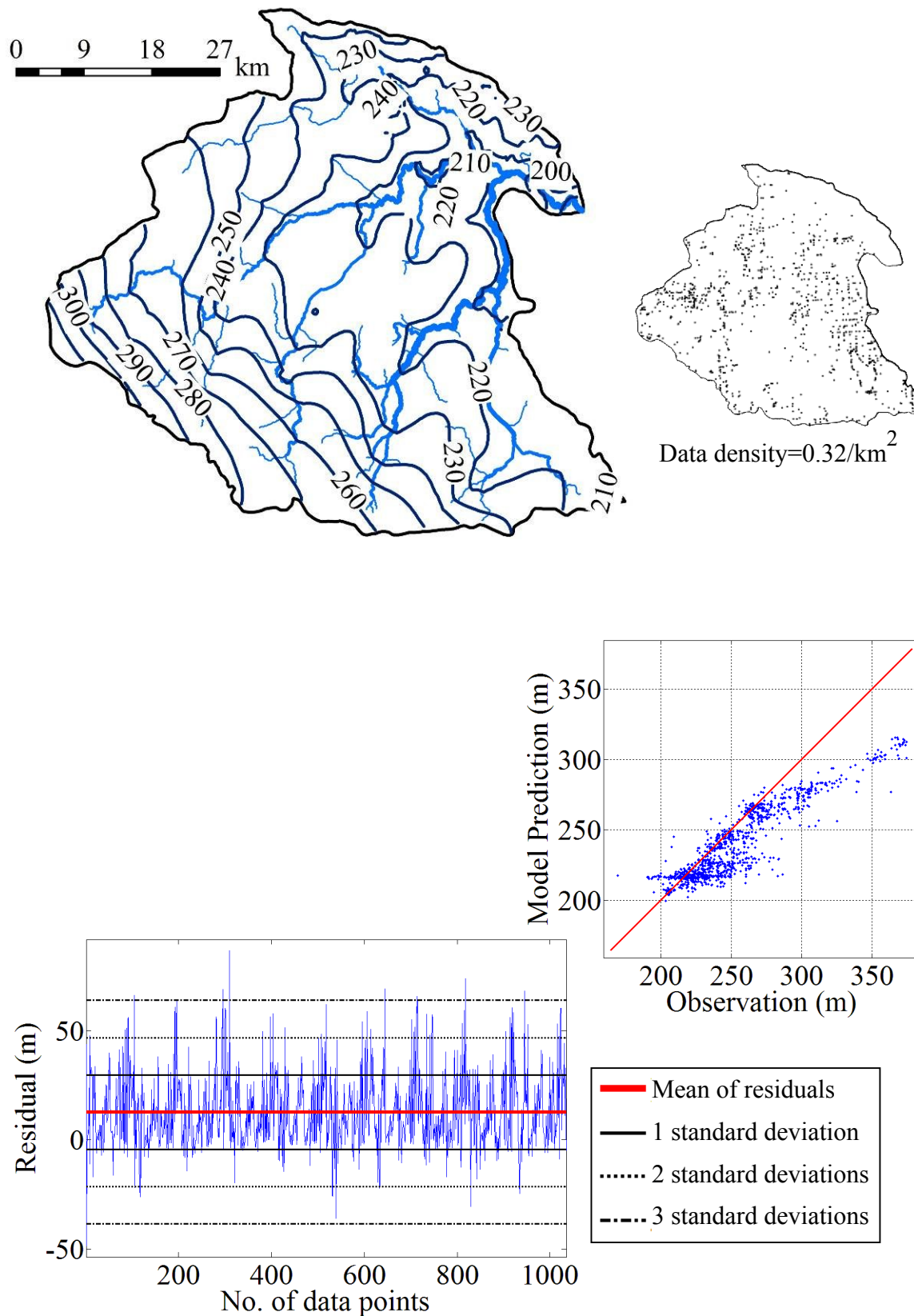


Figure 85: Analysis of the simulated heads in the Thunder Bay Watershed, glacial aquifer.

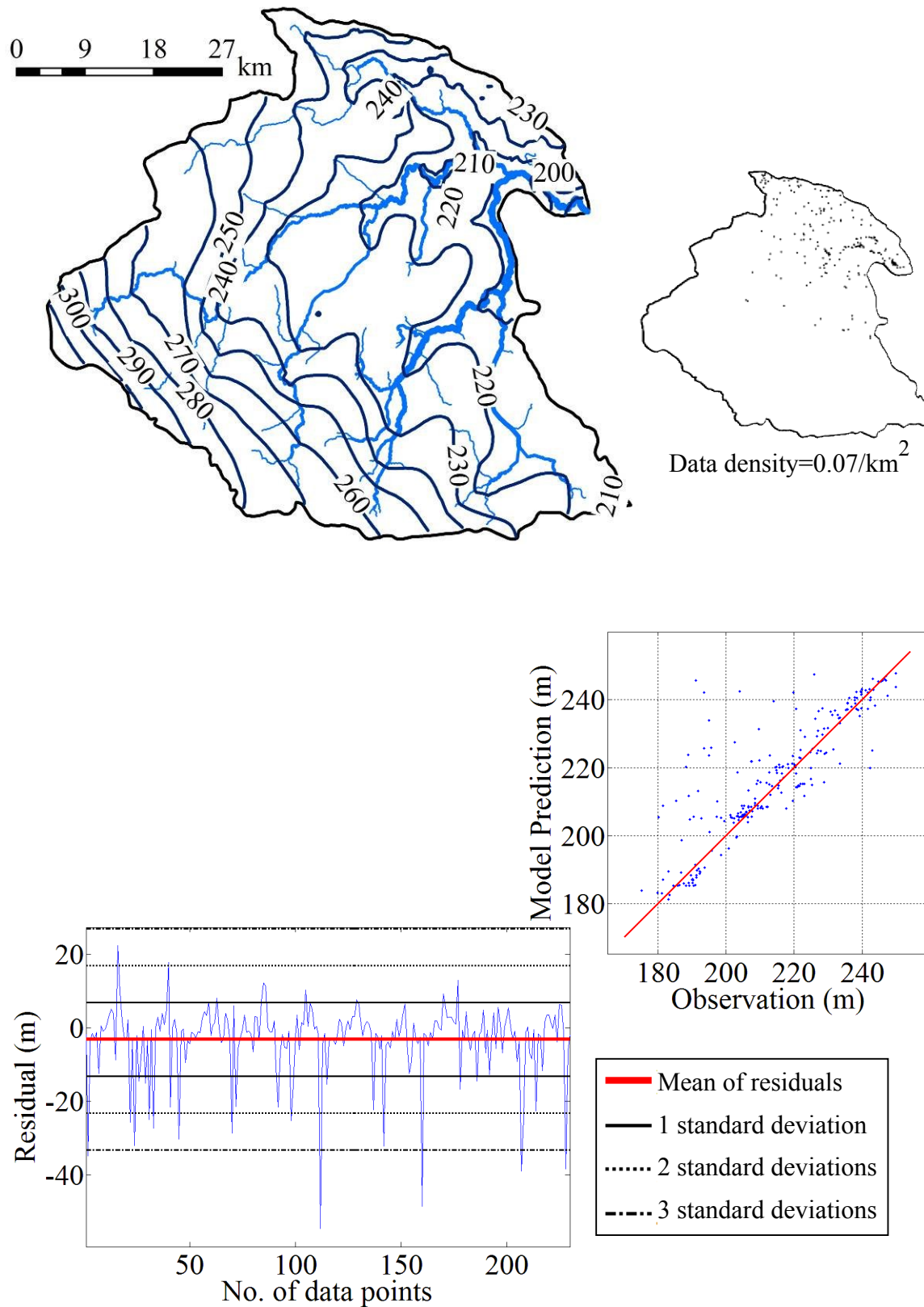


Figure 86: Analysis of the simulated heads in the Thunder Bay Watershed, bedrock aquifer.

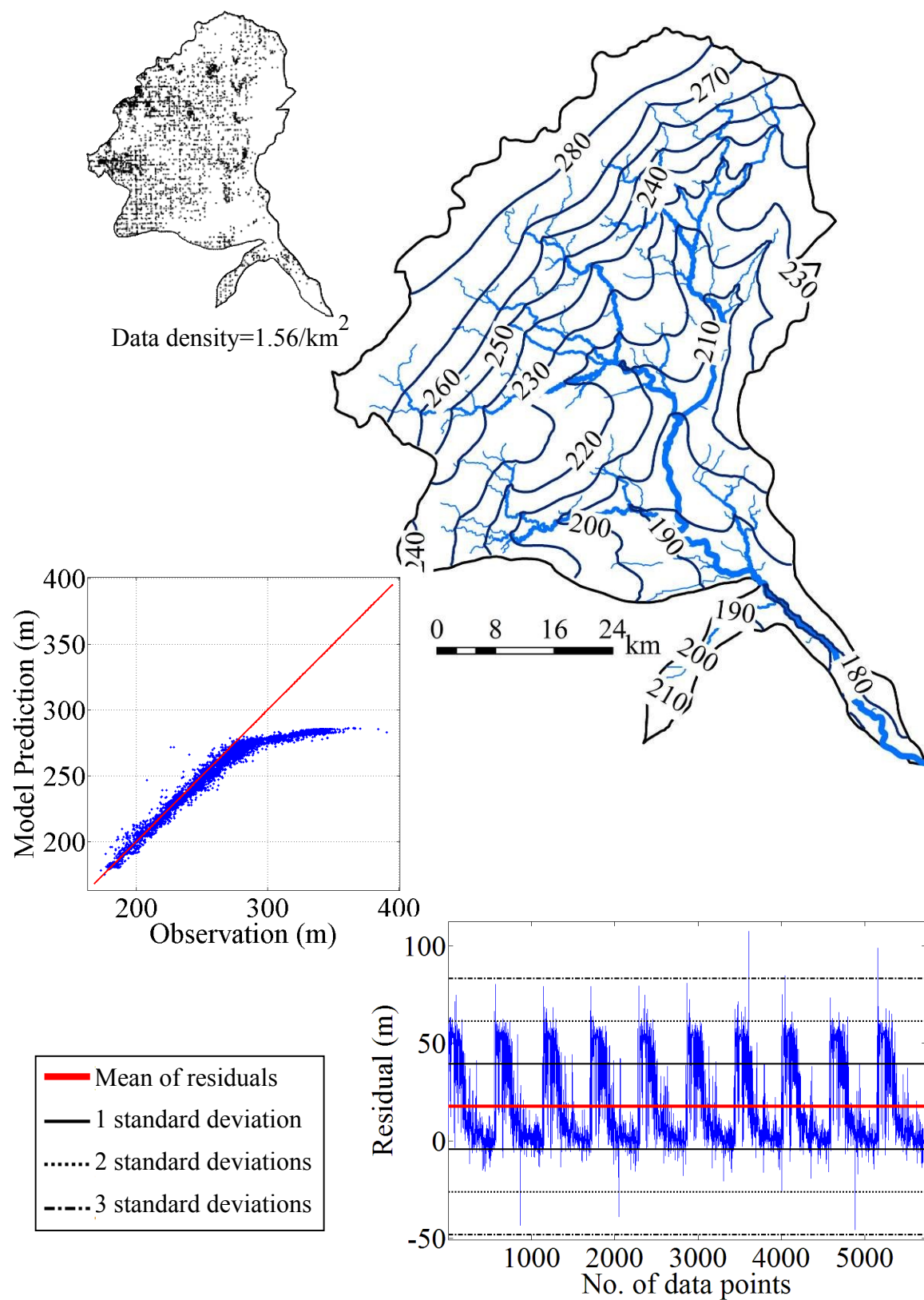


Figure 87: Analysis of the simulated heads in the Tittabawassee Watershed, glacial aquifer.

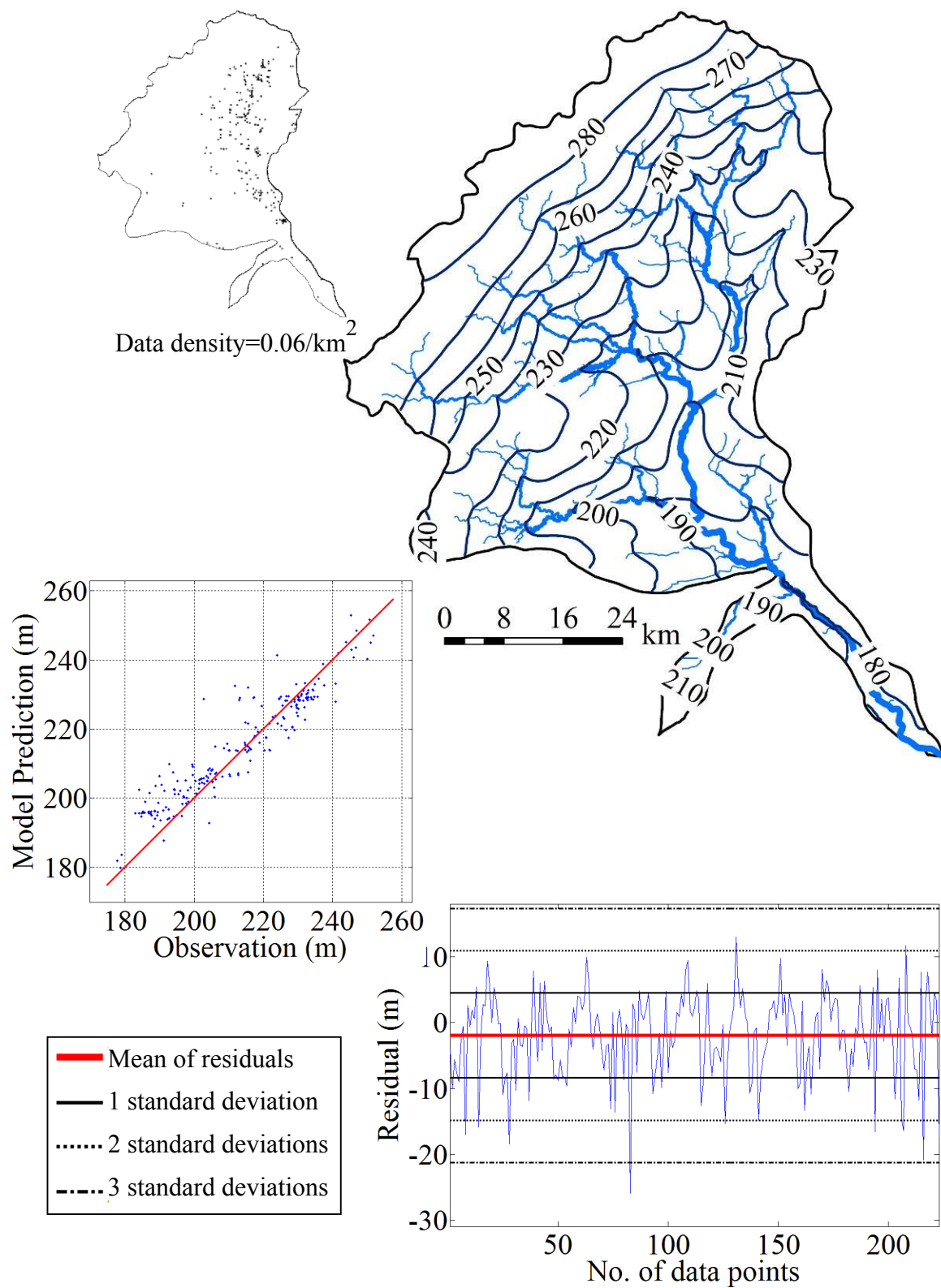


Figure 88: Analysis of the simulated heads in the Tittabawassee Watershed, bedrock aquifer.

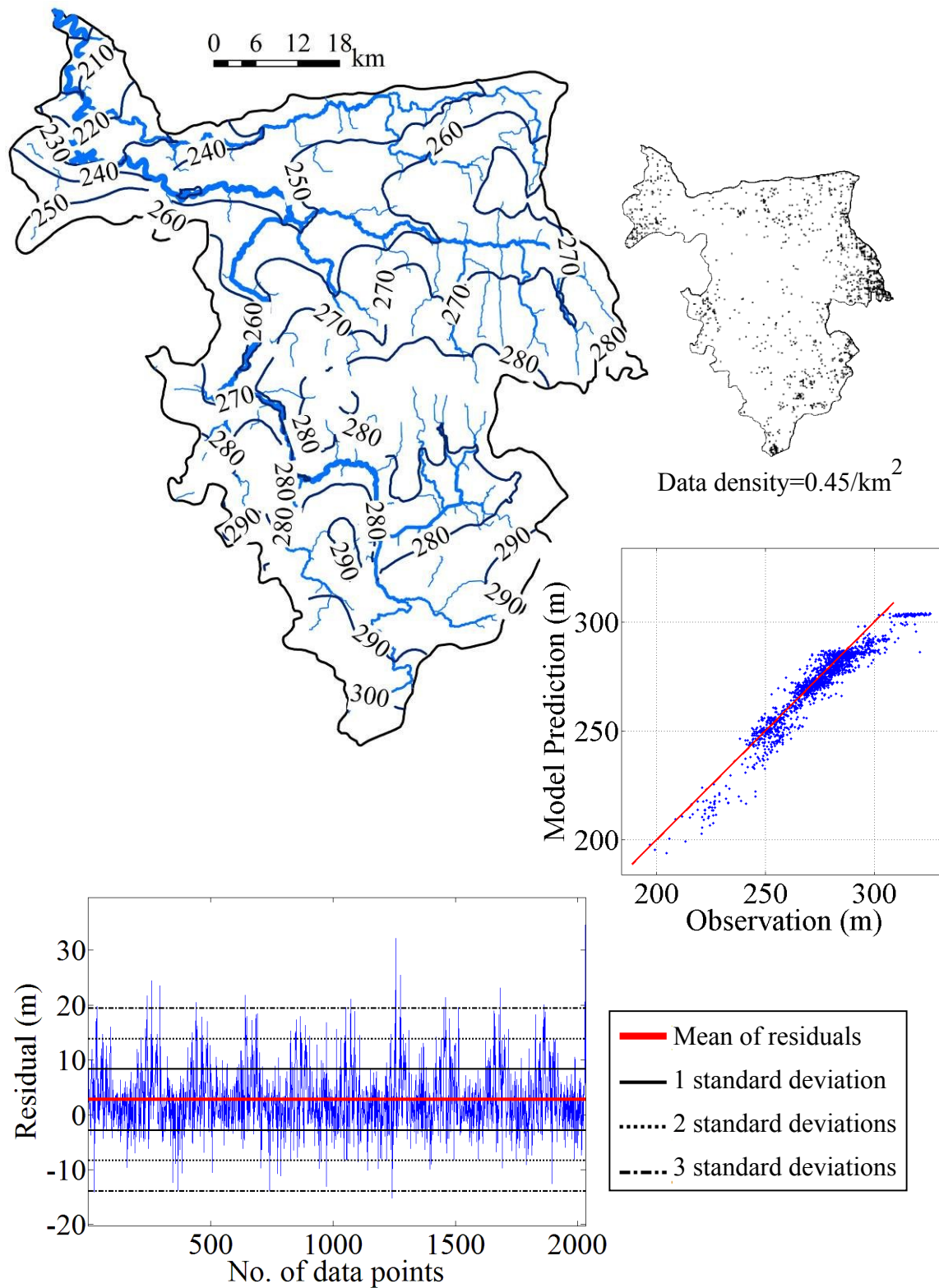


Figure 89: Analysis of the simulated heads in the Upper Grand River Watershed, glacial aquifer.

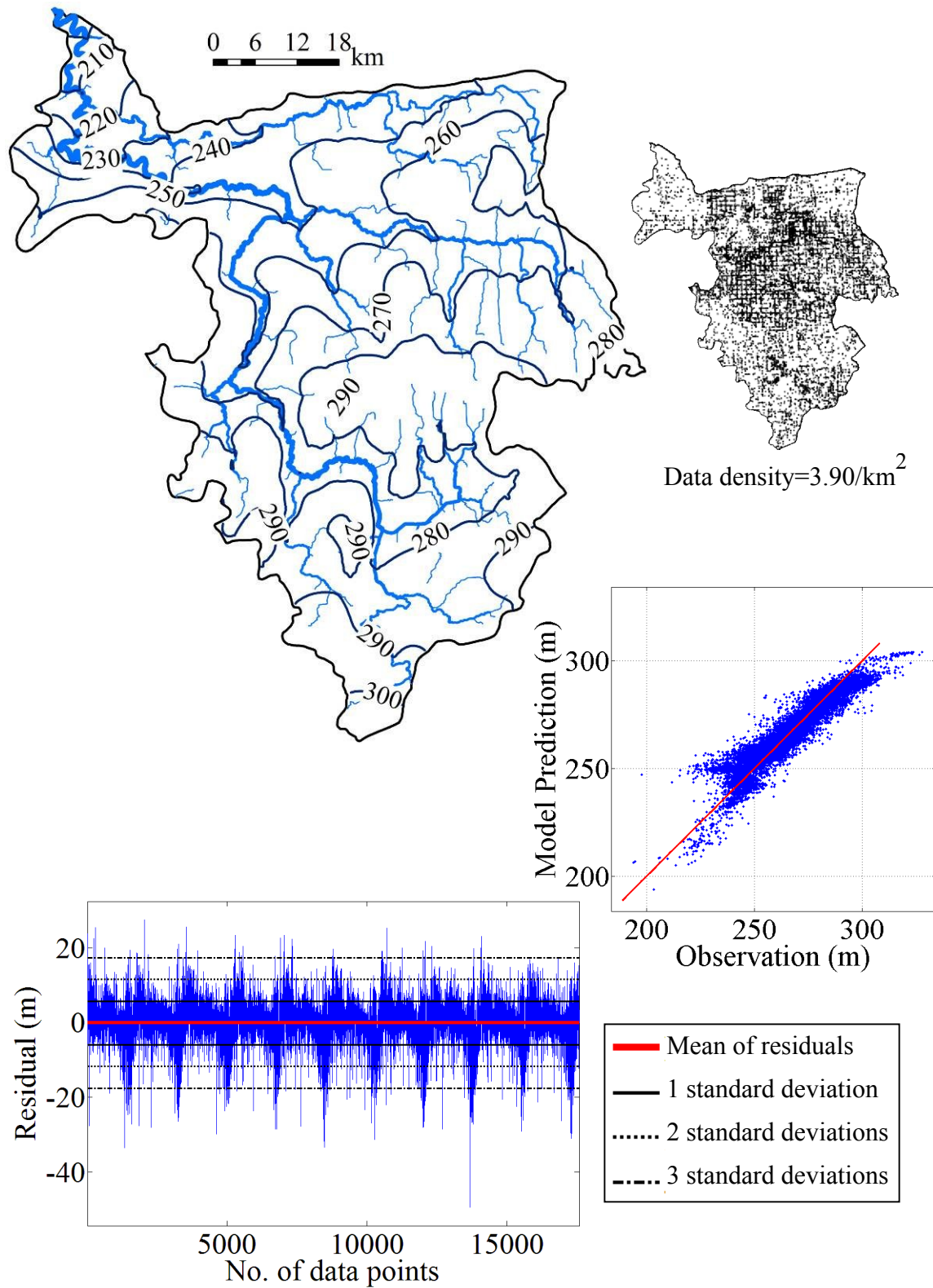


Figure 90: Analysis of the simulated heads in the Upper Grand River Watershed, bedrock aquifer.

Appendix F: Analysis of Pumping in the Southern Lower Peninsula

The SWL data that are used for the head comparisons conducted in this research represent the long-term averages of the groundwater levels in the watersheds. These water levels are recorded after the water wells are drilled and before the pumping in those wells starts. However, all of the water wells in the watersheds are not drilled at the same time and the construction dates change within a wide range between 1960s (sometimes even at earlier dates) and 2006.

Groundwater levels in the aquifers vary naturally, both seasonally and from year to year, over a range of several feet in most places (GWIM, 2006). Also, the water level that had been recorded in a well in 1970 doesn't reflect the changes due to pumping in a neighbor well that was drilled in 1980. In other words, transient impacts of the human induced stresses are not superimposed onto the data.

The cone of depression that has evolved over time within the Lansing area is a good example to demonstrate the temporal variability in the water levels. Bedrock aquifer in the Lansing area is the primary source of water for domestic, commercial, and industrial use (Holtschlag *et al.*, 1996). While in the 1970s, drawdown in the area reached its maximum levels because of the significant pumping, after late 1980s, locations of the pumping wells were changed to distribute the stress to a larger area and recover the water levels (Holtschlag *et al.*, 1996). To demonstrate the significant water level changes in the area, SWL data recorded in the bedrock wells that were drilled in two different periods (between 1970 and 1980, and between 1990 and 2000) is interpolated and shown in (Figure 91).

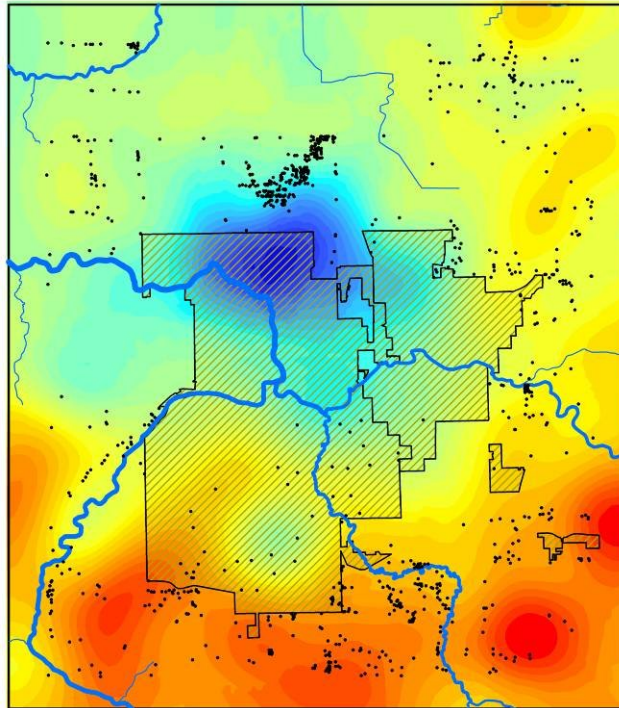
SWL (m)

269

215

Scale is non-linear

a) 1970-1980 period



SWL (m)

267

233

Scale is non-linear

b) 1990-2000 period

● Bedrock well

— Stream

▨ Lansing area

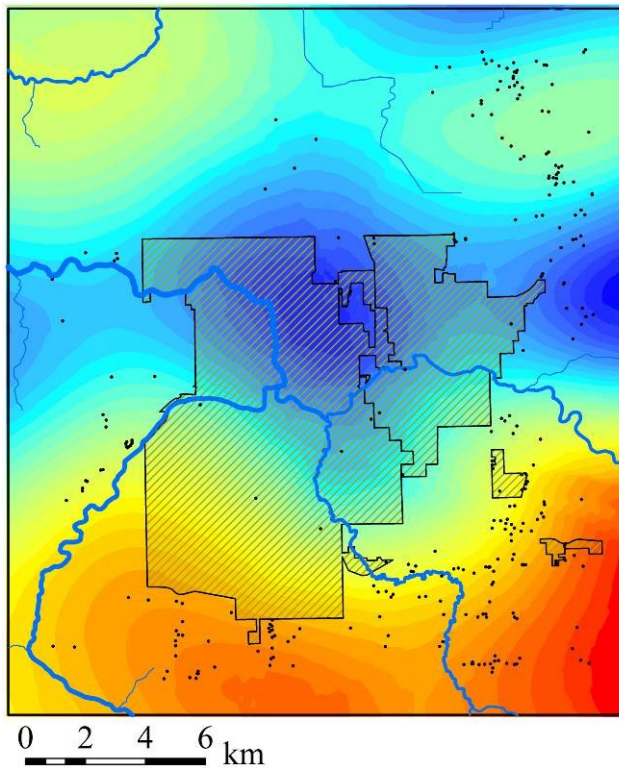


Figure 91: Interpolated SWL in the city of Lansing.

Revisiting the model of the Upper Grand River Watershed, one can clearly see the effect (strong local bias) of the pumping in the bedrock aquifer in the Lansing area (Figure 92).

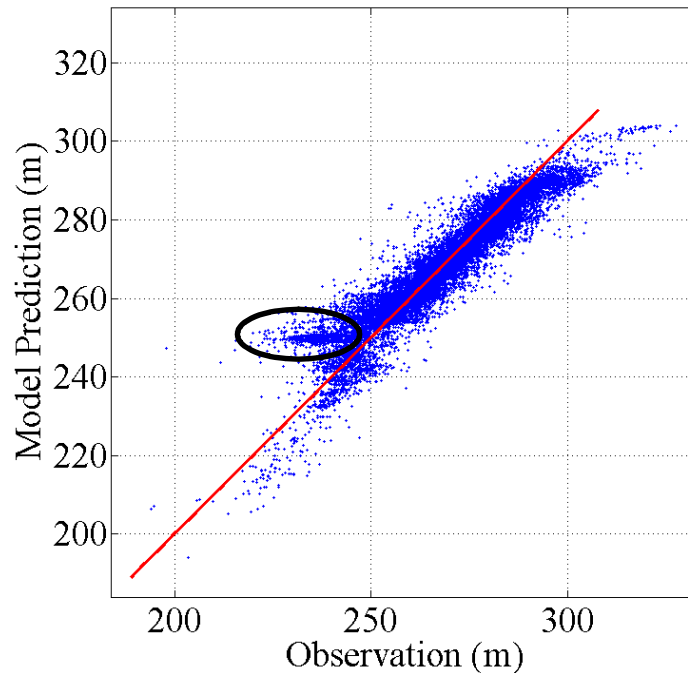


Figure 92: Revisiting the model results for the Upper Grand River. Circled area indicate the pumping effect.

Since the water wells are not simulated in any of the models, simulated heads cannot capture the impacts of pumping. However, pumping effect (drawdown) can be identified from the comparisons, especially when the total pumping discharge is significant over a long-term period. Furthermore, the bias shown in Figure 92 can be recovered if the pumping wells are enabled in the conceptual model. Even though there is not enough evidence to say that it is also a result of pumping, a similar bias for which the model systematically and at a local scale overestimates the data is also detected in the head comparisons for the bedrock aquifers in the Flint and Shiawassee Watersheds (Figure 93).

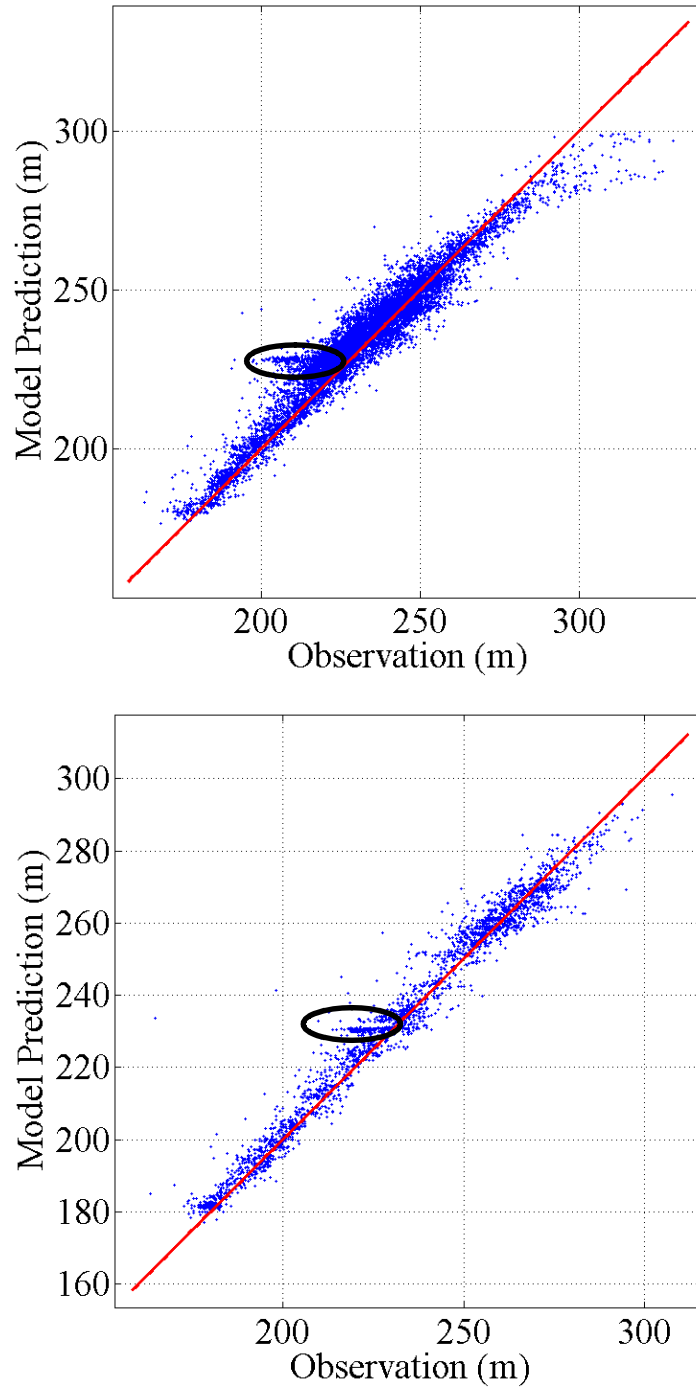


Figure 93: Identifying biases similar to that of the Upper Grand River case. Circled areas might potentially indicate the pumping effect. Above: Flint Watershed, Below: Shiawassee Watershed.

Appendix G: Definition of the Additional Model Statistics

Additional statistics that help to quantify the comparison between the simulated and measured heads are summarized in Table 18. A MATLAB script (Appendix I) is provided to generate the statistics in this table and to plot the graphics for the head comparisons illustrated in this dissertation.

Table 18: Statistics that are used to quantify the head comparisons.

Parameter (unit)	Definition
Residual Min (m)	Minimum value of residuals
Residual Max (m)	Maximum value of residuals
μ (m)	Mean value of residuals
σ (m)	One standard deviation of residuals around μ
< 0	Number of negative residuals
> 0	Number of positive residuals
Data Min (m)	Minimum measured head
Data Max (m)	Maximum measured head
Model Min (m)	Minimum simulated head
Model Max (m)	Maximum simulated head
RMSE (m)	Root mean square error
NOSD	Number of outliers
NRMSE (m)	Normalized root mean square error
R^2	Coefficient of determination
NS	Nash-Sutcliffe model efficiency coefficient

Residuals used in the analysis represent the true error between the measured and simulated heads (i.e. measurement minus prediction). The NOSD in Table 18 represents the

number of the outliers for the condition of

$$absolute(residuals) \geq absolute(mean(residuals) + 3\sigma(residuals)).$$

Root mean square error (RMSE) is frequently used in the groundwater modeling applications to measure the difference between the simulated and measured heads at the locations of the measurements. IGW's GIS interface allows the automatic extraction of the measured head values (above sea level) by subtracting the depth to water level recorded in Wellogig from the land surface elevation value extracted from the USGS-10 m DEM (sampled from the USGS-30 m DEM) at the well's location. RMSE is defined by the following formula [Equation (15)]:

$$RMSE = \sqrt{\frac{\sum_{i=1}^n (h_s - h_m)^2}{n}} \quad (15)$$

where n is the total number of measurements in a watershed, h_s is the simulated groundwater level, and h_m is the measured groundwater level.

NRMSE is the normalized value of RMSE which is calculated by dividing RMSE to the data range [Equation (16)]:

$$NRMSE = \frac{RMSE}{DR} \quad (16)$$

where DR is the data range.

The smaller the NRMSE for a model is the better the model predicts the reality.

Another measure of the ability of the model to predict the head field is Nash-Sutcliffe model efficiency coefficient (NS). NS is calculated with [Equation (17)]:

$$NS = 1 - \frac{\sum_{i=1}^n (h_s - h_m)^2}{(h_m - \overline{h_m})^2} \quad (17)$$

where n is the total number measurements in a watershed, h_s is the simulated groundwater level, h_m is the measured groundwater level, and $\overline{h_m}$ is the average of the measured groundwater levels.

The values of NS can range from $-\infty$ to 1. An efficiency value of 1 corresponds to a perfect match between the simulated and measured heads. An efficiency value of zero (NS=0) indicates that the simulated heads are as accurate as the mean of the measured heads. An efficiency value less than zero (NS<0) indicates that the measurements give a better representation of the flow field than the model predictions.

Appendix H: Detailed List of the Model Statistics

Table 19: Statistics for the model residuals, glacial aquifers.

Watershed Name	Glacial Aquifer							
	No. of Data Points	Residual						
		Min	Max	μ	σ	< 0	> 0	NOSD
Au Gres – Rifle	1,834	-35.4	101.5	5.7	11.3	493	1,341	56
Au Sable	3,184	-46.5	67.1	6.1	11.8	780	2,404	81
Birch – St. Clair	2,770	-25.3	32.1	-0.7	6.9	1,631	1,139	41
Black	369	-28.9	91.9	6.9	16.9	122	247	5
Cass	109	-22.7	27.4	3.9	19.6	33	76	0
Cheboygan	1,446	-33.5	102.8	16.6	21.6	258	1,188	3
Clinton	12,057	-43.9	46.9	3.9	7.1	3568	8,489	116
Flint	3,611	-25.6	51.7	7.1	10.2	886	2,725	12
Huron	19,938	-41.3	56.4	3.8	6.2	4,694	15,244	212
Kalamazoo	12,730	-50.1	55.0	3.4	8.1	4563	8,167	138
Kawkawlin	623	-23.0	20.1	-3.8	6.5	511	112	12
L. Grand River	14,162	-40.2	57.4	8.2	9.9	2,634	11,528	127
Manistee	5,222	-40.4	1,283	20.4	19.0	484	4,738	39
Maple	1,173	-25.8	31.6	3.3	6.1	338	835	18
Muskegon	15,054	-35.6	117.4	11.5	12.6	1,844	13,210	118
Pere – Marquette	10,227	-39.3	91.9	12.0	12.4	1,098	9,129	146
Pine	4,305	-47.6	59.1	5.3	7.2	795	3,510	41
Raisin	4,403	-28.5	41.0	2.4	6.4	1,495	2,908	38
Shiawassee	10,307	52.3	55.1	3.2	6.5	3,434	6,873	80
St. Joseph	15,448	-34.3	46.4	2.7	6.3	5,703	9,745	263
Thornapple	5,034	-34.3	55.5	8.0	8.1	774	4,260	17
Thunder Bay	1,035	-48.5	86.7	12.7	17.0	223	812	7
Tittabawassee	5,744	-45.7	107.6	17.6	21.9	1,038	4,706	3
U. Grand River	2,032	-15.2	34.6	2.8	5.5	648	1,384	16

Table 20: Statistics for the model performances, glacial aquifers.

Watershed Name	Glacial Aquifer							
	Head							
	Data		Model		RMSE	NRMSE	R ²	NS
	Min	Max	Min	Max				
Au Gres – Rifle	174	406	175	308	12.66	0.05	0.89	0.85
Au Sable	146	414	175	391	13.29	0.05	0.96	0.95
Birch – St. Clair	165	304	175	275	6.98	0.05	0.92	0.92
Black	170	398	180	320	18.20	0.08	0.91	0.85
Cass	178	261	180	253	8.72	0.11	0.78	0.72
Cheboygan	159	412	176	334	27.25	0.11	0.96	0.85
Clinton	165	350	173	313	8.09	0.04	0.98	0.97
Flint	173	343	177	300	12.38	0.07	0.95	0.90
Huron	196	335	204	306	7.24	0.05	0.83	0.76
Kalamazoo	145	350	175	310	8.76	0.04	0.90	0.88
Kawkawlin	167	244	176	225	7.57	0.10	0.80	0.71
L. Grand River	147	311	175	292	12.90	0.08	0.86	0.76
Manistee	150	444	176	378	27.85	0.09	0.91	0.80
Maple	186	288	193	264	6.96	0.07	0.89	0.85
Muskegon	161	445	175	399	17.04	0.06	0.96	0.92
Pere – Marquette	144	374	175	287	17.25	0.07	0.89	0.78
Pine	172	340	183	312	8.95	0.05	0.97	0.94
Raisin	179	335	200	316	6.85	0.04	0.94	0.93
Shiawassee	174	350	177	297	7.21	0.04	0.97	0.96
St. Joseph	155	360	176	349	6.90	0.03	0.95	0.94
Thornapple	157	297	187	272	11.42	0.08	0.86	0.73
Thunder Bay	169	375	199	316	21.26	0.10	0.82	0.67
Tittabawassee	173	390	175	286	28.11	0.13	0.89	0.64
U. Grand River	197	336	194	30.4	6.21	0.04	0.91	0.88

Table 21: Statistics for the model residuals, bedrock aquifers.

Watershed Name	Bedrock Aquifer							
	No. of Data Points	Residual						
		Min	Max	μ	σ	< 0	> 0	NOSD
Au Gres – Rifle	562	-18.4	19.4	-0.1	4.6	305	257	10
Birch – St. Clair	1,234	-27.8	28.8	-1.5	6.1	860	374	29
Black	158	-64.2	15.8	-13.2	17.4	121	37	17
Cass	2,159	-37.3	24.2	-0.1	5.7	1,129	1,030	44
Cheboygan	77	-56.3	47.9	-1.9	15.5	38	39	3
Clinton	181	-115.2	33.1	-0.9	13.3	85	96	3
Flint	9,750	-48.9	38.7	-2.4	6.1	6,584	3,166	263
Huron	2,358	-26.4	25.8	1.2	5.1	926	1,432	23
Kalamazoo	2,884	-28.7	43.7	3.3	7.0	929	1,955	44
Kawkawlin	1,735	-29.0	10.1	-4.7	4.3	1,520	215	335
L. Grand River	1,298	-39.9	44.1	-3.2	8.7	908	390	26
Maple	1,106	-19.3	25.4	-0.2	5.1	564	542	15
Pigeon	1,308	-26.4	17.2	-5.2	4.7	1,179	129	277
Raisin	1,733	-36.5	24.6	-5.7	8.5	1,236	497	72
Shiawassee	2,829	-68.9	25.5	-1.5	4.9	1,818	1,011	56
St. Joseph	972	-51.3	42.2	2.7	7.1	347	625	18
Thornapple	1,508	-28.6	22.9	2.1	5.5	533	975	11
Thunder Bay	230	-54.5	22.3	-3.1	10.0	142	88	10
Tittabawassee	223	-25.9	13.0	-1.9	6.4	131	92	4
U. Grand River	17,579	-49.4	27.4	-0.1	5.8	8,201	9,378	254

Table 22: Statistics for the model performances, bedrock aquifers.

Watershed Name	Bedrock Aquifer							
	Head							
	Data		Model		RMSE	NRMSE	R^2	NS
	Min	Max	Min	Max				
Au Gres – Rifle	172	277	175	271	4.57	0.04	0.96	0.96
Birch – St. Clair	170	295	176	272	6.25	0.05	0.93	0.94
Black	174	274	187	264	21.84	0.22	0.26	-0.30
Cass	173	275	178	253	5.71	0.05	0.87	0.87
Cheboygan	165	270	176	273	15.54	0.15	0.67	0.55
Clinton	110	322	173	312	13.26	0.06	0.88	0.87
Flint	163	329	177	300	6.55	0.04	0.93	0.91
Huron	167	308	173	290	5.25	0.04	0.95	0.94
Kalamazoo	179	351	183	310	7.74	0.04	0.95	0.94
Kawkawlin	166	229	176	222	6.38	0.10	0.88	0.61
L. Grand River	150	251	176	251	9.27	0.09	0.73	0.69
Maple	189	253	193	244	5.08	0.08	0.84	0.84
Pigeon	163	253	176	239	6.97	0.08	0.91	0.79
Raisin	168	340	187	316	10.26	0.06	0.99	0.96
Shiawassee	163	308	177	296	5.17	0.03	0.97	0.97
St. Joseph	224	364	235	348	7.62	0.05	0.93	0.91
Thornapple	179	286	188	272	5.93	0.05	0.91	0.89
Thunder Bay	175	250	181	248	10.48	0.14	0.71	0.67
Tittabawassee	178	252	180	253	6.70	0.09	0.89	0.86
U. Grand River	194	328	194	304	5.83	0.04	0.89	0.88

Appendix I: MATLAB Script for the Calculation of the Model Statistics

% Statistics and head comparison for the watershed models

```
data=xlsread('WATERSHED.NAME.DATA.xlsx');  
model=xlsread('WATERSHED.NAME.MODEL.xlsx');
```

% Eliminating zeros for data

```
data1=data(:);  
b=isnan(data1); %Detect NaN cells  
c=find(b==0); %Find non-zero cells  
datanew=data1(c); %Assign a new vector for non-zero cells  
datanew1=datanew(:); %New data column vector  
ndv=[1:1:size(datanew1(:))]; %New data vector
```

% Eliminating zeros for model

```
modell=model(:);  
b1=isnan(modell); %Detect NaN cells  
c1=find(b1==0); %Find non-zero cells  
modelnew=modell(c1); %Assign a new vector for non-zero cells  
modelnew1=modelnew(:); %New model column vector
```

% Residuals

```
res=datanew1-modelnew1; %Residuals  
plot1=plot(ndv,res)  
plot1=xlabel('No. of data points','FontSize',24,'FontName','Times','Fontweight','b')  
plot1=ylabel('Residual (m)','FontSize',24,'FontName','Times','Fontweight','b')  
plot1=title('Residuals for the Au Sable Watershed (Drift Aquifer)',...  
            'FontSize',24,'FontName','Times','Fontweight','b')
```

```

hold on

axis([1,max(ndv),min(res)-5,max(res)+5]);

hold on

mr=mean(res); %Mean of residuals

mrvec=ones(size(res)); %Mean residual vector

mrvec1=mr*mrvec;

plot2=plot(ndv,mrvec1)

set(plot2,'Color','Red','LineWidth',2.5);

hold on

% Standard deviation calculations

% 1 std

sdr1=std(res); %Standard deviation of residuals

msdr11=mr+sdr1; %Mean + 1 std

sdr1vec=ones(size(res)); %Standard deviation vector

sdr1vec1=msdr11*sdr1vec;

msdr12=mr-sdr1; %Mean - 1 std

sdr1vec2=msdr12*sdr1vec;

plot3=plot(ndv,sdr1vec1)

set(plot3,'Color','Black','LineWidth',2.5);

hold on

plot4=plot(ndv,sdr1vec2)

set(plot4,'Color','Black','LineWidth',2.5);

hold on

% 2 stds

msdr21=mr+2*sdr1; %Mean + 2 std

```

```

sdr2vec1=msdr21*sdr1vec;
msdr22=mr-2*sdr1 %Mean - 2 std
sdr2vec2=msdr22*sdr1vec;
plot5=plot(ndv,sdr2vec1,'.')
set(plot5,'Color','Black','LineWidth',2.5);
hold on
plot6=plot(ndv,sdr2vec2,'.')
set(plot6,'Color','Black','LineWidth',2.5);
hold on
% 3 stds
msdr31=mr+3*sdr1; %Mean + 3 std
sdr3vec1=msdr31*sdr1vec;
msdr32=mr-3*sdr1; %Mean - 3 std
sdr3vec2=msdr32*sdr1vec;
plot7=plot(ndv,sdr3vec1,'.')
set(plot7,'Color','Black','LineWidth',2.5);
hold on
plot8=plot(ndv,sdr3vec2,'.')
set(plot8,'Color','Black','LineWidth',2.5);
hold off
legend([plot2,plot3,plot5,plot7],'Mean of residuals',...
'1 standard deviation','2 standard deviations','3 standard deviations')
set(legend,'FontName','Times','FontSize',24,'Fontweight','b','Location','SouthWest')
set(gca,'FontSize',20,'FontName','Times')

```

% RMSE calculation

```
ressq=res.^2;  
par=sum(ressq);  
RMS=sqrt(par/length(datanew1)); %RMS  
NRMS=RMS./(max(datanew1)-min(datanew1)) %Normalized RMS
```

% Head comparison graph

```
plot9=plot(datanew1,modelnew1,'*','MarkerSize',2)  
plot9=xlabel('Observation (m)','FontSize',24,'FontName','Times','Fontweight','b')  
plot9=ylabel('Model Prediction (m)','FontSize',24,'FontName','Times','Fontweight','b')  
tchar=num2str(max(ndv));  
title(({ 'Head Comparison for the Au Sable Watershed (Drift Aquifer)';[tchar,' data points']}),...  
    'FontSize',24,'FontName','Times','Fontweight','b')  
set(gca,'FontSize',20, 'FontName', 'Times')  
hold on
```

%Coefficient of determination (R-square) calculation

```
mo=mean(datanew1); %Mean of observations  
mp=mean(modelnew1); %Mean of predictions  
odiff=datanew1-mo;  
pdiff=modelnew1-mp;  
term1=sum(odiff.*pdiff)  
term2=sqrt(sum(odiff.^2));  
term3=sqrt(sum(pdiff.^2));  
rsq=(term1./(term2.*term3)).^2;
```

% 45 degree line

```
if min(datanew1) < min(modelnew1) && max(datanew1) > max(modelnew1)
```

```

x1=[min(datanew1)-5:1:max(datanew1)+5];
y1=[min(datanew1)-5:1:max(datanew1)+5];
else
x1=[min(modelnew1)-5:1:max(modelnew1)+5];
y1=[min(modelnew1)-5:1:max(modelnew1)+5];
end
plot10=plot(x1,y1,'r','LineWidth',2.5)
if min(datanew1) < min(modelnew1) && max(datanew1) > max(modelnew1)
    axis([min(datanew1)-10 max(datanew1)+10 min(datanew1)-10 max(datanew1)+10])
else
    axis([min(modelnew1)-10 max(modelnew1)+10 min(modelnew1)-10 max(modelnew1)+10])
end
axis square
grid on
hold off
% Outliers
out=find(abs(res)>=abs(msdr31));
outs=size(out);
% Nash Sutcliffe model efficiency coefficient
NS=1-(sum((datanew1-modelnew1).^2)/sum((datanew1-mean(datanew1)).^2));
% Statistics summarized
RMS
NRMS
nofdata=size(datanew1)
mindata=min(datanew1)

```

```

minmodel=min(modelnew1)
maxdata=max(datanew1)
maxmodel=max(modelnew1)
nneg=find(res<0); %Number of negative residuals
sizeneg=size(nneg)
npos=find(res>0); %Number of positive residuals
sizepos=size(npos)
minres=min(res)
maxres=max(res)
meanres=mr
stdres=sdr1
std2res=msdr21
std3res=msdr31
outs
NS
rsq

```

LITERATURE CITED

Alley, W., T. E. Reilly, and O. L. Franke, 1999. Sustainability of ground water resources. U.S. Geological Survey Circular 1186, 86 p. <http://pubs.usgs.gov/circ/circ1186/>.

Anderson, M. P. and W. W. Woessner, 2002. Applied ground water modeling: Simulation of flow and advective transport. Academic Press, San Diego, USA, ISBN: 0-12-059485-4.

Barazzuoli, P., M. Bouzelboudjen, S. Cucini, L. Kiraly, O. Menicori, and N. Salleolini, 1999. Olocenic alluvial aquifer of the River Cornia coastal plain (southern Tuscany, Italy): Database design for ground water management. *Environmental Geology* 39(2): 123-143.

Barton, G., R. J. Mandle, and J. M. A. Baltusis, 1996. Predevelopment fresh heads in the glaciofluvial, Saginaw, Marshall aquifers in the Michigan Basin. U.S. Geological Survey Open-File Report 95-319, 21 p.

Batelaan, O, F. de Smedt, M. N. O. Valle, and W. Huybrechts, 1993. Development and application of a ground water model integrated in the GIS GRASS. In *HydroGIS 93: Application of Geographic Information Systems in Hydrology and Water Resources*. Vienna, Austria.

El-Kadi, A. I., A. A. Oloufa, A. A. Eltahan, and H. U. Malik, 1994. Use of geographic information systems in site-specific ground water modeling. *Ground Water* 32(4): 617-625.

El-Kadi, Aly (Ed.), 1995. Ground water models for resources analysis and management. CRC Press, Boca Raton, USA, ISBN: 0-56670-100-7.

Freeze, A. R. and J. A. Cherry, 1979. Groundwater. Prentice Hall, New Jersey, ISBN: 0-13-365312-9, 604 p.

Gogu, R. C., G. Carabin, V. Hallet, V. Peters, and A. Dassargues, 2001. GIS-based hydrogeological databases and ground water modeling. *Hydrogeology Journal* 9: 555-569.

Goodchild, M. F., 1996. The application of advanced information technology assessing environmental impacts, *SSSA Special Publications* (48).

Ground water Mapping and Inventory Project (GWIM), 2006. Technical Report. <http://gwmap.rsgis.msu.edu/>. [Accessed March 2010].

Haitjema, H. M. and S. M. Bruker, 2005. Are water tables a subdued replica of the topography? *Ground Water* 43(6): 781-786.

Henriksen, H. J., L. Trolborg, P. Nyegaard, T. O. Sonnenborg, J. C. Refsgaard, and B. Madsen, 2003. Methodology for construction, calibration, and validation of a national hydrological model of Denmark. *Journal of Hydrology* 280: 52-71.

- Hill-Rowley, R., T. McClain, and M. Malone, 2003. Static water level mapping in East Central Michigan. *Journal of American Water Resources Association* 39(1): 99-111.
- Hoaglund, J. R., G. C. Huffman, and N. G. Grannemann, 2002. Michigan Basin regional ground water flow discharge to three Great Lakes. *Ground Water* 40(4): 390-405.
- Hojberg, A. L., J. C. Refsgaard, F. van Geer, L. F. Jorgensen, and I. Zsuffa, 2007. Use of models to support the monitoring requirements in the water framework directive. *Water Resources Management* 21: 1649-1672.
- Holtschlag, D. J. and J. R. Nicholas, 1998. Indirect ground water discharge to the Great Lakes. U.S. Geological Survey Open Report: 98-579, 25p.
- Hunt, R. J., D. A. Saad, and D. M. Chapel, 2003. Numerical simulation of ground water flow in La Crosse County, Wisconsin, and into Nearby pools of the Mississippi River. U.S. Geological Survey Water Resources Investigations Report 03-4154, 44 p.
<http://pubs.usgs.gov/wri/wri034154/>.
- Johnston, C. M., T. G. Dewald, T. R. Bondelid, B. B. Worstell, L. D. McKay, A. Rea, R. B. Moore, and J. L. Goodall, 2009. Evaluation of catchment delineation methods for the medium-resolution national hydrography dataset. U.S. Geological Survey Scientific Investigations Report 2009-2533, 88 p. <http://pubs.usgs.gov/sir/2009/5233/>.
- Krause, P., D. P. Boyle, and F. Base, 2005. Comparison of different efficiency criteria for hydrological model assessment. *Advances in Geosciences* 5:89-97.
- Kuniansky, E. L., F. G. Gomez, and S. T. Gonzalez, 2004. Effect of aquifer development in irrigation practices on ground water availability in the Santa Isabel area, Puerto Rico. U.S. Geological Survey Water Resources Investigations Report 03-4303, 65 p.
<http://pubs.usgs.gov/wri/wri034303/>.
- Li, S. G., H. S. Liao, S. Afshari, M. Oztan, H. Abbas, and R. Mandle, 2009. A GIS-enabled hierarchical patch dynamics paradigm for modeling complex ground water systems across multiple spatial scales. In *Modelling of Pollutants in Complex Environmental Systems (Advanced Topics in Environmental Science)*. ILM Publications. Hertfordshire, UK.
- Li, S. G. and Q. Liu, 2006. Interactive Ground Water (IGW). *Environmental Modelling & Software* 21:417-418.
- Liao, H. S., S. G. Li, and R. Mandle, 2010. GIS-enabled multiscale modeling of a complex remediation site. In: *American Water Resources Association Spring Specialty Conference: Geographic Information Systems and Water Resources VI*.

Lubczynski, M. W. and J. Gurwin, 2005. Integration of various data sources for transient ground water modeling with spatio-temporally variable fluxes: Sardon study case, Spain. *Journal of Hydrology* 306: 71-96.

Marsicek, M., 2002. Geology of Michigan's Upper Peninsula.
http://www.msstate.edu/dept/geosciences/CT/TIG/WEBSITES/LOCAL/Spring2002/Michael_Marsicek/index.html. [Accessed March 2010].

Mende, A., A. Astorga, and D. Neumann, 2007. Strategy for ground water management in developing countries: A case study in northern Costa Rica. *Journal of Hydrology* 339: 109-124.

Michael, W. J., B. S. Minsker, D. Tcheng, A. J. Valocchi, and J. J. Quinn, 2005. *Water Resources Research* 41: 1-14.

National Oceanic and Atmospheric Administration (NOAA), 2011. Great Lakes water levels.
<http://www.glerl.noaa.gov/data/now/wlevels/levels.html>. [Accessed November 2010].

Neff, B. P., A. R. Piggott, and R. A. Sheets, 2006. Estimation of shallow groundwater recharge in the Great Lakes Basin. U.S. Geological Survey Scientific Investigations Report 2005-5284, 31 p. <http://pubs.usgs.gov/sir/2005/5284/>.

Refsgaard, J. C., A. L. Hojberg, I. Moller, M. Hansen, and V. Sondergaard, 2010. Ground water modeling in integrated water resources management: Visions for 2020. *Ground Water* 48(5): 633-648.

Neff, B. P., S. M. Day, A. R. Piggott, and L. M. Fuller, 2005. Base flow in the Great Lakes Basin. U.S. Geological Survey Scientific Investigations Report 2005-5217, 32p.
<http://pubs.usgs.gov/sir/2005/5217/>.

Rheaume, S. J., 1991. Hydrologic provinces of Michigan. U.S. Geological Survey Water Resources Investigations Report 91-4120, 73 p.

Seaber, P. R., P. F. Kapinos, and G. L. Knapp, 1987. Hydrologic unit maps. U.S. Geological Survey Water Supply Paper 2294, 66 p. <http://pubs.usgs.gov/wsp/wsp2294/>.

Simard, A., 2007. Predicting groundwater flow and transport using Michigan's statewide Wellogig database, Ph.D. dissertation, Michigan State University, 125 p.

Tiedeman, C. R., M. C. Hill, F. A. D'Agnese, and C. C. Faunt, 2003. Methods for using groundwater model predictions to guide hydrogeologic data collection, with application to the Death Valley regional groundwater flow system. *Water Resources Research* (39): 1-17.

Tim, U. S., D. Jain, and H. H. Liao, 1996. Interactive modeling of ground water vulnerability within a geographic information system environment. *Ground Water* 34(4): 618-627.

USGS, 2006. U.S. Geological Survey National Elevation Dataset. <http://ned.usgs.gov/>. [Accessed March 2010].

USGS, 2008. U.S. Geological Survey Shuttle Radar Topography Mission data. <http://seamless.usgs.gov/products/srtm3arc.php>. [Accessed March 2010].

USGS, 2009. U.S. Geological Survey NED release notes, 10 p. http://ned.usgs.gov/downloads/documents/NED_Release_Notes_Feb09.pdf. [Accessed March 2010].

USGS, 2010. U.S. Geological Survey National Hydrography Dataset. <http://nhd.usgs.gov/>. [Accessed March 2010].

Walton, W. C., 1992. Ground water modeling utilities. Lewis Publishers, Chelsea, MI, ISBN: 0-87371-679-5, 656 p.

Westjohn, D. B. and T. L. Weaver, 1998. Hydrogeologic framework of the Michigan basin regional aquifer system. U.S. Geological Survey Professional Paper 1418, 47 p.

Zheng, C. and R. Mia, 2010. IGW/DL: A digital library for teaching and learning hydrogeology and ground water modeling. *Ground Water* 48(3): 339-342.